

University of Alberta

Carbon-Carbon Bond Formation Promoted by Adjacent Rh and Ru Centres

By

Bryan Donald Rowsell



A thesis submitted to the Faculty of Graduate Studies and Research in partial fulfillment
of the
requirements for the degree of Doctor of Philosophy

Department of Chemistry

Edmonton, Alberta

Spring 2004



Library and
Archives Canada

Bibliothèque et
Archives Canada

Published Heritage
Branch

Direction du
Patrimoine de l'édition

395 Wellington Street
Ottawa ON K1A 0N4
Canada

395, rue Wellington
Ottawa ON K1A 0N4
Canada

Your file *Votre référence*
ISBN: 0-612-96316-0
Our file *Notre référence*
ISBN: 0-612-96316-0

The author has granted a non-exclusive license allowing the Library and Archives Canada to reproduce, loan, distribute or sell copies of this thesis in microform, paper or electronic formats.

L'auteur a accordé une licence non exclusive permettant à la Bibliothèque et Archives Canada de reproduire, prêter, distribuer ou vendre des copies de cette thèse sous la forme de microfiche/film, de reproduction sur papier ou sur format électronique.

The author retains ownership of the copyright in this thesis. Neither the thesis nor substantial extracts from it may be printed or otherwise reproduced without the author's permission.

L'auteur conserve la propriété du droit d'auteur qui protège cette thèse. Ni la thèse ni des extraits substantiels de celle-ci ne doivent être imprimés ou autrement reproduits sans son autorisation.

In compliance with the Canadian Privacy Act some supporting forms may have been removed from this thesis.

Conformément à la loi canadienne sur la protection de la vie privée, quelques formulaires secondaires ont été enlevés de cette thèse.

While these forms may be included in the document page count, their removal does not represent any loss of content from the thesis.

Bien que ces formulaires aient inclus dans la pagination, il n'y aura aucun contenu manquant.

Canada

Abstract

The binuclear complex $[\text{RhRu}(\text{CO})_3(\mu\text{-H})_2(\text{dppm})_2][\text{X}]$ (**1**) is prepared by protonation of $[\text{RhRu}(\text{CO})_3(\mu\text{-H})(\text{dppm})_2]$ ($\text{dppm} = \text{Ph}_2\text{PCH}_2\text{PPh}_2$, $\text{X} = \text{BF}_4^-$, CF_3SO_3^-). Treatment of **1** with CO affords the tetracarbonyl species $[\text{RhRu}(\text{CO})_4(\text{dppm})_2][\text{X}]$ (**2**), which yields the methylene-bridged species $[\text{RhRu}(\text{CO})_4(\mu\text{-CH}_2)(\text{dppm})_2][\text{X}]$ (**3**) upon treatment with CH_2N_2 at -78°C . Carbonyl removal using Me_3NO affords the tricarbonyl species $[\text{RhRu}(\text{CO})_3(\mu\text{-CH}_2)(\text{dppm})_2][\text{X}]$ (**4**). Compound **3** proved unreactive toward additional methylene incorporation, whereas **4** yielded several unidentified products upon exposure to CH_2N_2 . Compounds **3** and **4** react with PMe_3 to give $[\text{RhRu}(\text{CO})_3(\text{PMe}_3)(\mu\text{-CH}_2)(\text{dppm})_2][\text{X}]$ (**5**), in which coordination of PMe_3 occurs at Rh. Comparisons of the reactivity of **3** with analogous Rh/Os and Ir/Ru complexes are presented.

Compound **4**, generated *in situ*, reacts with a variety of alkynes to give C_3 -bridged species $[\text{RhRu}(\text{CO})_3(\mu\text{-}\eta^1:\eta^1\text{-C}(\text{R})=\text{C}(\text{R}')\text{CH}_2)(\text{dppm})_2][\text{CF}_3\text{SO}_3]$ ($\text{R}, \text{R}' = \text{CO}_2\text{Me}$ (**6**), CF_3 (**7**), CO_2Et (**8**); $\text{R} = \text{CH}_3$, $\text{R}' = \text{CH}(\text{COEt})_2$ (**9**), CH_2OH (**10**)). The regiochemistry of insertion for the unsymmetrical alkynes 2-butyne-1-ol diethylacetal and 2-butyne-1-ol was established by 2D NMR spectroscopy. Attempts to generate an isomer of **6** by diazomethane addition to $[\text{RhRu}(\text{CO})_3(\mu\text{-}\eta^1:\eta^1\text{-C}(\text{CO}_2\text{Me})=\text{C}(\text{CO}_2\text{Me}))(\text{dppm})_2][\text{X}]$ (**11**) failed, although CH_2N_2 addition to the tricarbonyl analogue $[\text{RhRu}(\text{OSO}_2\text{CF}_3)(\text{CO})_3(\mu\text{-}\eta^1:\eta^1\text{-C}(\text{CO}_2\text{Me})=\text{C}(\text{CO}_2\text{Me}))(\text{dppm})_2]$ (**12**) affords the methylene-bridged complex $[\text{RhRu}(\text{OSO}_2\text{CF}_3)(\text{CO})_3(\mu\text{-CH}_2)(\mu\text{-}\eta^1:\eta^1\text{-C}(\text{CO}_2\text{Me})=\text{C}(\text{CO}_2\text{Me}))(\text{dppm})_2]$ (**13**). Reaction of **6** with Me_3NO gives the rearrangement product $[\text{RhRu}(\text{CO})_2(\mu\text{-}\eta^1:\eta^3\text{-CHC}(\text{CO}_2\text{CH}_3)=\text{CH}(\text{CO}_2\text{CH}_3))(\text{dppm})_2][\text{CF}_3\text{SO}_3]$ (**14**). Propargyl alcohol reacts with **4**

giving the double-insertion product $[\text{RhRu}(\text{CO})_2(\mu, \eta^2: \eta^4\text{-CH}=\text{C}(\text{CH}_2\text{OH})\text{CH}=\text{C}(\text{CH}_2\text{OH})\text{CH}_2)(\text{dppm})_2][\text{CF}_3\text{SO}_3]$ (**15**).

Compound **4** also reacts with allene to give the trimethylene-methane-bridged complex $[\text{RhRu}(\text{CO})_2(\mu\text{-}\eta^3: \eta^1\text{-C}(\text{CH}_2)_3)(\text{dppm})_2][\text{CF}_3\text{SO}_3]$ (**16**). Addition of CO and PMe_3 gives the complexes $[\text{RhRu}(\text{CO})_2(\text{L})(\mu\text{-}\eta^3: \eta^1\text{-C}(\text{CH}_2)_3)(\text{dppm})_2][\text{CF}_3\text{SO}_3]$ ($\text{L} = \text{CO}$ (**17**), PMe_3 (**18**)), in which coordination of L occurs at Rh. Dimethylallene reacts with **4** to give the metallacyclopentanone complex $[\text{RhRu}(\text{CO})_3(\text{C}(\text{O})\text{CH}_2\text{CH}_2\text{C}(\text{=C}(\text{CH}_3)_2)(\text{dppm})_2][\text{CF}_3\text{SO}_3]$ (**19**). Treatment of **19** with H_2 affords the complex $[\text{RhRu}(\text{CO})_3(\text{H})_2(\text{C}(\text{O})\text{CH}_2\text{CH}_2\text{C}(\text{=C}(\text{CH}_3)_2)(\text{dppm})_2][\text{CF}_3\text{SO}_3]$ (**20**).

Protonation of **4** with triflic acid at $-80\text{ }^\circ\text{C}$ affords the methyl complex $[\text{RhRu}(\text{CO})_4(\mu\text{-CH}_3)(\text{dppm})_2][\text{CF}_3\text{SO}_3]$ (**21**) in which the methyl group is bound to Ru, with agostic interactions with Rh. The methyl migration to Rh is completed upon warming the solution to $-40\text{ }^\circ\text{C}$, yielding the methyl complex $[\text{RhRu}(\text{CO})_4(\text{CH}_3)(\text{dppm})_2][\text{CF}_3\text{SO}_3]$ (**22**). Subsequent warming to $0\text{ }^\circ\text{C}$ gives $[\text{RhRu}(\text{OSO}_2\text{CF}_3)(\text{CO})_3(\mu\text{-C}(\text{O})\text{CH}_3)(\text{dppm})_2][\text{CF}_3\text{SO}_3]$ (**23**) and further warming to ambient temperature gives $[\text{RhRu}(\text{OSO}_2\text{CF}_3)(\text{CO})_2(\mu\text{-C}(\text{O})\text{CH}_3)(\text{dppm})_2][\text{CF}_3\text{SO}_3]$ (**20**). Spectroscopic and structural data suggest an oxycarbene formulation for **23** and **20**.

**This thesis is dedicated to the memory of Margaret Eileen “Peggy”
Rowsell
(1946 – 2001)**

Acknowledgements

This document would not exist were it not for the love and support of many people. Firstly, I must thank my family for their unwavering support throughout the duration of my graduate studies. My father and mother provided me with the tools to succeed in life (and the occasional addition to my bank account), and my brother provided me with a prolonged challenge to succeed, as he had, in academics. Thanks must also go my sister-in-law, Nicole Robert, for returning sanity to my brother. My Nana, who played an integral role in raising me, not only gave me love and laughs but also proved a worthy Gin Rummy opponent and someone to whom I could both tell and learn excessively dirty jokes. The Edmonton section of the Rowsells, i.e. my cousin Raymond, should also be acknowledged for making the transition from self-centred Ontarian to red-necked Albertan just that much easier. There are no words to describe the love I have for my family, and “thank you” is simply not a sufficient enough phrase to convey the infinite gratitude I have for those I’ve just mentioned, but I’ll say it anyway. Thank you. I miss you, Mom.

As my extended family, I must thank Lijoy and Ann Ulahannan for providing me with *love*, support and prayer throughout all of the tribulations of recent years. The harbor you provided in the form of your open home, heart and mind were instrumental in my completion of my work.

Mad props must also go to my supervisor, Martin Cowie. He will be forever known as my academic father, though I’m sure he’ll disavow any connection, formal or otherwise, to yours truly once I’m out of earshot (heck, I’ll be lucky if he waits that long).

In any case, I thank you Marty, for providing me with a formidable academic challenge and for being a supervisor to whom I could almost always speak my mind. That is a luxury not many PhD students are given, and I am grateful for it. I promise I'll buy you another red pen and those two beers I owe you.

The Cowie group members have been supportive and entertaining over the years I've spent in this lab. Dr. (that still sounds funny to me) Steve Trepanier: I only regret not graduating before you...but thanks for taking me under your wing (even if that wing was only around for 2 hours a day). Amala Chokshi: I do so like fun things...that's why we always got along. Dr. James "Wiggy" Wigginton: cheers for showing me that not all Brits are metrosexuals and for surviving my snoring. Dr. James "Leslie" Dennett: even though you interrupted me countless times (though if I had tried to count, you'd have no doubt interrupted it), you've been a good friend and joke-fodder over the years of your Canadian exile...and I thank you. D. Jason Anderson: what else could be said about the nicest "b'y" this side of St. John's? It was a pleasure to work along side you for this long, but here's hoping you get a better haircut once you get your PhD. Rahul Samant: all I can say to you is "good luck"...you'll need it once Steve, Amala and I have left the building!

Past members and contributors cannot go unpunished, so I'd be remiss if I did not thank Dr. Robert Hilts (the best chemist I have ever, or probably will ever, work with), Dr. Dusan Ristic-Petrovic (the only man more opinionated than your humble narrator and truly one of the most clever people I've encountered) and Dr. Todd Graham (thanks for letting me steal your look).

No thesis in the Cowie group could go without a shout out to Camp X-Ray: Drs. Mike Ferguson and Bob McDonald. You guys have been professional and courteous, despite numerous attempts on my part to undermine your sanity. It was a pleasure to work with the two of you over the years, and I wish both of you nothing but success. Thank you for your help and instruction.

The friends I have made during the course of my career at the University of Alberta are extensive, and their friendship and support made my stay here all-the-more bearable. Mark Teshima, I thank for not only providing me with some good memories, but for introducing 'waird' to my vocabulary. You owe me a fresh Wunderbar™. Dr. Nathan (a.k.a. Hanthan) Jones provided me with a source of near-perfect academic intellectualism, a model toward which I'll perpetually attempt to attain. You've been a good friend over the past two years, and let's hope that continues throughout our lives and careers, provided I don't suffer from the aneurysm you so frequently predict. Dr. Duane "Fug" Stones, thanks for your North England (i.e. unpretentious) influence and for not grasping the fact that Manchester United sucks. Jeff Kirk is thanked for his humorous angst-ridden e-mails, all that Canadian Tire cashola and for making those years at McMaster Parking bearable.

I'd also like to acknowledge the following, in alphabetical order, for providing me with ample and enjoyable distractions (if I wrote something about everyone, this section would overwhelm the chemistry!): Shane Crerar; Ebbing de Jong; Liz Fryz & Dr. Mike Ferguson (look, you made it in twice!); Dr. Stephan Giessmann; Shelly Forgeron; Robin, Tracy and Trent Hamilton; Chris Harrison; Dr. Robert Lam; Dr. Chris Lee; Carolyn Leong; Chris McDonald; Dave Norman (and Fonda!!); Dr. Kim Roy; Glen Shoemaker &

Sarah Pelletier; Pankaj “Rocky” Sinha; Aaron Skelhorne & Dr. Myrlene Gee; James Sochan; Wendy Topic; Ross Witherall and anyone else that I no doubt forgot to mention.

Thanks a lot guys.

Last, but not least, I'd like to thank the support staff at U of A: the Secretaries, NMR Technicians, Spectral & Analytical Services, Electronics & Machine Shops, Stores, Purchasing and Glassblowers. I feel you are the hidden gems in this department, and little or no research would get done were it not for your tireless efforts. Thank you.

Keep it real, dog. Peace.

Table of Contents

Chapter 1: Introduction

(i)	Homogeneous vs. Heterogeneous Catalysts	1
(ii)	Monometallic vs. Polymetallic Complexes	4
(iii)	Polynuclear vs. Binuclear Complexes	6
(iv)	The Fischer-Tropsch (FT) Reaction	7
(v)	Fischer-Tropsch Mechanisms	9
(vi)	Oxygenates	16
(vii)	Goals of This Thesis	18
	References	19

Chapter 2: Methylene-Bridged Complexes of Rhodium/Ruthenium as Models for Bimetallic Fischer-Tropsch Catalysts

	Introduction	26
	Experimental	26
	Preparation of Compounds	27
	Results and Compound Characterization	34
	Discussion	53
	References	60

Chapter 3: Regioselective Alkyne Insertions into a "Rh(μ -CH₂)Ru" Moiety Yielding C₃- and C₅-Bridged Fragments

	Introduction	62
--	--------------	----

Experimental	63
Preparation of Compounds	64
Results and Compound Characterization	77
Discussion	97
Conclusions	105
References	107

Chapter 4: Coupling Between Allenes and Methylene Groups

Introduction	111
Experimental	112
Preparation of Compounds	113
Results and Compound Characterization	120
Discussion	131
Conclusions	138
References	139

Chapter 5: Methylene-to-Acyl Conversion: Models for Oxygenate Formation

Introduction	143
Experimental	144
Preparation of Compounds	144
Results and Compound Characterization	154
Discussion	176
Summary	181

References	182
Chapter 6	
Summary, Conclusions and Future Work	185
References	196
Appendix: Diazoalkane Complexes of Rh/Ru	
Introduction	199
Experimental	200
Preparation of Compounds	202
Results and Compound Characterization	204
Discussion	210
Conclusions	213
References	214

List of Tables

Chapter 2: Methylene-Bridged Complexes of Rhodium/Ruthenium as Models for Bimetallic Fischer-Tropsch Catalysts

Table 2.1. Spectroscopic Data for the Compounds	28
Table 2.2. Crystallographic Experimental Details	35
Table 2.3. Selected Distances and Angles for $[\text{RhRu}(\text{CO})_4(\text{dppm})_2]^+$	40
Table 2.4. Selected Distances and Angles for $[\text{RhRu}(\text{CO})_4(\mu\text{-CH}_2)(\text{dppm})_2]^+$	44
Table 2.5. Selected Distances and Angles for $[\text{RhRu}(\text{CO})_3(\text{PMe})_3(\mu\text{-CH}_2)(\text{dppm})_2]^+$	50
Table 2.6. A Comparison of Selected Structural Parameters for the compounds $[\text{MM}'(\text{CO})_4(\mu\text{-CH}_2)(\text{dppm})_2][\text{BF}_4]$ ($\text{MM}' = \text{RhOs}, \text{RhRu}, \text{IrRu}$)	58

Chapter 3: Regioselective Alkyne Insertions into a "Rh($\mu\text{-CH}_2$)Ru" Moiety Yielding C₃- and C₅-Bridged Fragments

Table 3.1. Spectroscopic Data for the Compounds	65
Table 3.2. Crystallographic Experimental Details	75
Table 3.3. Selected Distances and Angles for $[\text{RhRu}(\text{CO})_3(\mu\text{-}\eta^1:\eta^1\text{-C}(\text{CF}_3)=\text{C}(\text{CF}_3)\text{CH}_2)(\text{dppm})_2]^+$	82
Table 3.4. Selected Distances and Angles for $[\text{RhRu}(\text{CO})_3(\mu\text{-}\eta^1:\eta^1\text{-C}(\text{CO}_2\text{CH}_3)=\text{C}(\text{CO}_2\text{CH}_3)(\text{dppm})_2]^+$	87
Table 3.5. Selected Distances and Angles for $[\text{RhRu}(\text{CO})_2(\mu\text{-}\eta^2:\eta^4\text{-CH}=\text{C}(\text{CH}_2\text{OH})\text{CH}=\text{C}(\text{CH}_2\text{OH})\text{CH}_2)(\text{dppm})_2]^+$	94

Chapter 4: Coupling Between Allenes and Methylene Groups

Table 4.1. Spectroscopic Data for the Compounds	114
Table 4.2. Crystallographic Experimental Details	119
Table 4.3. Selected Distances and Angles for $[\text{RhRu}(\text{CO})_2(\text{C}(\text{O})\text{CH}_2\text{CH}_2\text{C}(\text{=C}(\text{CH}_3)_2)(\text{dppm})_2]^+$	128

Chapter 5: Methylene-to-Acyl Conversion: Models for Oxygenate Formation

Table 5.1. Spectroscopic Data for the Compounds	145
Table 5.2. Crystallographic Experimental Details	152
Table 5.3. Selected Distances and Angles for $[\text{RhRu}(\text{OSO}_2\text{CF}_3)(\text{CO})_3(\mu\text{-C}(\text{O})\text{CH}_3)(\text{dppm})_2]^+$	162
Table 5.4. Selected Distances and Angles for $[\text{RhRu}(\text{OSO}_2\text{CF}_3)(\text{CO})_2(\mu\text{-C}(\text{O})\text{CH}_3)(\text{dppm})_2]^+$	167
Table 5.5. Selected Distances and Angles for $[\text{RhRu}(\text{CH}_3)(\text{CO})_2(\mu\text{-Cl})(\mu\text{-CO})\text{-}(\text{dppm})_2]^+$	174

Appendix: Diazoalkane Complexes of Rh/Ru

Table A.1. Spectroscopic Data for the Compounds	201
Table A.2. Selected Distances and Angles for $[\text{RhOs}(\text{CO})_3(\mu\text{-N}_2\text{C}(\text{COH})\text{-}(\text{CO}_2\text{Et}))(\text{dppm})_2]^+$	207

List of Schemes and Figures

Chapter 1

Scheme 1.1	1
Scheme 1.2	10
Scheme 1.3	11
Scheme 1.4	12
Scheme 1.5	13
Scheme 1.6	14
Scheme 1.7	15
Scheme 1.8	16
Scheme 1.9	17
Scheme 1.10	18
Chart 1.1	7

Chapter 2: Methylene-Bridged Complexes of Rhodium/Ruthenium as Models for Bimetallic Fischer-Tropsch Catalysts

Scheme 2.1	34
Chart 2.1	51
Chart 2.2	55

Figure 2.1. Perspective view of $[\text{RhRu}(\text{CO})_4(\text{dppm})_2]^+$	39
Figure 2.2. $^{31}\text{P}\{^1\text{H}\}$ NMR spectrum of $[\text{RhRu}(\text{CO})_4(\mu\text{-CH}_2)(\text{dppm})_2]^+$	41
Figure 2.3. Perspective view of $[\text{RhRu}(\text{CO})_4(\mu\text{-CH}_2)(\text{dppm})_2]^+$	43
Figure 2.4. Perspective view of $[\text{RhRu}(\text{CO})_3(\text{PMe})_3(\mu\text{-CH}_2)(\text{dppm})_2]^+$	49

Chapter 3: Regioselective Alkyne Insertions into a "Rh($\mu\text{-CH}_2$)Ru" Moiety Yielding C₃- and C₅-Bridged Fragments

Scheme 3.1	78
Scheme 3.2	84
Scheme 3.3	85
Scheme 3.4	90
Scheme 3.5	98
Scheme 3.6	99
Scheme 3.7	100
Scheme 3.8	103

Figure 3.1. Perspective view of $[\text{RhRu}(\text{CO})_3(\mu\text{-}\eta^1:\eta^1\text{-C}(\text{CF}_3)=\text{C}(\text{CF}_3)\text{CH}_2)\text{-}(\text{dppm})_2]^+$	81
Figure 3.2. Perspective view of $[\text{RhRu}(\text{CO})_3(\mu\text{-}\eta^1:\eta^1\text{-C}(\text{CO}_2\text{CH}_3)=\text{C}(\text{CO}_2\text{CH}_3)\text{-}(\text{dppm})_2]^+$	86
Figure 3.3. Perspective view of $[\text{RhRu}(\text{CO})_2(\mu\text{-}\eta^2:\eta^4\text{-CH}=\text{C}(\text{CH}_2\text{OH})\text{CH}=\text{C}(\text{CH}_2\text{OH})\text{CH}_2)(\text{dppm})_2]^+$	93

Figure 3.4. Alternate view of $[\text{RhRu}(\text{CO})_2(\mu\text{-}\eta^2\text{:}\eta^4\text{-CH=C}(\text{CH}_2\text{OH})\text{CH=C-}(\text{CH}_2\text{OH})\text{CH}_2)(\text{dppm})_2]^+$	95
---	----

Chapter 4: Coupling Between Allenes and Methylene Groups

Scheme 4.1	112
Scheme 4.2	121
Scheme 4.3	125
Scheme 4.4	134
Scheme 4.5	138
Chart 4.1	136
Figure 4.1. Perspective view of $[\text{RhRu}(\text{CO})_2(\text{C}(\text{O})\text{CH}_2\text{CH}_2\text{C-}(\text{=C}(\text{CH}_3)_2)(\text{dppm})_2]^+$	127

Chapter 5: Methylene-to-Acyl Conversion: Models for Oxygenate Formation

Scheme 5.1	154
Scheme 5.2	169
Scheme 5.3	171
Scheme 5.4	172
Scheme 5.5	176
Scheme 5.6	179

Chart 5.1	164
Chart 5.2	168
Chart 5.3	175
Figure 5.1. ^1H NMR Spectrum of Methyl Isotopomers of $[\text{RhOs}(\text{CO})_4(\mu\text{-CH}_3)\text{-}(\text{dppm})_2]^{2+}$	155
Figure 5.2. Perspective view of $[\text{RhRu}(\text{OSO}_2\text{CF}_3)(\text{CO})_3(\mu\text{-C}(\text{O})\text{CH}_3)(\text{dppm})_2]^+$	161
Figure 5.3. Perspective view of $[\text{RhRu}(\text{OSO}_2\text{CF}_3)(\text{CO})_2(\mu\text{-C}(\text{O})\text{CH}_3)(\text{dppm})_2]^+$	166
Figure 5.4. Perspective view of $[\text{RhRu}(\text{CH}_3)(\text{CO})_2(\mu\text{-Cl})(\mu\text{-CO})(\text{dppm})_2]^+$	173
 Appendix: Diazoalkane Complexes of Rh/Ru	
Scheme A.1	208
Scheme A.2	209
Scheme A.3	212
Chart A.1	199
Chart A.2	211
Figure A.1. Perspective view of $[\text{RhOs}(\text{CO})_3(\mu\text{-N}_2\text{C}(\text{COH})(\text{CO}_2\text{Et}))(\text{dppm})_2]^+$	206

List of Abbreviations and Symbols

anal	analysis
approx.	approximately
BDA	2-butyn-1-ol dimethylacetal
ca.	circa (approximately)
calcd	calculated
COSY	Correlation Spectroscopy
δ	Chemical Shift
DMA	1,1-dimethylallene
DMA·HCl	Dimethylacetamide·hydrochloride
DMAD	dimethyl acetylenedicarboxylate
dppm	bis(diphenylphosphino)methane
ENNG	1-Ethyl-3-nitro-1-nitrosoguanidine
equiv	equivalent
Et	ethyl
FT	Fischer-Tropsch
h	hour
HMBC	Heteronuclear Multiple Bond Correlation
HMQC	Heteronuclear Multiple-Quantum Coherence Experiment
IR	infrared
Me	methyl

mg	milligram
min	minute
mL	millilitres
mmol	millimoles
MHz	megahertz
NMR	nuclear magnetic resonance
Ph	phenyl
THF	tetrahydrofuran
TMM	trimethylenemethane
μL	microlitres

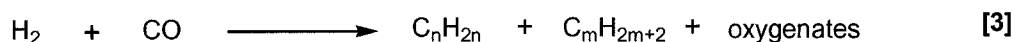
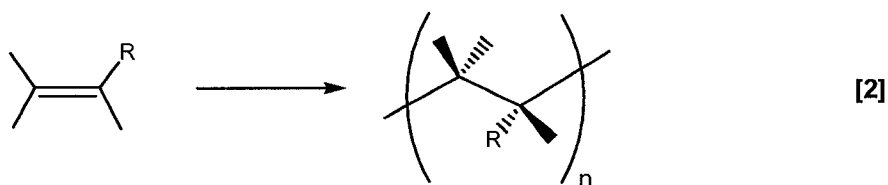
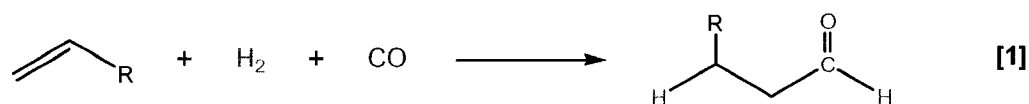
Chapter 1

Introduction

(i) Homogeneous vs. Heterogeneous Catalysts

The formation of carbon-carbon bonds is arguably one of the most important processes in chemistry being necessary in the formation of more complex hydrocarbons from smaller, simpler ones. Industrially, carbon-carbon bond formation is involved in a number of important processes such as olefin hydroformylation^{1,2} (reaction [1] in Scheme 1.1), olefin polymerization³ [2] and the Fischer-Tropsch (FT) process, (vide supra)⁴⁻⁸ [3],

Scheme 1.1



in which synthesis gas (H_2 and CO) is converted to a variety of hydrocarbons. The first two processes are well understood with long-standing success using well-defined, homogenous, metal-containing catalysts with a variety of ligand systems. The ability to use homogeneous catalysts has allowed detailed information about many of these systems

to be obtained. However, the majority of industrial catalysts are heterogeneous, and are less amenable to detailed study. Much less is known about these systems. Heterogeneous catalysts are usually exposed metal surfaces, either in the form of bulk material or as metals adsorbed on a solid support.⁹⁻¹¹ The chemical substrates are usually in the form of liquids or gasses, and are passed over these metal surfaces at the appropriate temperature and pressure. The difference in states of the catalysts and the reactants and products (assuming the products aren't solids) makes separation of the desired products from the catalyst much easier. This can allow for speedy and effective recovery of the products, and also allows for recycling of the catalyst. The rather harsh conditions under which these processes are performed (high temperatures, pressures and/or substrate or initiator concentrations) can affect the distribution of products, either directly through manipulation of the fundamental thermodynamics of the process or indirectly by affecting the catalyst and the nature of that catalyst's active site(s).

One significant drawback to employing a heterogeneous system is a lack of understanding of the fundamental steps that can affect the overall efficiency of the process. There are few readily available techniques that can quickly and effectively probe what is occurring on the surface of the catalyst. Due to this lack of pertinent information, very few heterogeneously catalyzed chemical processes are fully understood, and much work is needed to gain insight into the mechanism(s) at work. Without knowledge of the key mechanistic steps in the transformation of substrates into products, rational modification of the catalyst is not possible. Instead, an empirical or combinatorial approach¹² is often the only method for correlating the effect of catalyst modification and/or reaction conditions on the overall distribution of products.¹³

In order to gain some insight into the fundamental processes at work in heterogeneously catalyzed transformations, homogeneous complexes are often used as models for heterogeneous systems.¹⁴ These models have the major advantage of being soluble in organic solvents, allowing the use of a vast array of spectroscopic techniques that can greatly simplify characterization of the species involved and allow for easier elucidation of the possible mechanism(s) at work. Another significant advantage of homogeneous systems as models is the relative ease with which the catalyst can be modified. From metal substitution to a wholesale change of the ligand system, the effect of catalyst modification can be probed more easily than can the heterogeneous analogues. The obvious disadvantage of using homogeneous systems as models for heterogeneous systems is that there will no doubt be significant differences in the behaviour between soluble homogeneous metal complexes and the heterogeneous metal catalysts in a given chemical transformation. These potential differences notwithstanding, the elementary steps occurring on the molecular level should be identical in both systems.¹⁴⁻¹⁶

There are countless examples of relatively simple modifications in homogeneous systems where a change of metal and/or a change in the ligand system resulted in dramatic changes in either catalyst activity or selectivity in the resultant products. For example, BASF uses a cobalt catalyst system ($\text{Co}_2(\text{CO})_8/\text{HCo}(\text{CO})_4$) for the hydroformylation of propene, with resulting products being primarily the linear aldehyde.² A slight modification of the ligand system, using phosphines (L) as a modifier ($\text{Co}_2(\text{CO})_8/\text{HLC}(\text{CO})_3$), allows the reaction to be performed at significantly lower pressure, and results in the formation of primarily the linear product,^{2,17} albeit with a lower activity. A substitution of Rh for Co in the BASF system gives a nearly 50:50

mixture of linear and branched aldehydes, whereas using phosphine modification, the activity decreases, but the regioselectivity toward the linear product increases dramatically.¹⁷ In another recent example, van Leeuwen et al. showed that varying the steric bulk¹⁸ of the phosphines used can have a large effect on the regioselectivity of the process.¹⁹

(ii) Monometallic vs. Polymetallic Complexes

The aforementioned examples utilized mononuclear complexes as catalysts. Although these compounds are certainly easier to prepare, manipulate and characterize, they are not ideal models for metal surfaces, in which each metal is surrounded by adjacent metals. Complexes containing more than one metal atom (termed “clusters”) should therefore be a much more accurate model of a catalyst surface, mimicking to some degree the possible involvement of adjacent metal centres. These cluster compounds do however, have additional complexities associated with them, such as possessing metal-metal bonds and the availability of multiple coordination sites and binding modes for the incoming substrate(s).²⁰ The observation of hydrocarbyl fragments that are believed to be important surface-bound moieties in heterogeneous processes are more frequently observed in bi- and polymetallic compounds than in monometallic compounds; there are numerous bi- and polymetallic complexes containing important surface-bound carbon-containing species^{21,22} such as carbides,²³⁻²⁶ methynes²⁷⁻²⁹ and methylene^{30,31} groups. Although mononuclear methylenes (carbenes) have been characterized,³²⁻³⁴ no reports of late transition-metal carbides or methynes could be found.

The idea that a combination of metals can have marketable increases in a catalysts performance beyond the simple additive effect of the presence of an additional metal has been coined *synergism*, and was elegantly defined by Macaluso as “the force that can make $2 + 2 = 5$ ”.³⁵ Recently, this synergistic effect was exploited by Li et al., who found that addition of $\text{HMn}(\text{CO})_5$ to a well-known rhodium-based hydroformylation catalyst ($\text{Rh}_4(\text{CO})_{12}$) increased the activity of hydroformylation of 3,3-dimethylbut-1-ene by as much as 30%.³⁶

In addition to any potentially beneficial synergistic effects that are present, adjacent metals in bimetallic catalysts can also engage in a more specific form of synergism, called the “spillover effect”.³⁷ This effect arises when a substrate is adsorbed by one type of surface, and can then diffuse to another type of surface within the catalyst system, one that would not normally adsorb the substrate. In polynuclear cluster complexes, this can be mimicked somewhat by unsaturation at one or more of the metal centres in the complex. In mononuclear complexes, such as Vaska’s complex, $[\text{IrCl}(\text{CO})(\text{PPh}_3)_2]$,³⁸ Wilkinson’s Catalyst, $[\text{RhCl}(\text{PPh}_3)_3]$,³⁹ and Grubbs’ olefin metathesis catalysts, $[\text{Ru}(\text{=CHR})\text{Cl}_2(\text{PR}_3)_2]$ ³⁴ and $[\text{Ru}(\text{=CHPh})\text{Cl}_2(\text{C}_{21}\text{H}_{26}\text{N}_2)(\text{PCy}_3)]$,⁴⁰ their coordinative unsaturation is an important reason why these are effective catalysts for a variety of organic transformations.^{41,42} For polynuclear clusters, unsaturation is just as important in gauging the reactivity of the complexes. In a recent example, the coordinatively saturated hydrocarbyl-bridged cluster compound $[(\text{Cp}^*\text{Ru})_3(\mu\text{-H})_2(\mu\text{-CCH}_3)[\mu_3\text{-}\eta^2\text{-CH=CH}]]$ reacts with H_2 , but only at temperatures in excess of 100 °C and at high pressure (7 atm).⁴³ In contrast, one of the precursor complexes, $[(\text{Cp}^*\text{Ru}(\mu\text{-H}))_2(\mu_3\text{-H})_2]$, reacts with alkynes and olefins readily, presumably due to the relative ease

with which H₂ is lost, generating sites of coordinative unsaturation at one or more metal centres.⁴³

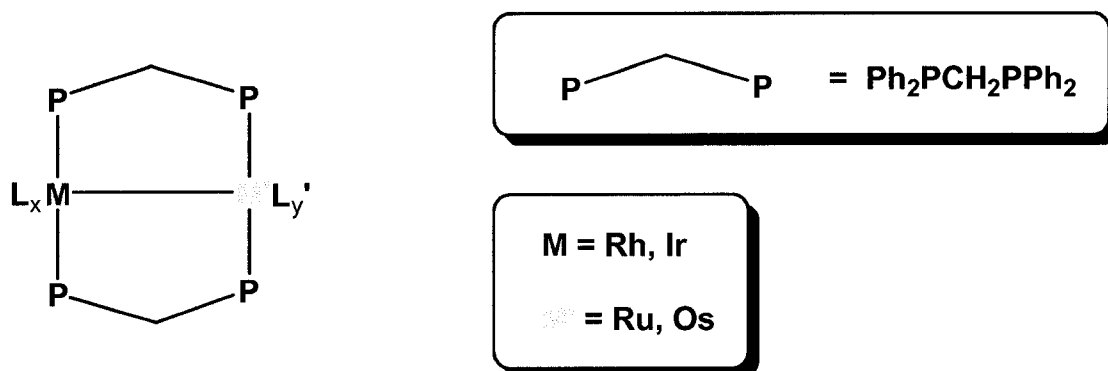
(iii) Polynuclear vs. Binuclear Complexes

Although complexes with a high degree of nuclearity can more closely model a catalysts' surface when compared to mononuclear counterparts, these complexes are notoriously difficult to study. In addition to the large number of ancillary ligands usually associated with high-nuclearity complexes, their poorer solubility compared to binuclear analogues makes their characterization more difficult. In addition, the presence of many adjacent metals can give rise to a wide range of reaction pathways, adding undesired complications. Smaller, simpler binuclear analogues are a compromise, possessing the solubility and ease of characterization of mononuclear complexes, yet still allowing for the study of synergistic effects associated with the presence of an adjacent metal as is present in polynuclear complexes.¹⁵

A requirement for the study of binuclear complexes is that the two metals must be held in close proximity by one or more bridging ligands. Furthermore, this bridging ligand system must be robust, i.e. must remain intact in their role to keep the metals together. If this is not the case, cooperativity effects between metals may be lost and the benefit of using binuclear complexes as surface models will be lost. The ligand bis(diphenylphosphino)methane,⁴⁴ or dppm, performs this task admirably. For late transition-metals, the strong M–P bonds generally keep the MM'₂P₄-framework of a dibridged MM'(dppm)₂ species shown in Chart 1.1 intact⁴⁵ while also serving as

convenient probes through the use of $^{31}\text{P}\{^1\text{H}\}$ and ^1H NMR spectroscopy to aid in

Chart 1.1



characterization. The ligands L and L', are usually chosen to be groups such as hydrides, carbonyls and hydrocarbyl fragments that are relevant to the organometallic chemistry we choose to study. There is a rich history of study of bis(dppm)-bridged, mixed-metal complexes in our group⁴⁵⁻⁶⁵ and others,^{44,66-71} with the ultimate goal being to develop a better understanding of the role of each of these metals in substrate transformation. Recently, more of an emphasis has been placed on combining different metals from groups 8 and 9.^{45,48,49,52,54,55,57-60,62-65}

(iv) The Fischer-Tropsch (FT) Reaction

The first reaction involving the use of synthesis gas ($\text{CO} + \text{H}_2$) to produce methane over a nickel catalyst was reported by Sabatier and Senderens in 1902.⁷² In 1923, Franz Fischer and Hans Tropsch had discovered the synthesis of various hydrocarbons from synthesis gas by using Fe and Co catalysts,⁷³ and by 1936, four FT

plants had been commissioned in Germany. These plants were subsequently used to meet the fuel demands later imposed by the Second World War. Today, the term Fischer-Tropsch synthesis is synonymous with the catalytic hydrogenation of carbon monoxide to form olefins, alkanes and oxygenates (see equation 3 in Scheme 1.1).

Although most of the world still relies almost exclusively on conventional oil supplies, the FT reaction is important in regions where oil reserves are minimal or non-existent, but where there is an abundance of alternate fossil fuels, such as coal or natural gas, which can also be used for the generation of synthesis gas. Currently, only SASOL (South African Synthetic Oil Limited), in South Africa, and Shell, in Malaysia, have operational FT plants, although many other companies are involved in the future construction of FT-based plants in various stages.^{6,74} Recently, it has been recommended that an FT plant be added to a multi-stage petrochemical plant in Alberta, Canada, in order to recycle some of the CO and H₂ that are side products of previous stages.⁷⁵ Clearly, fuels derived from the FT process will not challenge the current economic stranglehold that fuels derived from oil possesses, however the future importance of the FT process cannot be ignored.⁷⁴

The usefulness of the FT reaction lies in its diverse range of products formed. The product distribution is directly related to the conditions under which the FT reaction is carried out; therefore varying the pressure, temperature, catalyst, substrate concentrations, etc. can give rise to substantial variations in the nature of the products obtained. With iron-based catalysts, like those employed by SASOL,⁷⁴ the resultant products are primarily linear alkenes and oxygenates. Cobalt-based catalysts yield mostly linear alkanes and are currently the choice for the designs of more modern FT

plants.⁷⁴ Although ruthenium is an excellent catalyst and gives high molecular weight hydrocarbons and rhodium analogues give various hydrocarbons and oxygenates,⁷⁶ their high cost severely limits their use.

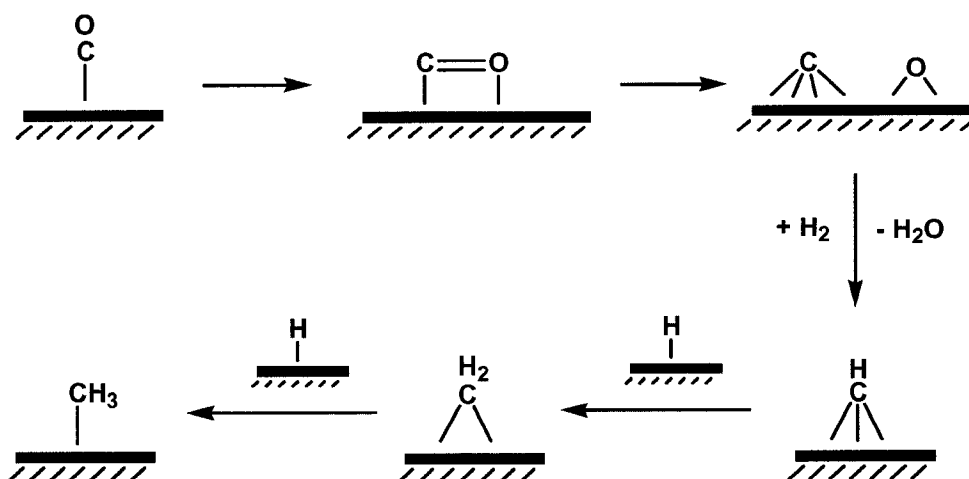
The differing reactivities of the different groups 8 and 9 metals in FT catalysis, coupled with recent reports of increased selectivities of bimetallic catalysts over monometallic ones in such processes as hydrogenation, alkene isomerization,⁷⁷ and oxidation of alcohols,⁷⁸ strongly suggest there is a role for bimetallic group 8/9 catalysts in FT chemistry. Reports of this increased selectivity have appeared,⁷⁹ and in one example the use of a Co/Ru catalyst showed increased turnover rate and preferential formation of C₅ and higher products with respect to those of monometallic catalysts.⁸⁰ Another Co/Ru catalyst has been shown to increase the activity of the catalytic hydroformylation of ethylene,⁸¹ and a rhodium-ruthenium catalyst has been shown to produce ethylene glycol with greater selectivity than the monometallic counterparts.⁸² Although the catalytic implications with regard to product distributions using bimetallic catalysts in FT chemistry have been extensively studied, little is known about the fundamental role of each metal. Even for the potentially simple monometallic FT catalysts, little is currently understood about the process and a number of proposals have been put forward to rationalize the products obtained.

(v) Fischer-Tropsch Mechanisms

The so-called carbide mechanism^{83,84} of the FT process can be artificially broken down into two steps. The first involves the conversion of syngas into C₁ hydrocarbyl

fragments as shown in Scheme 1.2. Carbon monoxide is adsorbed on the surface of the catalyst where it subsequently dissociates into surface-bound carbide and oxide moieties.

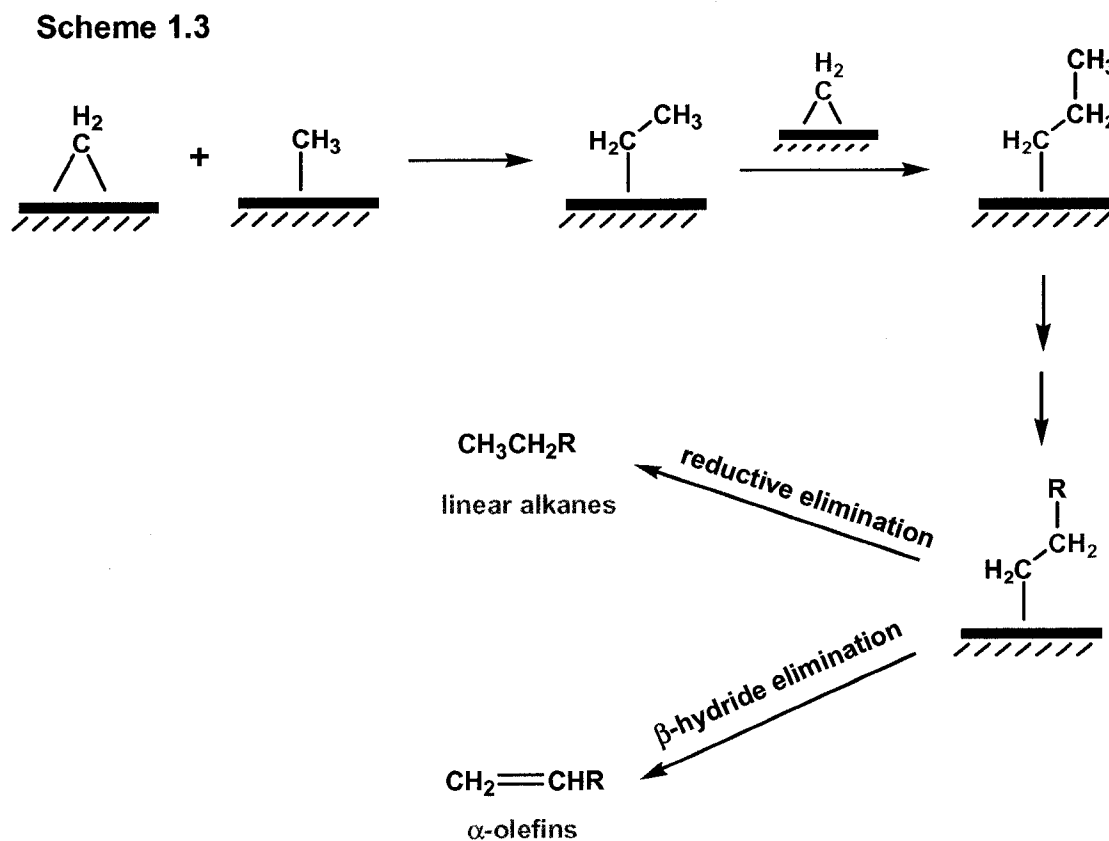
Scheme 1.2



Adsorption of H_2 on the catalyst surface results in the formation of surface hydrides, which then couple with the oxide atoms yielding water while also serving to reduce the carbide into methyne, methylene and methyl groups.

The greatest uncertainty relating to the FT process lies in the mechanisms of carbon-carbon bond formation, several of which have been proposed. Shortly after their initial report, Fischer and Tropsch proposed that carbon-carbon bonds are formed through the polymerization of the surface-bound methylene units.⁸³ This mechanism was challenged some 50 years later by Brady and Pettit, who reported that, surface-bound methylene groups, generated by passing diazomethane (CH_2N_2) over the catalyst in the absence of H_2 yielded only ethylene.⁸⁵ Only in the presence of H_2 did the diazomethane-generated methylene groups result in a normal FT distribution of hydrocarbons. This led

Brady and Pettit to propose that further reduction of some of the surface-bound methylenes to methyl groups occurred, and that C-C bond formation resulted from alkyl



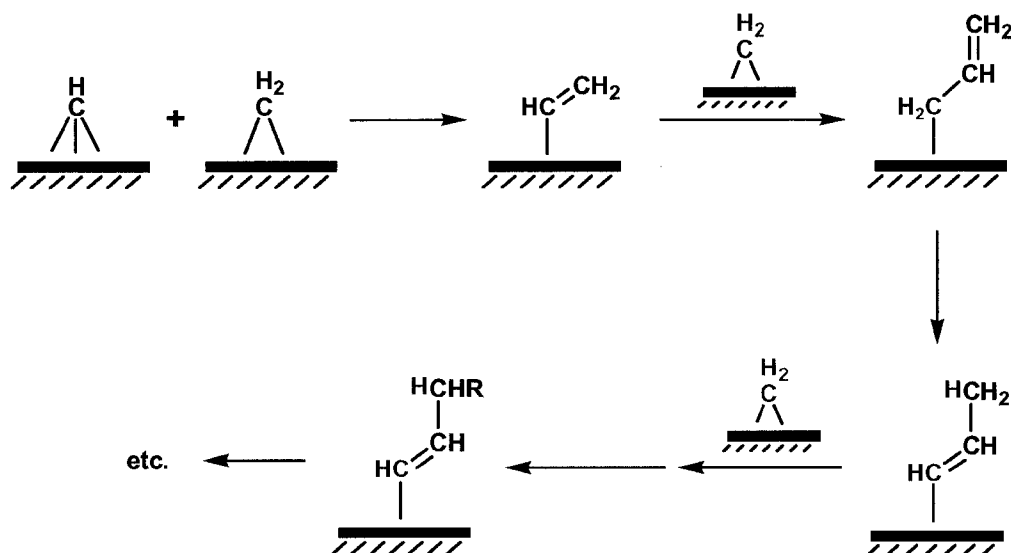
migration to the methylene groups forming longer, surface-bound alkylys. The resulting saturated and unsaturated products were the result of either reductive elimination of alkyl and hydride groups or β -hydride elimination, respectively, as diagrammed in Scheme 1.3.

Although the Brady-Pettit mechanism has been widely accepted in the literature, it is not without its shortcomings. Under normal FT conditions the yield of C_2 hydrocarbons produced is much less than those predicted by the Anderson-Schulz-Flory model,⁶ suggesting a fundamental difference between the C_2 -product formation and formation of C_n ($n > 2$) products. The FT reaction also produces small amounts of

branched hydrocarbons, which cannot be accounted for by this mechanism. Furthermore, it is known that α -olefins are the primary FT products (which are subsequently hydrogenated by the excess H_2 present),⁸ but this mechanism explains their production via β -hydrogen elimination, which seems unlikely on a catalyst surface believed to be already covered with hydrides, on which production of alkanes seems more probable.

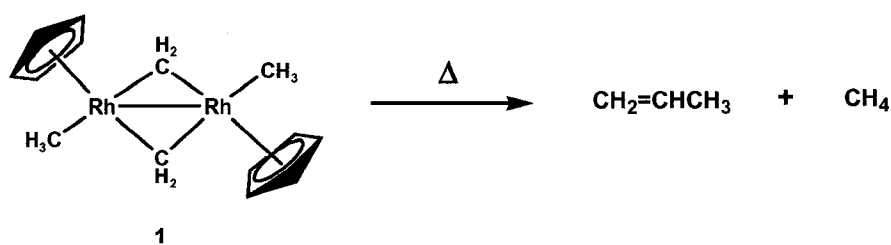
In order to overcome the inability of the Brady-Pettit mechanism to explain the low production of C_2 and branched hydrocarbons, Maitlis proposed the chain propagating steps involved migration of a vinyl (or alkenyl) species to methylene groups instead of migration of alkyl groups.⁸⁶ In such a proposal the formation of the initial C_2 (vinyl) species (possibly by coupling of methylene and methyne units) differs from the chain propagating steps, allowing a rationalization for the anomalous production of C_2 species compared to higher order hydrocarbons. In the chain propagating steps migration of a vinyl group onto a methylene group, forms the C_3 -containing allyl species, as diagrammed in Scheme 1.4. Isomerization of this allyl group (via 1,3-hydrogen shift)

Scheme 1.4



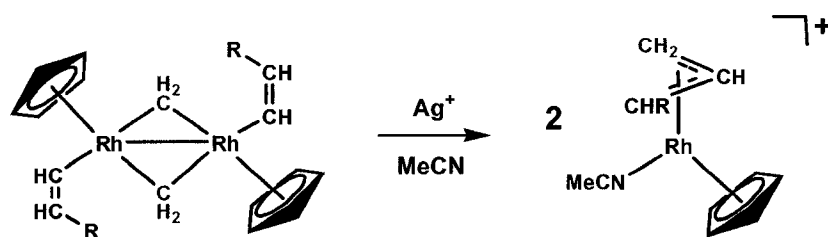
will generate a substituted vinyl group. Subsequent migrations of this substituted vinyl unit onto another methylene group followed by isomerization will propagate the mechanism and produce the observed long-chain hydrocarbons. Ironically, the suggestion for the involvement of vinyl species in C–C bond formation arose from studies on the bis-methylene-bridged species $[\text{Cp}^*\text{Rh}(\text{CH}_3)(\mu\text{-CH}_2)]_2$ (**1**) having adjacent methyl and methylene groups, which was being investigated as a model for the Brady-Pettit mechanism.⁸⁶ Heating complex **1** gives propene and methane,⁸⁶ as diagrammed in Scheme 1.5. Labelling experiments showed that the production of propene is not a result of coupling of a methyl with two methylene groups, followed by β -hydrogen elimination, but instead appeared to result from C-H activation of a methylene group to form a methyne/hydride species. Migration of a methyl group to the new bridging methyne unit followed by β -hydrogen elimination would give a vinyl/hydride. Coupling of the remaining CH_2 with the vinyl group, followed by reductive elimination, was proposed to give the observed propene.

Scheme 1.5



Facile migration of a vinyl group to an adjacent methylene moiety in $[\text{Cp}^*\text{Rh}(\text{CH}=\text{CH}_2)(\mu\text{-CH}_2)]_2$ was confirmed upon oxidation to yield the mononuclear allyl complex, shown in Scheme 1.6. In addition, a series of heterogeneous FT reactions with

Scheme 1.6

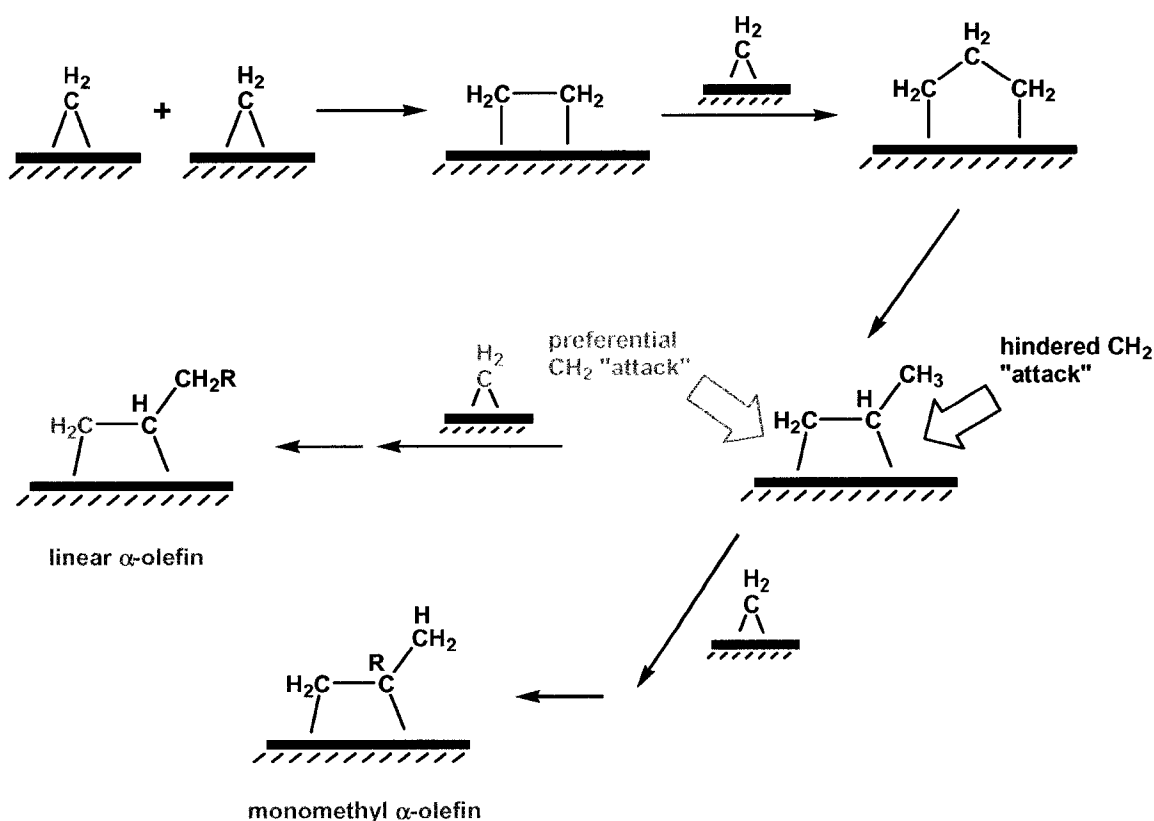


a Ru catalyst and using doubly-labelled $^{13}\text{C}_2\text{H}_2$ and $^{13}\text{CH}_2=^{13}\text{CHBr}$ as initiators have shown that high levels of $^{13}\text{C}_2$ incorporation into the hydrocarbon occurs, consistent with the proposed “alkenyl” mechanism shown in Scheme 1.4.^{87,88} One uncertainty in the “Maitlis Scheme” shown in Scheme 1.4 is the proposed isomerization of an allyl to an alkenyl species, for which only two examples have been observed.^{56,89} Furthermore, this isomerization is counterintuitive, owing to the well documented stability of allyl species.⁹⁰

A recent FT mechanism also based on C_2 species has been proposed by Dry,⁹¹ in which surface methylenes couple to form a surface-bound ethylene ligand, is shown in Scheme 1.7. Coupling of the ethylene with another methylene ligand yields a propanediyl-bridged (C_3H_6) species, which rearranges to form a surface-bound propene. Coupling of this olefin with a fourth methylene group can occur at the less hindered end leading subsequently to linear hydrocarbons or at the more hindered end to give the branched product.⁹¹ Clearly the former site of coupling will be favoured. The Dry

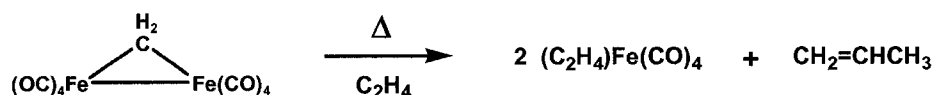
mechanism not only emphasizes the importance of the methylene unit, but also explains why methyl-branched hydrocarbons are the primary branched species observed in FT synthesis. The scheme also accounts for the anomalous yield of C₂ products in the Anderson-Shulz-Flory distribution, since the mechanism for C₂ production differs from the chain propagating steps.

Scheme 1.7



Pettit attempted to use a methylene-bridged di-iron complex, $[\text{Fe}_2(\text{CO})_8(\mu\text{-CH}_2)]_2$ (**2**), to model surface-bound methylenes.⁹² Upon heating of **2** to 55 °C under 400 psi of ethylene, propene is the major observed product (Scheme 1.8). Although Pettit proposed a mechanism involving (a) loss of a CO ligand followed by ethylene coordination, (b) insertion of ethylene into the Fe-CH₂ bond forming a C₃-bridged intermediate, (c) β -hydride elimination to give an allyl/hydride then (d) reductive elimination to afford

Scheme 1.8



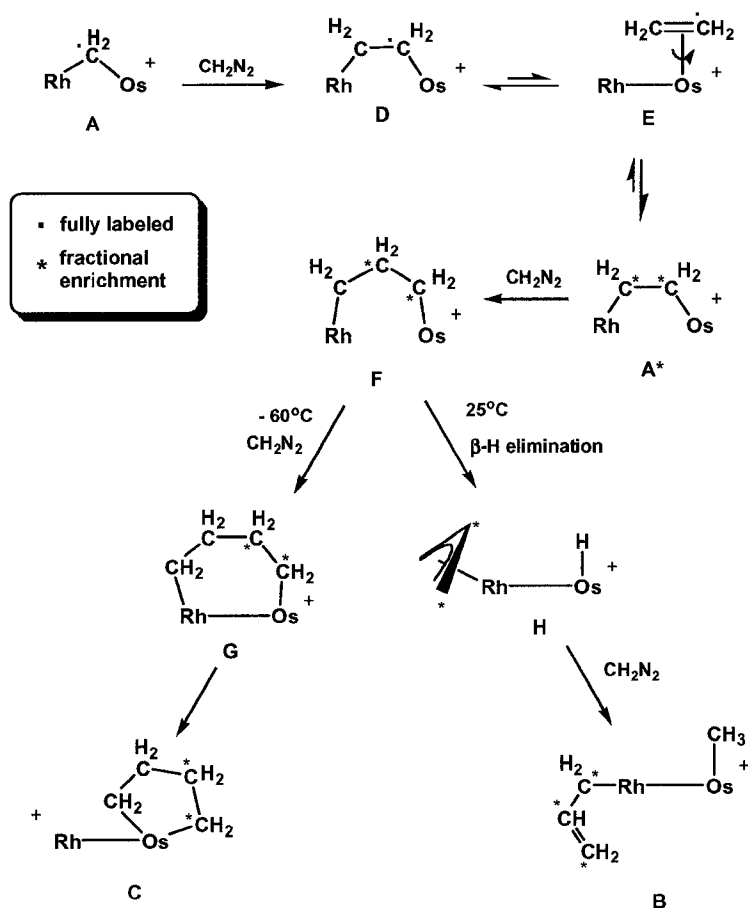
propene, none of the proposed intermediates were observed.^{92,93} The similarity of this proposed mechanism to the first few steps in the Dry proposal is striking.

Previous work in our group has shown that the reaction between the binuclear complex $[\text{RhOs}(\text{CO})_4(\text{dppm})_2][\text{X}]$ ($\text{dppm} = \mu\text{-Ph}_2\text{PCH}_2\text{PPh}_2$, $\text{X} = \text{anion}$) (**3**) and diazomethane appears to model the Dry proposal of sequential CH_2 coupling. Treatment of **3** with diazomethane can incorporate between one and four methylene units yielding methylene-bridged (**A**), allyl/methyl (**B**), or butanediyl (**C**) fragments on the metals, as shown in Scheme 1.9.⁵⁹ The C_2 -bridged (**D**) and the C_3 -bridged (**F**) appear to be excellent models for those proposed in the first two steps of the Dry mechanism.

(vi) *Oxygenates*

As mentioned earlier, alkanes and olefins are not the only products produced in the FT reaction. Other products include oxygenates such as alcohols, glycols and aldehydes. Although little mechanistic work has been carried out in efforts to explain the appearance of oxygenates, their formulation must occur by a different mechanism than that of hydrocarbons. From an organometallic perspective, it would seem that carbonyl migratory insertion is a feasible pathway to oxygen-containing products.^{94,95} This mechanism is referred to as the Pichler-Schulz mechanism,⁹⁶⁻⁹⁹ and is diagrammed in

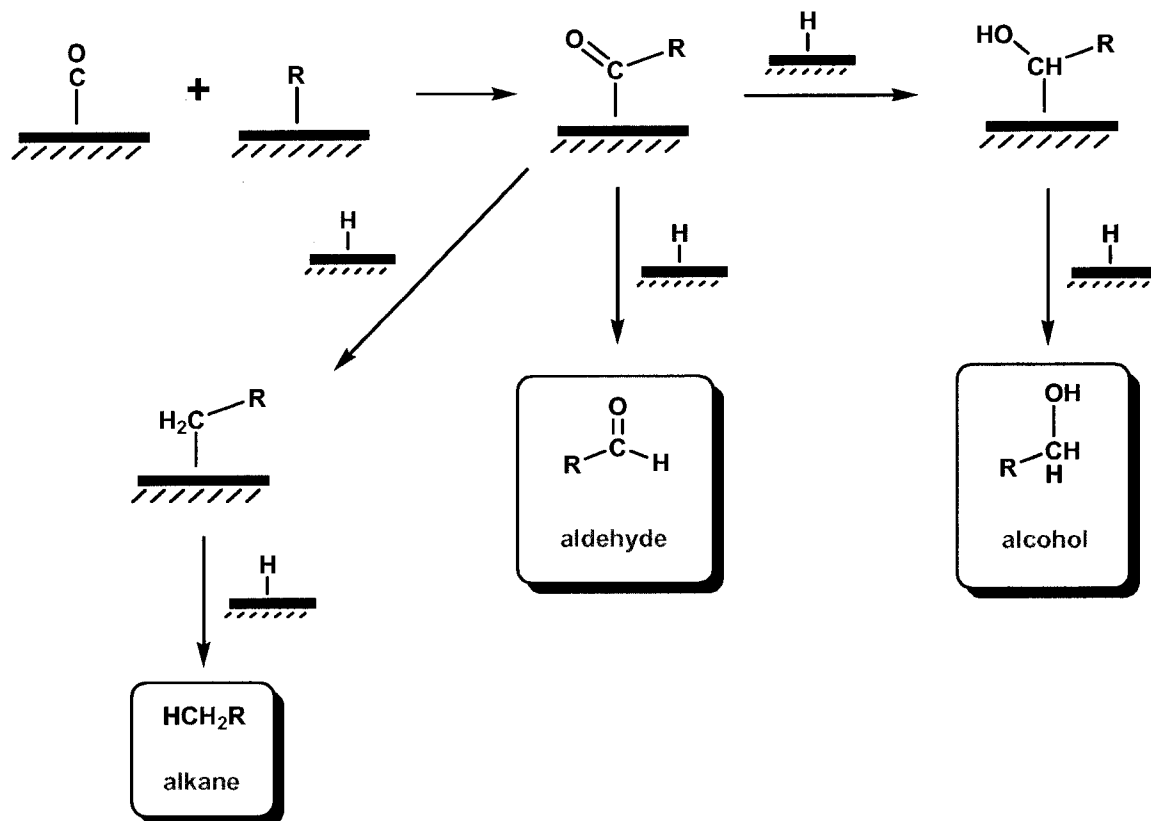
Scheme 1.9



Scheme 1.10. The alkyl group, presumably formed by one of the previously mentioned mechanisms, migrates to a carbonyl forming a surface acyl group, which can then undergo one of three possible transformations: (i) hydrogenation of the C=O bond followed by reductive elimination with a surface hydride group forming alcohols, (ii) immediate reductive elimination of the acyl group and a hydride forming aldehydes; or (iii) complete reduction of the acyl species forming an alkyl, which can then desorb as alkanes. All three steps have been observed in model systems. The complex $\text{CpFe}(\text{CH}_3\text{CO})(\text{CO})_2$ can react with silanes to undergo selective reduction forming

siloxylalkyl group (step (i)) or an alkyl group (step (iii)).¹⁰⁰ Step (ii) has been modeled by

Scheme 1.10



a binuclear complex, $[\text{Rh}_2(\mu\text{-CH}_3\text{CO})(\text{CO})_3(\text{dppm})_2]^+$ (**4**), where reaction of **4** with H_2 affords acetaldehyde.¹⁰¹

(vii) Goals of this Thesis

The high reactivity of the Rh/Os compound **3** toward diazomethane suggested that substitution of Os with the more labile Ru¹⁰² could lead to an increase in the reactivity of a Rh/Ru analogue of **3**, resulting perhaps in enhanced CH₂ incorporation. In any case, an

investigation of heterobinuclear complexes and a determination of roles of the different metals and of different metal combinations require that different combinations of metals be compared. For these reasons, the reactivity of the RhRu analogues of the RhOs system was investigated. As such, the primary goal of this thesis was to synthesize and investigate the reactivity of Rh/Ru complexes containing a bridging-methylene group. The reactivity of these Rh/Ru complexes with additional methylene groups and with unsaturated organic substrates was to be examined, with the ultimate goal of effecting carbon-carbon bond formation of relevance to the FT process. Also a comparison with the RhOs series of complexes will be made, wherever relevant. It was anticipated that such products may be effective models for the surface-bound species prevalent in the aforementioned FT mechanisms.

References:

1. Breit, B. *Acc. Chem. Res.* **2003**, *36*, 264.
2. Trzeciak, A.M.; Ziolkowski, J.J. *Coord. Chem. Rev.* **1999**, *192*, 883.
3. Imanishi, Y.; Naga, N. *Prog. Polym. Sci.* **2001**, *26*, 1147.
4. Van der Laan, G.P.; Beenackers, A. *Catal. Rev.-Sci. Eng.* **1999**, *41*, 255.
5. Schulz, H. *Appl. Catal. A* **1999**, *186*, 3.
6. Overett, M.J.; Hill, R.O.; Moss, J.R. *Coord. Chem. Rev.* **2000**, *206*, 581.
7. Davis, B.H. *Fuel Proc. Technol.* **2001**, *71*, 157.
8. Dry, M.E. *Catal. Today* **2002**, *71*, 227.
9. Leadbeater, N.E.; Marco, M. *Chem. Rev.* **2002**, 3217.
10. Serp, P.; Kalck, P. *Chem. Rev.* **2002**, *102*, 3085.

11. Brunel, D.; Bellocq, N.; Sutra, P.; Cauvel, A.; Lasperas, M.; Moreau, P.; Di Renzo, F.; Galarneau, A.; Fajula, F. *Coord. Chem. Rev.* **1998**, *178-180*, 1085.
12. Mittasch, A. *Adv. Catal.* **1950**, *2*, 81.
13. Richter, M.; Langpape, M.; Kolf, S.; Grubert, G.; Eckelt, R.; Radnik, J.; Schneider, M.; Pohl, M.-M.; Fricke, R. *Appl. Catal. B* **2002**, *36*, 261.
14. Coperet, C.; Chabanas, M.; Saint-Arroman, R.P.; Basset, J.-M. *Angew. Chem.-Int. Ed. Engl.* **2003**, *42*, 156.
15. Muetterties, E.L.; Stein, J. *Chem. Rev.* **1979**, *79*, 479.
16. Locatelli, F.; Candy, J.-P.; Didillon, B.; Niccolai, G.P.; Uzio, D.; Basset, J.-M. *J. Am. Chem. Soc.* **2001**, *123*, 1658.
17. Cornils, B.; Herrmann, W.A. *J. Catal.* **2003**, *216*, 23.
18. Tolman, C.A. *Chem. Rev.* **1977**, *77*, 313.
19. Kamer, P.C.J.; van Leeuwen, P.W.N.; Reek, J.N.H. *Acc. Chem. Res.* **2001**, *34*, 895.
20. Adams, R.D.; Cotton, F.A., Eds. *Catalysis by Di- and Polynuclear Metal Cluster Complexes*; Wiley: New York, 1998.
21. Zheng, C.; Apeloig, Y.; Hoffmann, R. *J. Am. Chem. Soc.* **1988**, *110*, 749.
22. Zaera, F. *Chem. Rev.* **1995**, *95*, 2651.
23. Adams, R.D.; Captain, B.; Fu, W.; Pellechia, P.J.; Smith, M.D. *Inorg. Chem.* **2003**, *42*, 2094.
24. Adams, R.D.; Chen, G.; Wu, W. *J. Cluster Sci.* **1991**, *2*, 271.
25. Korlann, S.; Diaz, B.; Bussell, M.E. *Chem. Mater.* **2002**, *14*, 4049.
26. Tachikawa, M.; Muetterties, E.L. *J. Am. Chem. Soc.* **1980**, *102*, 4541.

27. Kolis, J.W.; Holt, E.M.; Shriver, D.F. *J. Am. Chem. Soc.* **1983**, *105*, 7307.
28. Hriljac, J.A.; Swepston, P.N.; Shriver, D.F. *Organometallics* **1985**, *4*, 158.
29. Dutta, T.K.; Vites, J.C.; Jacobsen, G.B.; Fehlner, T.P. *Organometallics* **1987**, *6*, 842.
30. Herrmann, W.A. *Adv. Organomet. Chem.* **1982**, *20*, 159.
31. Davies, D.L.; Jeffery, J.C.; Miguel, D.; Sherwood, P.; Stone, F.G.A. *J. Organomet. Chem.* **1990**, *383*, 463.
32. Heinekey, D.M.; Radzewich, C.E. *Organometallics* **1998**, *17*, 51.
33. Fryzuk, M.D.; Gao, X.; Joshi, K.; McNeil, P.A.; Massey, R.L. *J. Am. Chem. Soc.* **1993**, *115*, 10581.
34. Schwab, P.; Grubbs, R.H.; Ziller, J.W. *J. Am. Chem. Soc.* **1996**, *118*, 100.
35. Macaluso, P. *Ind. Eng. Chem.* **1944**, *36*, 1071.
36. Li, C.; Widjaja, E.; Garland, M. *J. Am. Chem. Soc.* **2003**, *125*, 5540.
37. Conner, W.C.; Falconer, J.L. *Chem. Rev.* **1995**, *95*, 759.
38. Vaska, L.; Sloane, E.M. *J. Am. Chem. Soc.* **1960**, *82*, 1263.
39. Osborn, J.A.; Jardine, F.H.; Young, J.F.; Wilkinson, G. *J. Chem. Soc.* **1966**, 1711.
40. Scholl, M.; Ding, S.; Lee, C.W.; Grubbs, R.H. *Org. Lett.* **1999**, *1*, 953.
41. Brase, S.; Lauterwasser, F.; Ziegler, R.E. *Adv. Synth. Catal.* **2003**, *345*, 869.
42. Fagnou, K.; Lautens, M. *Chem. Rev.* **2003**, *103*, 169.
43. Takao, T.; Takemori, T.; Makoto, M.; Suzuki, H. *Organometallics* **2002**, *21*, 5190.
44. Puddephatt, R.J. *Chem. Soc. Rev.* **1983**, *12*, 99.
45. Antonelli, D.M.; Cowie, M. *Organometallics* **1990**, *9*, 1818.

46. Antonelli, D.M.; Cowie, M. *Inorg. Chem.* **1990**, *29*, 4039.
47. Antonelli, D.M.; Cowie, M. *Inorg. Chem.* **1990**, *29*, 3339.
48. Hilts, R.W.; Franchuk, R.A.; Cowie, M. *Organometallics* **1991**, *10*, 1297.
49. Hilts, R.W.; Franchuk, R.A.; Cowie, M. *Organometallics* **1991**, *10*, 304.
50. Antonelli, D.M.; Cowie, M. *Organometallics* **1991**, *10*, 2550.
51. Antonelli, D.M.; Cowie, M. *Organometallics* **1991**, *10*, 2173.
52. McDonald, R.; Cowie, M. *Inorg. Chem.* **1993**, *32*, 1671.
53. Wang, L.S.; McDonald, R.; Cowie, M. *Inorg. Chem.* **1994**, *33*, 3735.
54. Sterenberg, B.T.; Hilts, R.W.; Moro, G.; McDonald, R.; Cowie, M. *J. Am. Chem. Soc.* **1995**, *117*, 245.
55. George, D.S.A.; McDonald, R.; Cowie, M. *Organometallics* **1998**, *17*, 2553.
56. Wang, L.S.; Cowie, M. *Can. J. Chem.* **1995**, *73*, 1058.
57. Antwi-Nsiah, F.H.; Oke, O.; Cowie, M. *Organometallics* **1996**, *15*, 1042.
58. Sterenberg, B.T.; McDonald, R.; Cowie, M. *Organometallics* **1997**, *16*, 2297.
59. Trepanier, S.J.; Sterenberg, B.T.; McDonald, R.; Cowie, M. *J. Am. Chem. Soc.* **1999**, *121*, 2613.
60. Oke, O.; McDonald, R.; Cowie, M. *Organometallics* **1999**, *18*, 1629.
61. Graham, T.W.; Van Gastel, F.; McDonald, R.; Cowie, M. *Organometallics* **1999**, *18*, 2177.
62. George, D.S.A.; Hilts, R.W.; McDonald, R.; Cowie, M. *Organometallics* **1999**, *18*, 5330.
63. George, D.S.A.; Hilts, R.W.; McDonald, R.; Cowie, M. *Inorg. Chim. Acta* **2000**, *300*, 353.

64. Dell'Anna, M.M.; Trepanier, S.J.; McDonald, R.; Cowie, M. *Organometallics* **2001**, *20*, 88.
65. Trepanier, S.J.; McDonald, R.; Cowie, M. *Organometallics* **2003**, *22*, 2638.
66. Orth, S.D.; Terry, M.R.; Abboud, K.A.; Dodson, B.; McElwee-White, L. *Inorg. Chem.* **1996**, *35*, 916.
67. Elliot, D.J.; Holah, D.G.; Hughes, A.N.; Vittal, J.J.; Puddephatt, R.J. *Organometallics* **1993**, *12*, 1225.
68. Chaudret, B.; Delavaux, B.; Poilblanc, R. *Coord. Chem. Rev.* **1988**, *86*, 191.
69. Braunstein, P.; Faure, T.; Knorr, M. *Organometallics* **1999**, *18*, 1791.
70. Schreiner, S.; Setzer, M.M.; Gallaher, T.N. *Inorg. Chim. Acta* **1991**, *188*, 131.
71. Braunstein, P.; de Meric de Bellefon, C.; Oswald, B. *Inorg. Chem.* **1993**, *32*, 1649.
72. Sabatier, P.; Senderens, J.B. *Hebd. Seances Acad. Sci.* **1902**, *134*, 514.
73. Fischer, F.; Tropsch, T. *Brennst. Chem.* **1923**, *4*, 276.
74. Tullo, A.H. *Chem. Eng. News* **2003**, *July 21*, 18.
75. Tullo, A.H. *Chem. Eng. News* **2003**, *August 25*, 16.
76. Vannice, M.A. *J. Catal.* **1975**, *37*, 449.
77. Sinfelt, J.H. *Bimetallic Catalysts: Discoveries, Concepts and Applications*; Wiley: New York, 1983
78. da Silva, A.C.; Piotrowski, H.; Mayer, P.; Polborn, K.; Severin, K. *Eur. J. Inorg. Chem.* **2001**, 685.
79. Alexeev, O.S.; Gates, B.C. *Ind. Eng. Chem. Res.* **2003**, *42*, 1571.
80. Iglesia, E.; Soled, S.L.; Fiato, R.A.; Via, G.H. *J. Catal.* **1993**, *143*, 345.

81. Huang, L.; Xu, Y. *Catalysis Letters* **2000**, *69*, 145.
82. Dombek, B.D. *Organometallics* **1985**, *4*, 1707.
83. Fischer, F.; Tropsch, T. *Brennst. Chem.* **1926**, *7*, 97.
84. Fischer, F.; Tropsch, T. *Chem. Ber.* **1926**, *59*, 830.
85. Brady, R.C.; Pettit, R. *J. Am. Chem. Soc.* **1980**, *102*, 6181.
86. Maitlis, P.M.; Long, H.C.; Quyoun, R.; Turner, M.L.; Wang, Z.Q. *Chem. Commun.* **1996**, 1.
87. Long, H.C.; Turner, M.L.; Fornasiero, P.; Kaspar, J.; Graziani, M.; Maitlis, P.M. *J. Catal.* **1997**, *167*, 172.
88. Maitlis, P.M.; Quyoun, R.; Long, H.C.; Turner, M.L. *Appl. Catal. A* **1999**, *186*, 363.
89. Martinex, J.; Gill, J.B.; Adams, H.; Bailey, N.A.; Saez, I.M.; Sunley, G.J.; Maitlis, P.M. *J. Organomet. Chem.* **1990**, *394*, 2297.
90. Crabtree, R.H. *The Organometallic Chemistry of the Transition Metals*; John Wiley & Sons: New York, 1988, Chapter 7.
91. Dry, M.E. *Appl. Catal. A* **1996**, *138*, 319.
92. Sumner, C.E.; Riley, P.E.; Davis, R.E.; Pettit, R. *J. Am. Chem. Soc.* **1980**, *102*, 1752.
93. Sumner, C.E.; Collier, J.A.; Pettit, R. *Organometallics* **1982**, *1*, 1350.
94. Koga, N.; Morokuma, K. *Chem. Rev.* **1991**, *91*, 823.
95. Niu, S.; Hall, M.B. *Chem. Rev.* **2000**, *100*, 353.
96. Pichler, H.; Schulz, H. *Chem. Ing. Technol.* **1970**, *12*, 1160.
97. Masters, C. *Adv. Organomet. Chem.* **1979**, *19*, 63.

98. Muetterties, E.L.; Rhodin, T.N.; Bard, E.; Brucker, C.F.; Pretzer, W.R. *Chem. Rev.* **1979**, *79*, 91.
99. Rofer-DePoorter, C.K. *Chem. Rev.* **1981**, *81*, 447.
100. Akita, M.; Mitani, O.; Sayama, M.; Moro-oka, Y. *Organometallics* **1991**, *10*, 1394.
101. Eisenberg, R.; Shafiq, F.; Kramarz, K.W. *Inorg. Chim. Acta* **1990**, *213*, 111.
102. Huheey, J.E.; Keiter, E.A.; Keiter, R.L. *Inorganic Chemistry: Principles of Structure and Reactivity*; 4th ed.; Harper Collins: New York, 1993

Chapter 2

Methylene-Bridged Complexes of Rhodium/Ruthenium as Models for Bimetallic Fischer-Tropsch Catalysts: Comparisons with the Rh/Os and Ir/Ru Analogues

Introduction:

As noted in Chapter 1, the most promising system for the incorporation of methylene fragments in our series of group 8/9 heterobinuclear complexes is derived from $[\text{RhOs}(\text{CO})_4(\text{dppm})_2][\text{CF}_3\text{SO}_3]$.¹ This complex was found to incorporate up to four diazomethane-generated methylene units, depending on reaction conditions, as diagrammed in Scheme 1.9. The high FT activity of Ru, as well as the rich chemistry of diruthenium complexes in carbon-carbon bond formation,²⁻⁴ led us to extend the above Rh/Os chemistry to include the Rh/Ru combination of metals, and our preliminary findings on this system are reported herein, as are comparisons with the above Rh/Os¹ system and the related Ir/Ru⁵ system. From this comparison we hope to be able to address questions relating to the use of different metal combinations in carbon-carbon bond formation related to FT chemistry.

Experimental:

General Comments. All solvents were dried (using appropriate desiccants), distilled before use, and stored under a dinitrogen atmosphere. Reactions were performed under an argon atmosphere using standard Schlenk techniques. Diazomethane was generated from Diazald, which was purchased from Aldrich, as was the trimethylphosphine (1.0 M) solution in THF. The ¹³C-enriched Diazald was purchased from Cambridge Isotopes,

whereas ^{13}C O was purchased from Isotec Inc. The complex $[\text{RhRu}(\text{CO})_3(\mu\text{-H})(\text{dppm})_2]$ was prepared by a published procedure.⁶

The ^1H , $^{13}\text{C}\{^1\text{H}\}$, and $^{31}\text{P}\{^1\text{H}\}$ NMR spectra were recorded on a Varian iNova-400 spectrometer operating at 399.8 MHz for ^1H , 161.8 MHz for ^{31}P , and 100.6 MHz for ^{13}C . Infrared spectra were obtained on a Bomem MB-100 spectrometer. The elemental analyses were performed by the microanalytical service within the department.

For all the compounds reported, both the triflate (CF_3SO_3^-) and tetrafluoroborate (BF_4^-) salts were synthesized through the use of either triflic or tetrafluoroboric acid in the preparation of compound **1**, described below. Compounds having the triflate anion are labeled **a**, whereas those with tetrafluoroborate are labeled **b**. Since the spectroscopic data for the cations were found to be identical, irrespective of anion used, only the syntheses and spectroscopic data (Table 2.1) for the triflate salts are reported herein. However, crystal structure determinations described are for the tetrafluoroborate salts since our attempts to obtain suitable single crystals of the triflate salts were unsuccessful.

Preparation of Compounds:

(a) $[\text{RhRu}(\text{CO})_3(\mu\text{-H})_2(\text{dppm})_2][\text{CF}_3\text{SO}_3]$ (1a**).** The compound $[\text{RhRu}(\text{CO})_3(\mu\text{-H})(\text{dppm})_2]$ (100 mg, 0.095 mmol) was dissolved in 1.0 mL of THF, and 20 mL of diethyl ether was added slowly to produce a cloudy, brown solution. Triflic acid (8.5 μL , 14.1 mg, 0.096 mmol) was added dropwise, causing the precipitation of a yellow solid. The slurry was stirred for 2 h, and the light brown supernatant was removed. The

Table 2.1. Spectroscopic Data For Compounds.

Compound	IR (cm ⁻¹) ^{a,b}	NMR ^{d,e}		
		³¹ P{ ¹ H} (ppm) ^f	¹ H (ppm) ^{g,h}	¹³ C{ ¹ H} (ppm) ^{h,i}
[RhRu(CO) ₃ (μ-H) ₂ (dppm) ₂]- [CF ₃ SO ₃] (1a)	2044 (m), 1970 (br,s)	34.4 (m), 26.2 (dm)	3.87 (m, 4H), -9.65 (m, 2H)	197.0 (t, ² J _{PC} = 12 Hz, 2C), 182.6 (dt, ² J _{RhC} = 75 Hz, ² J _{PC} = 17 Hz, 1C)
[RhRu(CO) ₄ (dppm) ₂][CF ₃ SO ₃] (2a)	1987 (m), 1945 (m), 1906 (s)	35.4 (m), 27.1 (dm)	3.9 (m, 4H)	207.6 (t, ² J _{PC} = 13 Hz, 2C), 195.9 (t, ² J _{PC} = 15 Hz, 1C), 179.5 (m, ² J _{PC} = 15 Hz, ¹ J _{RhC} = 75 Hz, 1C)
[RhRu(CO) ₄ (μ- CH ₂)(dppm) ₂]- [CF ₃ SO ₃] (3a)	2043 (m), 2001 (m), 1963 (s), 1802 (m)	35.3 (om)	3.74 (m, 2H), 2.80 (m, 2H), 2.43 (m, 2H)	227.4 (m, 1C), 195.4 (dt, ² J _{PC} = 20 Hz, ¹ J _{RhC} = 66 Hz, 1C), 194.9 (m, 1C), 194.0 (t, ² J _{PC} = 12 Hz, 1C), 48.3 (dpq, ¹ J _{RhC} = 16 Hz, ² J _{PC} = 5 Hz)
[RhRu(CO) ₃ (μ- CH ₂)(dppm) ₂]- [CF ₃ SO ₃] (4a)	2018 (m), 1995 (s), 1957 (s) ^c	30.7 (m), 28.6 (dm) ^j	5.38 (m, 2H), 4.24 (m, 2H), 3.58 (m, 2H) ^j	96.2 (t, ² J _{PC} = 8 Hz, 1C), 195.2 (t, ² J _{PC} = 13 Hz, 1C), 189.1 (dt, ² J _{PC} = 14 Hz, ¹ J _{RhC} = 68 Hz, 1C), 97.0 (m) ^k

Table 2.1. Spectroscopic Data For Compounds (cont'd.)

[RhRu(PMe ₃)(CO) ₃ (μ-CH ₂)- (dppm) ₂][CF ₃ SO ₃] (5a)	1981 (s), 1965 (s), 1919 (s)	26.8 (m), 23.5 (dm), -34.4 (dm)	4.77 (m, 2H), 3.85 (m, 2H), 3.60 (m, 2H), 0.70 (d, ² J _{PH} = 10 Hz, 9H)	204.1 (t, ² J _{PC} = 10 Hz, 1C), 199.6 (om, 2C), 90.7 (m)
--	---------------------------------	---------------------------------------	--	---

^a IR abbreviations: s = strong, m = medium, w = weak, sh = shoulder. ^b CH₂Cl₂ solutions unless otherwise stated, in units of cm⁻¹. ^c in THF. ^d NMR abbreviations: s = singlet, d = doublet, t = triplet, m = multiplet, dm = doublet of multiplets, om = overlapping multiplets, br = broad, dt = doublet of triplets, dpq = doublet of pseudo-quintets. ^e NMR data at 25 °C in CD₂Cl₂ unless otherwise stated. ^f ³¹P chemical shifts referenced to external 85% H₃PO₄. ^g Chemical shifts for the phenyl hydrogens are not given. ^h ¹H and ¹³C chemical shifts referenced to TMS. ⁱ ¹³C{¹H} NMR performed with ¹³CO enrichment. ^j in acetone-d₆. ^k in THF-d₈.

remaining solid was recrystallized from $\text{CH}_2\text{Cl}_2/\text{Et}_2\text{O}$ (83% yield). Anal. Calcd for $\text{C}_{54}\text{H}_{46}\text{F}_3\text{O}_6\text{P}_4\text{RhRuS}$: C, 53.70; H, 3.84. Found: C, 53.75; H, 3.81.

(b) $[\text{RhRu}(\text{CO})_4(\text{dppm})_2][\text{CF}_3\text{SO}_3]$ (2a). Compound **1a** (100 mg, 0.081 mmol) was dissolved in 10 mL of CH_2Cl_2 and stirred under a CO atmosphere for 16 h. The orange solution was concentrated to 5 mL, and ether was added slowly to precipitate a yellow solid, which was recrystallized from $\text{CH}_2\text{Cl}_2/\text{Et}_2\text{O}$, washed with 3×15 mL of ether, and dried in vacuo (93% yield). Anal. Calcd for $\text{C}_{55}\text{H}_{44}\text{F}_3\text{O}_7\text{P}_4\text{RhRuS}$: C, 53.54; H, 3.59. Found: C, 53.61; H, 3.59.

(c) $[\text{RhRu}(\text{CO})_4(\mu\text{-CH}_2)(\text{dppm})_2][\text{CF}_3\text{SO}_3] \cdot 0.33\text{CH}_2\text{Cl}_2$ (3a·0.33CH₂Cl₂). Compound **2a** (254 mg, 0.206 mmol) was dissolved in 15 mL of CH_2Cl_2 and cooled to -78 °C. Diazomethane, generated from 290 mg of Diazald (1.347 mmol), was passed through the solution vigorously for the duration of CH_2N_2 production. The orange solution was stirred under the diazomethane atmosphere for 1 h, after which the vessel was allowed to warm to room temperature under a stream of argon. The solvent was removed in vacuo, and the orange residue dissolved in 5 mL of CH_2Cl_2 and filtered through Celite (in air). Ether was added dropwise to precipitate orange microcrystals (89% yield). Anal. Calcd for $\text{C}_{56.3}\text{H}_{46.7}\text{Cl}_{0.7}\text{F}_3\text{O}_7\text{P}_4\text{RhRuS}$: C, 53.03; H, 3.69; Cl, 1.83. Found: C, 52.86; H, 3.69; Cl, 1.71. The fractional methylene chloride (1/3) of crystallization resulted from facile desolvation upon removal of crystals from the mother liquor. However, storage under high vacuum did not result in complete solvent loss. Elemental analysis and ^1H NMR spectroscopy confirmed the presence of CH_2Cl_2 .

(d) [RhRu(CO)₃(μ-CH₂)(dppm)₂][CF₃SO₃] (4a). A 50 mL portion of acetone was added to a mixture of compound **3a** (126 mg, 0.101 mmol) and Me₃NO (13 mg, 0.17 mmol), resulting in a rapid color change from orange to dark red. The solution was filtered through Celite, and the solvent was removed in vacuo. The residue was recrystallized from acetone/ether/*n*-pentane (1:3:3), washed with 3 × 15 mL of ether, and dried in vacuo (53% yield). The highly air-sensitive nature of **4a** has prevented dependable elemental analysis results.

(e) [RhRu(PMe₃)(CO)₃(μ-CH₂)(dppm)₂][CF₃SO₃] (5a). Method i. Compound **3a** (100 mg, 0.080 mmol) was suspended in 15 mL of THF, and PMe₃ (160 μL of a 1.0 M THF solution, 0.160 mmol) was added. The solution was stirred for 2 h, after which the solvent was removed in vacuo. The yellow residue was recrystallized from CH₂Cl₂/ether, washed with 3 × 15 mL of ether, and dried in vacuo (72% yield). Anal. Calcd for C₅₈H₅₅F₃O₆P₃RhRuS: C, 53.75; H, 4.28. Found: C, 53.60; H, 4.27.

Method ii. Compound **4a** (20 mg, 0.016 mmol) was dissolved in 0.7 mL of CD₂Cl₂ in an NMR tube. PMe₃ (20 μL of a 1.0 M THF solution, 0.020 mmol) was added, and the solution was mixed for 5 min, during which time the color changed from red to yellow. ¹H and ³¹P NMR spectroscopy revealed complete conversion to **5a**.

(f) Reaction of 3 with Excess CH₂N₂. Compound **3**, as either the CF₃SO₃⁻ or BF₄⁻ salt (100 mg, 0.080 mmol), was dissolved in 0.7 mL of CD₂Cl₂ in an NMR tube, and diazomethane, generated from 100 mg (0.464 mmol) of Diazald, was passed through the headspace of the tube. The solution was mixed for 20 min with no noticeable color change. ¹H and ³¹P NMR spectroscopy revealed only the presence of **3** and ethylene.

(g) Reaction of 4 with CO. Compound **4**, as either the CF_3SO_3^- or BF_4^- salt (20 mg, 0.016 mmol), was placed in an NMR tube, and 0.7 mL of CD_2Cl_2 was added. Addition of carbon monoxide caused the solution to turn from red to orange-yellow immediately. ^{31}P and ^1H NMR spectroscopy confirmed complete conversion to compound **3**.

(h) Reaction of 4 with Excess CH_2N_2 . Compound **4**, as either the CF_3SO_3^- or BF_4^- salt (100 mg, 0.080 mmol), was dissolved in 0.7 mL of CD_2Cl_2 in an NMR tube, and diazomethane, generated from 100 mg (0.46 mmol) of Diazald, was passed through the headspace of the tube. The solution was mixed for 20 min with no noticeable color change. ^1H and ^{31}P NMR spectroscopy revealed the formation of at least three new uncharacterized products.

X-ray Data Collection.⁷ Data for all compounds in this chapter were collected by Drs. Robert McDonald and Robert Lam in the departmental X-Ray Structure Determination Laboratory on a Bruker P4/RA/SMART 1000 CCD diffractometer⁸ using Mo $\text{K}\alpha$ radiation at -80°C . Yellow crystals of $[\text{RhRu}(\text{CO})_4(\text{dppm})_2][\text{BF}_4]$ (**2b**) were obtained from slow diffusion of Et_2O into a concentrated CH_2Cl_2 solution of the compound. Orange crystals of $[\text{RhRu}(\text{CO})_4(\mu\text{-CH}_2)(\text{dppm})_2][\text{BF}_4]$ (**3b**) were obtained by slow diffusion of Et_2O into a concentrated CH_2Cl_2 solution of the compound. Although the triflate salt (**3a**) contained CH_2Cl_2 of crystallization, no solvent is present in crystals of the BF_4^- salt. Yellow crystals of $[\text{RhRu}(\text{PMe}_3)(\text{CO})_3(\mu\text{-CH}_2)(\text{dppm})_2][\text{BF}_4]$ (**5b**) were obtained from slow diffusion of Et_2O into a concentrated CH_2Cl_2 solution of the compound. Unit cell parameters for the compounds were obtained from a least-squares refinement of the setting angles of 4710 reflections for **2b**, 4386 reflections for compound

3b, and 6861 reflections for compound **5b** from the data collection. Space groups for **2b** and **5b** were determined to be $P2_1/c$, and that of **3b** was found to be $I2/a$ (a nonstandard setting of $C2/c$). The data for all compounds were corrected for absorption by use of the SADABS procedure.

Structure Solution and Refinement. All structures were solved by Drs. Robert McDonald and Robert Lam using direct methods (SHELXS-86),⁹ and refinement was completed using the program SHELXL-93.¹⁰ Hydrogen atoms were assigned positions on the basis of the geometries of their attached carbon atoms and were given thermal parameters 20% larger than those of attached carbons. Compound **2b** is disordered about the inversion center at (0, 0, 0), such that the metal sites are each composed of 1/2 occupancy of each metal (Rh/Ru). The only other atoms affected by the disorder are C(2) and C(3), which each appear at 1/2 occupancy at inversion-related sites. The BF_4^- ion was also disordered about the inversion center at (0, 1/2, 0). Despite the disorder, all atom positions were resolved and least-squares refinement proceeded well.

In compound **5b** both metals have similar coordination environments, so the identification of Rh or Ru is not obvious. However, interchanging the scattering factors for the two metals resulted in an obvious enlargement of the thermal parameters for the incorrectly labeled Rh atom and a contraction of those for Ru, indicating that too few electrons were at the former site and too many at the latter. At the same time, the residuals upon convergence for this model are marginally worse ($R_1 = 0.0521$, $wR_2 = 0.1300$) than for the correct model ($R_1 = 0.0506$, $wR_2 = 0.1200$). Both effects indicate that the original model, having the labeling reported, is correct. This model also agrees with

the spectroscopic data (vide infra). Crystallographic data for compounds **2b**, **3b**, and **5b** are given in Table 2.2.

Results and Compound Characterization:

The methylene-bridged complex $[\text{RhRu}(\text{CO})_4(\mu\text{-CH}_2)(\text{dppm})_2][\text{X}]$ (**3**) has been prepared from $[\text{RhRu}(\text{CO})_3(\mu\text{-H})(\text{dppm})_2]^6$ by the series of reactions shown in Scheme 2.1. Protonation of this monohydride, using either triflic acid or tetrafluoroboric acid yields $[\text{RhRu}(\text{CO})_3(\mu\text{-H})_2(\text{dppm})_2][\text{X}]$ ($\text{X} = \text{SO}_3\text{CF}_3$ (**1a**), BF_4 (**1b**)), as the respective

Scheme 2.1

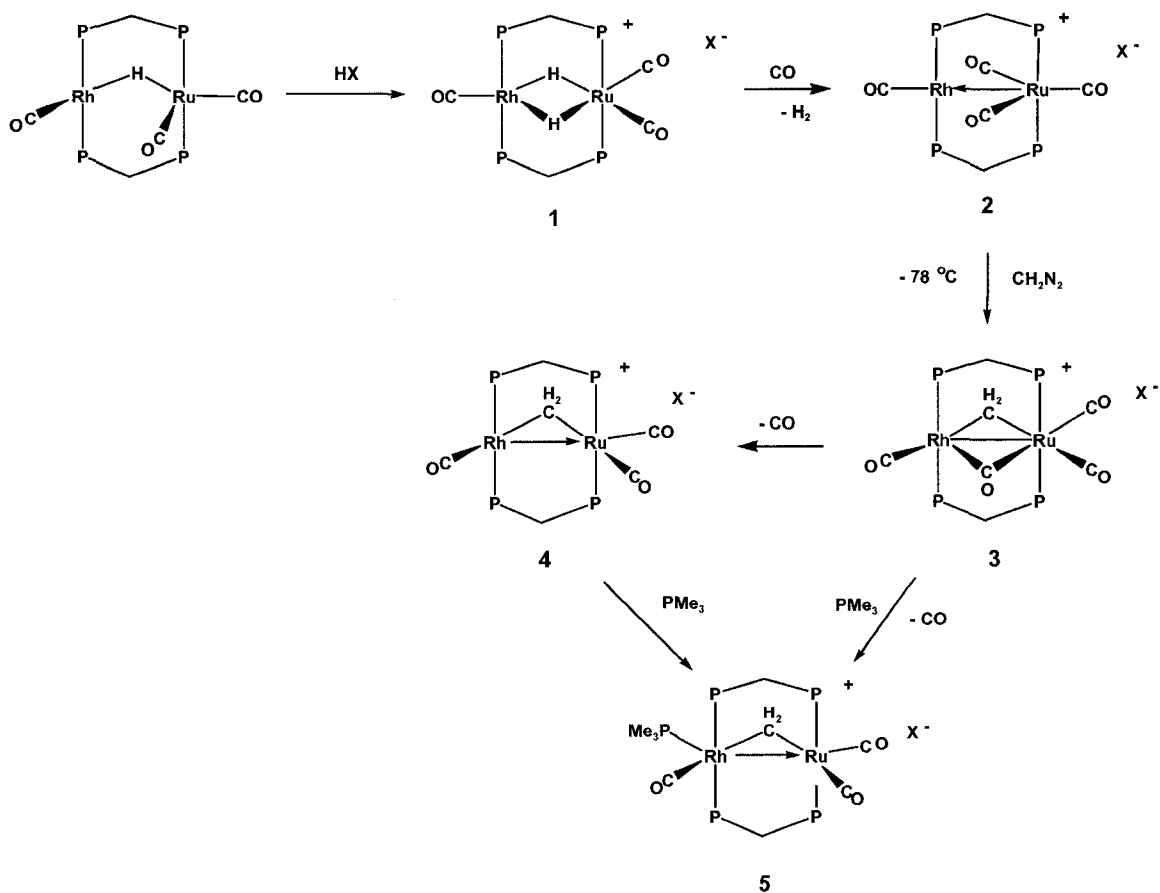


Table 2.2. Crystallographic Data for Compounds 2b, 3b and 5b.

	[RhRu(CO) ₄ (dppm) ₂][BF ₄] (2b)	[RhRu(CO) ₄ (μ-CH ₂)-(dppm) ₂][BF ₄] (3b)	[RhRu(PMe ₃)(CO) ₃ (μ-CH ₂)-(dppm) ₂][BF ₄]·2CH ₂ Cl ₂ (5b)
formula	C ₅₄ H ₄₄ BF ₄ O ₄ P ₄ RhRu	C ₅₅ H ₄₆ BF ₄ O ₄ P ₄ RhRu	C ₅₉ H ₅₉ BCl ₄ F ₄ O ₃ P ₅ RhRu
fw	1171.56	1185.59	1403.50
cryst dimens, mm	0.39 × 0.24 × 0.12	0.63 × 0.13 × 0.08	0.38 × 0.16 × 0.07
cryst. system	monoclinic	monoclinic	monoclinic
space group	<i>P</i> 2 ₁ / <i>c</i> (No. 14)	<i>I</i> 2/ <i>a</i> (No. 15)	<i>P</i> 2 ₁ / <i>c</i> (No. 14)
<i>a</i> , Å	11.5763(6) ^a	42.754(5) ^b	20.3808(13) ^c
<i>b</i> , Å	12.7597(7)	10.240(1)	12.7481(9)
<i>c</i> , Å	17.401(1)	23.590(3)	23.240(1)
<i>β</i> , deg	101.66 (1)	90.455(2)	91.495 (1)
<i>V</i> , Å ³	2516.8(2)	10327(2)	6036.0(7)
<i>Z</i>	2	8	4
<i>d</i> _{calcd} , g cm ⁻³⁴	1.546	1.525	1.544
<i>μ</i> , mm ⁻¹	0.815	0.796	0.889
diffractometer	Bruker P4/RA/SMART 1000 CCD ^d	Bruker P4/RA/SMART 1000 CCD ^d	Bruker P4/RA/SMART 1000 CCD ^d

Table 2.2 (cont'd.)

radiation (λ , Å)	graphite-monochromated Mo K α (0.710 73)	graphite-monochromated Mo K α (0.710 73)	graphite-monochromated Mo K α (0.710 73)
T , °C	-80	-80	-80
scan type	ϕ rotations (0.3°)/ ω scans (0.3°) (30 s exposures)	ϕ rotations (0.3°)/ ω scans (0.3°) (30 s exposures)	ϕ rotations (0.3°)/ ω scans (0.3°) (30 s exposures)
2θ (max), deg	52.76	52.82	52.82
no. of unique reflections	5141	10 526	12 333
no of observns	4489	8180	7751
no. of variables	340	626	703
range of abs corr factors	0.909-0.742	0.939-0.634	0.956-0.730
residual density, e/Å ³	0.59 to -0.36	1.48 to -0.70	1.21 to -1.10
$R_1(F_o^2 > 2s(F_o^2))^e$	0.0255	0.0415	0.0506
wR_2 (all data)	0.0690	0.1051	0.1200
GOF (s) ^f	1.028	1.010	0.951

^a Cell parameters obtained from least-squares refinement of 4710 centered reflections. ^b Cell parameters obtained from least-squares refinement of 4386 centered reflections. ^c Cell parameters obtained from least-squares refinement of 6861 centered reflections. ^d Programs for diffractometer operation, data reduction, and absorption were those supplied by Bruker. ^e $R_1 = \Sigma ||F_o| - |F_c|| / \Sigma |F_o|$; $wR_2 = [\Sigma \omega(F_o^2 - F_c^2)^2 / \Sigma \omega(F_o^4)]^{1/2}$. ^f $S = [\Sigma \omega(F_o^2 - F_c^2)^2 / (n - p)]^{1/2}$ (n = number of data, p = number of parameters varied; $w = [\sigma^2(F_o^2) + (a_0P)^2 + a_1P]^{-1}$, where $P = [\max(F_o^2, 0) = 2F_c^2]/3$. For **2b** $a_0 = 0.0368$ and $a_1 = 1.1895$; for **3b** $a_0 = 0.0587$ and $a_1 = 5.1691$; for **5b** $a_0 = 0.0527$ and $a_1 = 0.00$.

triflate or tetrafluoroborate salts (in subsequent discussions a compound number without **a** or **b** designation refers to the generic compound having either CF_3SO_3^- or BF_4^- anions). Both hydride ligands in **1** are chemically equivalent and appear as a multiplet at δ -9.55 in the ^1H NMR spectrum due to coupling to four phosphorus and one ^{103}Rh nuclei. The $^{31}\text{P}\{^1\text{H}\}$ NMR spectrum of **1** is characteristic of an AA'BB'X spin system found in these types of dppm-bridged heterobinuclear systems with the Rh-bound end of the diphosphine (δ 26.2) being slightly upfield from the Ru-bound end (δ 34.4). In the $^{13}\text{C}\{^1\text{H}\}$ NMR spectrum two carbonyl resonances are observed in a 2:1 intensity ratio. The more intense signal at δ 197.0 corresponds to the pair of chemically equivalent, Ru-bound carbonyls, while the other, at δ 182.6, displays 75 Hz coupling to Rh and corresponds to the terminal carbonyl on this metal.

Reaction of **1** with carbon monoxide results in elimination of H_2 and accompanying coordination of CO affording the cationic tetracarbonyl, $[\text{RhRu}(\text{CO})_4(\text{dppm})_2][\text{X}]$ (**2**), which displays three carbonyl resonances in the $^{13}\text{C}\{^1\text{H}\}$ NMR spectrum in a 1:1:2 intensity ratio at 25°C. The high-field resonance (δ 179.5), showing coupling of 75 Hz to Rh, is identified as that terminally bound to this metal, the intermediate signal at δ 195.9 is a triplet, displaying coupling to the pair of Ru-bound ^{31}P nuclei while the low-field resonance (also a triplet), integrating as two carbonyls, corresponds to the two Ru-bound CO ligands that are bent toward Rh. The slight downfield shift of these carbonyls is presumed to result from the interaction with the adjacent Rh, as has previously been observed.¹¹ However, it is clear that any interaction

of these carbonyls with Rh must be weak since no coupling to this nucleus is observed in the $^{13}\text{C}\{^1\text{H}\}$ NMR spectrum, and the IR spectrum of **2** shows only terminal carbonyls.

The solid-state structure of **2** confirms what is proposed based on spectroscopic data and this structure is shown for the cation in Figure 2.1, with relevant bond lengths and angles in Table 2.3. About Rh, the geometry is square planar in which Ru occupies one of the coordination sites. If the metal-metal bond is ignored, the geometry at Ru is best described as trigonal bipyramidal, in which the C(2)-Ru-C(3) angle, which is bisected by the metal-metal bond, has opened up to $131.7(2)^\circ$ with a corresponding decrease in the other carbonyl angles to $113.6(1)^\circ$ and $114.7(2)^\circ$. The Rh-Ru distance ($2.7870(3)$ Å) is normal for a single bond showing substantial contraction of the metal-metal separation compared to the intra-ligand P-P separation ($3.0176(6)$ Å). The X-ray structure also shows that C(2)O(2) and C(3)O(2'), although aimed towards Rh, remain terminally bound to Ru. The long Rh-C(2) and Rh-C(3) distances ($2.665(4)$ and $2.678(4)$ Å) confirm that any interaction between Rh and these carbonyls must be extremely weak.

Reaction of **2** with diazomethane at -78°C generates the methylene-bridged product $[\text{RhRu}(\text{CO})_4(\mu\text{-CH}_2)(\text{dppm})_2][\text{X}]$ (**3**) quantitatively, as shown in Scheme 2.2. The ^1H NMR spectrum reveals the resonance for the $\mu\text{-CH}_2$ group as a pseudo-quintet at δ 2.43 with essentially equal coupling to all four ^{31}P nuclei. No coupling of the methylene protons to Rh is obvious. This signal can be differentiated from the dppm methylene protons (at δ 3.74 and 2.80) by using broad-band ^{31}P decoupling, resulting in a collapse of the metal-bound methylene signal to a singlet while the dppm-methylene

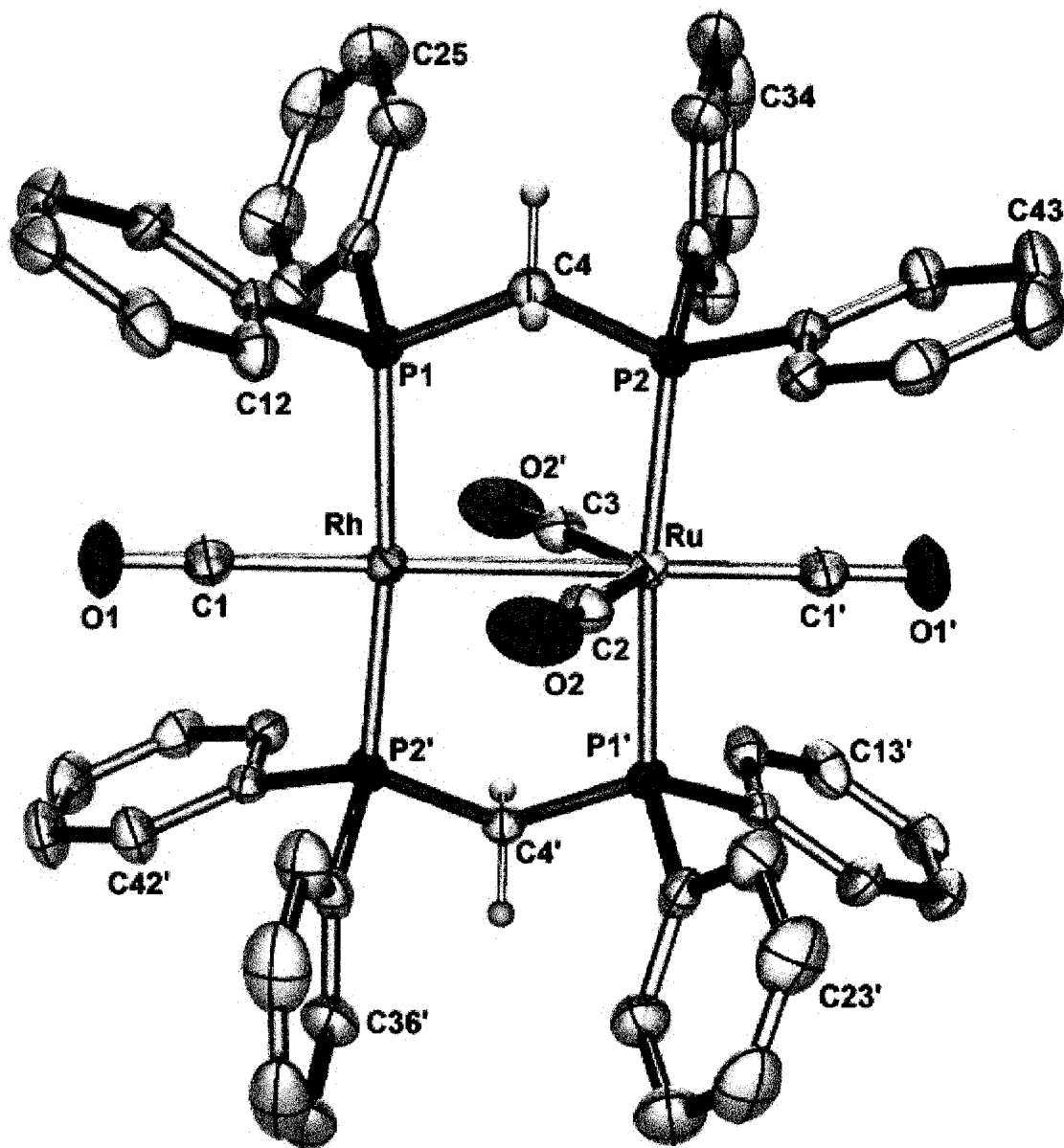


Figure 2.1: Perspective view of the $[\text{RhRu}(\text{CO})_4(\text{dppm})_2]^+$ complex cation of **2b** showing the atom-labeling scheme. Non-hydrogen atoms are represented by Gaussian ellipsoids at the 20% probability level. The methylene hydrogen atoms are shown with arbitrarily small thermal parameters, while the dppm phenyl hydrogens are not shown. Primed atoms are related to unprimed ones by inversion symmetry. Only one of the disordered structures is shown. For an explanation of the disorder see the Experimental Section.

Table 2.3: Selected Distances and Angles for Compound **2b**.*(i) Distances (Å)*

Atom 1	Atom 2	Distance	Atom 1	Atom 2	Distance
Rh	Ru	2.7870(3)	Ru	C(3)	1.950(4)
Rh	P(1)	2.3368(5)	P(1)	P(2)	3.0176(6) [†]
Rh	P(2') ^a	2.3346(5)	P(1)	C(4)	1.834(2)
Rh	C(1)	1.885(2)	P(2)	C(4)	1.834(2)
Rh	C(2)	2.665(4) [†]	O(1)	C(1)	1.126(3)
Rh	C(3)	2.678(4) [†]	O(2)	C(2)	1.218(4)
Ru	C(2)	1.969(4)	O(2')	C(3)	1.224(4)

[†] Non-bonded distance.

(ii) Angles (deg)

Atom1	Atom2	Atom3	Angle	Atom1	Atom2	Atom3	Angle
Ru	Rh	P(1)	92.41(1)	P(2)	Ru	C(3)	88.3(1)
Ru	Rh	P(2')	93.20(1)	C(1')	Ru	C(2)	113.6(1)
Ru	Rh	C(1)	179.13(8)	C(1')	Ru	C(3)	114.7(2)
P(1)	Rh	P(2')	173.78(2)	C(2)	Ru	C(3)	131.7(2)
P(1)	Rh	C(1)	87.47(7)	Rh	P(1)	C(4)	113.17(6)
P(2')	Rh	C(1)	86.96(7)	Ru	P(2)	C(4)	113.56(6)
Rh	Ru	C(2)	65.6(1)	Rh	C(1)	O(1)	179.7(3)
Rh	Ru	C(3)	66.1(1)	Ru	C(2)	O(2)	175.3(3)
P(1')	Ru	C(2)	89.7(1)	Ru	C(3)	O(2')	174.8(3)
P(1')	Ru	C(3)	91.5(1)	P(1)	C(4)	P(2)	110.7(1)
P(2)	Ru	C(2)	95.1(1)				

^a Primed atoms related to unprimed ones by the crystallographic inversion center at (0, 0, 0).

signals collapse to the expected AB quartet. It is important to point out that selective ^{31}P decoupling, in which only one of the two ^{31}P resonances is decoupled, is not possible in some of these compounds, due to the close proximity of the two resonances. In compound **3** the two sets of resonances are superimposed, as shown in Figure 2.2.

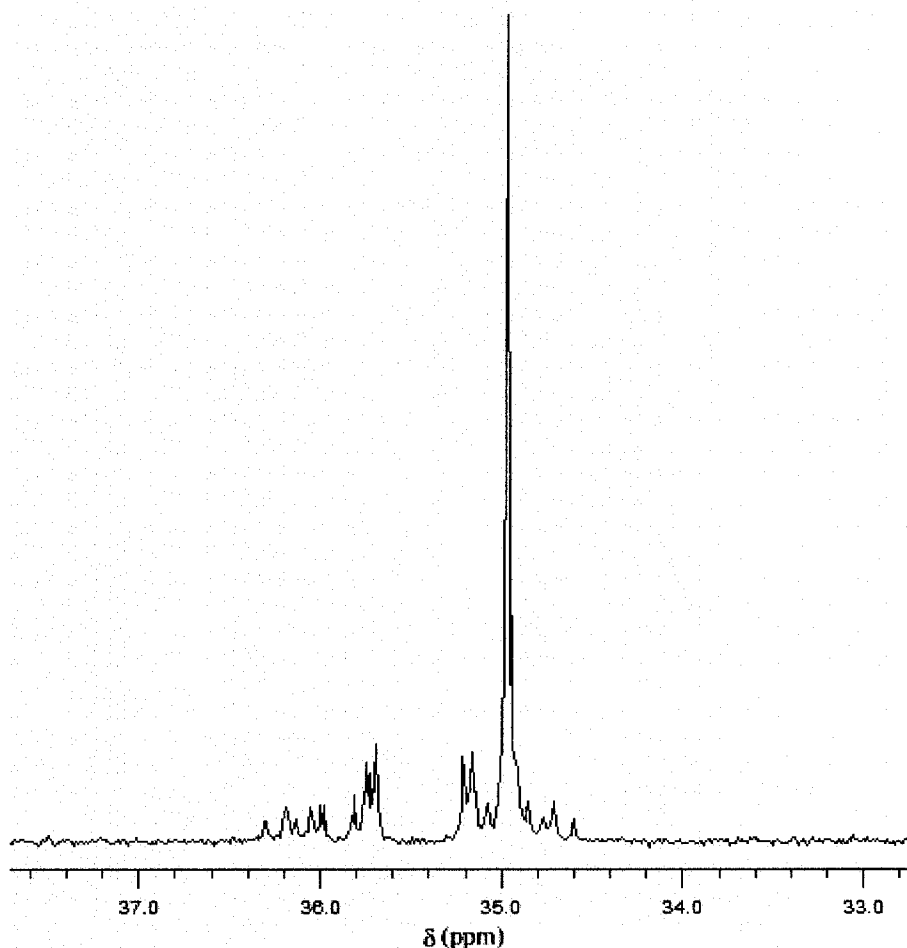


Figure 2.2: The $^{31}\text{P}\{^1\text{H}\}$ NMR spectrum of compound **3**.

The $^{13}\text{C}\{^1\text{H}\}$ NMR spectrum of a ^{13}CO -enriched sample of **3** shows the expected four resonances, with the lowest-field signal (δ 227.4) being attributed to the bridging CO ligand. Broad-band ^{31}P -decoupling experiments show that this carbonyl also displays a 25 Hz coupling to Rh, consistent with a strong semibridging interaction. The signal at δ

195.4 appears as a doublet of triplets with coupling to the Rh nucleus of 66 Hz, clearly indicating that it is Rh-bound. The remaining two carbonyl signals are due to the pair that are terminally bound to Ru. The ^{13}C resonance for the bridging methylene group ($^{13}\text{CH}_2$ -enriched sample) appears as a doublet of pseudo quintets at δ 48.3, displaying 16 Hz coupling to Rh and 5 Hz coupling to all phosphorus nuclei. The IR spectrum helps confirm the carbonyl bonding assignment, showing three terminal CO bands (2043, 2001 and 1963 cm^{-1}) and one for the semibridging CO (1802 cm^{-1}).

The structure of **3b** was confirmed by an X-ray structure determination and the complex cation is shown in Figure 2.3 with important bond lengths and angles given in Table 2.4. This compound has a doubly-bridged “A-frame” structure, in which the metals are bridged by the methylene group and a carbonyl on opposite faces of the “RhRuP₄” plane. The Rh-Ru separation ($2.9114(5)\text{ \AA}$) is longer than a normal single bond involving these metals and can be compared to that observed in **2b**, which is in the normal range of such bonds. However, this metal-metal separation is still significantly less than the intraligand P-P separations ($3.205(1)$ and $3.004(1)\text{ \AA}$), indicating a mutual attraction of the metals. In the absence of a metal-metal bond, we expect the Rh-Ru separation to be close to the intraligand P-P distance. If the Rh-Ru bond is ignored, the geometry about Ru can be viewed as octahedral while Rh has a tetragonal pyramidal geometry in which the apical site is occupied by the bridging carbonyl. This carbonyl can be considered as semi-bridging, although the asymmetry in the angles about the carbonyl carbon ($\text{Rh-C(2)-O(2)} = 130.4(3)^\circ$, $\text{Ru-C(2)-O(2)} = 141.1(3)^\circ$) is not as great as usually observed.¹² Surprisingly, the asymmetry in metal-carbonyl bond lengths is the

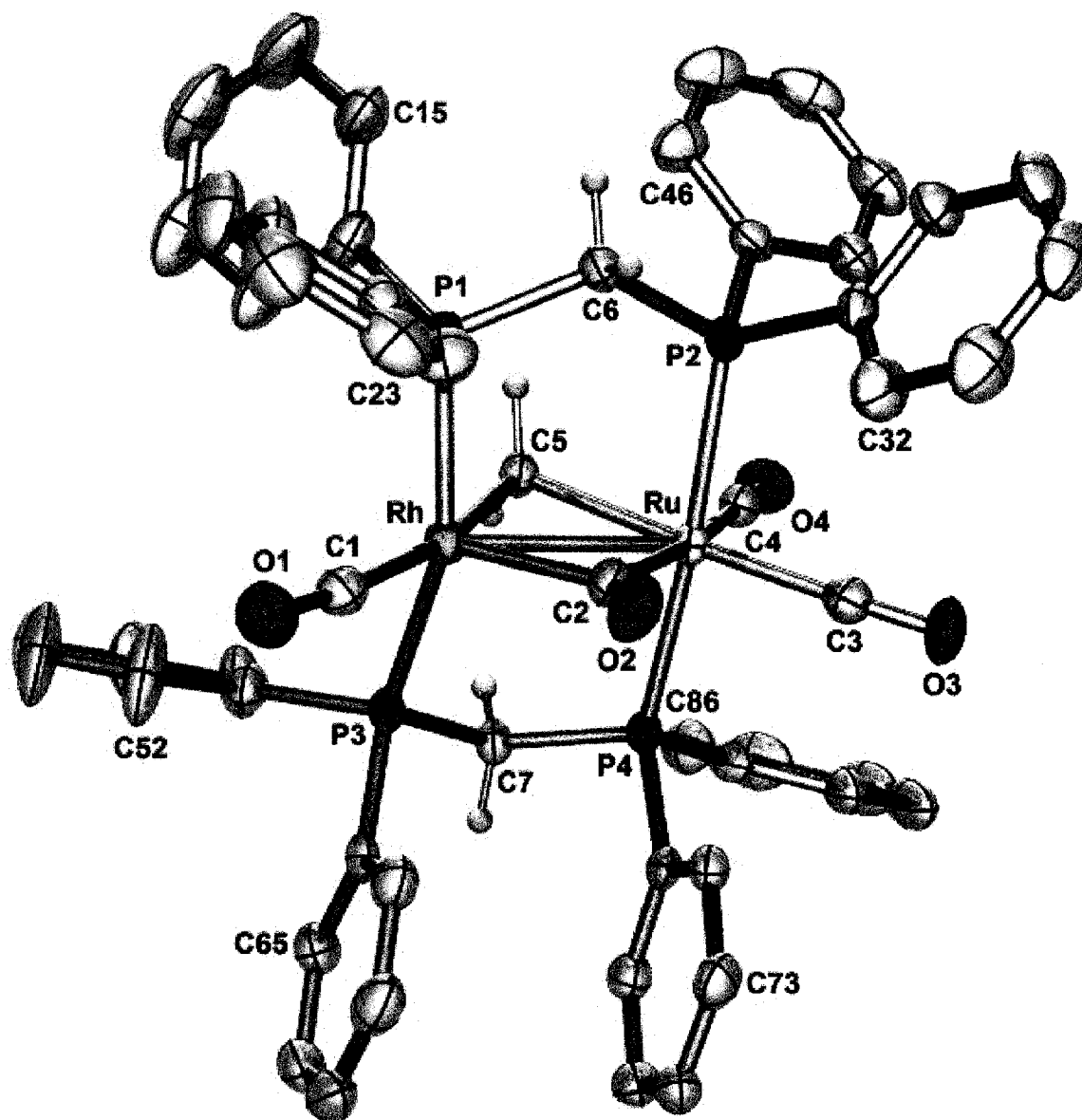


Figure 2.3: Perspective view of the $[\text{RhRu}(\text{CO})_4(\mu\text{-CH}_2)(\text{dppm})_2]^+$ cation of **3b** showing the atom-labeling scheme. Thermal parameters are as described for Figure 2.1.

Table 2.4: Selected Distances and Angles for Compound **3b**.*(i) Distances (Å)*

Atom 1	Atom 2	Distance	Atom 1	Atom 2	Distance
Rh	Ru	2.9114(5)	Ru	C(5)	2.213(3)
Rh	P(1)	2.305(1)	P(1)	P(2)	3.205(1) ^a
Rh	P(3)	2.351(1)	P(1)	C(6)	1.840(3)
Rh	C(1)	1.900(4)	P(2)	C(6)	1.853(4)
Rh	C(2)	2.021(3)	P(3)	P(4)	3.004(1) ^a
Rh	C(5)	2.089(3)	P(3)	C(7)	1.835(3)
Ru	P(2)	2.382(1)	P(4)	C(7)	1.835(3)
Ru	P(4)	2.382(1)	O(1)	C(1)	1.137(4)
Ru	C(2)	2.155(4)	O(2)	C(2)	1.164(4)
Ru	C(3)	1.927(4)	O(3)	C(3)	1.139(4)
Ru	C(4)	1.913(4)	O(4)	C(4)	1.136(4)

† Non-bonded distance.

(ii) Angles (deg)

Atom 1	Atom 2	Atom 3	Angle	Atom 1	Atom 2	Atom 3	Angle
Ru	Rh	P(1)	96.24(2)	C(1)	Rh	C(5)	167.9(1)
Ru	Rh	P(3)	94.68(2)	C(2)	Rh	C(5)	96.1(1)
Ru	Rh	C(1)	142.8(1)	Rh	Ru	P(2)	90.82(2)
Ru	Rh	C(2)	47.7(1)	Rh	Ru	P(4)	86.78(2)
Ru	Rh	C(5)	49.24(9)	Rh	Ru	C(2)	43.94(9)
P(1)	Rh	P(3)	156.12(3)	Rh	Ru	C(3)	135.6(1)
P(1)	Rh	C(1)	92.6(1)	Rh	Ru	C(4)	128.8(1)
P(1)	Rh	C(2)	95.3(1)	Rh	Ru	C(5)	45.65(9)
P(1)	Rh	C(5)	83.3(1)	P(2)	Ru	P(4)	174.72(3)
P(3)	Rh	C(1)	91.5(1)	P(2)	Ru	C(2)	87.8(1)
P(3)	Rh	C(2)	107.8(1)	P(2)	Ru	C(3)	93.6(1)
P(3)	Rh	C(5)	87.9(1)	P(2)	Ru	C(4)	91.6(1)
C(1)	Rh	C(2)	95.6(2)	Rh	Ru	C(2)	88.3(1)
				Rh	C(2)	O(2)	130.4(3)
				Ru	C(2)	O(2)	141.1(3)
				Rh	C(5)	Ru	85.1(1)

opposite of what one might expect with the Ru-C(2) distance (2.155(4)Å) being *longer* than Rh-C(2) (2.021(3) Å). Usually in semi-bridging carbonyls the shorter distance is associated with the metal that forms the more linear carbonyl arrangement (Ru in this case). The bridging methylene group is also unsymmetrically bridged, again being more tightly bound to Rh (Rh-C(5) = 2.089(3) Å, Ru-C(5) = 2.213(3) Å). It should be noted, however, that in **3b** all metal-ligand bonds are shorter for Rh than for Ru. This may be a consequence of the differences in coordination geometry, with greater repulsions giving rise to longer bonds at the more crowded Ru center. In addition, the carbonyls bound to Ru may also be elongated due to the trans influence of the bridging carbonyl and methylene groups.

A comparison with two other closely related compounds, [RhOs(CO)₄(μ-CH₂)(dppm)₂][BF₄]¹³ and [IrRu(CO)₄(μ-CH₂)(dppm)₂][BF₄]⁵ is of interest. The Rh/Ru and Rh/Os compounds have almost identical geometries with only minor variations in bond lengths and angles, so will not be discussed further at this point. However the Ir/Ru analogue has more substantial differences, although these differences are still not large. The major difference results from the bonding of the bridging carbonyl, which for the Ir/Ru compound is essentially symmetrically bridged. As a result, the Ir-C(2) and Ru-C(2) distances in the Ir/Ru analogue are comparable at 2.033(8) and 2.072(8) Å, respectively, in contrast to the more asymmetric Rh-C(2) and Ru-C(2) distances (2.021(3), 2.155(4) Å) in **3b**. In addition, the angles at the bridging carbonyl group in the Ir/Ru analogue (Ir-C(2)-O(2) = 134.4(7)°, Ru-C(2)-O(2) = 137.1(7)°) are also indicative of a more symmetrically bridging carbonyl. Accompanying the slight change in carbonyl bonding from **3b** to the Ir/Ru analogue is a corresponding shortening of the metal-metal

bond (to 2.8650(7) Å in the Ir/Ru species) and a corresponding bending back of the terminally bound iridium carbonyl ($C(5)-Ir-C(1) = 161.7(5)^\circ$) compared to the angle of $167.9(1)^\circ$ in **3b**. We will attempt to address the possible significance of these differences later.

Addition of excess diazomethane to compound **3** does not afford any new organometallic products, although ethylene is observed in both the 1H and $^{13}C\{^1H\}$ NMR spectra. Surprisingly, when $^{13}CH_2N_2$ is used in the reaction with **3**, no ^{13}C incorporation into the methylene bridge of **3** is observed. The only product of ^{13}C incorporation is $^{13}C_2H_4$. After extended exposure of **3** to CH_2N_2 , unreacted **3** is the only complex observed.

Reaction of **3** with trimethylamine-N-oxide results in carbonyl loss to yield the tricarbonyl product $[RhRu(CO)_3(\mu-CH_2)(dppm)_2][X]$ (**4**). The 1H NMR spectrum of **4** shows the metal-bound methylene unit at δ 5.38. As was the case for **3**, broad-band ^{31}P decoupling clearly allows us to distinguish the bridging $\mu-CH_2$ from the dppm methylenes (δ 4.24 and 3.58). The $^{13}C\{^1H\}$ NMR spectrum of a ^{13}CO -enriched sample of **4** shows the expected three carbonyl resonances, with the high-field signal appearing as a doublet of triplets ($^1J_{RhC} = 68$ Hz), confirming that this carbonyl is terminally bound to Rh, and the remaining two signals appear as triplets, corresponding to the two carbonyls that are bound to Ru. In a $^{13}CH_2$ -enriched sample of **4** the methylene carbon appears as a multiplet at δ 97.0 in the ^{13}C NMR spectrum. The IR spectrum of **4** shows three terminal CO stretches (ν_{CO} : 1931, 1966 and 1992 cm^{-1}). As expected, reaction of **4** with carbon monoxide regenerates **3**. Loss of a carbonyl from **3** necessitates a subtle change in the nature of the Rh-Ru bonding; in **4** we propose that the coordinative unsaturation that

results from CO loss is alleviated by formation of a dative Rh→Ru bond from the filled d_z^2 orbital on the square-planar Rh(+1) center.

Whereas the methylene-bridged compound **3** is not transformed into other species in the presence of additional diazomethane at ambient temperature, the tricarbonyl **4** reacts rapidly at temperatures as low as -78 °C. Unfortunately, even at -78 °C, the reaction of **4** with CH_2N_2 yields a mixture of at least 3 products which have not yet been identified.

Compounds **3** and **4** both react with PMe_3 , affording the phosphine adduct, $[\text{RhRu}(\text{PMe}_3)(\text{CO})_3(\mu\text{-CH}_2)(\text{dppm})_2][\text{X}]$ (**5**). The $^{31}\text{P}\{^1\text{H}\}$ NMR spectrum of **5** shows low-field multiplets for the Rh- and Ru-bound ends of the diphosphine ligands (δ 23.5 and 26.8, respectively) and a high-field doublet of multiplets at δ -34.4 , corresponding to the PMe_3 group. The large rhodium coupling ($^1J_{\text{RhP}} = 120$ Hz) for the PMe_3 group clearly identifies that this ligand is bound to Rh. In the related Ir/Ru complex, $[\text{IrRu}(\text{PMe}_3)(\text{CO})_3(\mu\text{-CH}_2)(\text{dppm})_2][\text{BF}_4]$, the PMe_3 group is again bound to the group 9 metal.⁵ As was observed in the Ir/Ru compound, the ^{31}P nucleus of PMe_3 in **5** shows coupling to both ends of the diphosphine ligands (in this case, the Rh- and Ru-bound ends). Unfortunately, the proximity of the two signals is not conducive to selective decoupling experiments, so the magnitude of the coupling to the two sets of dppm ^{31}P nuclei could not be determined. In related compounds, the PMe_3 group on one metal can display comparable or *greater* coupling to the ^{31}P nuclei on the *adjacent* metal than to those on the same metal.^{5,14} The $^1\text{H}\{^{31}\text{P}\}$ NMR spectrum of **5** confirms that the signal at δ 3.60 is due to the bridging methylene group. A ^{13}C NMR spectrum of a ^{13}CO -enriched sample of **5** shows only two carbonyl resonances in a 1:2 ratio. The high-field signal is

actually comprised of two overlapping multiplets (corresponding to the Rh-bound and one Ru-bound carbonyls) from which coupling information could not be extracted. The ^{13}C resonance for the bridging methylene group appears at δ 90.7, but coupling information again could not be extracted due to poor signal-to-noise ratio in the spectrum derived from an unenriched sample.

The X-ray structure of the cationic complex of **5b** is shown in Figure 2.4 with relevant bond lengths and angles given in Table 2.5. As indicated in the $^{31}\text{P}\{^1\text{H}\}$ NMR investigation, and confirmed in this X-ray study, the PMe_3 group is bound to Rh giving rise to an almost symmetrical ligand arrangement in which both metals have, in addition to the bridging groups, two terminally bound 2-electron-donor ligands; Rh is bound to the PMe_3 group and one carbonyl while Ru has two carbonyls. As in compound **3b**, the Rh-Ru separation in **5b** (2.8952(6) Å) is longer than a normal single bond (*cf.* compound **2b**: Rh-Ru = 2.7870(3) Å) but is again less than the intraligand P-P separation (3.002(2), 2.954(2) Å) suggesting attraction of the metals. In addition, a metal-metal bond (in some form) is needed to satisfy the valence electron counts of the metals. Two bonding extremes can be considered. If the positive charge of the complex is localized on Ru the metals have Rh(+1) and Ru(+2) oxidation states ($\mu\text{-CH}_2$ viewed as a dianionic ligand) and a dative Rh \rightarrow Ru bond is required to give Ru its preferred 18e configuration. However, if the positive charge is localized on Rh, the oxidation states are Rh(+2) and Ru(+1) with a conventional metal-metal bond as shown in Chart 2.1. We prefer the former formulation, in line with the common oxidation states of these metals.

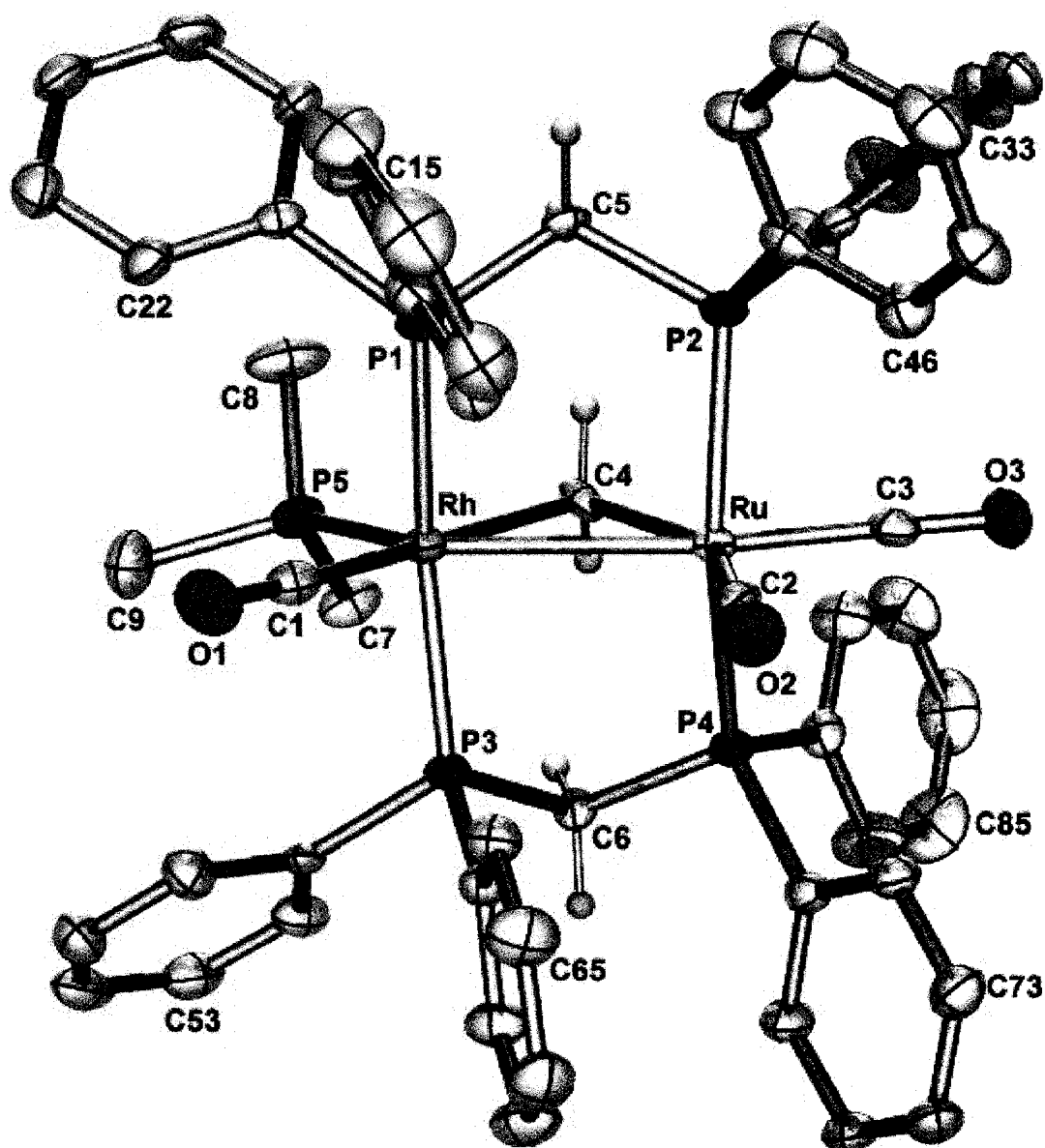


Figure 2.4: Perspective view of the $[\text{RhRu}(\text{PMe}_3)(\text{CO})_3(\mu\text{-CH}_2)(\text{dppm})_2]^+$ cation of **5b** showing the atom-labeling scheme. Thermal parameters are as described for Figure 2.1.

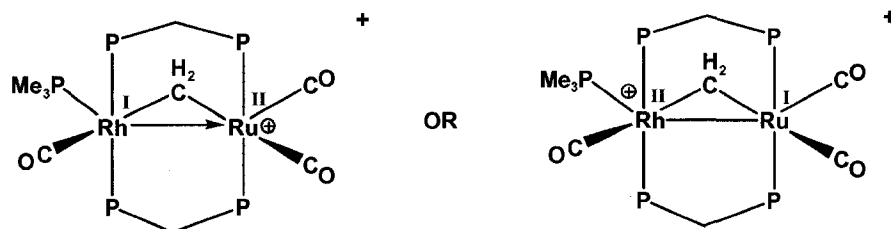
Table 2.5: Selected Distances and Angles for Compound **5b**.*(i) Distances (Å)*

Atom 1	Atom 2	Distance	Atom 1	Atom 2	Distance
Rh	Ru	2.8952(6)	P(1)	C(5)	1.833(5)
Rh	P(1)	2.340(1)	P(2)	C(5)	1.822(5)
Rh	P(3)	2.322(1)	P(3)	P(4)	2.954(2) [†]
Rh	P(5)	2.400(1)	P(3)	C(6)	1.830(4)
Rh	C(1)	1.900(5)	P(4)	C(6)	1.836(5)
Rh	C(4)	2.148(4)	P(5)	C(7)	1.826(5)
Ru	P(2)	2.352(1)	P(5)	C(8)	1.822(5)
Ru	P(4)	2.370(1)	P(5)	C(9)	1.809(6)
Ru	C(2)	1.934(5)	O(1)	C(1)	1.136(6)
Ru	C(3)	1.860(5)	O(2)	C(2)	1.130(5)
Ru	C(4)	2.117(5)	O(3)	C(3)	1.164(6)
P(1)	P(2)	3.002(2) [†]			

[†] Non-bonded distance.*(ii) Angles (deg)*

Atom 1	Atom 2	Atom 3	Angle	Atom 1	Atom 2	Atom 3	Angle
Ru	Rh	P(1)	88.90(4)	P(2)	Ru	C(4)	86.8(1)
Ru	Rh	P(3)	85.04(4)	P(4)	Ru	C(2)	100.5(2)
Ru	Rh	P(5)	129.91(4)	P(4)	Ru	C(3)	84.7(2)
Ru	Rh	C(1)	125.8(2)	P(4)	Ru	C(4)	84.3(1)
Ru	Rh	C(4)	46.8(1)	C(2)	Ru	C(3)	95.6(2)
P(1)	Rh	P(3)	165.55(5)	C(2)	Ru	C(4)	147.3(2)
P(1)	Rh	P(5)	99.17(5)	C(3)	Ru	C(4)	117.1(2)
P(1)	Rh	C(1)	85.2(2)	Rh	P(1)	C(5)	114.3(2)
P(1)	Rh	C(4)	91.6(1)	Ru	P(2)	C(5)	114.4(2)
P(3)	Rh	P(5)	94.77(5)	Rh	P(3)	C(6)	113.1(2)
P(3)	Rh	C(1)	87.7(2)	Ru	P(4)	C(6)	113.1(2)
P(3)	Rh	C(4)	93.8(1)	Rh	P(5)	C(7)	116.9(2)
P(5)	Rh	C(1)	104.2(2)	Rh	P(5)	C(8)	119.1(2)
P(5)	Rh	C(4)	83.4(1)	Rh	P(5)	C(9)	115.8(2)
C(1)	Rh	C(4)	172.2(2)	C(7)	P(5)	C(8)	98.4(3)
Rh	Ru	P(2)	92.99(4)	C(7)	P(5)	C(9)	101.5(3)
Rh	Ru	P(4)	93.28(4)	C(8)	P(5)	C(9)	102.0(3)
Rh	Ru	C(2)	99.6(2)	Rh	C(1)	O(1)	177.2(5)
Rh	Ru	C(3)	164.8(2)	Ru	C(2)	O(2)	178.1(5)
Rh	Ru	C(4)	47.7(1)	Ru	C(3)	O(3)	178.5(5)
P(2)	Ru	P(4)	161.04(4)	Rh	C(4)	Ru	85.5(2)
P(2)	Ru	C(2)	96.1(2)	P(1)	C(5)	P(2)	110.5(2)
P(2)	Ru	C(3)	84.5(2)	P(3)	C(6)	P(4)	107.3(2)

Chart 2.1



The PMe_3 group influences the structure in a number of subtle ways. Its size causes the diphosphines bound to Rh to bend away from it, and also causes a similar distortion at Ru, giving rise to P(1)-Rh-P(3) and P(2)-Ru-P(4) angles of $165.55(5)^\circ$ and $161.04(4)^\circ$ respectively - significantly distorted from the idealized 180° value. This PMe_3 group also appears to influence two of the metal-carbonyl distances. Although carbonyls C(1)O(1) and C(2)O(2) occupy similar positions on each metal, the former appears to be more tightly bound (Rh-C(1) = $1.900(5)$ Å, Ru-C(2) = $1.934(5)$ Å), presumably a consequence of greater π back-donation at Rh resulting from the basic PMe_3 group. Of some surprise is that the shortest metal-carbonyl distance is that of Ru-C(3) ($1.860(5)$ Å). It is becoming recognized that electronic effects can be transmitted through a metal-metal bond;^{15,16} in this case it appears that electron donation by the PMe_3 group to Rh can be transmitted via the Rh-Ru bond to C(3)O(3), which lies almost opposite this bond. This transmission of electron density from Rh to Ru can be rationalized considering the above bonding formulation, in which a dative Rh→Ru bond is proposed. Electron donation to Rh by the basic PMe_3 group would result in Rh being a better donor to Ru.

Although compound **5** is isoelectronic with **3**, resulting from replacement of one carbonyl group by the PMe_3 moiety, their geometries are significantly different. In **3** the Rh center has only one terminally bound ligand (a carbonyl) whereas in **5** Rh has two terminally bound groups. The presence of two terminal ligands bound to Rh in **5** is unexpected based on steric arguments, since the larger PMe_3 group should favor the carbonyl being pushed towards Ru, as observed in **3**, in which it is bridging. However, it appears that the terminal carbonyl is favored electronically since in this bonding mode it can more effectively function to remove electron density from Rh that is donated by the PMe_3 group. It is also interesting that the ligand arrangement on the metals is not symmetric. The “ $\text{Rh}(\text{CO})(\text{PMe}_3)$ ” fragment has been twisted away from the metal-metal bond more than the corresponding “ $\text{Ru}(\text{CO})_2$ ” fragment. As a result, the PMe_3 group lies significantly off the Rh-Ru vector ($\text{Ru-Rh-P}(5) = 129.91(4)^\circ$) whereas the carbonyl $\text{C}(3)\text{O}(3)$ is close to this vector ($\text{Rh-Ru-C}(3) = 164.8(2)^\circ$). It appears that this relative twisting about the metal centers allows the phenyl rings of the dppm ligands to fit in the interligand gaps in a gear-wheel arrangement. An inspection of Figure 2.4 shows that phenyl rings 1 and 6 are aimed into the cavity between the metals, opening up the Ru-Rh-C(1) angle, while phenyl ring 8 is aimed between C(3)O(3) and the bridging methylene group. Other phenyl groups are aiming between other ligand combinations or are twisted (phenyl rings 2 and 5) to avoid contacts with the PMe_3 group.

It is notable that for the three methylene-bridged compounds reported (**3**, **4** and **5**), there is a correlation between the ^1H and ^{13}C chemical shifts for the methylene groups (a high-field ^1H chemical shift corresponds to a high-field signal in the ^{13}C NMR spectrum and *vice versa*). Unfortunately, however, these NMR data are not helpful in establishing

whether or not there is a metal-metal bond. It has been noted¹⁷ that for metal-metal bonded species the ¹H NMR resonance for a bridging methylene group generally lies in the range δ 5 - 11, whereas the ¹³C resonance is also low-field, in the range δ 100 - 210. Both sets of resonances for compounds **3** and **5** are upfield from these ranges, although the Rh-CH₂-Ru angle in each compound (85.1(1)°, 85.5(2)°) lies within the range (73-88°) given for metal-metal bonded species.¹⁸ As noted earlier, we consider these complexes to be metal-metal bonded in spite of their long metal-metal separations.

Discussion:

The bridging methylene unit has been shown to be a pivotal fragment in FT chemistry, and has been implicated in carbon-carbon bond formation through a number of proposed pathways.¹⁹⁻²⁴ Following our success with coupling of up to four methylene fragments promoted by a Rh/Os¹ compound, we turned to the Rh/Ru combination of metals in order to determine the effect of substituting Os by the more labile Ru.²⁵ However, much of the chemistry reported herein is inconsistent with this interpretation and necessitates a consideration of not only Ru-for-Os replacement, but also a consideration of the effects of different *combinations* of metals (i.e. Rh/Ru vs. Rh/Os and Ir/Ru), as will be discussed.

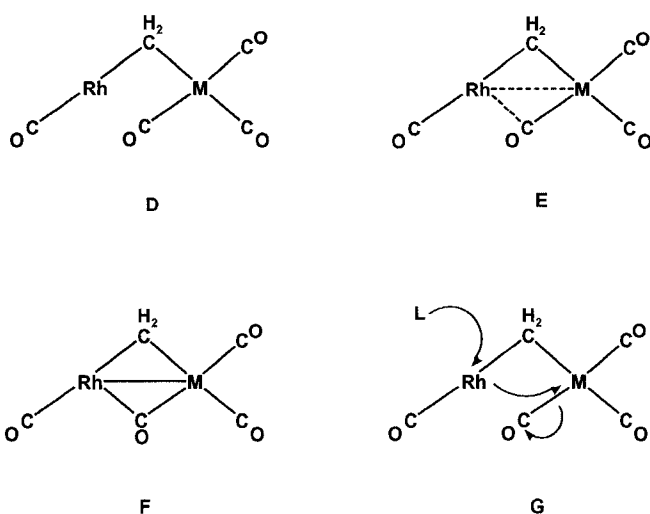
The transformations from [RhRu(CO)₃(μ -H)(dppm)₂] to [RhRu(CO)₄(μ -CH₂)(dppm)₂][X] (**3**), as shown in Scheme 2.1, are not surprising and parallel previous work done with the Rh/Os¹ and Ir/Ru⁵ combinations of metals. What is surprising is the subsequent lack of reactivity of **3** with diazomethane, compared to the analogous Rh/Os compound which reacts readily under similar conditions (Scheme 1.9). Although **3** and its Ir/Ru analogue do not incorporate additional methylene groups from diazomethane,

they do generate ethylene. Labeling studies in both compounds show that none of the labeled methylene from diazomethane becomes incorporated into the complexes nor does any of the metal-bridged methylene group become incorporated into the ethylene. In contrast, labeling studies for the Rh/Os compound, $[\text{RhOs}(\text{CO})_4(\mu\text{-CH}_2)(\text{dppm})_2][\text{X}]$, have shown that ethylene formation results from coupling of the metal-bridged methylene group with a second methylene group generated by diazomethane, presumably by diazomethane activation at the unsaturated Rh center. In this Rh/Os system, ethylene is either liberated from the complex or subsequent methylene incorporation occurs yielding the C₃- and C₄- containing species shown in Scheme 1.9.¹ The failure of ¹³CH₂-labeled **3** to transfer any of the label to the ethylene produced shows that a different mechanism for ethylene formation is operating, although what this mechanism is remains unclear.

In hopes of obtaining clues about the differing reactivities of the Rh/Os complex compared to those of Rh/Ru and Ir/Ru we compared their solid-state structures. However, the closely comparable structural parameters for these compounds (particularly the Rh/Ru and Rh/Os analogues) gave no obvious clue to the reactivity differences. Looking back at the transformation of $[\text{RhOs}(\text{CO})_4(\mu\text{-CH}_2)(\text{dppm})_2]^+$ into either $[\text{RhOs}(\text{CH}_2\text{CH}=\text{CH}_2)(\text{CH}_3)(\text{CO})_3(\text{dppm})_2]^+$ or $[\text{RhOs}(\text{CH}_2)_4(\text{CO})_3(\text{dppm})_2]^+$ (Scheme 1.9) it was clear that carbonyl loss accompanied these interesting examples of C-C bond formation. However, in the previous study¹ we had not established the stage at which carbonyl loss occurred or its relationship to the methylene-coupling reactions. In order to test the effect of carbonyl loss in the Rh/Ru system, the removal of one carbonyl by Me₃NO was effected, yielding the tricarbonyl species $[\text{RhRu}(\text{CO})_3(\mu\text{-CH}_2)(\text{dppm})_2][\text{X}]$ (**4**). Unlike the methylene-bridged tetracarbonyl precursor (**3**), which remains unaffected

by additional CH_2N_2 , compound **4** reacts readily yielding a mixture of products. Although we have been unable to characterize any of these products, the reactivity of **4** with diazomethane suggests that CO loss is pivotal in subsequent incorporation of methylene groups, leading to methylene coupling. It seemed, therefore, that the clue to the reactivity differences in the Rh/Ru and Rh/Os compounds may lie in their abilities to lose CO upon reaction with diazomethane. Two closely related extremes can be envisioned for methylene-bridged tetracarbonyl complexes of Rh/Ru and Rh/Os as diagrammed for **D** and **F** (dppm groups above and below the plane of the drawing are omitted) in Chart 2.2. In structure **D**, Rh is coordinatively unsaturated, whereas in the metal-metal bonded **F**, both metals have 18e configurations. Structure **D** should therefore be more susceptible to substrate addition, which might induce CO loss as diagrammed in

Chart 2.2



G. The coordinative saturation at Rh, resulting from substrate (L) addition can lead to dative-bond formation to M (Ru or Os) assisting in the labilization of a carbonyl. In

keeping with this proposal, the reaction of **3** with PMe_3 yields the substitution product **5**, which appears to have resulted from PMe_3 attack as diagrammed in structure **G**. That PMe_3 reacts readily with **3** whereas diazomethane does not, is presumably a result of the greater nucleophilicity of the former. With these ideas in mind, we looked back at the structures of $[\text{RhOs}(\text{CO})_4(\mu\text{-CH}_2)(\text{dppm})_2][\text{BF}_4]$ (**3b**), and the Rh/Os and Ir/Ru analogues to determine their relationship to the structures shown in Chart 2.2. Clearly, the transition from **D** to **F** is accompanied by a shortening of the metal-metal separation and by a change in the M-C-O angle from 180° to near 135° as this carbonyl assumes a bridging position. A comparison of structural parameters for the three methylene-bridged compounds under discussion is given in Table 2.6.

Clearly, none of the structures correspond to structure **D** in which all carbonyls are terminally-bound. However, based on the parameters given in Table 2.6, it is clear that the Ir/Ru compound is close to the symmetrically-bridged carbonyl extreme, **F** (atom numbering scheme as in Figure 2.3). In this compound the Ir-C(2)-O(2) and the Ru-C(2)-O(2) angles are comparable, as are the Ir-C(2) and Ru-C(2) distances. As shown in structure **F**, the symmetrical carbonyl bridge is accompanied by a metal-metal bond, consequently this Ir/Ru compound has the shortest metal-metal distance of the three. In addition, as the carbonyl group (C(2)-O(2)) moves to a bridging arrangement the C(5)-Rh-C(1) or C(5)-Ir-C(1) angle should decrease from 180° expected in structure **D** as interaction of this metal with C(2)-O(2) increases. Consistent with this argument, this angle is smallest for the Ir/Ru structure. The structures for the RhRu and RhOs compounds are extremely similar and seem to correspond best to the intermediate structure **E** in which one carbonyl (C(2)-O(2)) is semibridging. This is seen not only in

the asymmetry of the angles at the semibridging carbonyl ($\text{Rh-C(2)-O(2)} \approx 141^\circ$, $\text{M-C(2)-O(2)} \approx 130^\circ$) but also in the Rh-M distances of greater than 2.91 Å, which are significantly longer than a conventional Rh-Os or Rh-Ru bond, as shown for $[\text{RhOs}(\text{CF}_3\text{SO}_3)(\text{CO})_2(\mu\text{-C}(\text{CH}_3)\text{O})(\text{dppm})_2]^+$ and $[\text{RhRu}(\text{CO})_4(\text{dppm})_2]^+$ (**2**) ($\text{Rh-Os} \approx 2.71$ Å,²⁶ $\text{Rh-Ru} \approx 2.79$ Å) respectively. Although, as noted earlier, a comparison of **3b** and the Rh/Os analogue was not very helpful since both structures are very similar, it is useful to compare them in the context of the above discussion. So although the Rh-C(2) and M-C(2) distances (M = Ru, Os) are not significantly different in the two structures, other parameters given in Table 6 show a clear trend. Therefore, the differences between the Rh-C(2)-O(2) and M-C(2)-O(2) angles in the two structures are 10.7° (Rh/Ru) and 12.8° (Rh/Os), with the Rh/Ru structure tending slightly towards the symmetric extreme. This tendency is supported by a shorter Rh-M bond and a less linear C(5)-Rh-C(1) angle in the Rh/Ru compound, both of which suggest a tendency towards a symmetrically-bridged structure. These parameters, taken together, suggest that the Rh/Os compound, although clearly having a semibridging CO, tends most towards the structure type **D**. This tendency towards a symmetrically bridged carbonyl for the Rh/Ru compound compared to Rh/Os is also supported by the solution NMR studies. In **3** the semibridging carbonyl displays a somewhat larger coupling to Rh (25 Hz) compared to that observed (22 Hz) for the Rh/Os analogue,¹³ suggesting stronger binding to Rh in the former. We propose that the greater the tendency for the semibridging carbonyl to approach the “all terminal carbonyl” geometry (**D**), the weaker the interaction of this carbonyl with Rh, and the more readily it is displaced by an incoming nucleophile.

Table 2.6. A Comparison of Selected Structural Parameters for the Compounds

	MM'		
	RhOs ^b	RhRu (3) ^c	IrRu ^d
<i>(a) Bond-lengths (Å)</i>			
M-M' ^e	2.9413(4)	2.9114(5)	2.8650(7)
M'-C(2)	2.157(4)	2.155(4)	2.072(8)
M-C(2)	2.027(4)	2.021(3)	2.033(8)
M'-C(5)	2.210(4)	2.213(3)	2.305(12)
M-C(5)	2.088(4)	2.089(3)	2.045(11)
<i>(b) Angles (deg)</i>			
M'-C(2)-O(2)	141.7(3)	141.1(3)	137.1(7)
M-C(2)-O(2)	128.9(3)	130.4(3)	134.4(7)
C(5)-M-C(1)	169.1(2)	167.9(1)	161.7(5)

^a The atom numbering scheme used for all compounds is that used for compound **3** in Figure 2.3.

^b unpublished work.

^c this work.

^d reference 5.

^e M = Rh, Ir; M' = Ru, Os.

Although the structural differences between **3** and the RhOs analogue are subtle, presumably diazomethane (a weak nucleophile) can displace the carbonyl in the RhOs compound, but not in **3**.

The displacement of a carbonyl from these methylene-bridged tetracarbonyl complexes has been demonstrated for the addition of PMe_3 yielding $[\text{MM}'(\text{PMe}_3)(\text{CO})_3(\mu\text{-CH}_2)(\text{dppm})_2]^+$ as described earlier. Consistent with the above arguments carbonyl displacement occurs in the order of RhOs > RhRu > IrRu.²⁷ These observations support a proposal of carbonyl loss as diagrammed for species **G** above. It should be noted however, that carbonyl loss upon diazomethane attack in the RhOs compound may not occur as shown for the stronger nucleophile PMe_3 . In particular, it has been recently demonstrated for the RhOs system that carbonyl loss probably does not occur until after the coupling of *three* methylene groups, to give a C_3H_6 -bridged species.¹ Nevertheless, it appears as though the pivotal step that determines whether reaction of the methylene-bridged complexes with diazomethane occurs is whether diazomethane is capable of displacing the semi-bridging carbonyl from Rh. A bridging carbonyl that is too strongly bound to Rh does not allow diazomethane incorporation.

Although we recognize that the structural differences between **3** and its Rh/Os analogue are slight and are susceptible to over-interpretation, the most important aspect of these arguments is the recognition that a number of factors associated with *both* metals, including the nature of the metal-metal bonding and the nature of the bridged ligand interactions, are responsible for the reactivity of binuclear complexes.

References:

1. Trepanier, S.J.; Sterenberg, B.T.; McDonald, R.; Cowie, M. *J. Am. Chem. Soc.* **1999**, *121*, 2613.
2. Knox, S.A.R. *J. Organomet. Chem.* **1990**, *400*, 255.
3. Knox, S.A.R. *J. Cluster Sci.* **1992**, *3*, 385.
4. Akita, M.; Hua, R.; Knox, S.A.R.; Moro-oka, Y.; Nakanishi, S.; Yates, M.I. *J. Organomet. Chem.* **1998**, *569*, 71.
5. Dell'Anna, M.M.; Trepanier, S.J.; McDonald, R.; Cowie, M. *Organometallics* **2001**, *20*, 88.
6. Antonelli, D.M.; Cowie, M. *Organometallics* **1990**, *9*, 1818.
7. Further information may be obtained by contacting Dr. Robert McDonald (bob.mcdonald@ualberta.ca) and inquiring about sample numbers COW0125 (compound **2**), COW0134 (compound **3**) and COW0009 (compound **5**).
8. Programs for diffractometer operation, data reduction, and absorption correction were those supplied by Bruker.
9. Sheldrick, G.M. *Acta Crystallogr. Sect. A* **1990**, *46*, 467.
10. Sheldrick, G.M. *SHELXL-93*: Program for crystal structure determination; University of Gottingen: Gottingen, Germany, 1993.
11. George, D.S.A.; McDonald, R.; Cowie, M. *Organometallics* **1998**, *17*, 2553.
12. Crabtree, R.H.; Lavin, M. *Inorg. Chem.* **1986**, *25*, 805.
13. Trepanier, S.J.; Cowie, M. Unpublished results.
14. Oke, O.; McDonald, R.; Cowie, M. *Organometallics* **1999**, *18*, 1629.

15. Cowie, M.; Vasapollo, G.; Sutherland, B.R.; Ennett, J.P. *Inorg. Chem.* **1986**, *25*, 2648.
16. Sola, E.; Torres, F.; Jimenez, M.V.; Lopez, J.A.; Ruiz, S.E.; Lahoz, F.J.; Elduque, A.; Oro, L.A. *J. Am. Chem. Soc.* **2001**, *123*, 11925.
17. Puddephatt, R.J. *Polyhedron* **1988**, *7*, 767.
18. Herrmann, W.A. *Adv. Organomet. Chem.* **1982**, *20*, 159.
19. Biloen, P.; Sachtler, W.M.H. *Adv. Catal.* **1981**, *30*, 165.
20. Kaminsky, M.P.; Winograd, N.; Geoffroy, G.L.; Vannice, M.A. *J. Am. Chem. Soc.* **1986**, *108*, 1315.
21. Brady, R.C.; Pettit, R. *J. Am. Chem. Soc.* **1980**, *102*, 6181.
22. Brady, R.C.; Pettit, R. *J. Am. Chem. Soc.* **1981**, *103*, 1287.
23. Maitlis, P.M.; Long, H.C.; Quayoum, R.; Turner, M.L.; Wang, Z.Q. *Chem. Commun.* **1996**, 1.
24. Long, H.C.; Turner, M.L.; Fornasiero, P.; Kaspar, J.; Graziani, M.; Maitlis, P.M. *J. Catal.* **1997**, *167*, 172.
25. Huheey, J.E.; Keiter, E.A.; Keiter, R.L. *Inorganic Chemistry: Principles of Structure and Reactivity*; 4th ed.; Harper Collins: New York, 1993.
26. Trepanier, S.J.; McDonald, R.; Cowie, M. *Organometallics* **2003**, *22*, 2638.
27. Trepanier, S.J.; Rowsell, B.D.; Cowie, M. Unpublished Results.

Chapter 3

Regioselective Alkyne Insertions into a "Rh(μ -CH₂)Ru" Moiety Yielding C₃- and C₅-Bridged Fragments

Introduction:

The recent interest in bimetallic Fischer-Tropsch catalysts,¹⁻⁵ in which two different group 8 and 9 metals are used as catalysts, led us to study a series of methylene-bridged complexes involving the Rh/Os,⁶ Rh/Ru (Chapter 2) and Ir/Ru⁷ metal combinations as models for these bimetallic systems. To date, the Rh/Os system has proven to be the most promising, showing selective coupling of either three or four methylene groups to give allyl or butanediyl fragments, respectively (as shown in Scheme 1.9).⁶ Although no intermediates in the formation of these C₃ and C₄ products were observed beyond the methylene-bridged species, we proposed stepwise methylene insertions to give first a C₂H₄-bridged followed by a C₃H₆-bridged intermediate, the latter of which yielded the allyl or butanediyl groups by β -H elimination or an additional CH₂-insertion step, respectively. Our failure to observe the proposed C₂- or C₃-bridged intermediates led us to attempt to synthesize models for these species using alkynes and methylene groups as the C₂ and C₁ fragments, respectively, which could be combined to yield C₃ species. A recent report by Dry has alluded to the possible importance of surface-bound C₃ units in the FT process,⁸ produced by the condensation of bridging methylene groups and surface-bound olefins as the C₂ fragments.

In this chapter, attempts to synthesize C₃-bridged complexes via the coupling of methylene groups and alkynes promoted by the Rh/Ru combination of metals will be reported.

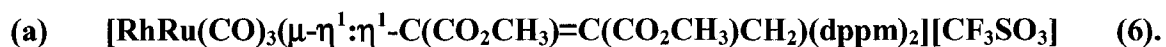
Experimental Section:

General Comments. All solvents were dried (using appropriate desiccants), distilled before use, and stored under a dinitrogen atmosphere. Reactions were performed under an argon atmosphere using standard Schlenk techniques. Diazomethane was generated from Diazald, which was purchased from Aldrich, as were trimethylamine-N-oxide dimethyl acetylenedicarboxylate, hexafluoro-2-butyne, diethyl acetylenedicarboxylate, propargyl alcohol, 2-butyne-1-yl diethyl acetal, and 2-butyne-1-ol. The ¹³C-enriched Diazald was purchased from Cambridge Isotopes, and ¹³CO was purchased from Isotech, Inc. The complexes [RhRu(CO)₄(μ-CH₂)(dppm)₂][CF₃SO₃] (**3**) and [RhRu(CO)₃(μ-CH₂)(dppm)₂][CF₃SO₃] (**4**) were prepared as described in Chapter 2.⁹ In all cases compound **4** was generated *in situ* from **3** in the presence of Me₃NO and filtered over Celite.

The ¹H, ¹³C{¹H}, ¹H-¹H COSY, ³¹P-³¹P COSY, and ³¹P{¹H} NMR spectra were recorded on a Varian iNova-400 spectrometer operating at 399.8 MHz for ¹H, 161.8 MHz for ³¹P and 100.6 MHz for ¹³C. The HMBC experiments were performed on a Varian Unity 500 MHz spectrometer, and infrared spectra were obtained on a Bomem MB-100 spectrometer. Elemental analyses were performed by the microanalytical service within the department. In a number of cases, elemental analyses are less satisfactory than desired owing to facile yet incomplete loss of CH₂Cl₂ of crystallization upon removal of the

crystals from the mother liquor. In all cases, however, the compounds were shown to be spectroscopically pure on the basis of NMR spectroscopy. The $^{31}\text{P}\{^1\text{H}\}$, ^1H , and $^{13}\text{C}\{^1\text{H}\}$ NMR and IR spectroscopic data are given in Table 3.1, while other relevant NMR data are provided in the text.

Preparation of Compounds:



Method i. A 10 mL portion of acetone was added to a mixture of compound **3** (135 mg, 0.111 mmol) and Me_3NO (13.75 mg, 0.185 mmol, 1.70 equiv), resulting in a rapid color change from orange to dark red. Dimethyl acetylenedicarboxylate (14 μL , 0.11 mmol, 1.0 equiv) was added, causing an immediate color change from dark red to orange. The solution was filtered over Celite, after which the solvent was removed *in vacuo*. The orange residue was recrystallized from CH_2Cl_2 /ether/pentane (1:3:1), and the orange solid was washed with 2×10 mL of ether and dried *in vacuo*, yielding 130.0 mg (0.0955 mmol, 86%) of product. The fractional CH_2Cl_2 of crystallization was established by elemental analysis and by ^1H NMR spectroscopy. Anal. Calcd for $\text{C}_{61.1}\text{H}_{52.2}\text{Cl}_{0.2}\text{F}_3\text{O}_{10}\text{P}_4\text{RhRuS}$ ($6 \cdot 0.1\text{CH}_2\text{Cl}_2$): C, 53.55; H, 3.84; Cl, 0.52. Found: C, 53.12; H, 3.76; Cl, 0.43.

Method ii. Dimethyl acetylenedicarboxylate (2.6 μL , 0.021 mmol) was added to a solution of $[\text{RhRu}(\text{CO})_4(\mu\text{-CH}_2)(\text{dppm})_2][\text{CF}_3\text{SO}_3]$ (**3**) (25 mg, 0.020 mmol) in 0.7 mL of CD_2Cl_2 in an NMR tube. The complete conversion to **6** was confirmed by ^1H and ^{31}P NMR spectroscopy in less than 1 h at ambient temperature.

Table 3.1. Spectroscopic Data For Compounds.

Compound	IR (cm ⁻¹) ^{a,b,c}	NMR ^{d,e}		
		³¹ P{ ¹ H} (ppm) ^f	¹ H (ppm) ^{g,h}	¹³ C{ ¹ H} (ppm) ^{h,i}
[RhRu(CO) ₃ (μ-η ¹ :η ¹ -C(CO ₂ CH ₃)=C(CO ₂ CH ₃)-CH ₂)(dppm) ₂][CF ₃ SO ₃] (6)	2039 (s), 2018 (s), 1968 (m), 1705 (br, m), 1574 (w) ^j	28.4 (m), 24.6 (dm)	4.58 (m, 2H), 3.72 (m, 2H), 3.15 (s, 3H), 2.65 (s, 3H), 1.48 (br, t, 2H)	194.0 (t, ² J _{PC} = 15 Hz, 1C), 193.2 (t, ² J _{PC} = 15 Hz, 1C), 191.1 (dt, ² J _{PC} = 12 Hz, ¹ J _{RhC} = 50 Hz, 1C), 15.3 (t, ² J _{PC} = 9 Hz, 1C)
[RhRu(CO) ₃ (μ-η ¹ :η ¹ -C(CF ₃)=C(CF ₃)CH ₂)-(dppm) ₂][CF ₃ SO ₃] (7)	2049 (s), 2019 (s), 1968 (s), 1574 (w) ^j	27.3 (m), 22.7 (dm)	4.37 (m, 2H), 4.55 (m, 2H), 1.82 (m, 2H)	194.0 (m, 1C), 193.1 (t, ² J _{PC} = 14 Hz, 1C), 191.3 (dt, ² J _{PC} = 12 Hz, ¹ J _{RhC} = 50 Hz, 1C), 13.8 (t, ² J _{PC} = 8 Hz, 1C) ^k
[RhRu(CO) ₃ (μ-η ¹ :η ¹ -C(CO ₂ Et)=C(CO ₂ Et)CH ₂)-(dppm) ₂][CF ₃ SO ₃] (8) ^l	2042 (m), 2016 (s), 1953 (m), 1695 (br, m), 1574 (m) ^j	28.3 (m), 25.0 (dm)	5.06 (m, 2H), 4.23 (m, 2H), 3.40 (q, 2H), 3.17 (q, 2H), 1.53 (m, 2H), 1.07 (t, 3H), 0.81 (t, 3H)	204.7 (t, ² J _{PC} = 13 Hz, 1C), 194.4 (td, ² J _{PC} = 13 Hz, ² J _{RhC} = 4 Hz, 1C) 190.9 (dt, ² J _{PC} = 13 Hz, ¹ J _{RhC} = 51 Hz, 1C)
[RhRu(CO) ₃ (μ-η ¹ :η ¹ -C(CH ₃)=C(CH(OEt) ₂)CH ₂)-(dppm) ₂][CF ₃ SO ₃] (9)	2024 (s), 1977 (sh), 1951 (s)	28.4 (m), 22.9 (dm)	4.97 (s, 1H), 4.75 (m, 2H), 4.41 (m, 2H), 3.70 (q, 2H), 3.59 (q, 2H), 1.45 (m, 2H), 1.33 (t, 6H), 0.07 (s, 3H)	201.4 (t, ² J _{PC} = 6 Hz, 1C), 193.8 (t, ² J _{PC} = 15 Hz, ² J _{RhC} = 7 Hz, 1C), 193.2 (dt, ² J _{PC} = 12 Hz, ¹ J _{RhC} = 52 Hz, 1C)

Table 3.1. Spectroscopic Data For Compounds (cont'd.)

[RhRu(CO) ₃ (μ-η ¹ :η ¹ -C(CH ₃)=C(CH ₂ OH)-CH ₂)(dppm) ₂][CF ₃ SO ₃] (10)	2024 (s), 1995 (m), 1950 (s)	28.3 (m), 22.4 (dm)	4.64 (m, 2H), 3.92 (d, 2H), 3.73 (m, 2H), 1.98 (s, 1H), 1.36 (m, 2H), 0.11 (s, 3H)	
[RhRu(CO) ₃ (μ-η ¹ :η ¹ -C(CO ₂ -CH ₃)=C(CO ₂ CH ₃))(dppm) ₂]- [CF ₃ SO ₃] (11b) ^l	2038 (s), 2019 (s), 1969 (s), 1726 (m) ^k	19.9 (om)	4.04 (m, 2H), 3.29 (m, 2H), 2.71 (s, 3H), 2.32 (s, 3H)	197.5 (m, 1C), 192.4 (t, ² J _{PC} = 13 Hz, 1C), 190.5 (m)
[RhRu(OSO ₂ CF ₃)(CO) ₂ -(μ-η ¹ :η ¹ -C(CO ₂ CH ₃)=C(CO ₂ CH ₃))(dppm) ₂] (12)	2003(s), 1945(s), 1356 (m) ^k	22.7 (m), 17.0 (dm) ^k	3.89 (m, 2H), 3.67 (m, 2H), 3.23 (s, 3H), 2.18 (s, 3H) ^k	206.9 (m, 1C), 192.2 (m, 1C) ^k
[RhRu(OSO ₂ CF ₃)(CO) ₂ -(μ-η ¹ :η ¹ -C(CO ₂ CH ₃)=C(CO ₂ CH ₃))(μ-CH ₂)(dppm) ₂] (13)	2027 (s), 1964 (s), 1703 (s), 1575 (w) ^{i,k}	26.2 (d, ¹ J _{RhP} = 142 Hz), 15.3 (s) ^k	4.42 (m, 2H), 3.66 (m, 2H), 3.34 (s, 3H), 2.74 (m, 2H), 1.70 (s, 3H) ^k	199.4 (m, 1C), 193.1 (m, 1C) ^k
[RhRu(CO) ₂ (μ-η ¹ :η ³ -CHC(CO ₂ CH ₃)=CH(CO ₂ CH ₃))- (dppm) ₂][CF ₃ SO ₃] (14)	1998 (s), 1969 (s) ^k	45.3 (m), 43.5 (m), 24.8 (cm), 29.4 (cm) ^k	5.90 (m, 1H), 4.90 (m, 1H), 4.35 (m, 1H), 3.79 (s, 3H), 3.52 (m, 1H), 3.32 (m, 1H), 2.82 (s, 3H) ^k	205.0 (t, ² J _{PC} = 13 Hz, 1C), 193.3 (dt, ² J _{PC} = 15 Hz, ¹ J _{RhC} = 67 Hz, 1C), 110.2 (dm, ¹ J _{RhC} = 21 Hz, 1C) ^k

Table 3.1. Spectroscopic Data For Compounds (cont'd.)

[RhRu(CO) ₂ (μ-η ² :η ⁴ -CH=C-(CH ₂ OH)CH=C(CH ₂ OH)-CH ₂)(dppm) ₂][CF ₃ SO ₃] (15)	1995 (s), 1957 (s)	66.7 (dd, J = 21, 124 Hz), 39.7 (ddd, J = 16, 84, 140 Hz), 27.8 (dd, J = 22, 46 Hz), 0.62 (ddd, J = 16, 46, 104 Hz)	6.03 (s, 1H), 5.03 (m, 1H), 4.36 (m, 1H), 3.71 (m, 1H), 3.60 (m, 1H), 3.44 (m, 1H), 3.24 (m, 1H), 2.86 (m, 1H), 2.80 (om, 2H), 2.55 (m, 1H), 2.03 (m, 1H), 0.77 (m, 1H)	200.3 (m, 1C), 192.2 (dm, ¹ J _{RhC} = 67 Hz, 1C), 3.6 (ddd, ¹ J _{RhC} = 16 Hz, ² J _{PC(trans)} = 64 Hz, ² J _{PC(cis)} = 5 Hz, 1C)
--	--------------------	---	---	---

^a IR abbreviations: s = strong, m = medium, w = weak, sh = shoulder. ^b CH₂Cl₂ solutions unless otherwise stated, in units of cm⁻¹. ^c Carbonyl stretches unless otherwise noted. ^d NMR abbreviations: s = singlet, d = doublet, t = triplet, m = multiplet, cm = complex multiplet, dm = doublet of multiplets, om = overlapping multiplets, br = broad, dt = doublet of triplets, dpq = doublet of pseudo-quintets. ^e NMR data at 25 °C in CD₂Cl₂ unless otherwise stated. ^f ³¹P chemical shifts referenced to external 85% H₃PO₄. ^g Chemical shifts for the phenyl hydrogens are not given. ^h ¹H and ¹³C chemical shifts referenced to TMS. ⁱ ¹³C{¹H} NMR performed with ¹³CO enrichment. ^j ν(C=C). ^k In acetone-*d*₆. ^l Spectroscopic parameters for the cation of **8a** are identical to those of **8b**.

(b) $[\text{RhRu}(\text{CO})_3(\mu\text{-}\eta^1\text{:}\eta^1\text{-C}(\text{CF}_3)=\text{C}(\text{CF}_3)\text{CH}_2)(\text{dppm})_2][\text{CF}_3\text{SO}_3]$ (**7**). Compound **4** was generated from a mixture of compound **3** (120 mg, 0.096 mmol) and Me_3NO (12.30 mg, 0.164 mmol, 1.70 equiv) in 15 mL of acetone as described above. Hexafluoro-2-butyne was passed through the headspace of the flask containing the solution of **4** for 1 min at a rate of *ca.* 10 mL/min, causing a slow colour change from dark red to dull orange. The solution was filtered over Celite and the solvent was removed in vacuo, yielding 70.5 mg (0.0510 mmol, 53%) of product. The orange residue was recrystallized from $\text{CH}_2\text{Cl}_2/\text{ether}$, and the orange solid was washed with 2×10 mL of ether and 1×10 mL of pentane and dried *in vacuo*. Anal. Calcd for $\text{C}_{59}\text{H}_{46}\text{F}_9\text{O}_6\text{P}_4\text{RhRuS}$ (**7**): C, 51.28; H, 3.36. Found: C, 50.45; H, 3.29.

(c) $[\text{RhRu}(\text{CO})_3(\mu\text{-}\eta^1\text{:}\eta^1\text{-C}(\text{CO}_2\text{CH}_2\text{CH}_3)=\text{C}(\text{CO}_2\text{CH}_2\text{CH}_3)\text{CH}_2)(\text{dppm})_2][\text{CF}_3\text{SO}_3]$ (**8**). Compound **4** was prepared, as noted above, in 10 mL of acetone using compound **3** (125 mg, 0.103 mmol) and Me_3NO (13.2 mg, 0.175 mmol, 1.70 equiv). Diethyl acetylenedicarboxylate (18 μL , 0.113 mmol, 1.1 equiv) was added, causing an immediate colour change from dark red to orange. The solution was filtered over Celite, after which the solvent was removed *in vacuo*, affording 107.4 mg (0.0773 mmol, 75%) of product. The orange residue was recrystallized from $\text{CH}_2\text{Cl}_2/\text{ether}$, and the orange solid was washed with 2×10 mL of ether and dried in vacuo. Anal. Calcd for $\text{C}_{63}\text{H}_{56}\text{F}_3\text{O}_{10}\text{P}_4\text{RhRuS}$ (**8**): C, 54.44; H, 4.06. Found: C, 54.01; H, 3.99.

(d) $[\text{RhRu}(\text{CO})_3(\mu\text{-}\eta^1\text{:}\eta^1\text{-C}(\text{CH}_3)=\text{C}(\text{CH}(\text{OCH}_2\text{CH}_3)_2)\text{CH}_2)(\text{dppm})_2][\text{CF}_3\text{SO}_3]$ (**9**). Compound **4** was prepared, as noted above, in 10 mL of acetone using compound **3** (156 mg, 0.128 mmol) and Me_3NO (16.5 mg, 0.219 mmol, 1.71 equiv), in 10 mL of acetone

and cooled to $-10\text{ }^{\circ}\text{C}$. 2-Butyn-1-ol diethylacetal (22 μL , 0.140 mmol, 1.1 equiv) was added, causing a slow color change from dark red to orange over the course of 5 min. The solution was stirred at $-10\text{ }^{\circ}\text{C}$ for 2 h, after which the solution was warmed to room temperature and filtered over Celite. The solvent was then removed *in vacuo*, the dull orange residue was recrystallized from CH_2Cl_2 /ether, and the orange-red solid was washed with $3 \times 15\text{ mL}$ of ether and dried *in vacuo*, yielding 104.6 mg (0.0768 mmol, 60%) of product. Anal. Calcd for $\text{C}_{63.2}\text{H}_{60.4}\text{Cl}_{0.4}\text{F}_3\text{O}_8\text{P}_4\text{RhRuS}$ ($9 \cdot 0.2\text{CH}_2\text{Cl}_2$): C, 55.04; H, 4.42; Cl, 1.05. Found: C, 54.54; H, 4.39; Cl, 0.71.

(e) $[\text{RhRu}(\text{CO})_3(\mu\text{-}\eta^1\text{:}\eta^1\text{-C}(\text{CH}_3)=\text{C}(\text{CH}_2\text{OH})\text{CH}_2)(\text{dppm})_2][\text{CF}_3\text{SO}_3]$ (**10**). Compound **4** was prepared, as noted above, in 10 mL of acetone using compound **3** (113 mg, 0.093 mmol) and Me_3NO (12.2 mg, 0.163 mmol, 1.75 equiv), in 10 mL of acetone. 2-Butyn-1-ol (8 μL , 0.107 mmol, 1.2 equiv) was added, causing an immediate colour change from dark red to orange. The solution was stirred for 1 h, after which the solution was filtered over Celite and the solvent was removed *in vacuo*. The bright orange residue was recrystallized from CH_2Cl_2 /ether/pentane (1:3:2), washed with $2 \times 10\text{ mL}$ of ether, and dried *in vacuo*, yielding 103.2 mg (0.0800 mmol, 86%) of product. Anal. Calcd for $\text{C}_{60}\text{H}_{56}\text{F}_3\text{O}_6\text{P}_4\text{RhRuS}$ (**10**): C, 54.88; H, 4.06. Found: C, 54.60; H, 4.03.

(f) $[\text{RhRu}(\text{CO})_3(\mu\text{-}\eta^1\text{:}\eta^1\text{-C}(\text{CO}_2\text{CH}_3)=\text{C}(\text{CO}_2\text{CH}_3))(\text{dppm})_2][\text{X}]$, $\text{X} = \text{BF}_4^-$ (**11a**), $\text{X} = \text{CF}_3\text{SO}_3^-$ (**11b**). Dimethyl acetylenedicarboxylate (20 μL , 0.126 mmol) was added to a solution of $[\text{RhRu}(\text{CO})_4(\text{dppm})_2][\text{X}]$ (**2**) (110 mg, 0.089 mmol) at $20\text{ }^{\circ}\text{C}$, dissolved in 10 mL of CH_2Cl_2 . No noticeable colour change resulted; however, NMR spectroscopy showed complete conversion to a new product. The solvent was removed *in vacuo*, and

the bright orange residue was recrystallized from $\text{CH}_2\text{Cl}_2/\text{Et}_2\text{O}$. The orange solid was washed with 2×15 mL of ether and dried *in vacuo*, yielding 114.0 mg (0.0730 mmol, 82%) of $\mathbf{11a} \cdot 2\text{CH}_2\text{Cl}_2$. Anal. Calcd for $\text{C}_{61}\text{H}_{58}\text{BCl}_4\text{F}_4\text{O}_7\text{P}_4\text{RhRu}$ ($\mathbf{11a} \cdot 2\text{CH}_2\text{Cl}_2$): C, 50.33; H, 3.73; Cl, 9.74. Found: C, 49.82; H, 3.35; Cl, 9.33.

(g) $[\text{RhRu}(\text{OSO}_2\text{CF}_3)(\text{CO})_2(\mu\text{-}\eta^1\text{:}\eta^1\text{-C}(\text{CO}_2\text{CH}_3)=\text{C}(\text{CO}_2\text{CH}_3))(\text{dppm})_2]$ (12**).** A Schlenk flask was charged with compound **11b** (40 mg, 0.0297 mmol) and Me_3NO (3.9 mg, 0.0519 mmol, 1.75 equiv). The flask was cooled to approximately 0°C , and 10 mL of acetone was added slowly. After 20 min the reaction changed colour from orange to orange-red. The reaction was stirred for another 15 min, after which the solution was slowly warmed to room temperature and filtered over Celite. The solvent was removed *in vacuo*, and the orange-red residue was recrystallized from acetone/ether/pentane (1:5:1), washed with 3×10 mL ether, and dried *in vacuo*, yielding 29.4 mg (0.0223 mmol, 75%) of product. Anal. Calcd for $\text{C}_{59}\text{H}_{50}\text{F}_3\text{O}_9\text{P}_4\text{RhRuS}$ (**12**): C, 53.68; H, 3.82. Found: C, 53.21; H, 3.92.

(h) $[\text{RhRu}(\text{OSO}_2\text{CF}_3)(\text{CO})_2(\mu\text{-CH}_2)(\mu\text{-}\eta^1\text{:}\eta^1\text{-C}(\text{CO}_2\text{CH}_3)=\text{C}(\text{CO}_2\text{CH}_3))(\text{dppm})_2]$ (13**).** Compound **12** (70.8 mg, 0.0520 mmol) was dissolved in 10 mL of acetone. Diazomethane was bubbled through the solution vigorously for 10 min, causing no noticeable color change. The solution was concentrated to 5 mL and filtered over Celite to remove any polymethylene that may have formed. The solvent was removed *in vacuo*, and the orange residue was recrystallized from acetone/ether/pentane (1:5:1), washed with 2×10 mL ether, and dried *in vacuo*, yielding 46.5 mg (0.0348 mmol, 67%) of

product. Owing to the air sensitivity of compound **13**, satisfactory elemental analyses could not be obtained.

(i) [RhRu(CO)₂(μ-η¹:η³-CHC(CO₂CH₃)=CH(CO₂CH₃))(dppm)₂][CF₃SO₃] (14). A 0.7 mL sample of acetone-*d*₆ was added to a mixture of compound **6** (35 mg, 0.026 mmol) and Me₃NO (3.23 mg, 0.043 mmol, 1.67 equiv) at 20 °C in an NMR tube. An immediate colour change from orange to dark orange occurred immediately upon mixing. Compound **14** was characterized entirely by ¹H, ²H, and ³¹P spectroscopy; elemental analyses were not obtained owing to its high air-sensitivity.

(j) [RhRu(CO)₂(μ-η²:η⁴-CH=C(CH₂OH)CH=C(CH₂OH)CH₂)(dppm)₂][CF₃SO₃] (15). Compound **4** was prepared, as noted above, in 10 mL of acetone using compound **3** (134 mg, 0.110 mmol) and Me₃NO (14.0 mg, 0.186 mmol, 1.69 equiv), in 15 mL of acetone. The solution was cooled to -78 °C, and propargyl alcohol (14 μL, 0.241 mmol, 2.2 equiv) was added, causing a gradual color change from dark red to light orange over the course of 2 min. The solution was brought to room temperature and filtered over Celite followed by removal of the solvent *in vacuo*. The orange residue was recrystallized from CH₂Cl₂/ether, and the orange-red solid was washed with 2 × 10 mL of ether and dried *in vacuo*, yielding 120.5 mg (0.0924 mmol, 84%) of product. Anal. Calcd for C_{60.1}H_{54.2}Cl_{0.2}F₃O₇P₄RhRuS (15·0.1CH₂Cl₂): C, 54.99; H, 4.16. Found: C, 54.20; H, 4.13.

(k) Reaction of 4 with Propyne. A Teflon-valved NMR tube was charged with 0.7 mL of a 0.05 M acetone-*d*₆ solution of **4** and was degassed by two freeze/pump/thaw cycles. Once the solution was frozen in liquid nitrogen, the tube was back-filled using a 5 mL flask previously filled with ca. 1 atm propyne. The solution was then warmed to -78 °C

for VT NMR analysis. Monitoring the $^{31}\text{P}\{^1\text{H}\}$ NMR between $-78\text{ }^\circ\text{C}$ and ambient temperature showed the presence of a large number of unidentified species.

(l) Reaction of 2 with 2-Butyne. A Teflon-valved NMR tube was charged with 0.7 mL of a 0.025 M acetone- d_6 solution of **4** and was degassed by two freeze/pump/thaw cycles. A 5 mL flask was charged with the room-temperature vapor pressure of 2-butyne (ca. 0.8 atm). The solution of **4** was frozen in liquid nitrogen, and the tube was back-filled using the flask containing the 2-butyne. The solution was then warmed to $-78\text{ }^\circ\text{C}$ for VT NMR analysis. Monitoring the $^{31}\text{P}\{^1\text{H}\}$ NMR spectrum between $-78\text{ }^\circ\text{C}$ and ambient temperature showed the presence of a large number of unidentified species.

(m) Reaction of 6 with Diazomethane. Compound **6** (15 mg, 0.011 mmol) was dissolved in 0.6 mL of CD_2Cl_2 in an NMR tube. Diazomethane gas was bubbled through the headspace of the NMR tube for *ca.* 5 min, causing no colour change. ^1H and $^{31}\text{P}\{^1\text{H}\}$ NMR spectroscopy after 20 h detected only the presence of **6**.

(n) Reaction of 15 with H_2 . Compound **15** (25 mg, 0.0192 mmol) was dissolved in 0.7 mL of CD_2Cl_2 in an NMR tube. Hydrogen gas was bubbled through the headspace of the tube, with no noticeable colour change. ^1H and $^{31}\text{P}\{^1\text{H}\}$ NMR spectroscopy detected the presence of $[\text{RhRu}(\mu\text{-H})_2(\text{CO})_3(\text{dppm})_2][\text{CF}_3\text{SO}_3]^9$ as well as several unidentified organic products.

(o) Attempted Reaction of 15 with $[(\text{Cp})_2\text{Fe}][\text{PF}_6]$. Compound **15** (20 mg, 0.0153 mmol) and $[(\text{Cp})_2\text{Fe}][\text{PF}_6]$ (10.1 mg, 0.0302 mmol, 1.97 equiv) were placed in an NMR

tube and dissolved in 0.7 mL of acetone, forming a green solution. $^{31}\text{P}\{^1\text{H}\}$ NMR spectroscopy after 14 h detected only the presence of **15**.

(p) Attempted Reaction of 15 with $[\text{NH}_4]_2[\text{IrCl}_6]$. Compound **15** (15.0 mg, 0.012 mmol) and $[\text{NH}_4]_2[\text{IrCl}_6]$ (10.1 mg, 0.023 mmol, 2.0 equiv) were placed in an NMR tube and dissolved in 0.6 mL of acetonitrile and 0.1 mL of D_2O . After sitting overnight, only starting material was observed by $^{31}\text{P}\{^1\text{H}\}$ NMR.

X-ray Data Collection.¹⁰ Pale yellow crystals of $[\text{RhRu}(\text{CO})_3(\mu\text{-}\eta^1\text{:}\eta^1\text{-C}(\text{CF}_3)=\text{C}(\text{CF}_3)\text{CH}_2)(\text{dppm})_2][\text{CF}_3\text{SO}_3]\cdot 1.5\text{CH}_2\text{Cl}_2$ (**7**) were obtained via slow diffusion of pentane into a CD_2Cl_2 solution of the compound. Data were collected (and later refined) by Drs. Robert McDonald and Michael J. Ferguson on a Bruker PLATFORM/SMART 1000 CCD diffractometer¹¹ using Mo $\text{K}\alpha$ radiation at -80°C . Unit cell parameters were obtained from a least-squares refinement of the setting angles of 5957 reflections from the data collection. The space group was determined to be $P2_1/n$ (an alternate setting of $P2_1/c$ [No. 14]). The data were corrected for absorption through use of the SADABS procedure. See Table 3.2 for a summary of crystal data and X-ray data collection information.

Red-orange crystals of $[\text{RhRu}(\text{CO})_3(\mu\text{-}\eta^1\text{:}\eta^1\text{-C}(\text{CO}_2\text{CH}_3)=\text{C}(\text{CO}_2\text{CH}_3))(\text{dppm})_2][\text{BF}_4]$ (**11a**) were obtained via slow diffusion of diethyl ether into a dichloromethane solution of the compound. Data were collected as for **7** above (see Table 3.2), and data were corrected for absorption via Gaussian integration (crystal dimensions measured and faces indexed). Unit cell parameters were obtained from a least-squares refinement of the

setting angles of 7423 reflections from the data collection, and the space group was determined to be $P\bar{1}$ (No. 2).

Orange crystals of $[\text{RhRu}(\text{CO})_2(\mu\text{-}\eta^2\text{:}\eta^4\text{-CH=C(CH}_2\text{OH)CH=C(CH}_2\text{OH)-CH}_2\text{)(dppm)}_2][\text{CF}_3\text{SO}_3]\cdot\text{CH}_2\text{Cl}_2$ (**15**) were obtained via slow diffusion of diethyl ether into a dichloromethane solution of the compound. Data were collected and corrected for absorption as for **7** above (see Table 3.2). Unit cell parameters were obtained from a least-squares refinement of the setting angles of 3321 reflections from the data collection. The space group was determined to be $P2_1/n$ (an alternate setting of $P2_1/c$ [No. 14]).

Structure Solution and Refinement. The structure of **7** was solved using direct methods (SHELXS-86).¹² Refinement was completed using the program SHELXL-93.¹³ Hydrogen atoms were assigned positions on the basis of the geometries of their attached carbon atoms and were given thermal parameters 20% greater than those of the attached carbons. Although the presence of 1.5 equiv of CD_2Cl_2 in the crystals was confirmed by ^2H NMR, the atoms of these solvent molecules could not be unambiguously located in difference Fourier syntheses; only smeared out regions of electron density were found, for which suitable disorder models could not be found. These solvent molecules were therefore handled using the SQUEEZE routine as implemented in the PLATON^{14,15} program system, in which the contribution of the disordered solvent electron density to the intensity data was calculated, and the refinement continued using data with this contribution removed. The final model for **7** was refined to values of $R_1(F) = 0.0398$ (for 10 314 data with $F_o^2 \geq 2\sigma(F_o^2)$) and $wR_2(F^2) = 0.1031$ (for all 12464 independent data).

Table 3.2. Crystallographic Data for Compounds 7, 11a and 15.

	[RhRu(CO) ₃ (μ-η ¹ :η ¹ - C(CF ₃)=C(CF ₃)CH ₂)- (dppm) ₂][CF ₃ SO ₃] (7)	[RhRu(CO) ₃ (μ-η ¹ :η ¹ - C(CO ₂ CH ₃)=C(CO ₂ CH ₃))- (dppm) ₂][BF ₄] (11a)	[RhRu(CO) ₂ (μ-η ² :η ⁴ - CH=C(CH ₂ OH)CH=C- (CH ₂ OH)CH ₂)(dppm) ₂][CF ₃ SO ₃] (15)
formula	C _{60.5} H ₄₉ Cl ₃ F ₉ O ₆ P ₄ RhRuS	C ₆₁ H ₅₄ BCl ₄ F ₄ O ₇ P ₄ RhRu	C ₆₁ H ₅₆ Cl ₂ F ₃ O ₇ P ₄ RhRuS
fw	1171.56	1185.59	1403.50
cryst dims, mm	0.34 × 0.24 × 0.20	0.44 × 0.37 × 0.36	0.32 × 0.14 × 0.03
cryst. system	monoclinic	triclinic	monoclinic
space group	<i>P2₁/n</i> (an alternate setting of <i>P2₁/c</i>)	<i>P</i> 1 (No. 2)	<i>P2₁/n</i> (an alternate setting of <i>P2₁/c</i>)
<i>a</i> , Å	12.4541(7) ^a	11.5463(8) ^b	11.988(1) ^c
<i>b</i> , Å	19.1183(11)	14.731(1)	22.217(2)
<i>c</i> , Å	25.8616(14)	19.101(1)	22.280(2)
<i>α</i> , deg	90.0	87.334(1)	90.0
<i>β</i> , deg	97.6146(11)	76.823(1)	104.662(2)
<i>γ</i> , deg	90.0	85.017(1)	90.0
<i>V</i> , Å ³	6103.4 (6)	3150.2(4)	5740.9(8)
<i>Z</i>	4	2	4
<i>d</i> _{calcd} , g cm ⁻³	1.642	1.534	1.607
<i>μ</i> , mm ⁻¹	0.866	0.835	0.855

Table 3.2. (cont'd...)

radiation (λ , Å)	graphite-monochromated Mo K α (0.71073)	graphite-monochromated Mo K α (0.71073)	graphite-monochromated Mo K α (0.71073)
T , °C	-80	-80	-80
scan type	ω scans (0.2°) (25 s exposures)	ω scans (0.2°) (20 s exposures)	ω scans (0.2°) (30 s exposures)
2θ (max), deg	52.76	52.76	52.88
no. of unique reflections	12464 ($R_{\text{int}} = 0.0462$)	12744 ($R_{\text{int}} = 0.0272$)	11524 ($R_{\text{int}} = 0.1008$)
no of observns	10 314 [$F_o^2 \geq 2\sigma(F_o^2)$]	10 311 [$F_o^2 \geq 2\sigma(F_o^2)$]	6446 [$F_o^2 \geq 2\sigma(F_o^2)$]
range of transmn factors	0.8458-0.7571	0.7987-0.7112	0.9748-0.7714
no. of data/restraints/params	12 464 [$F_o^2 \geq -3\sigma(F_o^2)$]/0/730	12 744 [$F_o^2 \geq -3\sigma(F_o^2)$]/0/754	11 524 [$F_o^2 \geq -3\sigma(F_o^2)$]/0/723
residual density, e/Å ³	0.59 to -0.36	1.48 to -0.70	1.21 to -1.10
$R_1(F_o^2 > 2\sigma(F_o^2))^e$	0.0398	0.0496	0.0699
$wR_2[F_o^2 \geq -3\sigma(F_o^2)]^e$	0.1031	0.1423	0.1770
GOF (s) ^f	1.037 [$F_o^2 \geq -3\sigma(F_o^2)$]	1.054 [$F_o^2 \geq -3\sigma(F_o^2)$]	0.985 [$F_o^2 \geq -3\sigma(F_o^2)$]

^a Cell parameters obtained from least-squares refinement of 5957 centered reflections. ^b Cell parameters obtained from least-squares refinement of 7423 centered reflections. ^c Cell parameters obtained from least-squares refinement of 3321 centered reflections. ^d Programs for diffractometer operation, data reduction, and absorption were those supplied by Bruker. ^e $R_1 = \Sigma ||F_o| - |F_c|| / \Sigma |F_o|$; $wR_2 = [\Sigma w(F_o^2 - F_c^2)^2 / \Sigma w(F_o^4)]^{1/2}$ Refinement on F_o^2 for all reflections (having $F_o^2 \geq -3\sigma(F_o^2)$). wR_2 and S based on F_o^2 ; R_1 based on F_o , with F_o set to zero for negative F_o^2 . The observed criterion of $F_o^2 > 2\sigma(F_o^2)$ is used only for calculating R_1 and is not relevant to the choice of reflections for refinement. ^f $S = [\Sigma w(F_o^2 - F_c^2)^2 / (n - p)]^{1/2}$ (n = number of data, p = number of parameters varied; $w = [\sigma^2(F_o^2) + (a_0P)^2 + a_1P]^{-1}$, where $P = [\max(F_o^2, 0) = 2F_c^2]/3$. For **7** $a_0 = 0.0603$ and $a_1 = 0.8779$; for **11a** $a_0 = 0.00822$ and $a_1 = 3.9605$; for **15** $a_0 = 0.0808$ and $a_1 = 0.00$.

The structure of **11a** was solved using the direct-methods program SHELXS-86, and refinement was completed using the program SHELXL-93, during which the hydrogen atoms were treated as for **7**. One of the chlorine atoms of a solvent dichloromethane molecule was found to be disordered; this atom was split into two positions, which were assigned occupancy factors of 0.75 and 0.25 and were allowed to refine independently. The final model for **11a** was refined to values of $R_1(F) = 0.0496$ (for 10 311 data with $F_o^2 \geq 2\sigma(F_o^2)$) and $wR_2(F^2) = 0.1423$ (for all 12744 independent data).

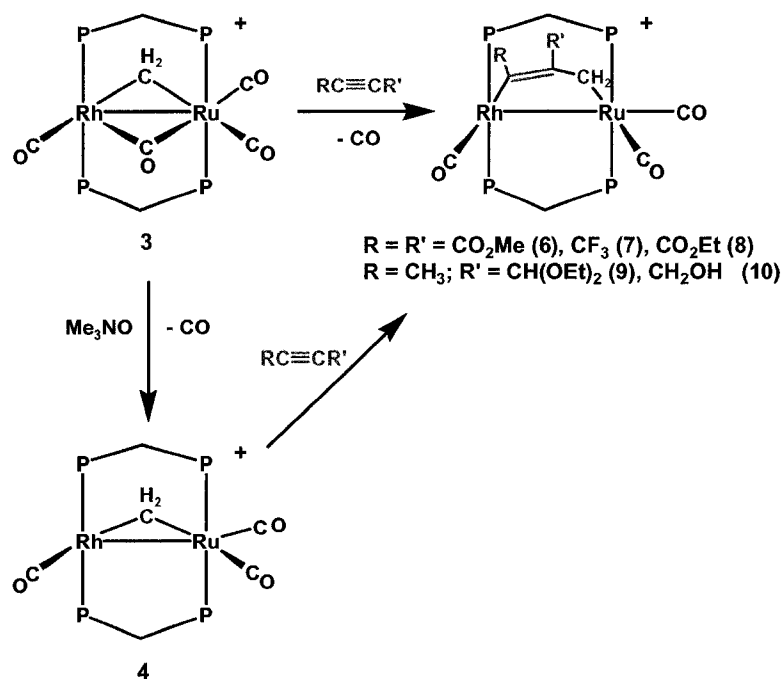
The structure of **15** was solved using the direct-methods program SHELXS-86, and refinement was completed using the program SHELXL-93, during which the hydrogen atoms were treated as for **7**. The final model for **15** was refined to values of $R_1(F) = 0.0699$ (for 6446 data with $F_o^2 \geq 2\sigma(F_o^2)$) and $wR_2(F^2) = 0.1770$ (for all 11524 independent data).

Results and Compound Characterization:

Reaction of the methylene-bridged, tetracarbonyl species $[\text{RhRu}(\text{CO})_3(\mu\text{-CH}_2)(\mu\text{-CO})(\text{dppm})_2][\text{CF}_3\text{SO}_3]$ (**3**) with a number of alkynes has been attempted. Although this reaction proceeds readily with dimethyl acetylenedicarboxylate (DMAD), yielding $[\text{RhRu}(\text{CO})_3(\mu\text{-}\eta^1\text{:}\eta^1\text{-C}(\text{CO}_2\text{Me})=\text{C}(\text{CO}_2\text{Me})\text{CH}_2)(\text{dppm})_2][\text{CF}_3\text{SO}_3]$ (**6**), the reactions with other alkynes proceed sluggishly, requiring hours or days to reach completion at ambient temperature. However, removal of a carbonyl from **3**, using trimethylamine-*N*-oxide to give the tricarbonyl $[\text{RhRu}(\text{CO})_3(\mu\text{-CH}_2)(\text{dppm})_2][\text{CF}_3\text{SO}_3]$ (**4**)⁹ *in situ*, results in instantaneous reaction with a number of alkynes to give the same products as with **3**, as shown in Scheme 3.1. With the symmetric alkynes $\text{RC}\equiv\text{CR}$ ($\text{R} = \text{CO}_2\text{Me}, \text{CF}_3, \text{CO}_2\text{Et}$),

reaction with **4** yields the products $[\text{RhRu}(\text{CO})_3(\mu\text{-}\eta^1\text{:}\eta^1\text{-C}(\text{R})=\text{C}(\text{R})\text{CH}_2)\text{-}$

Scheme 3.1



(dppm)₂][CF₃SO₃] (R = CO₂Me (**6**), CF₃ (**7**), CO₂Et (**8**)), in which alkyne insertion into the Rh-CH₂ bond of the precursor has occurred. All products display very similar ³¹P{¹H} NMR spectra (see Table 3.1), having two complex multiplet patterns between δ 22 and 29, in which the higher field signal in each case displays coupling to Rh. In all cases, the presence of three terminally bound carbonyls is confirmed by the ¹³C{¹H} NMR spectra of ¹³CO-enriched products in which the high-field resonance in each case shows coupling to Rh of *ca.* 50 Hz, confirming this signal as resulting from the Rh-bound carbonyl. In the case of compound **7**, one of the Ru-bound carbonyls also displays 4 Hz coupling to Rh. This carbonyl is assigned as opposite the Rh-Ru bond, since such coupling has been observed when Rh and a carbonyl are mutually trans at an intervening

metal.¹⁶ The IR spectra of the three compounds confirm the terminal binding for all carbonyl ligands and also display the C=C stretch of the dimetallacyclopentene moiety at 1574 cm⁻¹. A broad carbonyl stretch at 1705 cm⁻¹ is observed for the carboxylate group of **6**, while that of **8** appears at 1695 cm⁻¹. In all cases, the ¹H NMR spectra of compounds **6-8** display the dppm-methylene resonances in the range δ 3.7-5.1 and the metal-bound methylene group between approximately δ 1.5 and 1.8. The two dppm resonances are consistent with different environments on either side of the "RhRuP₄" plane and have the typical appearance, which simplifies to an AB quartet upon broad-band ³¹P decoupling. The metal-bound methylene group in each case appears as a triplet, showing coupling to the Ru-bound ³¹P nuclei, consistent with alkyne insertion having occurred into the Rh-CH₂ bond. In addition to the above ¹H resonances, compound **6** displays two separate resonances for the methyl groups of the inserted DMAD molecule, and **8** shows the corresponding resonances for the two inequivalent ethyl groups. The inequivalence of the two methyl groups of **6** and the two ethyl groups of **8** is consistent with the insertion products diagrammed in Scheme 3.1. By the same token, the ¹⁹F NMR spectrum of **7** displays two broad singlets at δ -46.7 and -61.9 for the inequivalent CF₃ groups. Additional support for alkyne insertion into the Rh-CH₂ bond comes from the ¹³C{¹H} NMR spectra of ¹³CH₂-enriched samples of **6** and **7**, which show the methylene resonances as triplets at δ 15.3 and 13.8, respectively, displaying coupling to only the Ru-bound ³¹P nuclei. In contrast, the methylene resonance in the precursor (2-¹³CH₂) appears at δ 97.0 and shows coupling to all four ³¹P nuclei and to Rh (25 Hz).⁹

Support for the structures proposed for complexes **6 - 8** comes from the X-ray structure determination of compound **7**. A representation of the complex cation is

diagrammed in Figure 3.1, with relevant bond lengths and angles given in Table 3.3. Although both dppm ligands are bridging the metals in the common manner, in which these groups are essentially trans on each metal, there is significant twisting of the two coordination geometries about the metal-metal vector, to give an average torsion angle of approximately 26° . This staggering of the ligands on adjacent metals may occur to minimize nonbonded contacts, which otherwise would be quite severe because of the short Rh-Ru distance ($2.7771(3) \text{ \AA}$), and may also result from the strain imposed by the bridging C_3 fragment. As deduced from the spectral data, alkyne insertion into the Rh- CH_2 bond of **4** has occurred, leaving the Ru- CH_2 bond intact. Within the resulting C_3 -bridged fragment the bond lengths and angles are as expected. The C(4)-C(5) distance ($1.344(4) \text{ \AA}$) is typical of a double bond,¹⁷ while the C(4)-C(7), C(5)-C(6), and C(5)-C(8) bond lengths ($1.499(4)$, $1.505(4)$, $1.513(4) \text{ \AA}$, respectively) are typical of single bonds between sp^2 and sp^3 carbons.^{17,18} Similarly, the angles at C(4) and C(5) are also consistent with sp^2 hybridization of these atoms, while the smaller Ru-C(6)-C(5) angle ($114.2(2)^\circ$) is consistent with sp^3 hybridization at C(6), although this is still larger than the idealized 109.5° . It should be noted that twisting of the two metal octahedra about the Rh-Ru bond to give a somewhat eclipsed geometry would result in an ever larger angle at C(6), lending support to the argument that the staggered geometry results from strain imposed by the bridging C_3 ligand. The shorter Rh-C(4) bond compared to Ru-C(6) ($2.095(3)$ vs. $2.171(3) \text{ \AA}$) also probably reflects the hybridization difference of these two carbon atoms.

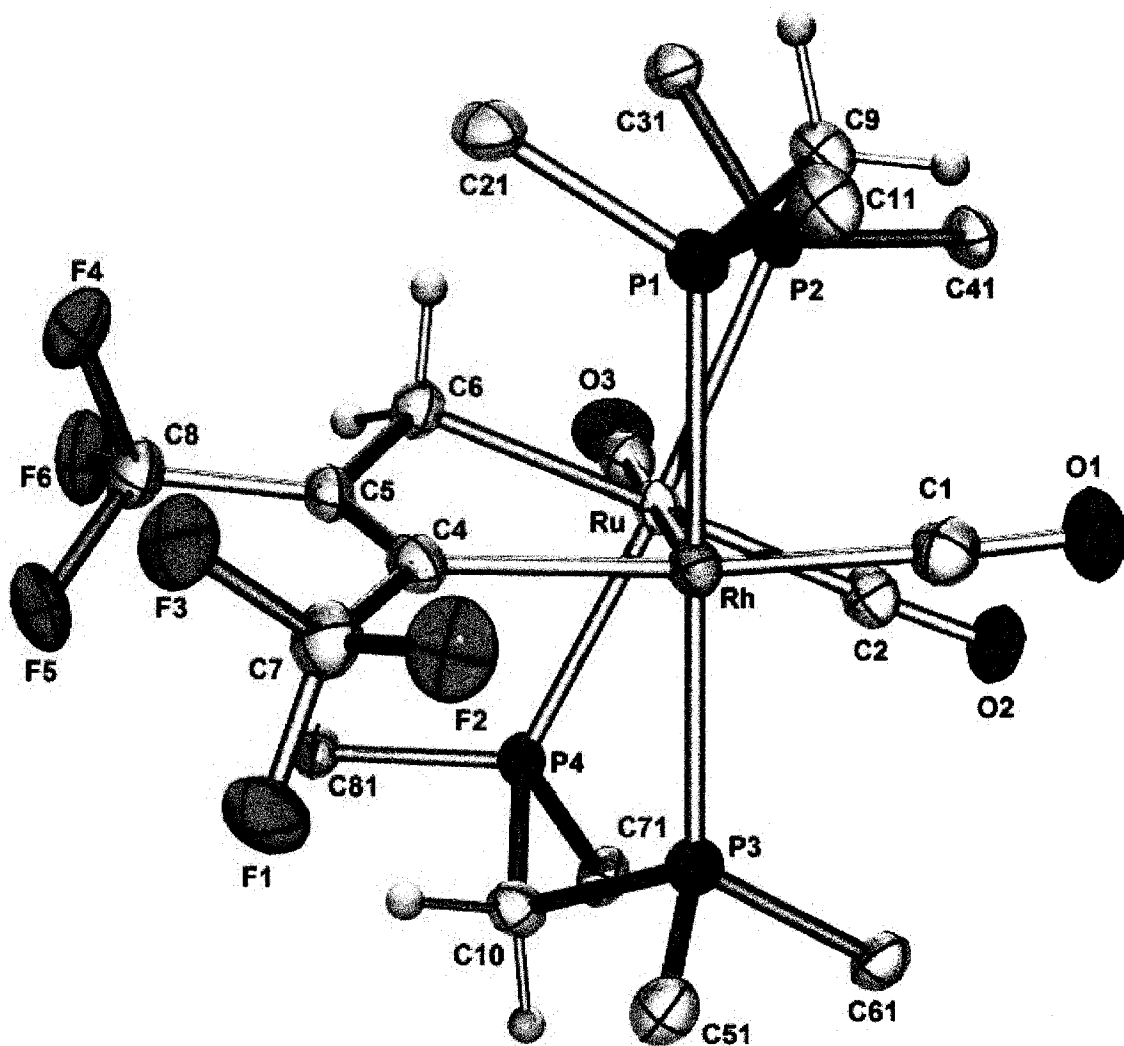


Figure 3.1: Perspective view of the complex cation of compound 7, showing the numbering scheme. Thermal ellipsoids are drawn at the 20% level except for methylene hydrogens, which are drawn arbitrarily small. Phenyl groups, except for ipso carbons, are omitted.

Table 3.3: Selected Distances and Angles for Compound 7.*(i) Distances (Å)*

Atom 1	Atom 2	Distance	Atom 1	Atom 2	Distance
Rh	Ru	2.7771(3)	P(1)	C(9)	1.832(3)
Rh	P(1)	2.3324(8)	P(2)	C(9)	1.843(3)
Rh	P(3)	2.3327(8)	P(3)	P(4)	3.0062(9) ^a
Rh	C(1)	1.891(3)	O(1)	C(1)	1.130(4)
Rh	C(4)	2.095(3)	O(2)	C(2)	1.139(4)
Ru	P(2)	2.3928(7)	O(3)	C(3)	1.147(3)
Ru	P(4)	2.4045(7)	C(4)	C(5)	1.344(4)
Ru	C(2)	1.945(3)	C(4)	C(7)	1.499(4)
Ru	C(3)	1.851(3)	C(5)	C(6)	1.505(4)
Ru	C(6)	2.171(3)	C(5)	C(8)	1.513(4)
P(1)	P(2)	3.091(1) ^a			

(ii) Angles (deg)

Atom 1	Atom 2	Atom 3	Angle	Atom 1	Atom 2	Atom 3	Angle
Ru	Rh	P(1)	94.35(1)	P(4)	Ru	C(3)	89.88(9)
Ru	Rh	P(3)	87.73(1)	P(4)	Ru	C(6)	86.56(8)
Ru	Rh	C(1)	92.96(9)	C(2)	Ru	C(3)	92.9(1)
Ru	Rh	C(4)	84.80(8)	C(2)	Ru	C(6)	174.3(1)
P(1)	Rh	P(3)	177.92(3)	C(3)	Ru	C(6)	92.8(1)
P(1)	Rh	C(1)	86.7(1)	Rh	P(1)	C(9)	108.4(1)
P(1)	Rh	C(4)	89.07(8)	Ru	P(2)	C(9)	116.49(9)
P(3)	Rh	C(1)	93.13(10)	P(2)	Ru	P(4)	175.75(3)
P(3)	Rh	C(4)	91.19(8)	P(2)	Ru	C(2)	89.89(9)
C(1)	Rh	C(4)	175.0(1)	Rh	C(1)	O(1)	177.3(3)
Rh	Ru	P(2)	89.40(1)	Ru	C(2)	O(2)	178.1(3)
Rh	Ru	P(4)	92.20(1)	Ru	C(3)	O(3)	178.6(3)
Rh	Ru	C(2)	90.64(8)	Rh	C(4)	C(5)	123.3(2)
Rh	Ru	C(3)	175.7(1)	Rh	C(4)	C(7)	112.9(2)
Rh	Ru	C(6)	83.64(7)	C(5)	C(4)	C(7)	123.7(3)
P(2)	Ru	P(4)	175.75(3)	C(4)	C(5)	C(6)	122.2(3)
P(2)	Ru	C(2)	89.89(9)	C(4)	C(5)	C(8)	123.9(3)
P(2)	Ru	C(3)	88.27(9)	C(6)	C(5)	C(8)	113.3(2)
P(2)	Ru	C(6)	89.71(8)	Ru	C(6)	C(5)	114.2(1)
P(4)	Ru	C(2)	94.03(9)				

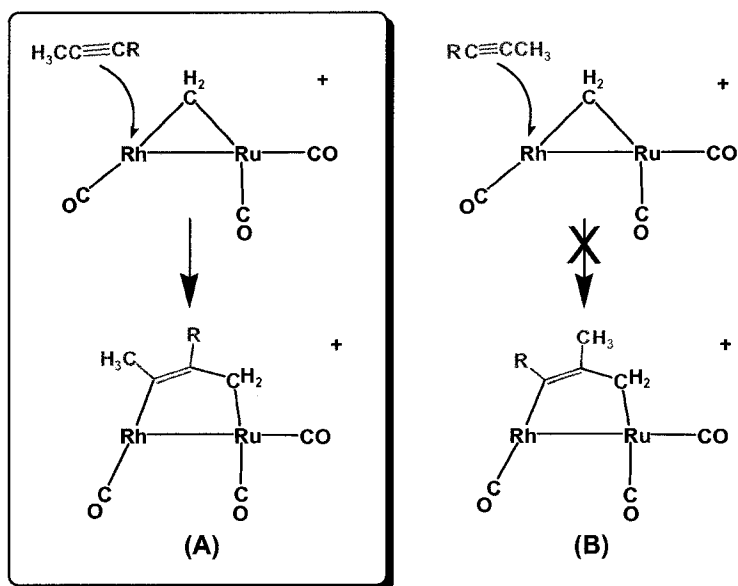
^a Non-bonded distance.

It was hoped that compound **6** might be susceptible to further methylene incorporation to yield a C₄-bridged species containing one methylene group bound to each metal with a DMAD moiety in between. Unfortunately, treatment of **6** with diazomethane under a variety of conditions afforded no new organometallic species.

The unsymmetrical alkynes 2-butyn-1-yl dimethylacetal (BDA) and 2-butyn-1-ol also react readily with **4**, giving the products $[\text{RhRu}(\text{CO})_3(\mu\text{-}\eta^1\text{:}\eta^1\text{-C}(\text{R})=\text{C}(\text{R}')\text{CH}_2)(\text{dppm})_2][\text{CF}_3\text{SO}_3]$ (R = CH₃; R' = CH(CO₂Et)₂ (**9**), CH₂OH (**10**)), in which alkyne insertion into the Rh-CH₂ bond has again occurred. These products are analogous to compounds **6** - **8** and show spectroscopic parameters (see Table 3.1) very similar to these products. Although compounds **9** and **10** could, in principle, give rise to two isomers resulting from alkyne insertion into the Rh-CH₂ bond, in which either the methyl substituent or the oxygen-containing substituent ends up adjacent to the methylene group, as shown in Scheme 3.2, only the latter is observed. The regiochemistry in each of compounds **9** and **10** was established on the basis of 2-D NMR techniques. In a heteronuclear multiple bond correlation (HMBC) experiment, two- and three-bond carbon-hydrogen coupling is observed, while four-bond carbon-hydrogen coupling is not. In these experiments, coupling between the carbon of the methylene group and the single hydrogen of the adjacent CH(CO₂Et)₂ group in **9** or the pair of CH₂(OH) hydrogens of **10** was observed, while coupling of the metal-bound methylene group with the methyl group on the bound alkyne of each compound was not observed. This clearly establishes the geometry as **A** and not **B**. The driving force for the observed

regiochemistry of the alkyne insertions is unclear, it is presumed that the phenyl rings on the dppm ligands might help guide the alkyne into the orientation shown in Scheme 3.2.

Scheme 3.2

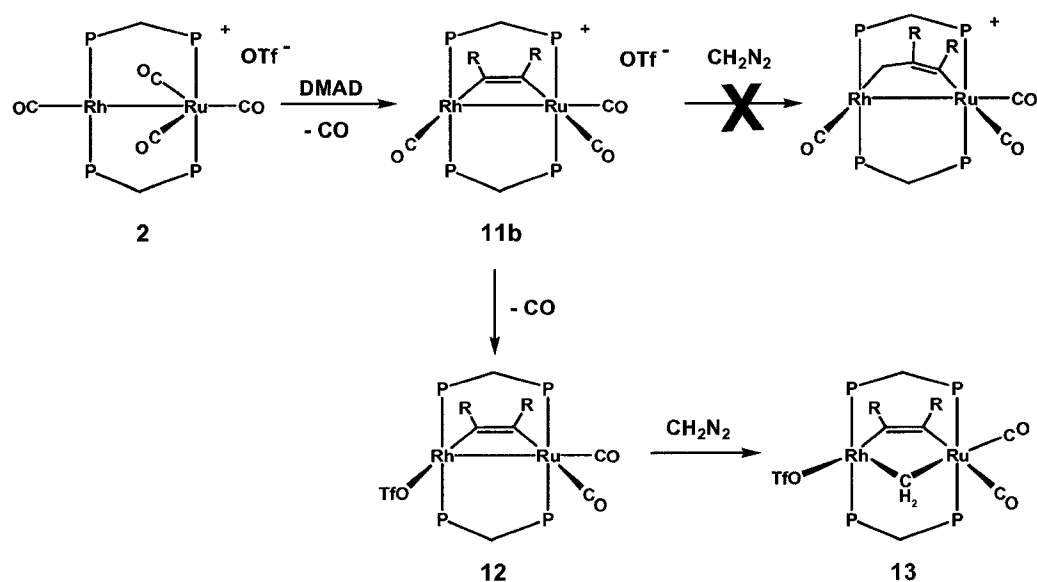


The nonactivated alkynes, acetylene, propyne, and 2-butyne, apparently do not give the analogous insertion products but yield a complex mixture of unidentified products over a range of temperatures between -80 and -20 °C has not been pursued further.

The C_2 -bridged species $[\text{RhRu}(\text{CO})_3(\mu\text{-}\eta^1\text{:}\eta^1\text{-C}(\text{CO}_2\text{Me})=\text{C}(\text{CO}_2\text{Me}))\text{-}(\text{dppm})_2][\text{X}]$ ($\text{X} = \text{BF}_4$ (**11a**), CF_3SO_3 (**11b**)) were obtained by the reaction of dimethyl acetylenedicarboxylate with $[\text{RhRu}(\text{CO})_4(\text{dppm})_2][\text{X}]$, accompanied by CO loss. In solution, the spectral characteristics of the cations of **11a** and **11b** are identical, although complete spectral data were obtained only for **11b**. The methyl protons appear as two

singlets in the ^1H NMR spectrum (δ 2.71 and 2.32), indicating two chemically inequivalent methyl environments, consistent with the structure shown in Scheme 3.3. In addition, the presence of two dppm-methylene resonances indicates "front-back" asymmetry in the complex. Both ^{31}P resonances in the $^{31}\text{P}\{^1\text{H}\}$ NMR spectrum are

Scheme 3.3



overlapping, giving rise to a complex pattern centered at δ 19.9, while the $^{13}\text{C}\{^1\text{H}\}$ NMR data and the IR spectrum indicate that the three carbonyls are terminally bound (see Table 3.1).

The structure of **11a** was confirmed by an X-ray structure determination, and a representation of the complex cation is diagrammed in Figure 3.2, with important bond lengths and angles given in Table 3.4. The alkyne moiety bridges the metals in a parallel arrangement in which the C(4)-C(5) axis is almost parallel to the metal-metal axis.

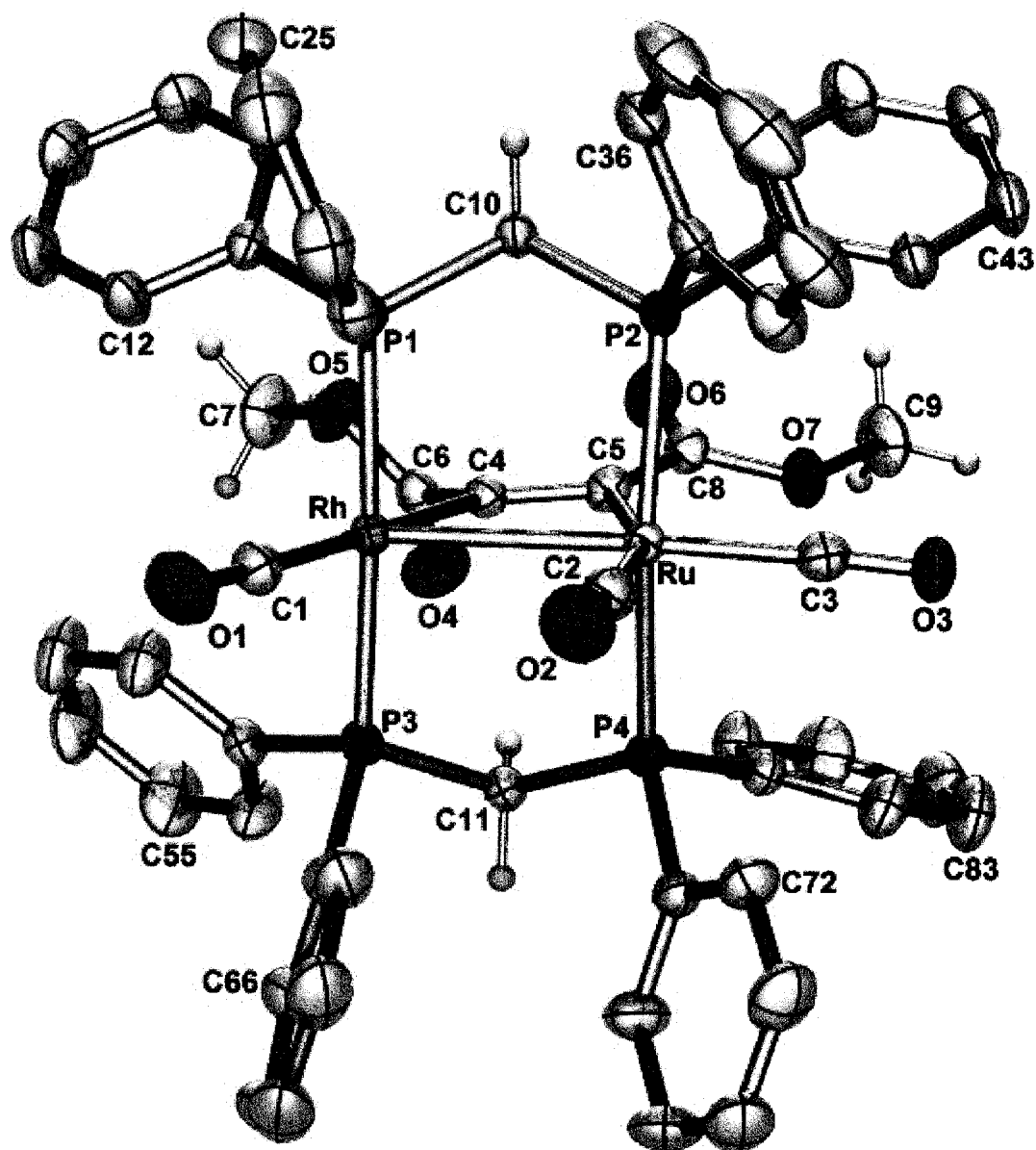


Figure 3.2: Perspective view of the complex cation of compound 11a. Thermal ellipsoids are as described in Figure 1. Each phenyl ring carbon is numbered from C(*n*1) to C(*n*6) starting at the ipso carbon, where *n* = 1 to 8 for the eight phenyl rings.

Table 3.4: Selected Distances and Angles for Compound **11a**.*(i) Distances (Å)*

Atom 1	Atom 2	Distance	Atom 1	Atom 2	Distance
Rh	Ru	2.8627(4)	Ru	C(3)	1.858(4)
Rh	P(1)	2.3123(9)	Ru	C(5)	2.070(3)
Rh	P(3)	2.312(1)	O(1)	C(1)	1.144(5)
Rh	C(1)	1.898(4)	O(1)	C(1)	1.144(5)
Rh	C(4)	2.110(4)	O(2)	C(2)	1.130(5)
Ru	P(2)	2.390(1)	O(3)	C(3)	1.138(5)
Ru	P(4)	2.410(1)	C(4)	C(5)	1.332(5)
Ru	C(2)	1.950(4)			

(ii) Angles (deg)

Atom 1	Atom 2	Atom 3	Angle	Atom 1	Atom 2	Atom 3	Angle
Ru	Rh	P(1)	91.19(2)	P(2)	Ru	C(3)	90.2(1)
Ru	Rh	P(3)	92.71(3)	P(2)	Ru	C(5)	81.6(1)
Ru	Rh	C(1)	118.3(1)	P(4)	Ru	C(2)	98.2(1)
Ru	Rh	C(4)	62.6(1)	P(4)	Ru	C(3)	86.1(1)
P(1)	Rh	P(3)	172.60(3)	P(4)	Ru	C(5)	83.6(1)
P(1)	Rh	C(1)	91.1(1)	C(2)	Ru	C(3)	97.4(1)
P(1)	Rh	C(4)	88.6(1)	C(2)	Ru	C(5)	158.9(1)
P(3)	Rh	C(1)	92.55(1)	C(3)	Ru	C(5)	103.7(1)
P(3)	Rh	C(4)	87.6(1)	Rh	C(1)	O(1)	177.5(4)
C(1)	Rh	C(4)	179.1(1)	Ru	C(2)	O(2)	175.2(4)
Rh	Ru	P(2)	92.37(2)	Ru	C(3)	O(3)	176.8(4)
Rh	Ru	P(4)	90.65(2)	Rh	C(4)	C(5)	122.3(3)
Rh	Ru	C(2)	84.8(1)	Rh	C(4)	C(6)	114.9(3)
Rh	Ru	C(3)	176.2(1)	C(5)	C(4)	C(6)	122.5(3)
Rh	Ru	C(5)	74.1(1)	Ru	C(5)	C(4)	100.7(3)
P(2)	Ru	P(4)	163.54(4)	Ru	C(5)	C(8)	133.5(3)
P(2)	Ru	C(2)	98.2(1)	C(4)	C(5)	C(8)	125.7(3)

However, the alkyne is not symmetrically bound to both metals but is offset slightly toward Ru. As a result, the Ru-C(5)-C(4) angle ($100.7(3)^\circ$) is substantially smaller than the expected value of near 120° , while the Ru-C(5)-C(8) angle ($133.5(3)^\circ$) has opened up substantially from the expected value. By contrast, the angles at C(4) appear quite normal and are close to 120° . This asymmetry also manifests itself in a difference in Rh-C(4) and Ru-C(5) distances ($2.110(4)$ vs $2.070(3)$ Å). Apart from the asymmetric binding of the alkyne, other parameters within this bound hydrocarbyl unit are normal. Therefore, the C(4)-C(5) separation ($1.332(5)$ Å) is typical for a double bond,¹⁷ and the C(5)-C(4)-C(6) and C(4)-C(5)-C(8) angles are all near the expected 120° . The metal-metal separation ($2.8627(4)$ Å) is typical of a single bond, showing significant contraction relative to the intraligand nonbonded P-P distances of $3.015(1)$ and $3.011(1)$ Å.

Surprisingly, the C₂-bridged **11** fails to react with diazomethane to yield a C₃-bridged product analogous to compounds **6** - **10**. The targeted species would be an isomer of compound **6**, in which the methylene group was adjacent to Rh rather than Ru. However, reaction with diazomethane could be induced upon CO removal from **11b** (*vide infra*).

Removal of a carbonyl from **11b**, using Me₃NO, yields a dicarbonyl product, [RhRu(OSO₂CF₃)(CO)₂(μ-η¹:η¹-C(CO₂Me)=C(CO₂Me))(dppm)₂] (**12**). The dicarbonyl formulation is supported by the two carbonyl stretches in the IR spectrum (2003 , 1945 cm⁻¹) and the carbonyl resonances in the ¹³C{¹H} NMR spectrum, at δ 206.9 and 192.2. Neither of these carbonyls displays coupling to Rh, indicating that both are bound to Ru,

and the absence of one of these carbonyls on Rh suggests that the coordination site vacated by the carbonyl is now occupied by the triflate anion; anion coordination at Rh upon CO loss was observed in a related RhOs compound.¹⁹ Although the triflate anion is generally weakly coordinating,²⁰ its coordination is common and has been observed in numerous Rh compounds.¹⁹⁻³⁰ The possibility that a solvent molecule is coordinated to Rh instead of the triflate anion was excluded on the basis that the spectral parameters for **12** are essentially identical (apart from slight chemical shift differences) in CH₂Cl₂ and in acetone. In addition, the IR spectrum of **12** in CH₂Cl₂ shows an S-O stretch for the triflate group at 1356 cm⁻¹, consistent with coordination of this group.²⁰ The parallel coordination mode of the alkyne is supported by the appearance of two methyl resonances in the ¹H NMR spectrum, which shows the asymmetry expected based on the two different metals. All other spectroscopic parameters are similar to those of **11b**, adding further support to our proposal that no gross geometry change has occurred on transformation of **11b** to **12**.

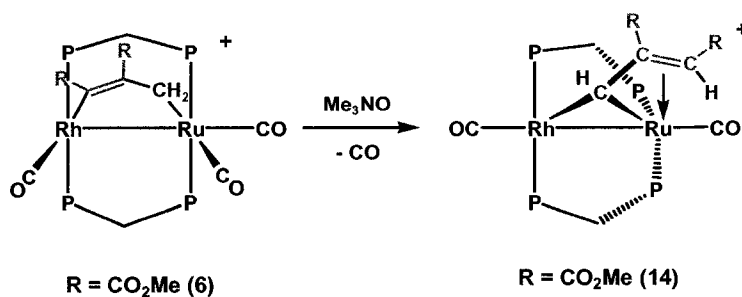
Treatment of **12** with diazomethane results in methylene group insertion into the Rh-Ru bond to give the methylene- and alkyne-bridged complex [RhRu(OSO₂CF₃)(CO)₂(μ-CH₂)(μ-DMAD)(dppm)₂] (**13**), as shown in Scheme 3.3. Again, the ¹³C{¹H} NMR spectrum shows no coupling of either carbonyl resonance to Rh, indicating that both remain bound to Ru. In the ¹H NMR spectrum the dppm methylene groups (δ 4.42, 2.74) have their usual appearance, which simplifies to an AB quartet upon broadband ³¹P decoupling. The metal-bridged methylene group appears as a pseudoquintet at δ 3.66, displaying coupling to all four ³¹P nuclei. Selective ³¹P decoupling of either ³¹P resonance results in simplification of the ¹H resonance of the

bridging methylene group to a triplet, and broadband ^{31}P decoupling yields a singlet. The absence of Rh coupling is not unusual since two-bond Rh-H coupling in hydrocarbyl fragments is usually less than 3 Hz.^{6,19,31}

The $^{31}\text{P}\{^1\text{H}\}$ NMR spectrum of **13** is atypical, appearing as a singlet (δ 26.2) for the Ru end of the diphosphines and a doublet (δ 15.3, $^1J_{\text{Rh-P}} = 142$ Hz) for the Rh end. A similar, unusually simple spectrum has been observed previously;³² in the present case the simplified spectrum appears to result from small intraligand P-P coupling, presumably a consequence of opening up of the dppm P-C-P angles upon cleavage of the Rh-Ru bond. We have previously noted a significant decrease in intraligand P-P coupling on cleavage of the metal-metal bond in related compounds.³⁰

Carbonyl removal from **6** using Me_3NO results in a hydrogen shift within the C_3 moiety and subsequent rearrangement to yield $[\text{RhRu}(\text{CO})_2(\mu\text{-}\eta^1\text{:}\eta^3\text{-CHC}(\text{CO}_2\text{CH}_3)=\text{CH}(\text{CO}_2\text{CH}_3))(\text{dppm})_2][\text{CF}_3\text{SO}_3]$ (**14**) as diagrammed in Scheme 3.4. This rearrangement is accompanied by a dramatic change in the $^{31}\text{P}\{^1\text{H}\}$ NMR spectrum from an AA'BB'X spin system in which there are two pairs of chemically inequivalent ^{31}P

Scheme 3.4



nuclei to an ABCDX spin system in which all four ^{31}P nuclei are chemically inequivalent. The appearance of only two carbonyls (one on each metal) in the $^{13}\text{C}\{^1\text{H}\}$ NMR spectrum confirms the loss of one carbonyl. In the ^1H NMR spectrum four resonances are observed for the four dppm-methylene protons and two signals appear for the inequivalent methyl groups of the DMAD ligand. Only one of the hydrogens that originated from the methylene group of **6** was unambiguously identified in the ^1H NMR spectrum (at δ 5.90). However, the ^2H NMR spectrum of a deuterium isotopomer of **14**, $[\text{RhRu}(\text{CO})_2(\mu\text{-}\eta^1\text{:}\eta^3\text{-C(D)C(CO}_2\text{Me)=CD(CO}_2\text{Me))}(\text{dppm})_2][\text{CF}_3\text{SO}_3]$, prepared from the $\mu\text{-CD}_2$ isotopomer of **6**, revealed the missing resonance of the vinylic deuterium at δ 3.90, typical for such a species.³³ The presence of this proton was confirmed by HMQC NMR experiments on compound **14**, in which the proton at δ 3.90 correlated with a carbon resonance at δ 55.0, also typical of such an arrangement.^{34,35} If a sample of **14** is prepared from $^{13}\text{CH}_2$ -enriched **3**, the single hydrogen at δ 5.90 shows 175 Hz coupling to the ^{13}C nucleus, confirming that these nuclei are mutually bonded. That this ^{13}C nucleus has only one proton attached was confirmed by both the presence of a positive signal in the $^{13}\text{C}\{^1\text{H}\}$ APT NMR spectrum and the appearance of a doublet of doublet of multiplets in the ^{13}C NMR spectrum with coupling of 175 Hz to only a single hydrogen nucleus. In the $^{13}\text{C}\{^1\text{H}\}$ NMR spectrum this carbon, at δ 110.2, appears as a doublet of multiplets. The large splitting of 73 Hz was confirmed to be due to coupling to phosphorus, based on ^{31}P decoupling experiments, and the magnitude of this coupling suggests a close-to-trans arrangement of the CH moiety and one end of the diphosphine unit. Selective ^{31}P decoupling experiments show that this large coupling is due to a Ru-bound phosphine. In the $^{13}\text{C}\{^1\text{H},^{31}\text{P}\}$ NMR spectrum the resonance due to the CH group

displays 23 Hz coupling to Rh, consistent with this unit occupying a bridging position. On the basis of these NMR data the structure shown in Scheme 3.4 is proposed, which is very similar to that confirmed in an X-ray study for $[\text{Ir}_2\text{H}(\text{CO})_2(\mu, \eta^1: \eta^3\text{-HCC}(\text{Et})\text{C}(\text{H})\text{Et})(\text{dppm})_2][\text{CF}_3\text{SO}_3]$, previously studied in our group.³³ Unfortunately, we were unable to obtain crystals of **14** suitable for an X-ray study, to confirm the proposed geometry.

The reaction of **4** with propargyl alcohol ($\text{HC}\equiv\text{CCH}_2\text{OH}$) occurs very differently than with the previously noted alkynes, yielding a product that has incorporated two alkyne molecules. Even if less than 2 equiv of the alkyne is utilized, only the "double-insertion" product $[\text{RhRu}(\text{CO})_2(\mu\text{-}\eta^2: \eta^4\text{-CH}=\text{C}(\text{CH}_2\text{OH})\text{CH}=(\text{CH}_2\text{OH})\text{CH}_2)(\text{dppm})_2][\text{CF}_3\text{SO}_3]$ (**15**) is obtained, together with unreacted starting material. The structure of this compound has been established by X-ray crystallography, and a representation of the complex cation of **15** is shown in Figure 3.3, with important bond lengths and angles given in Table 3.5. This structure determination clearly confirms that two alkynes have coupled in a head-to-tail manner with the methylene group, to form a rhodacyclohexadiene fragment. Both olefinic bonds of this rhodacyclohexadiene unit are also π -bonded to Ru, with Ru-C distances varying from 2.202(7) to 2.395(8) Å. As a consequence of the binding of this diolefin to Ru, the C(3)-C(4) and C(5)-C(6) bonds (1.39(1) and 1.39(1) Å) are somewhat elongated compared to normal double bonds.¹⁷ Although the Rh-C(3)-C(4)-C(5)-C(6) fragment is very close to planar, the methylene carbon (C(7)) lies 0.85(1) Å out of this plane. This is shown clearly in the alternate view of **15** shown in Figure 3.4. Both diphosphine ligands are bent back, away from the bridging hydrocarbyl group, with P(2)-Rh-P(4) and P(1)-Ru-P(3) angles of 105.61(7)°

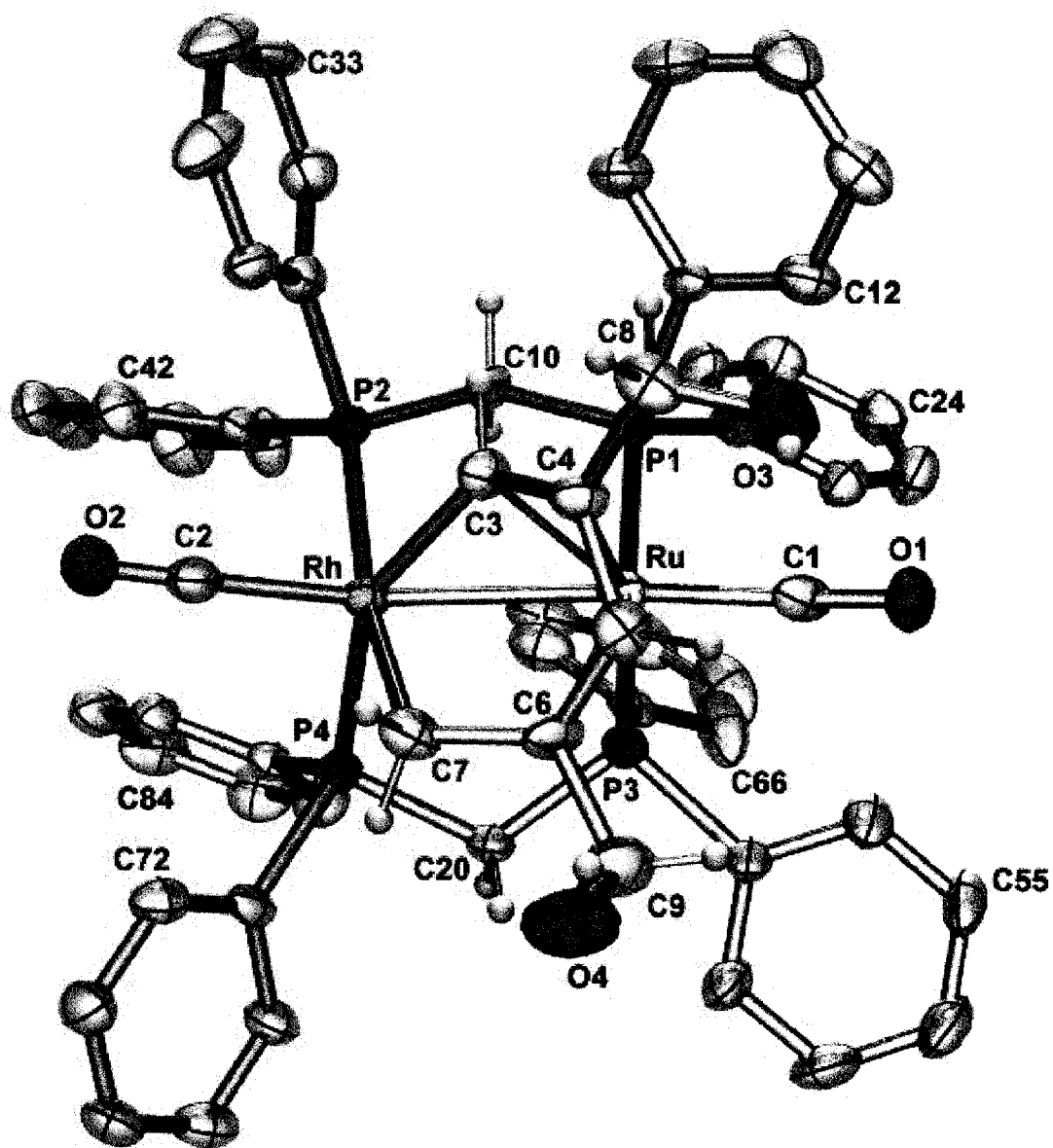


Figure 3.3: Perspective view of the complex cation of compound 15. Thermal ellipsoids and numbering are as described in Figure 2, except that the hydroxyl protons are also shown arbitrarily small.

Table 3.5. Selected Distances and Angles for Compound 15.*(i) Distances (Å)*

Atom 1	Atom 2	Distance	Atom 1	Atom 2	Distance
Rh	Ru	2.7722(8)	Ru	C6	2.395(8)
Rh	P2	2.369(2)	P1	P2	3.131(3) [†]
Rh	P4	2.362(1)	P3	P4	3.142(3) [†]
Rh	C2	1.912(8)	O1	C1	1.149(8)
Rh	C3	2.043(7)	O2	C2	1.125(9)
Rh	C7	2.116(8)	O3	C8	1.412(9)
Ru	P1	2.337(2)	O4	C9	1.50(1)
Ru	P3	2.330(1)	C3	C4	1.39(1)
Ru	C1	1.873(8)	C4	C5	1.43(1)
Ru	C3	2.202(7)	C4	C8	1.53(1)
Ru	C4	2.270(7)	C5	C6	1.39(1)
Ru	C5	2.227(8)	C6	C7	1.48(1)

(ii) Angles (deg)

Atom 1	Atom 2	Atom 3	Angle	Atom 1	Atom 2	Atom 3	Angle
Ru	Rh	P2	94.21(5)	P1	Ru	C6	161.0(1)
Ru	Rh	P4	98.24(5)	P3	Ru	C1	93.6(2)
Ru	Rh	C2	159.7(2)	P3	Ru	C3	137.1(1)
Ru	Rh	C3	51.8(2)	P3	Ru	C4	154.9(2)
Ru	Rh	C7	77.8(2)	P3	Ru	C5	122.6(2)
P2	Rh	P4	105.61(7)	P3	Ru	C6	91.5(1)
P2	Rh	C2	92.1(3)	C1	Ru	C3	129.2(3)
P2	Rh	C3	82.2(2)	C1	Ru	C4	97.1(3)
P2	Rh	C7	168.2(2)	C1	Ru	C5	84.2(3)
P4	Rh	C2	98.5(2)	C1	Ru	C6	101.8(3)
P4	Rh	C3	149.9(2)	C3	Ru	C4	36.2(3)
P4	Rh	C7	84.3(2)	C3	Ru	C5	66.6(3)
C2	Rh	C3	110.4(3)	C3	Ru	C6	77.6(3)
C2	Rh	C7	92.7(3)	C4	Ru	C5	37.0(3)
C3	Rh	C7	86.1(3)	C4	Ru	C6	64.1(3)
Rh	Ru	P1	94.53(5)	C5	Ru	C6	34.8(3)
Rh	Ru	P3	90.43(5)	Ru	C1	O1	174.4(7)
Rh	Ru	C1	170.1(2)	Rh	C2	O2	177.9(8)
Rh	Ru	C3	46.8(1)	Rh	C3	Ru	81.5(2)
Rh	Ru	C4	75.8(1)	Rh	C3	C4	129.9(6)
Rh	Ru	C5	86.0(2)	Ru	C3	C4	74.6(4)
Rh	Ru	C6	69.0(1)	Ru	C4	C3	69.2(4)
P1	Ru	P3	98.27(8)	Ru	C4	C5	69.8(4)

(ii) *Angles (deg) (cont'd...)*

P1	Ru	C1	93.9(2)	Ru	C4	C8	130.1(5)
P1	Ru	C3	84.2(2)	C3	C4	C5	119.3(7)
P1	Ru	C4	103.6(2)	C3	C4	C8	121.6(7)
P1	Ru	C5	139.1(2)	C5	C4	C8	118.9(7)

† Non-bonded distance.

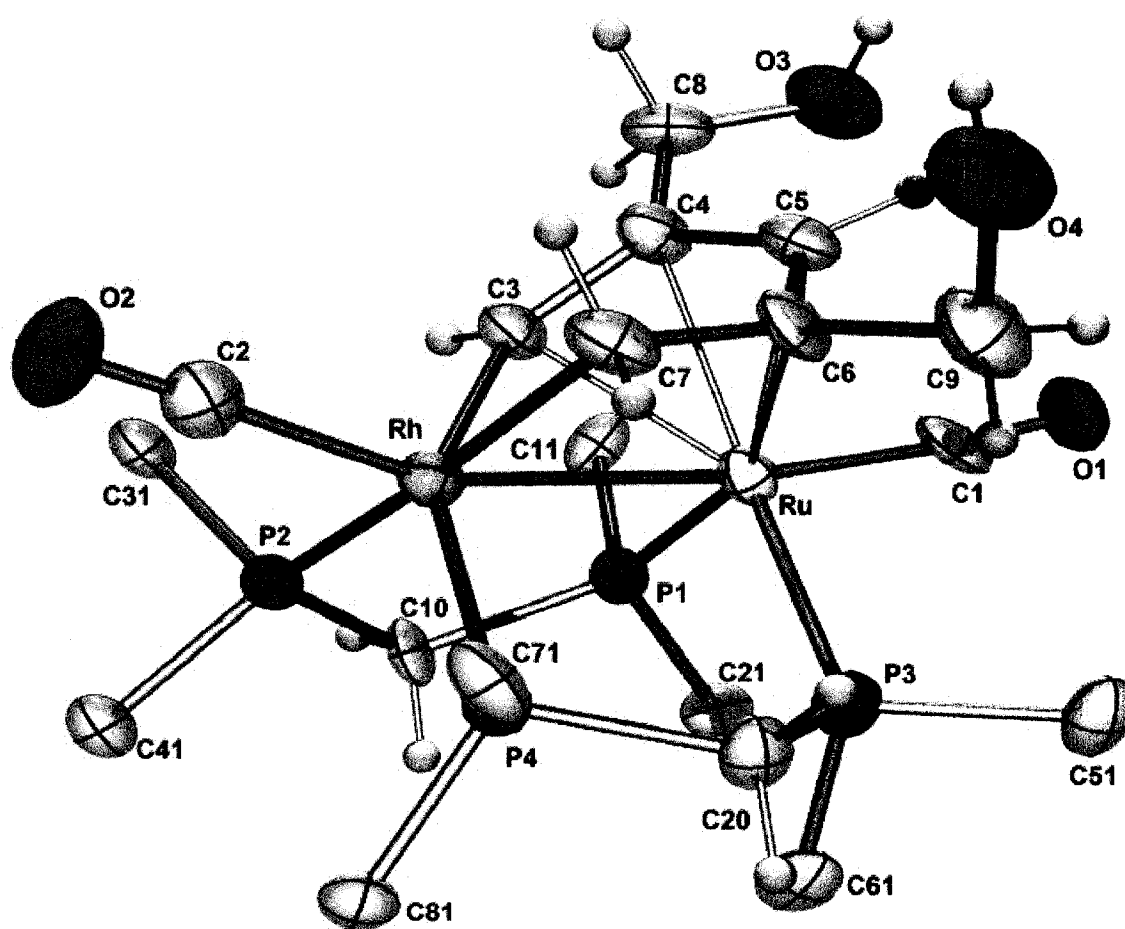


Figure 3.4: Alternate view of the cation of **15** in which the phenyl carbons, except for the ipso carbons, are omitted.

and $98.27(8)^\circ$, respectively. The geometry at both metals can be described as octahedral. At Rh, the hydrocarbyl group resulting from coupling of the methylene group and two alkynes occupies two cis positions, as do the two ends of the diphosphines; the carbonyl on this metal is opposite the metal-metal bond. Ruthenium has a rather similar geometry except that two of the mutually cis coordination sites are occupied by the two π -interactions involving the metallacyclohexadienyl fragment.

Although both Rh-C bonds of the metallacycle are normal, that involving the vinylic fragment (Rh-C(3) = 2.043(7) Å) is significantly shorter than the Rh-alkyl bond (Rh-C(7) = 2.116(8) Å) at the other end. This difference presumably reflects (in part) the differences in hybridization of both carbon atoms;¹⁸ however, additional shortening of the Rh-vinyl bond may be due to π back-bonding from the metal.

NMR spectroscopic studies suggest that the structure described above is maintained in solution. For example, the $^{31}\text{P}\{^1\text{H}\}$ NMR spectrum shows four separate phosphorus resonances and the ^1H NMR spectrum shows a separate resonance for each of the four dppm methylene hydrogens. In addition, the protons on the methylene group of the hydrocarbyl fragment are chemically distinct (δ 2.03 and 0.77) and display coupling to the Rh-bound ^{31}P nuclei. The resonance for the vinylic proton of C(5) of the diolefin fragment is observed at δ 6.03 as a singlet, showing no coupling to Rh or to its bound phosphine ligands. That of the proton on C(3) is not observed, but is shown by a ^1H COSY NMR experiment to be at δ 7.60 on the basis of its very weak coupling to the proton on C(5). Similarly, both alcoholic protons are coincident at δ 2.80, and ^1H COSY experiments show coupling of these protons to the pairs of adjacent methylene protons at

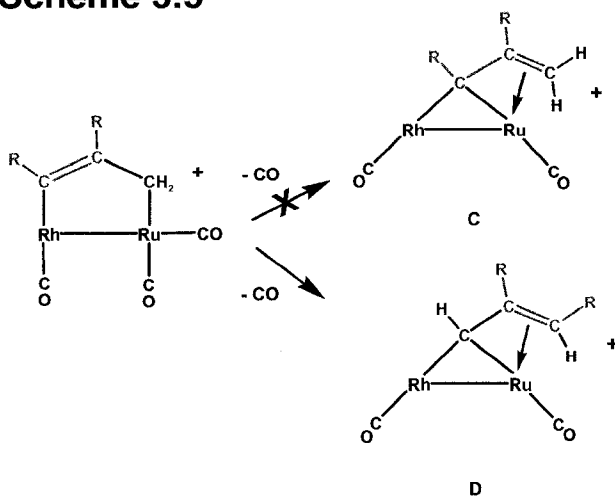
δ 3.71 and 3.60 and at δ 3.24 and 2.55. The $^{13}\text{C}\{^1\text{H}\}$ NMR and IR spectra show that both carbonyls are terminally bound, and the former spectrum establishes that one is bound to each metal on the basis of the 67 Hz coupling of one of these to Rh.

Discussion:

Our earlier observation of facile coupling of diazomethane-derived methylene groups at a Rh/Os core⁶ to yield either allyl or butanediyl fragments suggested to us the intermediacy of a C_3H_6 -bridged propanediyl species. Elimination of a β -hydrogen from the central carbon of this C_3 intermediate would yield the allyl group, whereas insertion of an additional methylene group would yield the butanediyl fragment. We have attempted to model this putative C_3 -bridged species by insertion of alkynes into one of the metal- CH_2 bonds of $[\text{RhRu}(\text{CO})_4(\mu\text{-CH}_2)(\text{dppm})_2][\text{CF}_3\text{SO}_3]$ (**3**). Although this reaction proceeds with varying degrees of success, depending on the alkyne, the anticipated products are obtained much more readily by first converting **3** into the tricarbonyl, $[\text{RhRu}(\text{CO})_3(\mu\text{-CH}_2)(\text{dppm})_2][\text{CF}_3\text{SO}_3]$ (**4**), followed by the reactions with alkynes. The resulting products, $[\text{RhRu}(\text{CO})_3(\mu\text{-}\eta^1\text{:}\eta^1\text{-RC=C(R')CH}_2)(\text{dppm})_2][\text{CF}_3\text{SO}_3]$ ($\text{R} = \text{R}' = \text{CO}_2\text{Me}$ (**6**), CF_3 (**7**), CO_2Et (**8**); $\text{R} = \text{Me}$, $\text{R}' = \text{CH}(\text{OEt})_2$ (**9**), $\text{R}' = \text{CH}_2\text{OH}$ (**10**)), have the so-formed C_3 fragment bridging the metals with the vinylic end of this fragment bound to Rh and the alkyl end bound to Ru. This arrangement is analogous to that proposed for the putative C_3H_6 fragment in the Rh/Os system.⁶ Although insertion of the nonactivated alkynes, acetylene, propyne, and 2-butyne, into the Rh- CH_2 bond of **3** or **4** would have given rise to better models for the above C_3H_6 -bridged intermediate,⁶ these simple insertion products did not result. Instead, mixtures of unidentified products

resulted. The products of alkyne insertion in this report are in contrast to the products previously obtained from alkyne insertion in " $\text{Fe}_2(\mu\text{-CH}_2)$ ",^{34,36} " $\text{Ru}_2(\mu\text{-CH}_2)$ ",³⁷⁻⁴¹ " $\text{FeRu}(\mu\text{-CH}_2)$ ",³⁵ and " $\text{Rh}_2(\mu\text{-CH}_2)_2$ "⁴² units, in which the resulting C_3 fragments could be viewed as vinyl carbenes. Unlike our bridging " $\text{RC}=\text{C}(\text{R}')\text{CH}_2$ " unit, which functions as a neutral two-electron donor, the vinyl carbene functions as a four-electron donor. We

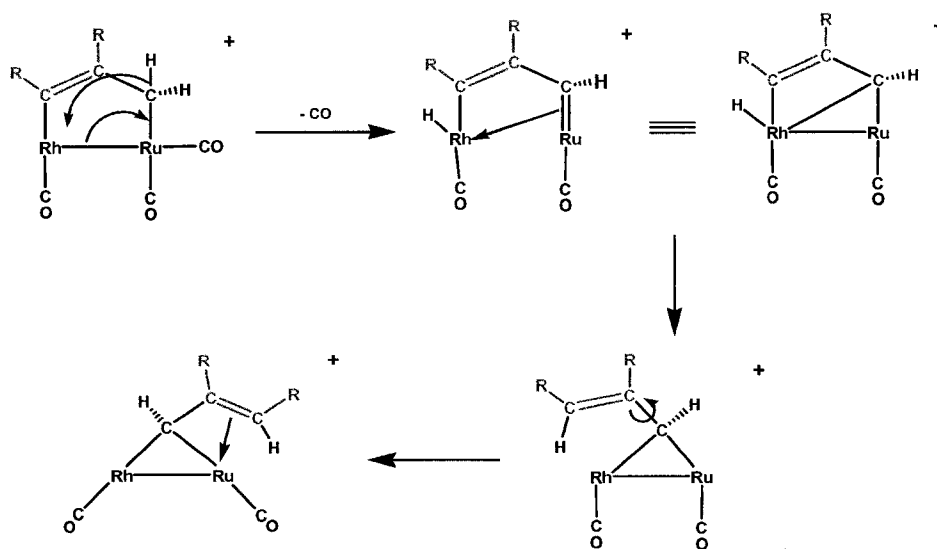
Scheme 3.5



therefore anticipated that removal of a carbonyl from our dimetallacyclopentene complexes could lead to a transformation of the bridging hydrocarbyl group to a vinyl carbene (C) with the two-electron deficiency resulting from CO loss being alleviated by the ligand transformation shown in Scheme 3.5 (dppm groups above and below the plane of the page are omitted for the sake of clarity). Surprisingly, carbonyl loss from **6** does not generate the anticipated product, but instead yields compound **14**, corresponding to the isomer **D**, in which a 1,3-hydrogen shift and an accompanying rearrangement has occurred, moving the fragment originating from the alkyne molecule from the Rh end to the Ru end of the complex.

The reason for this isomerization is not clear, although having a hydrogen on the bridging carbene carbon, as observed in **14**, rather than a larger CO₂Me group, as in the anticipated product, is sterically favoured. The proposed mechanism for this transformation is shown in Scheme 3.6. The methylene group adjacent to Ru in **6** is in a

Scheme 3.6

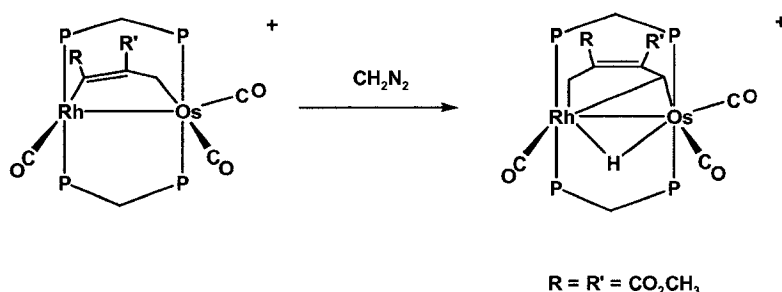


β position to Rh, and the attached hydrogen appears to be in a position that may be favourable toward β -elimination. This type of β -elimination has been observed in the Rh/Os system with a bridging C₄ unit (vide infra). Reductive elimination of the vinylic end of the C₃ moiety with the hydride followed by rotation of the alkene end will complete the migration. Analogous hydrogen migrations have previously been observed in related chemistry in which the vinyl carbene products, [Fe₂(CO)₇(μ , η^1 : η^3 -C(H)C(H)C(H)Ph)]³⁶ and [Ir₂H(CO)₂(μ , η^1 : η^3 -C(H)C(R)C(H)R)(dppm)₂][CF₃SO₃] (R = C₂H₅),³³ were obtained. In these examples, as for compound **14** in this report, the products have a less substituted carbene carbon than would have resulted without

hydrogen migration. Although the origin of the above diiridium species appears to differ, having resulted from alkyne attack at a methyl complex, we now believe that it also proceeded via a methylene-bridged alkyne adduct and that subsequent alkyne insertion and hydrogen migration occurred much as proposed for the above Fe₂ system and for the RhRu system reported herein.

Diazomethane addition to **6**, in an attempt to transform the C₃-bridged species into a C₄-bridged product did not afford any new complexes. This is in contrast to the RhOs analogue in which the targeted methylene incorporation is observed (Scheme 3.7).⁴³ It is unclear why the RhOs analogue of **6** incorporates a methylene group to yield a new C₄-bridged species while compound **6** does not. Both complexes appear to have the same steric limitations at the Rh centre, where presumably initial CH₂N₂ coordination will take place.

Scheme 3.7



In the case of the unsymmetrical alkynes, MeC≡CCH(OEt)₂ and MeC≡CCH₂OH, insertion occurs to yield the products having the bulkier CH(OEt)₂ and CH₂OH groups adjacent to the methylene group. This is in contrast to the regiochemistry demonstrated

for the insertion of unsymmetrical alkynes into the methylene bridges of the complexes $[\text{Ru}_2(\text{NCMe})(\text{CO})_2(\text{Cp})_2(\mu\text{-CH}_2)]$,⁴¹ $[\text{Ru}_2(\text{NCMe})(\text{CO})\text{Cp}_2(\mu\text{-CH}_2)_2]$,³⁷ and $[\text{FeRu}(\text{CO})_3\text{Cp}_2(\mu\text{-CH}_2)]$,³⁵ in which the less sterically crowded alkyne carbon usually ended up bonded to the methylene group. In the reaction of $[\text{Ru}_2(\text{NCMe})(\text{CO})_2(\text{Cp})_2(\mu\text{-CH}_2)]$ with 3-phenyl-2-propyn-1-ol ($\text{PhC}\equiv\text{CCH}_2\text{OH}$), insertion gave both isomers.⁴¹ Clearly the steric demands of the dppm-bridged system differ substantially from those of the above Cp complexes.

In all alkyne-insertion reactions reported herein, insertion has occurred into the Rh-CH₂ bond rather than the Ru-CH₂ bond. This presumably reflects the coordinative unsaturation at Rh, allowing alkyne coordination at this metal, followed by insertion into the adjacent Rh-CH₂ bond.

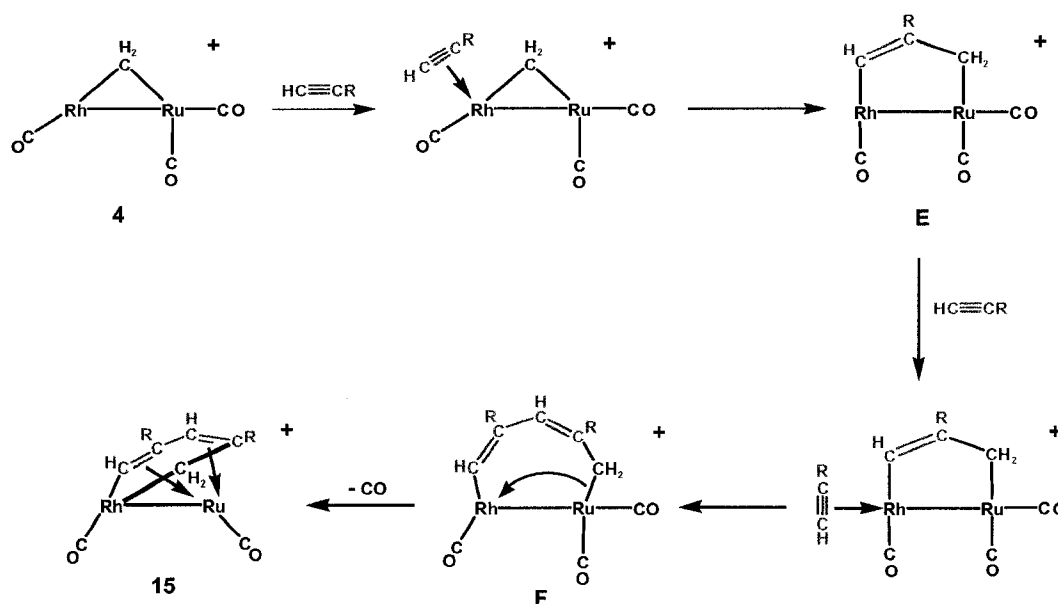
We attempted to obtain the isomeric C₃-bridged species $[\text{RhRu}(\text{CO})_3(\mu\text{-}\eta^1\text{:}\eta^1\text{-CH}_2\text{C}(\text{R})=\text{C}(\text{R}))(\text{dppm})_2][\text{CF}_3\text{SO}_3]$, in which the methylene group was adjacent to Rh instead of Ru, by reaction of the alkyne-bridged product $[\text{RhRu}(\text{CO})_3(\mu\text{-}\eta^1\text{:}\eta^1\text{-C}(\text{CO}_2\text{Me})=\text{C}(\text{CO}_2\text{Me}))(\text{dppm})_2][\text{CF}_3\text{SO}_3]$ (**11b**) with diazomethane. We had assumed that diazomethane coordination and activation would occur at the unsaturated Rh center with subsequent CH₂ insertion into the Rh-alkyne bond. Formation of the C₃-bridged product by this route would more closely model the formation of the putative C₃H₆-bridged intermediate from the ethylene-bridged precursor in the Rh/Os chemistry.⁶ Furthermore, this would also model a key step in the Dry mechanism for carbon-carbon chain growth in FT chemistry.⁸ However, the alkyne-bridged product **11b** proved to be unreactive toward diazomethane. Either diazomethane coordination at Rh is blocked by

the CO₂Me group adjacent to this metal, or insertion into the stronger bond between Rh and the sp² carbon is not favored. This bond is presumably further strengthened by the adjacent electron-withdrawing CO₂Me substituent.⁴⁴ Methylene insertion into a metal-carbon bond of an alkyne-bridged complex has been observed;³⁹ however, in this case the alkyne bridged the metals in an arrangement perpendicular to, rather than parallel to, the metal-metal bond. We have previously noted reactivity differences between isomeric complexes in which the alkyne was bound in either a perpendicular or parallel arrangement,^{45,46} so we have attempted to generate a perpendicular alkyne complex from **11b**. In the parallel mode the alkyne functions as a neutral two-electron donor, whereas in the perpendicular mode it is a four-electron donor. Removal of a carbonyl should induce a rotation of the alkyne group to perpendicular in order to alleviate the resulting electron deficiency. Instead however, carbonyl loss is accompanied by coordination of the triflate anion at Rh, thereby alleviating the resulting unsaturation and yielding a product (**12**), shown in Scheme 3.3, very much like the precursor, in which the alkyne group remains parallel to the metals. Nevertheless, this product does react with diazomethane, although not to give a product of methylene insertion into the Rh-alkyne bond. Instead, methylene insertion into the Rh-Ru bond has occurred, to give the methylene- and alkyne-bridged **13**. This product is analogous to a dirhodium compound, [Rh₂Cl₂(μ-CH₂)(μ-CF₃C=CCF₃)(dppm)₂], previously prepared by us by reaction of the alkyne-bridged precursor with diazomethane.⁴⁷ As an interesting contrast, it should be noted that subsequent studies with the RhOs system have shown that methylene insertion into the Rh-C bond of the alkyne-bridged complex [RhOs(CO)₃(μ-η¹:η¹-C(CO₂Me)=C(CO₂Me))(dppm)₂]⁺ does give the targeted C₃-bridged [RhOs(CO)₃(μ-

$\eta^1:\eta^1\text{-CH}_2\text{C}(\text{CO}_2\text{Me})=\text{C}(\text{CO}_2\text{Me})\text{)}(\text{dppm})_2]^+$.¹⁹ The reasons for this reactivity difference between the RhRu and the RhOs analogues are not understood.

With the terminal alkyne, propargyl alcohol, the single-insertion product analogous to compounds **6** - **10** is not observed. Instead, reaction with 2 equiv. occurs to give the C₅-bridged $[\text{RhRu}(\text{CO})_2(\mu\text{-}\eta^2:\eta^4\text{-CH}=\text{C}(\text{CH}_2\text{OH})\text{CH}=\text{C}(\text{CH}_2\text{OH})\text{CH}_2)\text{-(dppm)}_2][\text{CF}_3\text{SO}_3]$ (**15**). Stepwise insertion of both alkynes into the Rh-CH₂ bond in a head-to-tail manner has occurred with the more bulky substituent (CH₂OH) ending up adjacent to the methylene group. We propose that this double insertion occurs as diagrammed in Scheme 3.8 (dppm groups omitted for clarity). Coordination of the first

Scheme 3.8



alkyne at Rh leads to insertion into the Rh-CH₂ bond to give the C₃-bridged product **E**. This proposed intermediate has a geometry like those of **9** and **10**, with the bulkier alkyne substituent adjacent to the methylene group. The small hydrogen substituent on the

carbon bound to Rh presumably allows for coordination of a second alkyne at this metal, leading to the second insertion reaction which gives a C₅-bridged species. We assume that strain within this initially formed seven-membered dimetallacycle (F) leads to migration of the CH₂ end to Rh, giving a rhodacyclohexadiene moiety, which forms two π interactions with Ru, accompanied by carbonyl loss. Double insertions involving the internal alkynes described earlier do not occur owing to the inability of the second alkyne to coordinate to Rh in the monoinsertion products **6** - **10** because of steric repulsions involving the substituent on the carbon bound to Rh. Double insertions of alkyne into a single bridging methylene unit to give C₅-bridged moieties have been observed,^{36,38,48,49} and in a couple of these cases coupling of internal alkynes was observed. Presumably, the steric demands of these "Fe₂(CO)_x", "W₂(CO)_x" and "Ru₂Cp₂" core frameworks, for which double insertions of internal alkynes were observed, are lower than for the "RhRu(dppm)₂" framework reported herein, for which a second insertion was observed only for the terminal alkyne, propargyl alcohol. A double insertion was also reported for the bis-methylene-bridged complex [Cp**Rh*(NCMe)(μ -CH₂)₂]₂,⁴² in which stepwise alkyne insertion involving *both* methylene units, accompanied by coupling of the two resulting C₃ fragments, was proposed.

Compound **15** seems ideally suited to either reductive elimination via C-C bond formation yielding a cyclopentadiene fragment or hydrogenolysis of the Rh-C bonds to give a substituted pentadiene. Attempts to induce reductive elimination by mild heating (refluxing THF) or by oxidation by ferricinium hexafluorophosphate or ammonium hexachloroiridate(IV)⁵⁰ failed; no reaction was observed in either case. Reaction of **12** with H₂ does yield the expected binuclear hydride product, [RhRu(CO)₃(μ -

$\text{H})_2(\text{dppm})_2][\text{CF}_3\text{SO}_3]_3$,⁹ however the other expected product, $\text{H}_2\text{C}=\text{C}(\text{CH}_2\text{OH})-\text{C}(\text{H})=\text{C}(\text{CH}_2\text{OH})\text{CH}_3$, or the fully hydrogenated $\text{H}_3\text{CCH}(\text{CH}_2\text{OH})\text{CH}_2\text{CH}(\text{CH}_2\text{OH})\text{CH}_3$ was not detected; the complex mixture of organic products observed in the ^1H NMR spectrum of the reaction mixture was not analyzed.

Conclusions:

The insertion of a variety of alkynes into the Rh-CH₂ group of the methylene-bridged species $[\text{RhRu}(\text{CO})_3(\mu\text{-CH}_2)(\text{dppm})_2][\text{CF}_3\text{SO}_3]$ (**4**) occurs readily. In all cases studied the first product is either observed or assumed to be the single-insertion product in which the resulting "RC=C(R')CH₂" moiety bridges the metals with the terminal vinylic carbon bound to Rh and the methylene group bound to Ru. This is consistent with all previous studies from our group on "Rh($\mu\text{-CH}_2$)M" complexes (M = Ru, Os), in which coordinative unsaturation at Rh allows substrate coordination at this metal and subsequent substrate insertion into the Rh-CH₂ bond.^{6,9,19,51} In Chapter 2, the PMe_3 adduct of **4** models the initial ligand adduct, clearly demonstrating coordination at Rh adjacent to the bridging methylene group. Surprisingly, the reverse process of methylene insertion into the Rh-C bond of the alkyne-bridged product $[\text{RhRu}(\text{CO})_3(\mu\text{-}\eta^1:\eta^1\text{-}(\text{CO}_2\text{Me})\text{C}=\text{C}(\text{CO}_2\text{Me}))(\text{dppm})_2][\text{X}]$ (**11**) did not occur in the RhRu system, but does occur for the RhOs analogue, giving $[\text{RhOs}(\text{CO})_3(\mu\text{-}\eta^1:\eta^1\text{-CH}_2(\text{CO}_2\text{Me})\text{-C}=\text{C}(\text{CO}_2\text{Me}))(\text{dppm})_2]^+$ for reasons which are unclear.

In the cases in which the alkyne substituents (R,R') were not the same, regioselective insertion occurred, giving the product in which the larger substituent was adjacent to the methylene group. For propargyl alcohol the small hydrogen on one end of

the alkyne appears to allow subsequent coordination of a second propargyl alcohol molecule at Rh followed by a second insertion to give a C₅-bridged product.

The C₃-bridged products containing the $\mu\text{-}\eta^1\text{:}\eta^1\text{-RC=C(R')CH}_2$ groups are effective models for the proposed C₃H₆-bridged intermediates obtained by coupling of three methylene groups in a related Rh/Os system. Our success at isolating the alkyne-insertion products, where the C₃H₆-bridged species could not be observed, probably relates to the absence of hydrogens on the β -carbon atom in the former, eliminating the possibility of β -hydrogen elimination as a decomposition pathway. Unfortunately, apart from the double-insertion of propargyl alcohol, subsequent insertions into the Rh–C bond of the C₃-bridged products were not observed. Therefore we were unable to convert the model C₃-bridged systems into C₄ products by reaction with diazomethane. Our failure to convert the C₃ to C₄ products is not understood, especially considering the facile conversion of C₃ to C₅ products with propargyl alcohol. Furthermore, the RhOs analogues of the C₃-bridged products do accept a methylene unit from diazomethane affording an interesting C₄-bridged hydride species (Scheme 3.6).

As noted in Chapter 2, substitution of Os by Ru in these mixed-metal Rh/M (M = Ru, Os) complexes does not always lead to predictable changes in reactivity. So, in this chapter the reactivity described above in which the Rh/Os compounds $[\text{RhOs}(\text{CO})_3(\mu\text{-DMAD})(\text{dppm})_2][\text{CF}_3\text{SO}_3]$ and $[\text{RhOs}(\text{CO})_3(\mu\text{-}\eta^1\text{:}\eta^1\text{-C}(\text{CO}_2\text{Me})=\text{C}(\text{CO}_2\text{Me}))(\text{dppm})_2][\text{CF}_3\text{SO}_3]$ incorporate an additional methylene group whereas the Rh/Ru analogues don't react is puzzling. These differences are particularly puzzling when one

considers that both reactions occur at the Rh centre. Clearly the influence of the adjacent group 8 metal is subtle yet profound, significantly modifying the reactivity at Rh.

References:

1. Sun, S.; Fujimoto, K.; Yoneyama, Y.; Tsubaki, N. *Fuel* **2002**, *81*, 1583.
2. Tsubaki, N.; Sun, S.L.; Fujimoto, K. *J. Catal.* **2001**, *199*, 236.
3. Kariya, N.; Fukuoka, A.; Ichikawa, M. *Appl. Catal. A* **2002**, *233*, 91.
4. Maunula, T.; Ahola, J.; Salmi, T.; Haario, H.; Harkonen, M.; Luoma, M.; Pohjola, V.J. *Appl. Catal. B* **1997**, *12*, 287.
5. Adesina, A.A. *Appl. Catal. A* **1996**, *138*, 345.
6. Trepanier, S.J.; Sterenberg, B.T.; McDonald, R.; Cowie, M. *J. Am. Chem. Soc.* **1999**, *121*, 2613.
7. Dell'Anna, M.M.; Trepanier, S.J.; McDonald, R.; Cowie, M. *Organometallics* **2001**, *20*, 88.
8. Dry, M.E. *Catal. Today* **2002**, *71*, 227.
9. Rowsell, B.D.; Trepanier, S.J.; Lam, R.; McDonald, R.; Cowie, M. *Organometallics* **2002**, *21*, 3228.
10. Further information may be obtained by contacting Dr. Robert McDonald (bob.mcdonald@ualberta.ca) and inquiring about sample numbers COW0231 (compound **7**), COW0036 (compound **11**) and COW0209 (compound **15**).
11. Programs for diffractometer operation, data reduction, and absorption correction were those supplied by Bruker.
12. Sheldrick, G.M. *Acta Crystallogr. Sect. A* **1990**, *46*, 467.

13. Sheldrick, G.M. *SHELXL-93*: Program for crystal structure determination; University of Gottingen: Gottingen, Germany, 1993.
14. Spek, A.L. *Acta Crystallogr.* **1990**, *A46*, C34. PLATON-a multipurpose crystallographic tool.; Utrecht University, Utrecht, The Netherlands.:
15. Spek, A.L. *Acta. Crystallogr.* **1990**, *A46*, C34. PLATON-a multipurpose crystallographic tool; Utrecht University: Utrecht, The Netherlands, 1990.
16. George, D.S.A.; Hiltz, R.W.; McDonald, R.; Cowie, M. *Organometallics* **1999**, *18*, 5330.
17. Allen, F.H.; Kennard, O.; Watson, D.G.; Brammer, L.; Orpen, A.G.; Taylor, R. *J. Chem. Soc.-Perkin Trans. 2* **1987**, S1.
18. $r_c(\text{sp}^3) = 0.77 \text{ \AA}$; $r_c(\text{sp}^2) = 0.74 \text{ \AA}$.
19. Chokshi, A.; Graham, T.W.; McDonald, R.; Cowie, M. Manuscript in preparation.
20. Lawrance, G.A. *Chem. Rev.* **1986**, *86*, 17.
21. Gerisch, M.; Krumper, J.R.; Bergman, R.G.; Tilley, T.D. *Organometallics* **2003**, *22*, 47.
22. Berenguer, J.H.; Bernechea, M.; Fornies, J.; Gomez, J.; Lalinde, E. *Organometallics* **2002**, *21*, 2314.
23. Nuckel, S.; Burger, P. *Organometallics* **2001**, *20*, 4345.
24. Vincente, J.; Gil-Rubio, J.; Bautista, D. *Inorg. Chem.* **2001**, *40*, 2636.
25. Dias, E.L.; Brookhart, M.; White, P.S. *Organometallics* **2000**, *19*, 4995.
26. Lefort, L.; Lachicotte, R.J.; Jones, W.D. *Organometallics* **1998**, *17*, 1420.
27. Jimenez, M.V.; Sola, E.; Egea, M.A.; Huet, A.; Francisco, A.C.; Lahoz, F.J.; Oro, L.A. *Inorg. Chem.* **2000**, *39*, 4868.

28. Shafiq, F.; Eisenberg, R. *J. Organomet. Chem.* **1994**, *472*, 337.
29. Rowsell, B.D.; Cowie, M. Unpublished results.
30. Trepanier, S.J.; McDonald, R.; Cowie, M. *Organometallics* **2003**, *22*, 2638.
31. Sterenberg, B.T.; Hiltz, R.W.; Moro, G.; McDonald, R.; Cowie, M. *J. Am. Chem. Soc.* **1995**, *117*, 245.
32. McDonald, R.; Cowie, M. *Organometallics* **1990**, *9*, 2468.
33. Torkelson, J.R.; McDonald, R.; Cowie, M. *Organometallics* **1999**, *18*, 4134.
34. Dyke, A.F.; Knox, S.A.R.; Naish, P.J.; Taylor, G.E. *J. Chem. Soc.-Chem. Commun.* **1980**, 803.
35. Gracey, B.P.; Knox, S.A.R.; Macpherson, K.A.; Orpen, A.G.; Stobart, S.R. *J. Chem. Soc.-Dalton Trans.* **1985**, 1935.
36. Sumner, C.E.; Collier, J.A.; Pettit, R. *Organometallics* **1982**, *1*, 1350.
37. Akita, M.; Hua, R.; Nakanishi, S.; Tanaka, M.; Morooka, Y. *Organometallics* **1997**, *16*, 5572.
38. Adams, P.Q.; Davies, D.L.; Dyke, A.F.; Knox, S.A.R.; Mead, K.A.; Woodward, P. *J. Chem. Soc.-Chem. Commun.* **1983**, 222.
39. Colborn, R.E.; Dyke, A.F.; Knox, S.A.R.; Macpherson, K.A.; Orpen, A.G. *J. Organomet. Chem.* **1982**, *239*, C15.
40. Colborn, R.E.; Davies, D.L.; Dyke, A.F.; Knox, S.A.R.; Mead, K.A.; Orpen, A.G.; Guerchais, J.E.; Roue, J. *J. Chem. Soc.-Dalton Trans.* **1989**, 1799.
41. Dennett, J.N.L., Ph.D. Thesis, Chapter 4, University of Bristol, Bristol, UK, 2000.
42. Kaneko, Y.; Suzuki, T.; Isobe, K.; Maitlis, P.M. *J. Organomet. Chem.* **1998**, *554*, 155.

43. Chokshi, A.; Trepanier, S.J.; Cowie, M. Unpublished results.
44. Elschenbroich, C.; Salzer, A. *Organometallics, A Concise Introduction*; VCH Publishers: New York, 1989.
45. George, D.S.A.; McDonald, R.; Cowie, M. *Can. J. Chem.* **1996**, *74*, 2289.
46. Wang, L.S.; Cowie, M. *Can. J. Chem.* **1995**, *73*, 1058.
47. McKeer, I.R.; Sherlock, S.J.; Cowie, M. *J. Organomet. Chem.* **1988**, *352*, 205.
48. Navarre, D.; Parlier, A.; Rudler, H.; Daran, J.C. *J. Organomet. Chem.* **1987**, *322*, 103.
49. Levisalles, J.; Rose-Munch, F.; Rudler, H.; Daran, J.C.; Dromzee, Y.; Jeannin, Y. *J. Chem. Soc.-Chem. Commun.* **1981**, 152.
50. Saez, I.M.; Andrews, D.G.; Maitlis, P.M. *Polyhedron* **1988**, *7*, 827.
51. Rowsell, B.D.; Chokshi, A.; Trepanier, S.J.; Graham, T.W.; McDonald, R.; Ferguson, M.J.; Cowie, M. Manuscript in preparation.

Chapter 4

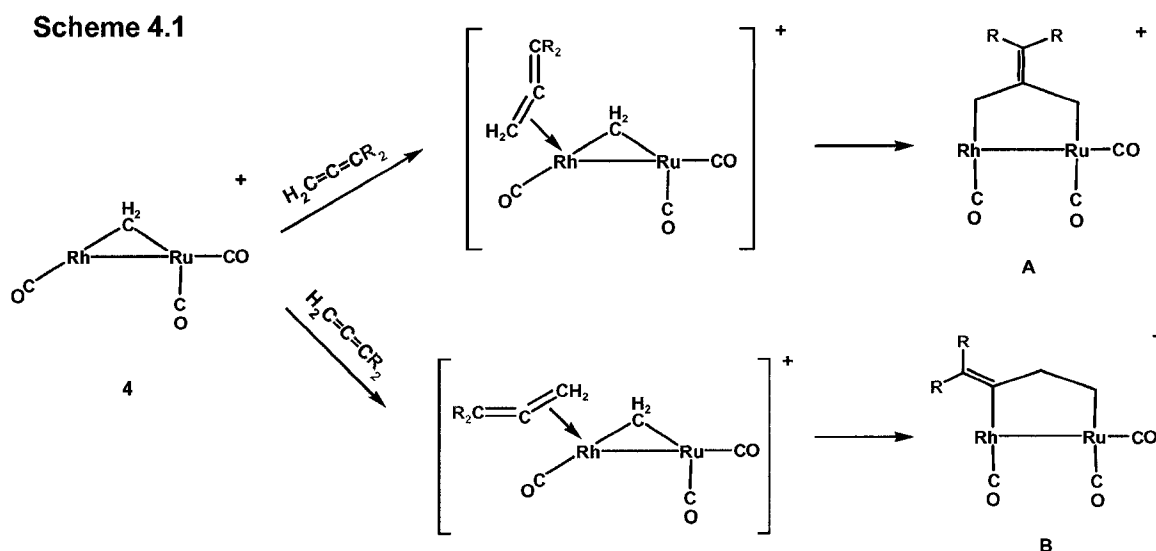
Coupling Between Allenes and Methylene Groups

Introduction:

In Chapter 2, we discussed the synthesis and characterization of the methylene-bridged complex $[\text{RhRu}(\text{CO})_3(\mu\text{-CH}_2)(\text{dppm})_2][\text{CF}_3\text{SO}_3]$ (**4**), and began to investigate its potentially rich chemistry. Chapter 3 dealt with additions of alkynes to **4**, resulting in the formation of one or two carbon-carbon bonds by sequential alkyne insertion into the Rh-C bonds giving C_3 - or C_5 -bridged species, respectively.

A natural progression from the use of alkynes is the utilization of another series of doubly-unsaturated organic compounds, cumulenes. Cumulenes, though they contain two available π systems like alkynes, are a closer analogue to ethylene and can potentially produce C_3 -bridged species more directly analogous to those of the C_3H_6 intermediates prepared in the Rh/Os system.¹

There are several different ways that the cumulene could interact with the unsaturated Rh centre, as diagrammed in Scheme 4.1. For the cases of substituted cumulenes, it is anticipated that coordination through the bulkier end will be sterically unfavoured. This being the case, the incoming cumulene can coordinate in two different geometries, leading to the products **A** and **B**. Although product **B** contains β -hydrogens, and as such may be susceptible to decomposition through β -hydrogen elimination, product **A** does not have β -hydrogens so may demonstrate increased stability.¹



In this chapter we attempt the synthesis of the C₃-bridged species **A** or **B** by the reaction of [RhRu(CO)₃(μ-CH₂)(dppm)₂][X] with some cumulene molecules.

Experimental:

General Comments. All solvents were dried (using appropriate desiccants), distilled before use, and stored under a dinitrogen atmosphere. Reactions were performed under an argon atmosphere using standard Schlenk techniques. Diazomethane was generated from Diazald, which was purchased from Aldrich, as was the trimethylphosphine (1.0 M) solution in THF. The dimethylallene and methylallene were purchased from Fluka. The ¹³C-enriched Diazald was purchased from Cambridge Isotopes, whereas ¹³CO was purchased from Isotec Inc. The allene was purchased from Praxair, Inc.

The ¹H, ¹³C{¹H}, and ³¹P{¹H} NMR spectra were recorded on a Varian iNova-400 spectrometer operating at 399.8 MHz for ¹H, 161.8 MHz for ³¹P, and 100.6 MHz for ¹³C.

Infrared spectra were obtained on a Bomem MB-100 spectrometer. The elemental analyses were performed by the microanalytical service within the department.

Spectroscopic data for all compounds are given in Table 4.1.

Preparation of Compounds:

(a) [RhRu(CO)₂(μ-η³:η¹-C(CH₂)₃)(dppm)₂][CF₃SO₃] (16). A Schlenk Flask was charged with the compound [RhRu(CO)₄(μ-CH₂)(dppm)₂][CF₃SO₃] (85 mg, 0.068 mmol) (**3**) and Me₃NO (8.70 mg, 0.116 mmol, 1.7 eq.). The flask was cooled to – 8 °C using a salt-water/ice bath, evacuated, then back-filled to *ca.* 1 atm with allene, then 5 mL of acetone was added to the flask, causing the solution colour to change immediately from red to yellow-orange. The ice bath was removed and the solution was stirred for 1 h, after which it was filtered over Celite. The filtrate was concentrated to *ca.* 2 mL, and subsequent dropwise addition of Et₂O caused the formation of an orange solid. The supernatant was removed and the solid was washed with 2 x 15 mL Et₂O and dried *in vacuo* (yield: 54 mg, 65%). Anal. Calcd for C₅₇H₅₀F₃O₅P₄RhRuS: C, 55.52; H, 4.09. Found: C, 55.69; H, 4.09.

(b) [RhRu(CO)₃(μ-η³:η¹-C(CH₂)₃)(dppm)₂][CF₃SO₃] (17). Compound **16** (100 mg, 0.081 mmol) was dissolved in 4 mL CH₂Cl₂ and carbon monoxide gas was passed over the solution for *ca.* 5 min. The solution slowly turned from yellow-orange to orange. After 0.5 h of stirring, the solution was concentrated to *ca.* 3 mL using a stream of Ar gas. Slow addition of 15 mL of Et₂O resulted in the precipitation of orange microcrystals. The supernatant was removed and the crystals were dried *in vacuo* (yield:

Table 4.1. Spectroscopic Data For Compounds.

Compound	IR (cm ⁻¹) ^{a,b,c}	NMR ^{d,e}		
		³¹ P { ¹ H} (ppm) ^f	¹ H (ppm) ^{g,h}	¹³ C { ¹ H} (ppm) ^{h,i}
[RhRu(CO) ₂ (μ-η ³ :η ¹ -C(CH ₂) ₃)(dppm) ₂]-[CF ₃ SO ₃] (16)	2021 (m), 1951 (s)	30.9 (om)	4.30 (m, 2H), 3.90 (m, 2H), 4.02 (s, 2H), 1.98 (d, ³ J _{PH} = 8 Hz, 2H), 1.49 (t, ³ J _{PH} = 8 Hz, 2H)	194.5 (m, 1C), 191.7 (m, 1C), 13.8 (s, 1C)
[RhRu(CO) ₃ (μ-η ³ :η ¹ -C(CH ₂) ₃)(dppm) ₂]-[CF ₃ SO ₃] (17)	2010 (m), 1980 (m), 1935 (m)	30.4 (m), 13.2 (dm)	4.16 (m, 2H), 4.06 (m, 2H), 2.64 (d, ³ J _{PH} = 9 Hz, 2H), 1.79 (s, 2H), 1.52 (t, ³ J _{PH} = 9 Hz, 2H)	205.2 (m, 1C), 198.7 (m, 1C), 184.2 (dm, ¹ J _{RhC} = 57 Hz, 1C)
[RhRu(CO) ₂ (PMe ₃)(μ-η ³ :η ¹ -C(CH ₂) ₃)(dppm) ₂]-[CF ₃ SO ₃] (18)		26.3 (m), 13.3 (dm), - 34.6 (dm) ^j	4.32 (m, 2H), 4.12 (m, 2H), 1.86 (s, br, 2H), 1.73 (m, br, 2H), 1.50 (s, br, 2H), 0.39 (d, ² J _{PH} = 7 Hz, 9H) ^j	
[RhRu(CO) ₂ (C(O)CH ₂ CH ₂ C-(=C(CH ₃) ₂)(dppm) ₂)-[CF ₃ SO ₃] (19)	1975 (m), 1910 (s), 1798 (m)	35.5 (m), 20.4 (dm)	3.58 (m, 2H), 3.41 (m, 2H), 2.73 (m, 2H), 1.31 (s, 3H), 0.96 (s, 3H), 0.37 (m, 2H)	250.7 (dt, ¹ J _{RhC} = 33 Hz, ² J _{PC} = 8 Hz, 1C) 220.2 (m, 1C), 202.4 (t, ² J _{PC} = 23 Hz, 1C)

Table 4.1. (cont'd.)

[RhRu(CO) ₂ (H) ₂ C(O)CH ₂ C H ₂ -C(=C(CH ₃) ₂)- (dppm) ₂]-[CF ₃ SO ₃] (20)	2155 (m), ^k 2126 (m), ^k 2053 (m), 2000 (s), 1683 (m)	31.9 (m), 22.3 (dm)	3.94 (m, 2H), 3.60 (m, 2H), 1.99 (s, 3H), 1.73 (m, 2H), 1.16 (s, 3H), 0.93 (m, 2H), -7.89 (m, 1H), -10.01 (m, 1H)	236.3 (dt, ¹ J _{RhC} = 28 Hz, ² J _{PC} = 7 Hz, 1C), 196.8 (m, 1C), 190.7 (t, ² J _{PC} = 11 Hz, 1C)
---	--	------------------------	---	--

^a IR abbreviations: s = strong, m = medium, w = weak. ^b CH₂Cl₂ solutions, in units of cm⁻¹. ^c Carbonyl stretches unless otherwise noted. ^d NMR abbreviations: s = singlet, d = doublet, t = triplet, m = multiplet, cm = complex multiplet, dm = doublet of multiplets, om = overlapping multiplets, br = broad, dt = doublet of triplets. ^e NMR data at 25 °C in CD₂Cl₂. ^f ³¹P chemical shifts referenced to external 85% H₃PO₄. ^g Chemical shifts for the phenyl hydrogens are not given. ^h ¹H and ¹³C chemical shifts referenced to TMS. ⁱ ¹³C{¹H} NMR performed with ¹³CO enrichment. ^j data obtained at -60 °C. ^k ν_(M-H)

80 mg, 78%). Anal. Calcd for $C_{58}H_{50}F_3O_6P_4RhRuS$: C, 55.24; H, 4.00. Found: C, 55.23; H, 3.87.

(c) **[RhRu(CO)₂(PMe₃)(μ-η³:η¹-C(CH₂)₃)(dppm)₂][CF₃SO₃] (18)**. Compound **16** (10 mg, 0.008 mmol) was dissolved in 0.7 mL of CD₂Cl₂ and cooled to –77 °C. To this was added 9 μL of a 1.0 M solution of PMe₃ in THF (0.009 mmol, 1.1 eq.) causing no noticeable colour change. However, monitoring the solution at –80 °C by NMR spectroscopy showed essentially quantitative conversion into a new compound **18**. This was the only product formed between –80 °C and –40 °C, however, at temperatures higher than –40 °C this product began to decompose into several unidentified products. As a result, characterization of **18** was achieved by ³¹P {¹H} and ¹H NMR spectroscopy at the lower temperatures.

(d) **[RhRu(CO)₂(C(O)CH₂CH₂C(=C(CH₃)₂))(dppm)₂][CF₃SO₃]·0.5CH₂Cl₂ (19)**. A Schlenk Flask was charged with 115 mg (0.092 mmol) of [RhRu(CO)₄(μ-CH₂)(dppm)₂][CF₃SO₃] (**3**), 9.5 μL of dimethyl allene (0.096 mmol, 1.04 eq.) along with 6 mL of acetone. The solution then was cooled to –10 °C, and 6 mL of a 0.025 M solution of Me₃NO in acetone (0.150 mmol, 1.7 eq.) was added dropwise, causing the immediate colour change from yellow to dark-red to orange. The solution was stirred for 1 h, after which it was warmed to ambient temperature then filtered over Celite. The solvent was removed *in vacuo* and the orange residue was dissolved in 2 mL of CH₂Cl₂. Orange microcrystals precipitated after dropwise addition of 17 mL of Et₂O. The supernatant was removed and the crystals were dried *in vacuo* (yield: 70 mg, 57%).

Anal. Calcd for $C_{60.5}H_{55}ClF_3O_6P_4RhRuS$: C, 54.62; H, 4.17; Cl, 2.66. Found: C, 54.80; H, 4.16; Cl, 2.16.

(d) $[RhRu(H)_2(CO)_2(C(O)CH_2CH_2C(=C(CH_3)_2))(dppm)_2][CF_3SO_3]$ (20).

Compound **19** (67 mg, 0.052 mmol) was dissolved in 5 mL of CH_2Cl_2 . Hydrogen gas was passed over the solution for *ca.* 5 min, after which no noticeable colour change occurred. The solution was stirred under H_2 for 1 h, the solvent was removed *in vacuo*, and the orange residue was dissolved in 2 mL of CH_2Cl_2 . Slow addition of 10 mL of Et_2O caused formation of a dark orange solid. The supernatant was removed and the solid was washed with 2 x 10 mL of Et_2O and dried *in vacuo* (yield: 52 mg, 77%). Anal. Calcd for $C_{60}H_{56}F_3O_6P_4RhRuS$: C, 55.86; H, 4.38. Found: C, 55.23; H, 4.29.

(e) Reaction of 16 with CH_2N_2 . Compound **16** (10 mg, 0.008 mmol) was dissolved in 0.7 mL of CD_2Cl_2 in an NMR tube then cooled to *ca.* 0 °C. Diazomethane was passed over the solution for 5 min. The NMR tube was shaken to mix the gas into the solution and was allowed to sit for 30 min at 0 °C. The diazomethane was removed *in vacuo* and the tube was back-filled with Ar. $^{31}P\{^1H\}$ NMR spectroscopy detected the presence of numerous unidentified products.

(f) Reaction of 17 with PMe_3 . Compound **17** (15 mg, 0.012 mmol) was dissolved in 0.7 mL of CD_2Cl_2 . To this, 12 μ L of PMe_3 (1.0 M in THF, 0.012 mmol) was added, causing the colour to change from yellow to dull-orange. The mixture was allowed to react for 30 min, after which the $^{31}P\{^1H\}$ NMR spectrum revealed the presence of numerous unidentified products.

X-ray Data Collection.² Orange crystals of $[\text{RhRu}(\text{CO})_2(\text{C}(\text{O})\text{CH}_2\text{CH}_2\text{C}(\text{=C}(\text{CH}_3)_2))(\text{dppm})_2][\text{CF}_3\text{SO}_3] \cdot (\text{CH}_3)_2\text{CO}$ (**19**) were obtained by slow diffusion of diethyl ether into an acetone solution of the compound. Data were collected and the structures solved and refined by Dr. Michael J. Ferguson on a Bruker PLATFORM/SMART 1000 CCD diffractometer³ using Mo $K\alpha$ radiation at -80 °C. Unit cell parameters were obtained from a least-squares refinement of the setting angles of 3998 reflections from the data collection. The space group was determined to be $P\bar{1}$ [No. 2]. Data were corrected for absorption through use of the SADABS procedure. See Table 4.2 for a summary of crystal data and X-ray data collection information.

Structure Solution and Refinement. The structure for compound **19** was solved using automated Patterson location of the heavy metal atoms and structure expansion via the DIRDIF-99⁴ program system. Refinement was completed using the program SHELXL-93.⁵ Hydrogen atoms were assigned positions based on the geometries of their attached carbon atoms and were given thermal parameters 20% greater than those of the attached carbons. The final model for **19** refined to values of $R(F) = 0.0560$ (for 11148 data with $F_o^2 \geq 2\sigma(F_o^2)$) and $wR(F^2) = 0.1377$ (for all 18118 data).

Table 4.2. Crystallographic Data for Compound 19.

	[RhRu(CO) ₂ (C(O)CH ₂ CH ₂ C(=C(CH ₃) ₂)(dppm) ₂]- [CF ₃ SO ₃] ⁻ ·(CH ₃) ₂ CO (19)
formula	C ₆₃ H ₆₀ F ₃ O ₇ P ₄ RhRuS
fw	1346.03
cryst dimens, mm	0.17 × 0.16 × 0.14
cryst system	triclinic
space group	<i>P</i> $\bar{1}$ (No. 2)
<i>a</i> , Å	13.228 (1) ^a
<i>b</i> , Å	15.403 (2)
<i>c</i> , Å	15.544 (2)
α deg	75.761 (2)
β , deg	74.776 (2)
γ , deg	72.884 (2)
<i>V</i> , Å ³	2871.1 (5)
<i>Z</i>	2
<i>d</i> _{calcd} , g cm ⁻³	1.557
μ , mm ⁻¹	0.762
radiation (λ , Å)	graphite-monochromated Mo K α (0.71073)
<i>T</i> , °C	-80
scan type	ω scans (0.2°) (25s exposures)
2 θ (max), deg	52.70
no. of unique reflections	11377 (<i>R</i> _{int} = 0.053)
no of observns	11148 [<i>F</i> _o ² ≥ 2 σ (<i>F</i> _o ²)]
range of transmn factors	0.9008–0.8813
no. of data/restraints/params	18118 [<i>F</i> _o ² ≥ -3 σ (<i>F</i> _o ²)] / 0 / 724
residual density, e/Å ³	1.104 to -1.353
<i>R</i> ₁ (<i>F</i> _o ² > 2 σ (<i>F</i> _o ²)) ^b	0.0560
<i>wR</i> ₂ [<i>F</i> _o ² ≥ -3 σ (<i>F</i> _o ²)] ^b	0.1377
GOF (s) ^c	0.953 [<i>F</i> _o ² ≥ -3 σ (<i>F</i> _o ²)]

^a Cell parameters obtained from least-squares refinement of 3998 centered reflections. ^b $R_1 = \sum ||F_o| - |F_c|| / \sum |F_o|$; $wR_2 = [\sum w(F_o^2 - F_c^2)^2 / \sum w(F_o^4)]^{1/2}$ Refinement on *F*_o² for all reflections (having *F*_o² ≥ -3 σ (*F*_o²)). *wR*₂ and *S* based on *F*_o²; *R*₁ based on *F*_o, with *F*_o set to zero for negative *F*_o². The observed criterion of *F*_o² > 2 σ (*F*_o²) is used only for calculating *R*₁ and is not relevant to the choice of reflections for refinement. ^c $S = [\sum w(F_o^2 - F_c^2)^2 / (n - p)]^{1/2}$ (*n* = number of data, *p* = number of parameters varied; $w = [\sigma^2(F_o^2) + (0.0638P)^2]^{-1}$, where $P = [\max(F_o^2, 0) = 2F_c^2]/3$).

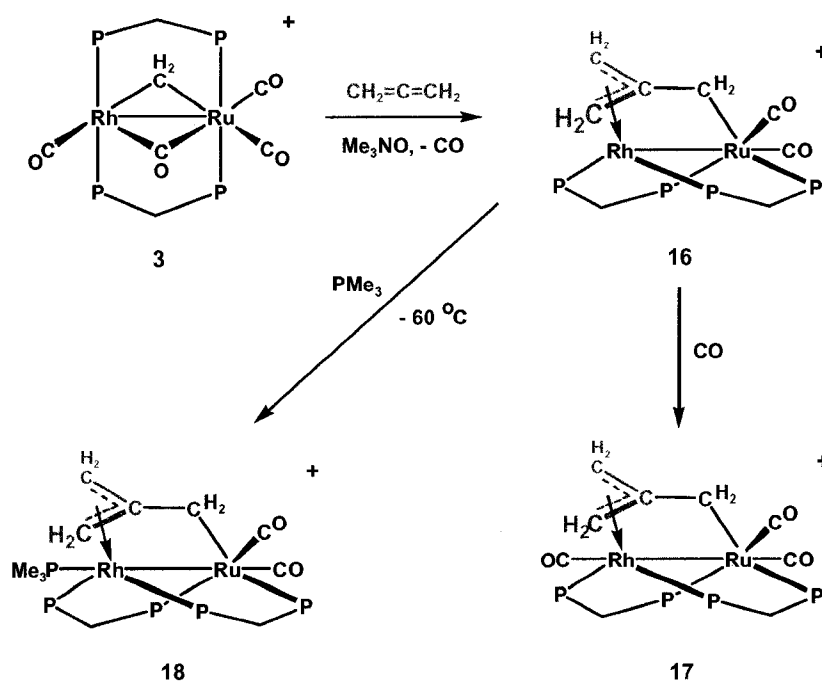
Results and Compound Characterization:

The attempted reactions between the methylene-bridged tetracarbonyl species $[\text{RhRu}(\text{CO})_4(\mu\text{-CH}_2)(\text{dppm})_2][\text{CF}_3\text{SO}_3]$ (**3**) and a number of cumulenes were unsuccessful, giving no observed reaction after several hours at ambient temperature. However, removal of a carbonyl from **3** using trimethylamine-N-oxide, to form the previously studied tricarbonyl analogue $[\text{RhRu}(\text{CO})_3(\mu\text{-CH}_2)(\text{dppm})_2][\text{CF}_3\text{SO}_3]$ (**4**) did result in facile reactions with the cumulenes. It proved most convenient to carry out these reactions by generating **4** from **3** *in situ* in the presence of Me_3NO and the organic substrate of interest.

In the first of these reactions, compound **3** and Me_3NO , under an atmosphere of allene ($\text{H}_2\text{C}=\text{C}=\text{CH}_2$) at $-10\text{ }^\circ\text{C}$, yields only one product, $[\text{RhRu}(\text{CO})_2(\mu\text{-}\eta^3\text{:}\eta^1\text{-C}(\text{CH}_2)_3)(\text{dppm})_2][\text{CF}_3\text{SO}_3]$ (**16**) in which the allene moiety has apparently inserted into the Rh-C bond of the methylene bridge followed by rearrangement to give the observed trimethylenemethane-bridged (TMM) product, as diagrammed in Scheme 4.2. The ^1H NMR spectrum of **16** shows two broad multiplets for the dppm methylene protons at δ 4.30 and 3.90, and three higher-field proton resonances due to the three CH_2 groups in the TMM fragment. The *syn* protons of the η^3 -bound end of the TMM group appear as a broad singlet at δ 4.02, while the *anti* protons appear as a broad doublet ($^3J_{\text{PH}} = 8\text{ Hz}$) at δ 1.98 showing coupling to one of the Rh-bound ends of the diphosphine ligand. The third methylene group, corresponding to that being η^1 -bound to Ru appears as a triplet ($^3J_{\text{PH}} = 8\text{ Hz}$) at δ 1.49 displaying coupling to both Ru-bound ends of the diphosphines. Previous studies in a series of methyl-substituted η^3 -allyl complexes $[\eta^3\text{-(2-CH}_3\text{-C}_3\text{H}_4)\text{RhL}_2]$ ($\text{L}_2 =$

$\text{Me}_2\text{PCH}_2\text{CH}_2\text{PMe}_3$ (dmpe), $(p\text{-Me-C}_6\text{H}_4)_2\text{PCH}_2\text{CH}_2\text{P}(\text{C}_6\text{H}_4\text{-}p\text{-Me})_2$ (dptpe),
 $\text{Ph}_2\text{PCH}_2\text{CH}_2\text{CH}_2\text{PPh}_2$ (dppp) or $\text{Ph}_2\text{PCH}=\text{CHPPh}_2$ (*cis*-dppe) which are structurally
 very similar to the structure proposed for the Rh-end of compound **16**, showed a very
 similar pattern in which the *syn* protons appear as broad singlets at lower field (ranging
 from δ 3.20 to 4.00) and the *anti* protons appear as broad doublets at somewhat higher
 field (δ 2.36 to 2.71) with $^3J_{\text{PH}} = 6$ Hz.⁶

Scheme 4.2



The $^{13}\text{C}\{^1\text{H}\}$ NMR spectrum of a ^{13}CO -enriched sample of **16** shows the presence
 of two carbonyls as complex multiplets at δ 194.5 and 191.7, and the lack of Rh-coupling
 indicates that neither carbonyl is bound to this metal. The IR spectrum, showing two
 terminal CO bands at 2021 and 1951 cm^{-1} confirms that these groups are terminally-
 bound. The HMBC and HMQC 2D NMR spectra in acetone- d_6 for **16** show that the two

terminal chemically equivalent carbons of the η^3 -allyl fragment appear at δ 73.0, whereas the Ru-bound methylene group appears at δ 13.8. Unfortunately, the quaternary carbon could not be detected. The COSY 2D NMR spectrum in acetone- d_6 also shows that the geminal protons on the η^3 -allyl fragment are weakly coupled to each other, and to the Ru-bound methylene end of the TMM ligand. These couplings could not be resolved in the 1D NMR spectrum, however. Treatment of a (μ - $^{13}\text{CH}_2$)-enriched sample of **3** with allene gave the complex $[\text{RhRu}(\text{CO})_2(\mu\text{-}\eta^3\text{:}\eta^1\text{-C}(\text{CH}_2)_2(^{13}\text{CH}_2)(\text{dppm})_2)[\text{CF}_3\text{SO}_3]$, in which the ^{13}C label remained adjacent to Ru (i.e. the red CH_2 in Scheme 4.2). No detectable scrambling occurred over several hours in solution.

Although the nature of the bonding in **16** is equivocal, and can be represented in a number of ways, differing in the nature of the Rh-Ru bond and the oxidation-state assignments of the metals, the compound is clearly coordinatively unsaturated. This being the case, the possibility of anion coordination cannot be ignored. Triflate, although generally accepted as a weakly coordinating anion,⁷ is known to coordinate to metals. Although the observed $\nu_{(\text{SO})}$ stretch in **16** at 1289 cm^{-1} is in the range that is generally considered diagnostic of an ionic triflate, we have observed cases in which such a value is observed for coordinated triflate anions (Chapter 5).⁸ Furthermore, the ^{19}F NMR spectrum is not diagnostic for coordination with the fluorines being remote from the coordinated oxygens at the opposite end of the anion. Substitution of CF_3SO_3^- with the less coordinating BF_4^- should allow ^{19}F NMR spectroscopy to be used to detect any anion coordination. In the case for **16-BF₄**, no such coordination is observed. Unfortunately, single crystals suitable for an X-ray study could not be obtained for **16** so the proposed structure could not be unambiguously confirmed. Nevertheless, all the spectroscopic data

obtained supports the TMM structure shown in Scheme 4.2.

Although further CH₂ incorporation into **16**, by reaction with CH₂N₂, was unsuccessful, it does appear that the unsaturated Rh centre of the compound is reactive toward other nucleophiles. Treatment of **16** with carbon monoxide at room temperature affords the tricarbonyl analogue [RhRu(CO)₃(μ-η³:η¹-C(CH₂)₃)(dppm)₂][CF₃SO₃] (**17**) seen in Scheme 4.2. The ¹H NMR spectrum of **17** is very similar to that of its precursor **16**. The dppm methylenes appear as low-field multiplets at δ 4.16 and 4.06 whereas the TMM moiety remains intact with no major changes, apart from a large high-field shift of the *syn* resonance from δ 4.06 to 1.79. The ¹³C{¹H} NMR spectrum of a ¹³CO-enriched sample of **17** shows three carbonyl signals, two Ru-bound signals at δ 205.2 and 198.7 and one Rh-bound resonance appearing as a doublet of multiplets (¹J_{RhC} = 57 Hz) at δ 184.2. The IR spectrum confirms the presence of three terminal carbonyls, showing three distinct bands at 2010, 1980 and 1935 cm⁻¹. ¹³C NMR studies of the addition of ¹³CO to unlabelled **16** at ambient temperature shows that the added carbonyl ligand binds to Rh, with no detectable CO scrambling occurring over a 16 h period. The ³¹P{¹H} NMR spectrum changes dramatically from a complex overlapping multiplet in **16** to a normal AA'BB'X spectrum with the Ru-end of the phosphines appearing at δ 30.4 and the Rh-end resonance being greatly shifted upfield to δ 13.2.

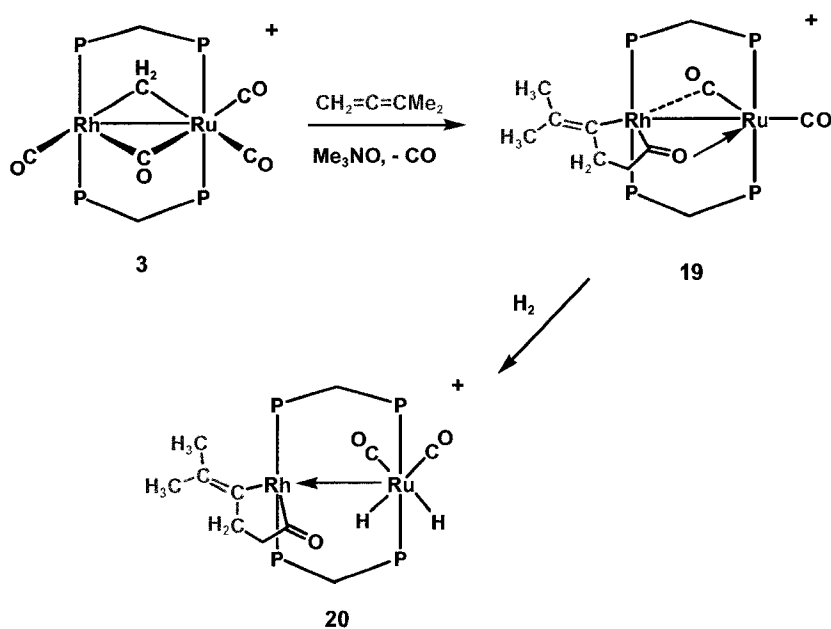
Treatment of **16** with PMe₃ at -60 °C results in quantitative formation of the PMe₃-adduct [RhRu(CO)₂(PMe₃)(μ-η³:η¹-C(CH₂)₃)(dppm)₂][CF₃SO₃] (**18**). ³¹P{¹H} NMR spectroscopy of **18** shows two new resonances at δ 26.3 and 13.3 for the dppm ligands and a new high-field resonance at δ -34.6, corresponding to the PMe₃ group. A large coupling is observed (112 Hz), which serves to identify the PMe₃ ligand as Rh-

bound. The ^1H NMR spectrum at $-60\text{ }^\circ\text{C}$ shows two dppm-methylene resonances at δ 4.32 and 4.12 in addition to three equally intense broad resonances at δ 1.86, 1.73 and 1.50. The protons of the PMe_3 group appear as a broad doublet ($^2J_{\text{PH}} = 7\text{ Hz}$) at δ 0.34. Spectroscopically, this compound is very similar to that of the CO addition product **17**, with the TMM fragment apparently remaining intact, as shown in Scheme 4.2. Unfortunately, suitable single crystals of either **17** or **18** could not be obtained, and subsequent warming of the solution of **18** resulted in the appearance of numerous broad signals in the $^{31}\text{P}\{^1\text{H}\}$ NMR spectrum, thereby preventing further characterization.

The reaction of dimethylallene (DMA) with the *in situ* generated **4**, yields the double-insertion product $[\text{RhRu}(\text{CO})_2(\text{C}(\text{O})\text{CH}_2\text{CH}_2\text{C}(\text{=C}(\text{CH}_3)_2)(\text{dppm})_2][\text{CF}_3\text{SO}_3]$ (**19**) shown in Scheme 4.3. In the $^{31}\text{P}\{^1\text{H}\}$ NMR spectrum of **19** the ruthenium-bound phosphorus nuclei appear as a multiplet at δ 35.3 with the rhodium-bound phosphorus nuclei appearing as a doublet of multiplets at δ 20.4. ^1H NMR spectroscopy shows four multiplets of equal intensities at δ 3.58 and 3.41 (dppm methylenes), 2.73 and 0.73 (organic fragment), in addition to two methyl singlets at δ 1.31 and 0.96. The dppm- CH_2 groups were distinguished from those on the organic fragment by use of $^1\text{H}\{^{31}\text{P}\}$ NMR spectroscopy, where the dppm-methylenes appear as AB quartets upon broad-band phosphorus decoupling, and those on the organic fragment remain unchanged. In the $^{13}\text{C}\{^1\text{H}\}$ NMR spectrum, one relatively low-field carbonyl signal is observed at δ 250.7, appearing as a doublet of triplets. The absence of Ru-bound phosphine coupling to this carbon nucleus argues against a bridging-carbonyl formulation. However, coupling to rhodium is observed ($^1J_{\text{RhC}} = 33\text{ Hz}$) and, along with the low-field chemical shift of this

resonance,⁸⁻¹³ suggests that this carbonyl has undergone an insertion to form an acyl complex. The carbonyl at δ 220.2 is likely semi-bridging in nature with unresolved coupling to Rh; the final signal at δ 202.4 is assigned as terminally-bound to Ru on the basis that there is no Rh coupling. In the IR spectrum of **19** three types of CO bands are observed, a terminal carbonyl at 1975 cm^{-1} , a semi-bridging carbonyl at 1910 cm^{-1} and an

Scheme 4.3



acyl carbonyl band at 1798 cm^{-1} . Although the acyl stretch seems a little blue-shifted compared to most bridging acyls,^{9,10,12,13} stretches similar to that of **19** have been previously reported^{8,14} and are diagnostic in determining the amount of carbene character for the sp^2 carbon. The $^{13}\text{C}\{^1\text{H}\}$ NMR and IR data suggest that in **19** that carbon has little carbene character associated with it.

The structure of **19** was confirmed by an X-ray structure determination, with a

representation of the complex cation shown in Figure 4.1 and relevant bond lengths and angles given in Table 4.3. Clearly the DMA has undergone a 1,2-insertion into the Rh-C bond of the methylene bridge, accompanied by migration of the organic fragment to a carbonyl group. The bond angles C(5)-C(6)-Rh ($112.3(3)^\circ$) and Rh-C(3)-C(4) ($118.0(4)^\circ$) are slightly less than the ideal 120° for an sp^2 type carbon, indicative of the ring strain in the group. The strain is also evident in the small C(6)-Rh-C(3) angle of $84.6(2)^\circ$, which is common in other structurally characterized late-metal mononuclear metallacyclopentanone complexes.^{14,15} The C(6)-C(5)-C(4)-C(3)-Rh fragment is quite planar, with the largest out-of-plane deviation belonging to C(4) ($0.051(7)$ Å). In addition, the organic fragment appears to be more tightly bound at the ketonic carbon (Rh-C(3) = $1.915(5)$ Å) than at the vinylic carbon (Rh-C(6) = $2.077(5)$ Å), again common in these types of complexes.^{14,15} Although the Rh-C(3) distance suggests some carbene character associated with this carbon, this is not supported by the C(3)-O(3) distance of $1.234(6)$ Å, which is normal for a C=O bond distance, and is not indicative of significant carbene character.¹⁶ Certainly, the spectroscopic evidence, noted above, did not suggest significant carbene character. The O(3)-Ru distance of $2.449(4)$ Å is also longer than complexes where the acyl moiety is considered to have more oxy-carbene character,⁹ but most certainly corresponds to a bonding interaction, being much shorter than the predicted van der Waals separation of *ca.* 3.15 Å.^{17,18} Presumably the acyl oxygen cannot approach closer to the Ru to optimize the orbital overlap owing to the strain that would result at the metallacycle end of the ligand. The Ru-O(3)-C(3) angle ($107.5(3)^\circ$) is more acute than predicted (idealized value of 120 for an sp^2 oxygen),

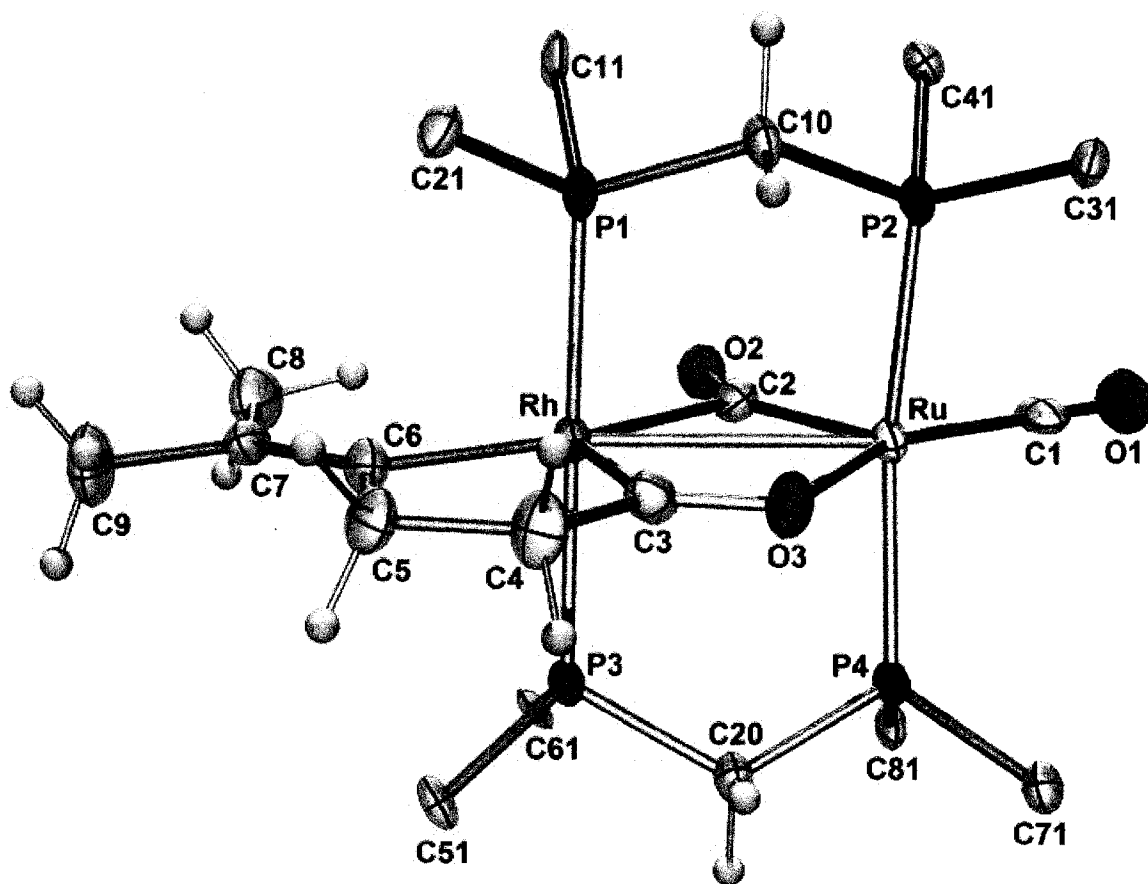


Figure 4.1: Perspective view of the complex cation of compound **19**, showing the numbering scheme. Thermal ellipsoids are drawn at the 50% level except for hydrogens, which are drawn arbitrarily small. Phenyl groups, except for ipso carbons, are omitted.

Table 4.3: Selected Distances and Angles for Compound 19.*(i) Distances (Å)*

Atom 1	Atom 2	Distance	Atom 1	Atom 2	Distance
Rh	Ru	2.9833(6)	P1	P2	3.089(2) [§]
Rh	P1	2.368(2)	P3	P4	3.090(2) [§]
Rh	P3	2.36(1)	O1	C1	1.160(6)
Rh	C2	2.238(5)	O2	C2	1.162(5)
Rh	C3	1.915(5)	O3	C3	1.234(6)
Rh	C6	2.077(5)	C3	C4	1.497(7)
Ru	P2	2.36(1)	C4	C5	1.536(7)
Ru	P4	2.34(1)	C5	C6	1.510(7)
Ru	O3	2.449(4)	C6	C7	1.329(7)
Ru	C1	1.837(5)	C7	C8	1.488(7)
Ru	C2	1.919(5)	C7	C9	1.520(7)

[§] Non-bonded distance

(ii) Angles (deg)

Atom 1	Atom 2	Atom 3	Angle	Atom 1	Atom 2	Atom 3	Angle
Ru	Rh	P1	90.23(4)				
Ru	Rh	P3	89.56(4)	O3	Ru	C2	108.2(1)
Ru	Rh	C2	40.01(13)	C1	Ru	C2	104.0(2)
Ru	Rh	C3	73.59(16)	Ru	O3	C3	107.5(3)
Ru	Rh	C6	158.1(1)	C6	C7	C8	122.8(5)
P1	Rh	P3	175.71(5)	C6	C7	C9	121.5(5)
C2	Rh	C3	113.6(2)	C8	C7	C9	115.7(4)
C2	Rh	C6	161.8(2)	C5	C6	C7	125.8(5)
C3	Rh	C6	84.6(2)	Rh	C6	C5	112.3(3)
Rh	Ru	P2	92.31(4)	Rh	C6	C7	122.0(4)
Rh	Ru	P4	93.01(4)	C4	C5	C6	112.6(4)
Rh	Ru	O3	59.59(8)	Rh	C3	O3	119.3(4)
Rh	Ru	C1	152.6(1)	Rh	C3	C4	118.0(4)
Rh	Ru	C2	48.6(1)	C4	C3	O3	122.7(4)
P2	Ru	P4	169.51(5)	Rh	C2	O2	120.5(4)
O3	Ru	C1	147.8(1)	Ru	C2	O2	148.0(4)

another indication that the orbital overlap between Ru and O(3) has not been optimized.

Within the organic fragment, all the bond distances and angles appear normal,¹⁹ indicating little if any delocalization within this group. The double bond of the DMA group, between C(6) and C(7), remains intact with a typical C(sp²)=C(sp²) distance of 1.329(7) Å. Single bonds within the fragment between sp² and sp³ hybridized carbon atoms (C(3)-C(4) = 1.497(7) Å, C(5)-C(6) = 1.510(7) Å) and sp³/sp³ carbon atoms (C(4)-C(5) = 1.536(7) Å) are also well within the normal range for such bonds. Within the planar group, the bond angles (with the exception of Rh-C(6)-C(5)) are all approximately 120°, with a slightly enlarged C(5)-C(6)-C(7) angle of 125.8(5)° (presumably to minimize the non-bonded contact between the C(9)H₃ methyl group and the C(5)H₂ methylene group). All other parameters within the complex appear normal.

Figure 4.1 also confirms the presence of a semibridging carbonyl as suggested by the ¹³C{¹H} NMR spectrum (*vide supra*), with a Ru-C(2)-O(2) angle of 148.0(4)° accompanied by a smaller Rh-C(2)-O(2) angle of 120.5(4)°. As is typical for semibridging carbonyls, the carbonyl is more linear with respect to the metal to which it is σ-bound, and the Ru-C(2) bond (1.919(5) Å) is significantly shorter than the Rh-C(2) interaction (2.238(5) Å), also typical for a semibridging CO.

The metal-metal distance of 2.9833(6) Å is outside the range normally associated with Rh-Ru bonds in complexes of this type (Chapter 2),²⁰⁻²² but the slight contraction compared to the intraligand P-P distances (3.089(2) and 3.090(2) Å) indicates some level of attraction between the metals. The nature of the bridging acyl group largely affects the degree to which these metals will interact. In **19**, the C(3)-O(3)-Ru bond angle, as noted,

is already somewhat strained at $107.5(3)^\circ$. Any shortening of the metal-metal distance would result in a more acute C(3)-O(3)-Ru bond angle, and thus weaken the Ru-O(3) interaction by reducing the overlap of the lone pair on O(3) with the empty d orbital on Ru.

Addition of H_2 to a concentrated dichloromethane solution of **19** affords the dihydride complex $[RhRu(H)_2(CO)_2(C(O)CH_2CH_2C(=C(CH_3)_2))(dppm)_2][CF_3SO_3]$ (**20**). The 1H NMR spectrum of **20** shows that the metallacyclopentanone moiety remains intact, with the only major difference compared to the 1H NMR spectrum of **19** being the appearance of two high-field multiplets at δ -7.89 and -10.01. The appearance of two resonances at such high field is inconsistent with an η^2-H_2 complex.^{23,24} Unfortunately, the broadness of the hydride signals does not allow us to establish the coupling involved and leaves ambiguity in the nature of their bonding and their connectivity diagrammed in Scheme 4.3. Upon broad-band phosphorus decoupling these two resonances became broad multiplets, and the close proximity of the two ^{31}P resonances rules out selective decoupling experiments. The IR spectrum of **20** shows two terminal CO bands at 2053 and 2000 cm^{-1} , in addition to one acyl carbonyl band at 1683 cm^{-1} . Two new bands appear at 2155 and 2126 cm^{-1} , well within the accepted range for terminally-bound hydrides to second-row transition metals.²³⁻²⁷ Confirmation by reacting **19** with D_2 and observing the isotopic shift of the bands has not been performed. The $^{13}C\{^1H\}$ NMR spectrum of **20** contains two ruthenium-bound terminal carbonyls at δ 196.8 and 190.7 along with the resonance for the acyl carbonyl at δ 236.3 with 28 Hz coupling to Rh.

Discussion:

As noted earlier, we have attempted to model the sequential transformation of C_1 -containing species to ones containing higher order hydrocarbyl fragments through the reactions of the methylene-bridged complexes $[\text{RhRu}(\text{CO})_x(\mu\text{-CH}_2)(\text{dppm})_2]^+$ ($x = 3, 4$) with unsaturated organic substrates. In Chapter 3 we showed that alkyne insertion into the Rh-carbon bond of the bridging-methylene group in $[\text{RhRu}(\text{CO})_3(\mu\text{-CH}_2)(\text{dppm})_2][\text{CF}_3\text{SO}_3]$ (**4**), yielded a series of C_3 -bridged products in which the C_3 fragment was bound to Rh by the vinylic end of the C_3 fragment and to Ru at the opposite methylene end. In this chapter we have investigated the reactions of **4** with allene and substituted allenes in attempts to form an analogous series of C_3 -bridged products. As anticipated, compound **4** reacts readily with cumulated olefins. Assuming that substrate insertions occurred at the Rh- CH_2 bond, as previously demonstrated in alkyne reactions (Chapter 3), two products seemed possible, as shown in Scheme 4.1.

Although **4** reacted instantly with allene, the product obtained was neither of those anticipated in Scheme 4.1, instead forming $[\text{RhRu}(\text{CO})_2(\mu\text{-}\eta^3\text{:}\eta^1\text{-C}(\text{CH}_2)_3)(\text{dppm})_2][\text{CF}_3\text{SO}_3]$ (**16**), as diagrammed in Scheme 4.2. This type of arrangement for a bridging trimethylenemethane (TMM) moiety has been observed previously with a variety of metal combinations.²⁸⁻³¹ In the present chemistry, we propose that allene coordination occurs at Rh, followed by insertion into the Rh- CH_2 bond to yield the C_3 -bridged species **A**, as shown in Scheme 4.1. This product is recognized as a substituted η^1 -allyl fragment bound to both Rh and Ru, and like many η^1 -allyl complexes, is unstable and tends to rearrange to an η^3 -allyl complex with

accompanying expulsion of one CO ligand, to give the product shown in Scheme 4.2. It is interesting that the η^1 - to η^3 -allyl rearrangement occurs at Rh and not Ru. We assume that the stronger Ru-CH₂ bond of the putative intermediate A (in Scheme 4.1) favours retention of this bond instead of the weaker Rh-CH₂ bond, the latter of which is cleaved to form the η^3 -allyl linkage. It may also be that the more crowded environment at Ru, necessitated by its strong tendency to have an 18e configuration also favours η^3 -binding at Rh. NMR evidence at low temperature shows that **16** is formed in appreciable amounts even at temperatures as low as -80 °C, with no intermediates being detected. In a related study by Knox and coworkers substitution of the labile acetonitrile ligand in the complex [Ru₂(CO)(MeCN)(μ -CH₂)(μ -CO)(η^5 -C₅H₅)₂] by allene yielded an analogous trimethylenemethane-bridged product, and again no evidence for intermediates was obtained.³¹ This proposal is directly analogous to the previously reported alkyne insertions in both our Rh/Ru²⁰ and Rh/Os³² systems, as well as those reported by Knox,³¹ Pettit³³ and Hudler.³⁴

Although most mononuclear TMM complexes are prone to fluxionality with respect to the TMM ligand,^{31,35} compound **16** is static with no scrambling of the ¹³CH₂ group that is bound to Ru occurring at temperatures as high as +30 °C. The σ -bound end of the TMM fragment in **16** and in [Ru₂(μ -C(CH₂)₃)(μ -CO)₂(Cp)₂] anchors the group and prevents the propeller-like rotation that might occur from an η^3 - η^1 - η^3 -type allyl rearrangement. Although this diruthenium compound did not display rotation of the trimethylene group, the compound is fluxional with respect to the carbonyl ligands.³¹ Compound **16** shows no such dynamic behaviour of the carbonyls.

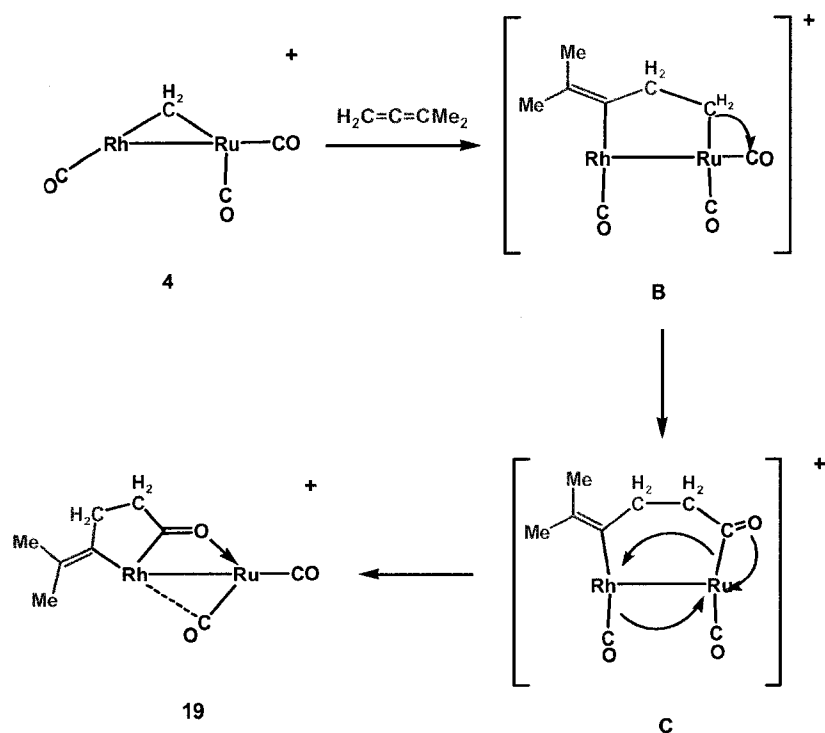
Attempts to incorporate additional CH₂ groups into **16** by reaction with diazomethane at a variety of temperatures did not yield isolable or identifiable products. At low diazomethane concentrations **16** did not react while at high concentrations a complex mixture of unidentified products resulted.

The proposed conversion of the η^1 -allyl group to η^3 was apparently accompanied by a carbonyl loss, suggesting that addition of CO, or another 2-electron donor might reverse the process leading to observation of the putative η^1 -allyl intermediate, or a related species. Although **16** does react with CO and PMe₃ to yield the adducts [RhRu(CO)₂(L)(μ - η^3 : η^1 -C(CH₂)₃)(dppm)₂][CF₃SO₃] (L = CO (**17**), PMe₃ (**18**)), this was not accompanied by rearrangement of the allyl moiety. The Rh centre in **16** has a 16e configuration so ligand incorporation can occur to give an 18e species while retaining an η^3 -allyl coordination mode. Both adducts **17** and **18** are labile, and under vacuum carbonyl loss from **17** and quantitative conversion to **16** occurs, while the PMe₃ adduct **18** is only stable below -40 °C; at higher temperatures decomposition occurs to a mixture of unidentifiable products.

Reaction of **4** with dimethylallene (DMA) does not yield a product analogous to **16**, but instead forms the unusual metallacyclopentanone-containing species [RhRu(CO)₂(C(O)CH₂CH₂C(=C(CH₃)₂))(dppm)₂][CF₃SO₃] (**19**). We suggest that coordination of the dimethylallene ligand at Rh occurs with subsequent insertion into the Rh-CH₂ bond to give species **B** diagrammed earlier in Scheme 4.1, and shown again in Scheme 4.4. It appears that subsequent migratory insertion of the resulting Ru-bound alkyl group to a Ru-bound carbonyl occurs, as shown in Scheme 4.4 to give an

intermediate **C**₄-bridged species, **C**. Migration of the acyl carbon from Ru to Rh, forming the 5-membered metallacycle is accompanied by coordination of the acyl oxygen to Ru and migration of the Rh-bound carbonyl to Ru to yield the final product **19**. We were unable to detect intermediates in this transformation, even at $-80\text{ }^{\circ}\text{C}$. This type of metallacyclopentanone organic fragment has been observed before in mononuclear complexes,^{14,15,36} but **19** appears to be the first binuclear example of such a fragment. Support for intermediate **B** comes from related chemistry involving the Rh/Os

Scheme 4.4



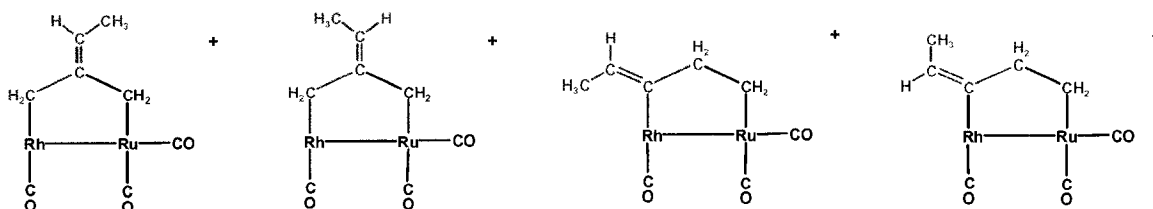
combination of metals in which a product analogous to intermediate **B** was observed and characterized³⁷. The failure of this Rh/Os analogue to undergo migratory insertion involving a carbonyl is in line with the lower migratory insertion tendencies of 3rd row metals, presumably as a result of stronger metal-carbon bonds involving these metals.³⁸

Attempts to liberate an organic product, such as $\text{Me}_2\text{C}=\text{CHCH}_2\text{CH}_2\text{C}(\text{O})\text{H}$ by hydrogenolysis of the Rh-C bonds of **19** or hydrogenated products such as 4-methyl-pent-3-enal, by treatment with H_2 failed. Instead, the dihydride complex $[\text{RhRu}(\text{H})_2(\text{CO})_2(\text{C}(\text{O})\text{CH}_2\text{CH}_2\text{C}(\text{=C}(\text{CH}_3)_2))(\text{dppm})_2][\text{CF}_3\text{SO}_3]$ (**20**) is formed in which H_2 has oxidatively added to the complex, leaving the metallacyclopentanone fragment intact. We suggest that the hydride ligands are bound to Ru, while the metallacyclopentanone fragment is bound to Rh, inhibiting reductive elimination of the organic fragment. Unfortunately, the breadth of the hydride signals in the NMR spectrum prevented unambiguous placement of the hydride ligands. Experiments are underway in order to determine the nature of these hydrides, such as IR spectroscopy of the isotopomer $[\text{RhRu}(\text{D})_2(\text{CO})_2(\text{C}(\text{O})\text{CH}_2\text{CH}_2\text{C}(\text{=C}(\text{CH}_3)_2))(\text{dppm})_2][\text{CF}_3\text{SO}_3]$ (**20-D₂**), and the $^1\text{H}/^{31}\text{P}$ HMQC 2D NMR experiments, both of which might confirm the terminal nature of these hydrides and their location on Ru. The weakly coordinating nature of the acyl oxygen to Ru in **19** allows for facile displacement by reaction with H_2 .

As noted earlier, two modes of cumulene coordination at Rh would give rise to two different insertion products (**A** and **B**). Although neither of these were obtained, the species appear to be intermediates in the formation of the trimethylenemethane (**16**) and metallacyclopentanone (**19**) products observed. We propose that initial formation of **A** and **B** is dictated by the steric interactions involving the hydrogen or methyl substituents on allene and dimethylallene, and the dppm phenyl rings. It appears that the less-sterically hindered allene ($\text{R} = \text{H}$) follows the path leading through intermediate **A**, whereas the bulkier dimethylallene ($\text{R} = \text{Me}$) appears to follow the other path, through intermediate **B**. Methylallene ($\text{R} = \text{Me}$ and H) is intermediate between the two steric

extremes of allene and 1,1-dimethylallene so it was of interest to determine the nature of the product with this monosubstituted allene. Unfortunately, treatment of **4** with methylallene gave a complex mixture of products which may contain both of the possible insertion products **A** and **B** shown in Scheme 4.1. If this is the case, *each* of these regioisomers could give rise to two *more* isomers detailing the location of the methyl group, all four of which are diagrammed in Chart 4.1. The components of this mixture could not be identified, however. It is not clear why the methylallene reacts so differently, particularly when the analogous chemistry with RhOs leads cleanly to a product analogous to **16** (*vide infra*).

Chart 4.1



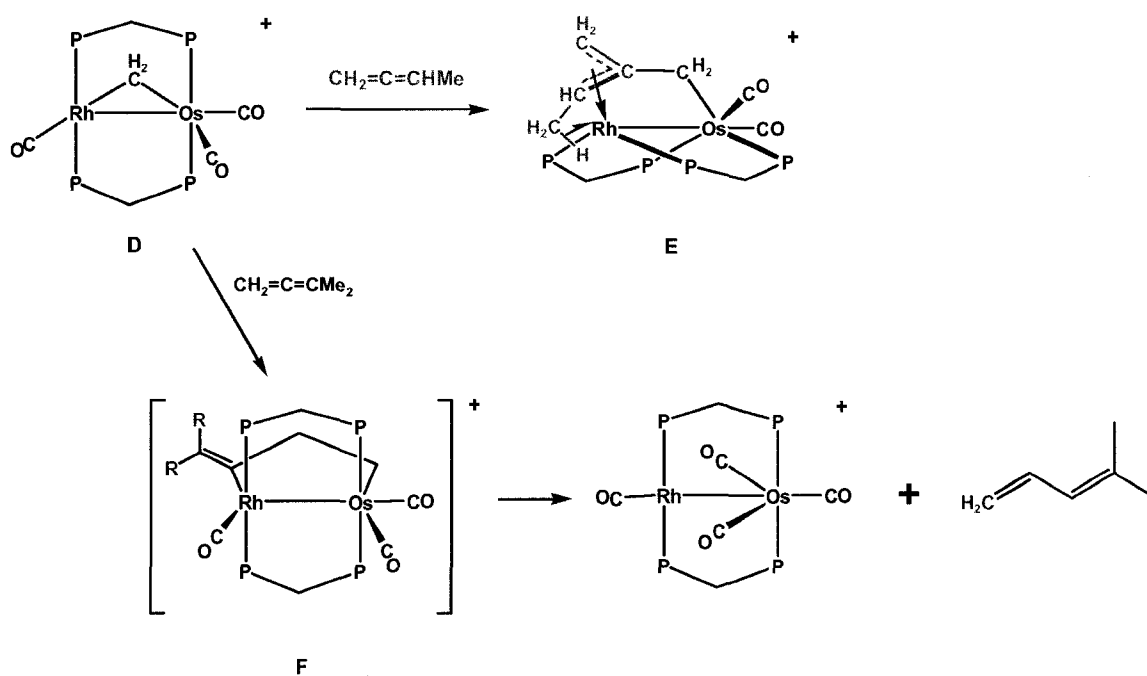
As described in earlier chapters, the reactivity of the Rh/Ru complexes can have similarities with those of Rh/Os, but can also display some unexpected differences. The same dichotomy is observed in the reactions of the two metal combinations with allenes. Both $[\text{RhRu}(\text{CO})_3(\mu\text{-CH}_2)(\text{dppm})_2]^+$ and its Rh/Os analogue react with allene gas to yield the TMM-bridged complexes $[\text{RhM}(\text{CO})_2(\mu\text{-}\eta^3\text{:}\eta^1\text{-C}(\text{CH}_2)_3)(\text{dppm})_2]^+$ ($\text{M} = \text{Ru}, \text{Os}$). In addition, both TMM-bridged complexes coordinate CO or PMe_3 forming the adducts $[\text{RhM}(\text{CO})_2(\text{L})(\mu\text{-}\eta^3\text{:}\eta^1\text{-C}(\text{CH}_2)_3)(\text{dppm})_2]^+$ ($\text{L} = \text{CO}, \text{PMe}_3$), while retaining the original TMM coordination mode.

The other allenes investigated react differently for the pair of metal combinations. The difference in the reactivity with methylallene has been noted above. With RhOs the TMM-bridged species shown in Scheme 4.5 was obtained. Interestingly, the agostic C-H interaction of the methyl substituent observed in the RhOs chemistry is analogous to the CO and PMe_3 adducts (**17** and **18**) observed in the chemistry described herein, in which the C-H bond supplied the pair of electrons to Rh instead of CO or PMe_3 . The reasons for the dramatic chemical differences upon substitution of Os for Ru in the reactions with methyl allene are unclear, although it should be noted that with the Rh/Os complex, reaction with methyl allene was capricious, yielding mixtures of products under all but one set of conditions tried. It may be that under the right (yet-to-be determined) conditions, a Rh/Ru analogue of **E** might be obtained.

With dimethylallene, the Rh/Ru complex yields the complex $[\text{RhRu}(\text{CO})_2(\text{C}(\text{O})\text{CH}_2\text{CH}_2\text{C}(\text{=C}(\text{CH}_3)_2))(\text{dppm})_2]^+$ (**19**), whereas with $[\text{RhOs}(\text{CO})_3(\mu\text{-CH}_2)(\text{dppm})_2]^+$, the products are $[\text{RhOs}(\text{CO})_4(\text{dppm})_2]^+$ and 1,1-dimethylbutadiene. As noted earlier, initial coordination of dimethylallene at Rh is assumed, leading to intermediate **B**. We suggest that this occurs in both cases, and indeed the intermediate **F** in Scheme 4.5 has been observed in the Rh/Os system, though its existence is

ephemeral.³⁷ With the Rh/Os complex, β -hydrogen elimination occurs followed by reductive elimination of the butadiene. Upon changing Os for Ru, the tendency for C-H activation decreases going to the second-row metal and the tendency for migratory insertion to a carbonyl increases. In this case the latter is formed leading to the metallacyclopentanone species observed.

Scheme 4.5



Conclusions:

Although the reactions of the methylene-bridged $[\text{RhRu}(\text{CO})_3(\mu\text{-CH}_2)(\text{dppm})_2][\text{CF}_3\text{SO}_3]$ (**4**) with allene and 1,1-dimethylallene did not yield the targeted C_3 -bridged products outlined in Scheme 4.1, they did yield two interesting and unusual

classes of compounds, which appear to proceed, in the early steps of the reactions, through the species proposed in this scheme. The very different products obtained in the reactions of dimethylallene with the Rh/Ru and Rh/Os compounds presents dramatic evidence that changes in metal combinations can give rise to different products. As noted in Chapter 1, the use of different metal combinations is a potential way to tailor the types of products obtained in FT and other processes. The work described herein has shown that the greater migratory insertion tendency of 2nd row metals compared to their 3rd row congeners can give rise to acyl products with the former, from which presumably oxygenates can be obtained.

References:

1. Trepanier, S.J.; Sterenberg, B.T.; McDonald, R.; Cowie, M. *J. Am. Chem. Soc.* **1999**, *121*, 2613.
2. Further information may be obtained by contacting Dr. Robert McDonald (bob.mcdonald@ualberta.ca) and inquiring about sample number COW0140 (compound **19**).
3. Programs for diffractometer operation, data reduction, and absorption correction were those supplied by Bruker.
4. Beurskens, P.T.; Beurskens, G.; de Gelder, R.; Garcia-Granda, S.; Isreal, R.; Gould, R.O.; Smits, J.M.M. *DIRDIF-99 program system*; Crystallography Laboratory, University of Nijmegen: The Netherlands, 1999.

5. Sheldrick, G.M. *SHELXL-93*: Program for crystal structure determination; University of Gottingen: Gottingen, Germany, 1993.
6. Fryzuk, M.D. *Inorg. Chem.* **1982**, *21*, 2134.
7. Lawrance, G.A. *Chem. Rev.* **1986**, *86*, 17.
8. Trepanier, S.J.; McDonald, R.; Cowie, M. *Organometallics* **2003**, *22*, 2638.
9. Shafiq, F.; Kramarz, K.W.; Eisenberg, R. *Inorg. Chim. Acta* **1993**, *213*, 111.
10. Ferguson, G.S.; Wolczanski, P.T. *J. Am. Chem. Soc.* **1986**, *108*, 8293.
11. Bonnesen, P.V.; Baker, A.T.; Hersh, W.H. *J. Am. Chem. Soc.* **1986**, *108*, 8304.
12. Casey, C.P.; Palermo, R.E.; Rheingold, A.L. *J. Am. Chem. Soc.* **1986**, *108*, 549.
13. Johnson, K.A.; Gladfelter, W.L. *Organometallics* **1990**, *9*, 2101.
14. Karel, K.J.; Tulip, T.H.; Ittel, S.D. *Organometallics* **1990**, *9*, 1276.
15. Theopold, K.H.; Becker, P.N.; Bergman, R.G. *J. Am. Chem. Soc.* **1982**, *104*, 5250.
16. Orpen, A.G.; Brammer, L.; Allen, F.H.; Kennard, O.; Watson, D.G.; Taylor, R. *J. Chem. Soc.-Perkin Trans. 2* **1989**, S1.
17. Bondi, A. *J. Phys. Chem.* **1964**, *68*, 441.

18. The van der Waal's radius for Ru was approximated using the experimentally determined value for that belonging to Pd = 1.63 Å.
19. Allen, F.H.; Kennard, O.; Watson, D.G.; Brammer, L.; Orpen, A.G.; Taylor, R. *J. Chem. Soc.-Perkin Trans. 2* **1987**, S1.
20. Rowsell, B.D.; McDonald, R.; Ferguson, M.J.; Cowie, M. *Organometallics* **2003**, *22*, 2944.
21. Rowsell, B.D.; Trepanier, S.J.; Lam, R.; McDonald, R.; Cowie, M. *Organometallics* **2002**, *21*, 3228.
22. Sterenberg, B.T., PhD Thesis, Chapter 5, University of Alberta, Edmonton, Alberta, Canada, 1997.
23. Bianchini, C.; Perez, P.J.; Peruzzini, M.; Zanobini, F.; Vacca, A. *Inorg. Chem.* **1991**, *30*, 279.
24. Lenero, K.A.; Kranenburg, M.; Guari, Y.; Karner, P.C.J.; van Leeuwen, P.W.N.M.; Sabo-Etienne, S.; Chaudret, B. *Inorg. Chem.* **2003**, *42*, 2859.
25. Lehner, H.; Matt, D.; Togni, A.; Thouvenot, R.; Venanzi, L.M.; Albinati, A. *Inorg. Chem.* **1984**, *23*, 4254.
26. Balch, A.L.; Davis, B.J.; Neve, F.; Olmstead, M.M. *Organometallics* **1989**, *8*, 1000.
27. Antonelli, D.M.; Cowie, M. *Organometallics* **1990**, *9*, 1818.

28. Chetcuti, M.J.; Fanwick, P.E.; Grant, B.E. *Organometallics* **1991**, *10*, 3003.
29. Ward, J.S.; Pettit, R. *J. Chem. Soc.-Chem. Commun.* **1970**, 1419.
30. Whitesides, T.H.; Slaven, R.W. *J. Organomet. Chem.* **1974**, *67*, 99.
31. Fildes, M.J.; Knox, S.A.R.; Orpen, A.G.; Turner, M.L.; Yates, M.I. *J. Chem. Soc.-Chem. Commun.* **1989**, 1680.
32. Chokshi, A.; Graham, T.W.; McDonald, R.; Cowie, M. Manuscript in preparation.
33. Sumner, C.E.; Collier, J.A.; Pettit, R. *Organometallics* **1982**, *1*, 1350.
34. Navarre, D.; Parlier, A.; Rudler, H.; Daran, J.C. *J. Organomet. Chem.* **1987**, *322*, 103.
35. Albright, T.A.; Hofmann, P.; Hoffmann, R. *J. Am. Chem. Soc.* **1977**, *99*, 7546.
36. Theopold, K.H.; Bergman, R.G. *J. Am. Chem. Soc.* **1980**, *102*, 5694.
37. Chokshi, A., M.Sc. Thesis, University of Alberta, Edmonton, Alberta, Canada, 2004.
38. Huheey, J.E.; Keiter, E.A.; Keiter, R.L. *Inorganic Chemistry: Principles of Structure and Reactivity*; 4th ed.; Harper Collins: New York, 1993.

Chapter 5

Methylene-to-Acyl Conversion: Models for Oxygenate Formation

Introduction:

As was noted in Chapter 1, alkanes and olefins are not the only products of the Fischer-Tropsch (FT) reaction. Oxygenates, in the form of aldehydes, ketones and alcohols, are common particularly when rhodium catalysts are used.¹ Unfortunately, little is known about the mechanism involved in the formation of these oxygenates. A proposal introduced by Pichler and Schulz,² and later revised by others,^{3,4} is based on the well-studied migratory insertion reactions of carbonyl and methyl groups,⁵ in which the resulting acyl groups give rise to the appropriate oxygenated products, as diagrammed in Scheme 1.10.

Our interest in the roles of different metals in bimetallic FT catalysts included the formation of oxygenates, so we set out to investigate alkyl and acyl formation from bridging methylene groups. Transformations of these groups at binuclear cores have been reported for several dppm- or dmpm-bridged (dmpm = Me₂PCH₂PMe₂) binuclear complexes involving the Rh/Rh,⁶ Ru/Ru^{7,8} and Rh/Os⁹ combinations of metals.

In this chapter, we investigate the conversion of a bridging methylene into an acyl group on a Rh/Ru complex.

Experimental:

General Comments. All solvents were dried (using appropriate desiccants), distilled before use, and stored under a dinitrogen atmosphere. Reactions were performed under an argon atmosphere using standard Schlenk techniques. Diazomethane was generated from Diazald, which was purchased from Aldrich, as was the trimethylphosphine (1 M) solution in THF, and the triflic acid. The ^{13}C -enriched Diazald was purchased from Cambridge Isotopes, whereas ^{13}CO was purchased from Isotec Inc.

The ^1H , $^{13}\text{C}\{^1\text{H}\}$, and $^{31}\text{P}\{^1\text{H}\}$ NMR spectra were recorded on a Varian iNova-400 spectrometer operating at 399.8 MHz for ^1H , 161.8 MHz for ^{31}P , and 100.6 MHz for ^{13}C . Infrared spectra were obtained on a Bomem MB-100 spectrometer. The elemental analyses were performed by the microanalytical service within the department.

Spectroscopic data for all compounds are given in Table 5.1.

Preparation of Compounds

(a) **[RhRu(OSO₂CF₃)(CO)₂(μ-C(O)CH₃)(dppm)₂][CF₃SO₃] (20).** The compound [RhRu(CO)₄(μ-CH₂)(dppm)₂][CF₃SO₃] (3) (100 mg, 0.080 mmol) was dissolved in 5 mL of CH₂Cl₂. To this, 8.0 μL of triflic acid (0.090 mmol) was added and the solution was stirred for 1 h. The orange solution was concentrated under a stream of Ar to *ca.* 2 mL and orange microcrystals slowly began to precipitate. Diethyl ether (20 mL) was added dropwise to the slurry. The supernatant was removed and the crystals were

Table 5.1. Spectroscopic Data For Compounds.

Compound	IR (cm ⁻¹) ^{a,b,c}	NMR ^{d,e}		
		³¹ P{ ¹ H} (ppm) ^f	¹ H (ppm) ^{g,h}	¹³ C{ ¹ H} (ppm) ^{h,i}
[RhRu(OSO ₂ CF ₃)(CO) ₂ - (μ-C(O)CH ₃)(dppm) ₂]- [CF ₃ SO ₃] (20)	2045 (s), 1989(s)	20.8 (m), 16.9 (dm)	3.64 (m, 2H), 2.59 (m, 2H), 1.99 (s, br, 3H)	270.3 (dm, ¹ J _{RhC} = 33 Hz, 1C), 204.2 (m, 1C), 180.4 (m, 1C)
[RhRu(CO) ₄ (μ- CH ₃)(dppm) ₂]-[CF ₃ SO ₃] ₂ (21)		24.2 (dm), 20.8 (m)	4.10 (m, 2H), 3.63 (m, 2H), 0.30 (s, br, 3H)	219.5 (m, 1C), 190.4 (m, 1C), 187.7 (m, 1C), 183.4 (dt, ¹ J _{RhC} = 79 Hz, ² J _{PC} = 15 Hz, 1C)
[RhRu(CH ₃)(CO) ₄ (dppm) ₂]- [CF ₃ SO ₃] ₂ (22)		28.7 (dm), 23.0 (m)	3.41 (m, 4H), 1.66 (dt, ³ J _{PH} = 8 Hz, ² J _{RhH} = 4 Hz, 3H)	221.6 (m, br, 2C), 186.3 (m, br, 2C)
[RhRu(OSO ₂ CF ₃)(CO) ₃ - (μ-C(O)CH ₃)(dppm) ₂]- [CF ₃ SO ₃] (23)	2090 (m), 2016 (s), 1732 (m)	21.9 (s, br), 6.8 (d, br)	3.30 (m, 2H), 3.22 (m, 2H), 2.03 (s, 3H)	304.8 (dm, ¹ J _{RhC} = 38 Hz, 1C), 250.3 (m, 1C), 196.6 (m, 1C), 184.9 (m, 1C)

Table 5.1. (cont'd)

[RhRu(OSO ₂ CF ₃)(CO) ₂ - (μ-C(O)CH ₃)(dppm) ₂]- [CF ₃ SO ₃] (24)	2015 (s), 1956 (s)	22.7 (m), 17.6 (dm)	3.77 (m, 2H), 3.32 (m, 2H), 1.93 (s, br, 3H)	293.3 (s, br, 1C), 196.3 (t, ² J _{PC} = 14 Hz), 186.8 (dt, ¹ J _{RhC} = 75 Hz, ² J _{PC} = 14 Hz, 1C)
[RhRu(OSO ₂ CF ₃)(CO) ₄ (μ- H)(dppm) ₂][CF ₃ SO ₃] (25a)	2072 (m), 2040 (s), 1999 (m), 1880 (m)	27.3 (m), 25.1 (m)	5.07 (m, 2H), 3.79 (m, 2H), -10.41 (m, 1H)	
[RhRu(BF ₄)(μ-H)(CO) ₄ - (dppm) ₂][BF ₄] (25b)		27.1 (om)	4.52 (m, 2H), 3.81 (m, 2H), -11.07 (m, 1H)	
[RhRu(CH ₃)(CO) ₂ (μ-Cl)(μ- CO)(dppm) ₂][CF ₃ SO ₃] (26a)	2013 (s), 1986 (s), 1711 (m)	29.0 (m), 23.0 (dm)	4.12 (m, 2H), 3.32 (m, 2H), -0.21 (t, ³ J _{PH} = 6 Hz, 3H)	246.4 (m, 1C), 199.4 (t, ² J _{PC} = 12 Hz, 1C), 188.8 (dt, ¹ J _{RhC} = 76 Hz, ² J _{PC} = 13 Hz, 1C)

^a IR abbreviations: s = strong, m = medium, w = weak, sh = shoulder. ^b CH₂Cl₂ solutions unless otherwise stated, in units of cm⁻¹. ^c Carbonyl stretches unless otherwise noted. ^d NMR abbreviations: s = singlet, d = doublet, t = triplet, m = multiplet, cm = complex multiplet, dm = doublet of multiplets, om = overlapping multiplets, br = broad, dt = doublet of triplets, dpq = doublet of pseudoquintets. ^e NMR data at 25 °C in CD₂Cl₂ unless otherwise stated. ^f ³¹P chemical shifts referenced to external 85% H₃PO₄. ^g Chemical shifts for the phenyl hydrogens are not given. ^h ¹H and ¹³C chemical shifts referenced to TMS. ⁱ ¹³C{¹H} NMR performed with ¹³CO enrichment.

washed with 2×15 mL of ether and dried *in vacuo* (72 mg, 66% yield). Anal. Calcd. for $C_{56}H_{47}F_6O_9P_4RhRuS_2$: C, 49.10; H, 3.46. Found: C, 49.22; H, 3.45.

(b) $[RhRu(CO)_4(\mu-CH_3)(dppm)_2][CF_3SO_3]_2$ (21**).** Triflic acid (0.70 μ L, 0.0079 mmol) was added to a CD_2Cl_2 (0.7 mL) of **3** (7.1 mg, 0.0056 mmol) in an NMR tube at -78 °C. No noticeable colour change resulted. Compound **21** was characterized only by NMR spectroscopy, since warming the solution above -40 °C resulted in conversion to **22** and subsequent heating to ambient temperature resulted in conversion to compounds **23** and **24** (*vide infra*).

(c) $[RhRu(CO)_4(\mu-CH_2D)(dppm)_2][CF_3SO_3]_2$ (21-CH₂D**).** Deuterated triflic acid (0.70 μ L, 0.0079 mmol) was added to a CD_2Cl_2 (0.7 mL) of **3** (7.1 mg, 0.0056 mmol) in an NMR tube at -78 °C. 1H NMR spectroscopy indicated a mixture of both **21** and **21-CH₂D**.

(d) $[RhRu(CO)_4(\mu-CD_2H)(dppm)_2][CF_3SO_3]_2$ (21-CD₂H**).** Triflic acid (0.70 μ L, 0.0079 mmol) was added to a CD_2Cl_2 (0.7 mL) of $[RhRu(\mu-CD_2)(CO)_4(dppm)_2][CF_3SO_3]$ (**3-CD₂**) (7.1 mg, 0.0056 mmol) in an NMR tube at -78 °C. 1H NMR spectroscopy indicated a mixture of the three isotopomers **21**, **21-CH₂D** and **21-CD₂H**.

(e) $[RhRu(CO)_4(CH_3)(dppm)_2][CF_3SO_3]_2$ (22**).** An NMR sample was prepared as described in part (b). The sample was then warmed to -40 °C. Complete conversion of **21** to **22** occurred over the course of approximately 1.5 h. As with compound **21**, **22** was

characterized by NMR spectroscopy alone, since warming above $-20\text{ }^{\circ}\text{C}$ resulted in conversion to **23** and **24**.

(f) [RhRu(OSO₂CF₃)(CO)₃(μ-C(O)CH₃)(dppm)₂][CF₃SO₃] (23). Method (i). An NMR sample was prepared as described in part (b). The sample was then warmed to $20\text{ }^{\circ}\text{C}$. Near total conversion of **21** to **23** occurred over the course of approximately 0.5 h.

Method (ii). An NMR tube was charged with both CO and 15 mg (0.0109 mmol) of **20**. To this, 0.7 mL of CD₂Cl₂ was added, and the orange slurry was transformed to a clear yellow solution upon mixing. ³¹P{¹H} and ¹H NMR spectroscopy confirmed complete conversion to **23**. Anal. Calcd. for C₅₇H₄₇F₆O₁₀P₄RhRuS₂: C, 48.97; H, 3.39. Found: C, 49.44; H, 3.43.

(h) Attempted reaction of 20 with H₂. A Teflon valved NMR tube was charged with 10 mg of the compound dissolved in 0.7 mL of CD₂Cl₂. H₂ was then passed over the solution to purge the headspace above the solution of Ar and pressurize to *ca.* 1 atm of H₂. The reaction was monitored by ³¹P{¹H} NMR spectroscopy over several days, and only the presence of **20** was detected.

(g) [RhRu(OSO₂CF₃)(CO)₂(μ-C(O)CH₃)(dppm)₂][CF₃SO₃] (24). [RhRu(CO)₃(PMe₃)-(μ-CH₂)(dppm)₂][CF₃SO₃] (**5**) (74 mg, 0.057 mmol) was dissolved in 10 mL of CH₂Cl₂, after which 5.5 μL (0.062 mmol) of triflic acid was added, causing an immediate colour change from orange to orange-yellow. Compound **24** was characterized by NMR spectroscopy alone, since any attempt to crystallize it resulted in isomerization to **24** and **20**.

(h) $[\text{RhRu}(\text{X})(\text{CO})_4(\mu\text{-H})(\text{dppm})_2][\text{X}]$ ($\text{X} = \text{CF}_3\text{SO}_3^-$ (**25a**) or BF_4^- (**25b**)). Although **25** was prepared with both the triflate (**25a**) and fluoborate (**25b**) anions, the synthesis described is for **25a**. Synthesis of **25b** is identical except for the use of tetrafluoroboric instead of triflic acid and using the BF_4^- salt of the precursor complex. Compound **2** (53 mg, 0.043 mmol) was dissolved in 10 mL of CH_2Cl_2 affording a bright yellow solution. Triflic acid was added dropwise (5.0 μL , 0.057 mmol) causing no colour change. The solution was stirred for 30 min, after which it was concentrated to *ca.* 1 mL. Dropwise addition of 15 mL of ether caused the precipitation of yellow microcrystals. The supernatant was removed and the yellow solid was washed with 3×10 mL ether and dried *in vacuo* (44.0 mg, 74% yield). Anal. Calcd for $\text{C}_{57}\text{H}_{47}\text{F}_6\text{O}_{10}\text{P}_4\text{RhRuS}_2$: C, 48.60; H, 3.28. Found: C, 48.13; H, 3.19.

(i) **Attempted reaction of 25a with CH_2N_2 .** A Teflon valved NMR tube was charged with 10 mg of the compound dissolved in 0.7 mL of CD_2Cl_2 . Diazomethane was then passed over the solution to purge the headspace above the solution of Ar and pressurize to *ca.* 1 atm of CH_2N_2 . The reaction was monitored by $^{31}\text{P}\{^1\text{H}\}$ NMR spectroscopy over several days, after which only **25a** was detected.

(j) $[\text{RhRu}(\text{CH}_3)(\text{CO})_2(\mu\text{-Cl})(\mu\text{-CO})(\text{dppm})_2][\text{X}]$ ($\text{X} = \text{CF}_3\text{SO}_3^-$ (**26a**) or BF_4^- (**26b**)). As with **25**, the synthesis described for **26** is that of the triflate complex, **26a**. Compound **3** (76 mg, 0.061 mmol) and $\text{DMA}\cdot\text{HCl}^{10}$ (8.2 mg, 0.067 mmol) were dissolved in 10 mL of acetone and stirred for 1 h. The yellow solution was concentrated to *ca.* 5 mL, to which 10 mL of ether was added dropwise resulting in the precipitation of bright yellow crystals. The supernatant was removed and the yellow microcrystals were washed with 2

× 10 mL ether and dried *in vacuo* (68.0 mg, 89% yield). Anal. Calcd. for $C_{55}H_{47}ClF_3O_6P_4RhRuS$: C, 52.58; H, 3.77. Found: C, 52.51; H, 3.78.

X-ray Data Collection.¹¹ Red crystals of $[RhRu(OSO_2CF_3)(CO)_2(\mu-C(O)CH_3)(dppm)_2][CF_3SO_3] \cdot 2MeNO_2$ (**20**) were obtained by slow diffusion of diethyl ether into a nitromethane solution of the compound. Data were collected on a Bruker PLATFORM/SMART 1000 CCD diffractometer¹² using Mo $K\alpha$ radiation at -80 °C. Unit cell parameters were obtained from a least-squares refinement of the setting angles of 5538 reflections from the data collection. The space group was determined to be $P2_1/c$ [No. 14]. The data were corrected for absorption through use of the SADABS procedure. See Table 5.2 for a summary of crystal data and X-ray data collection information.

Orange crystals of $[RhRu(OSO_2CF_3)(CO)_3(\mu-C(O)CH_3)(dppm)_2][CF_3SO_3]$ (**23**) were obtained by slow diffusion of diethyl ether into a dichloromethane solution of the complex. Data were collected and corrected for absorption as for **20** (*vide supra*). Unit cell parameters were obtained from a least-squares refinement of the setting angles of 7413 reflections from the data collection. The space group was determined to be $P2_1/n$ (an alternate setting of $P2_1/c$ [No. 14]).

Yellow crystals of $[RhRu(CH_3)(CO)_2(\mu-Cl)(\mu-CO)(dppm)_2][BF_4]$ (**26b**) were obtained by slow diffusion of diethyl ether into a dichloromethane solution of the complex. Data were collected and corrected for absorption as for **20** (*vide supra*). Unit cell parameters were obtained from a least-squares refinement of the setting angles of 7146 reflections from the data collection. The space group was determined to be $P2_1/n$.

Structure Solution and Refinement. The structure for **20** was solved using automated Patterson location of the heavy metal atoms and structure expansion via the DIRDIF-96 program system.¹³ Refinement was completed using the program SHELXL-93.¹⁴ Hydrogen atoms were assigned positions based on the geometries of their attached carbon atoms and were given thermal parameters 20% greater than those of the attached carbons. The final model for **20** refined to values of $R_1(F) = 0.0488$ (for 8659 data with $F_o^2 \geq 2\sigma(F_o^2)$) and $wR_2(F^2) = 0.1083$ (for all 12368 data).

The structure for **23** was solved using automated Patterson location of the heavy metal atoms and structure expansion via the DIRDIF-99 program system.¹⁵ Refinement was as for **20** above, using similar hydrogen atom location procedures. One end of one of the diphosphine ligands (involving P(3)) was found to be disordered such that the two phosphorous positions were approximately 0.2 Å apart. All attached atoms (C(51) to C(66) and attached hydrogens) were displaced over two slightly different positions. All disordered atoms were assigned equal occupancy factors and allowed to refine independently; although the P(3A) and P(3B) were refined anisotropically, the attached carbons were refined isotropically. The final model for **23** refined to values of $R_1(F) = 0.0393$ (for 10496 data with $F_o^2 \geq 2\sigma(F_o^2)$) and $wR_2(F^2) = 0.1076$ (for all 11881 data).

The structure for **26b** was solved using direct methods (SHELXS-86)¹⁶ and refinement was completed using the program SHELXL-93. The final model for **26b** refined to values of $R_1(F) = 0.0571$ (for 7085 data with $F_o^2 \geq 2\sigma(F_o^2)$) and $wR_2(F^2) = 0.1653$ (for all 11004 data).

Table 5.2. Crystallographic Data for Compounds 20, 23 and 26b.

	[RhRu(OSO ₂ CF ₃)(μ-C(O)CH ₃)(CO) ₂ (dppm) ₂]-[CF ₃ SO ₃] ₂ ·2MeNO ₂ (20)	[RhRu(OSO ₂ CF ₃)(μ-C(O)CH ₃)(CO) ₃ (dppm) ₂][CF ₃ SO ₃] (23)	[RhRu(μ-Cl)(μ-CO)(CO) ₂ (CH ₃)(dppm) ₂][BF ₄] ₂ ·CH ₂ Cl ₂ (26b)
formula	C ₅₈ H ₅₃ F ₆ N ₂ O ₁₃ P ₄ RhRuS ₂	C ₅₇ H ₄₇ F ₆ O ₁₀ P ₄ RhRuS ₂	C ₅₅ H ₄₉ BCl ₃ F ₄ O ₃ P ₄ RhRu
fw	1492.00	1397.93	1278.96
cryst dimens, mm	0.18 × 0.13 × 0.07	0.59 × 0.44 × 0.28	0.31 × 0.18 × 0.11
cryst. system	monoclinic	monoclinic	monoclinic
space group	<i>P2</i> ₁ / <i>c</i> (No. 14)	<i>P2</i> ₁ / <i>n</i> (an alternate setting of <i>P2</i> ₁ / <i>c</i> [No. 14])	<i>P2</i> ₁ / <i>n</i> (an alternate setting of <i>P2</i> ₁ / <i>c</i> [No. 14])
<i>a</i> , Å	14.8521 (8) ^a	10.1306 (5) ^b	17.3516 (9) ^c
<i>b</i> , Å	24.463 (1)	21.393 (1)	11.9257 (6)
<i>c</i> , Å	16.8317 (9)	26.908 (1)	26.464 (1)
<i>β</i> , deg	94.520 (10)	98.0403 (8)	100.251 (1)
<i>V</i> , Å ³	6096.5 (6)	5774.3 (5)	5388.7 (4)
<i>Z</i>	4	4	4
<i>d</i> _{calcd} , g cm ⁻³	1.626	1.608	1.576
<i>μ</i> , mm ⁻¹	0.775	0.807	0.911

Table 5.2. (cont'd)

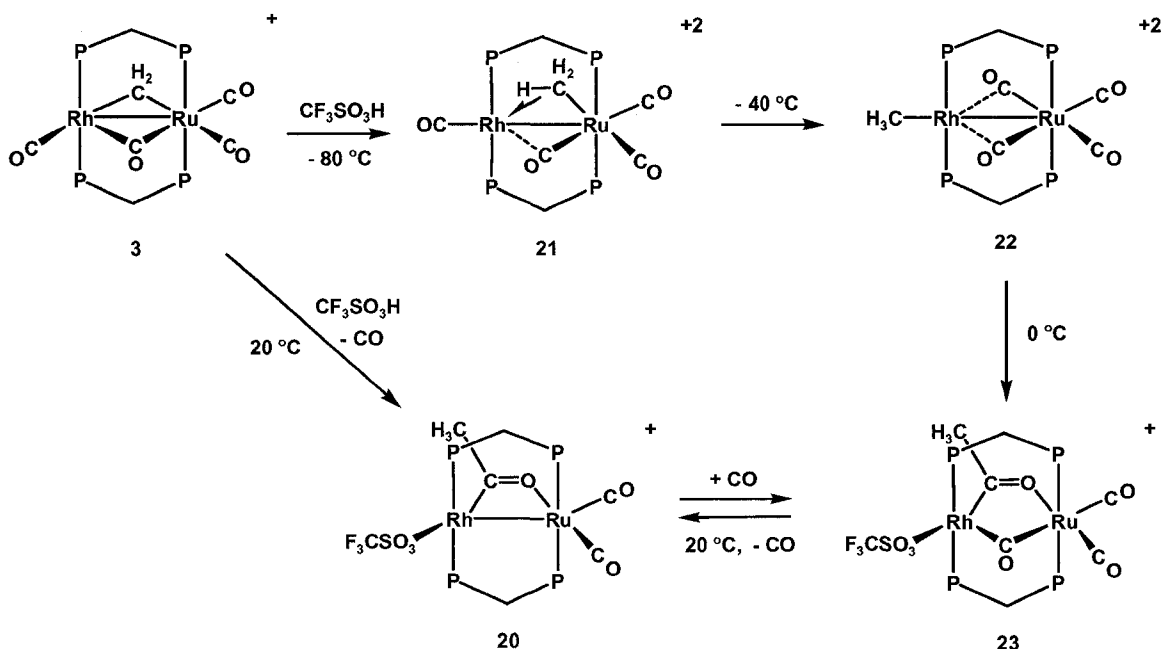
radiation (λ , Å)	graphite-monochromated Mo K α (0.71073)	graphite-monochromated Mo K α (0.71073)	graphite-monochromated Mo K α (0.71073)
T , °C	-80	-80	-80
scan type	ω scans (0.2°) (30 s exposures)	ω scans (0.3°) (20 s exposures)	ϕ rotations (0.3°) / ω scans (0.3°) (30 s exposures)
2θ (max), deg	52.76	52.86	52.80
no. of unique reflections	12368	11 881 ($R_{\text{int}} = 0.0191$)	11004 ($R_{\text{int}} = 0.0573$)
no of observns	8659 [$F_o^2 \geq 2\sigma(F_o^2)$]	10 496 [$F_o^2 \geq 2\sigma(F_o^2)$]	7085 [$F_o^2 \geq 2\sigma(F_o^2)$]
range of transmn factors	0.9478–0.8732	0.8055–0.6474	0.9064–0.7654
no. of data/restraints/params	12 368 [$F_o^2 \geq -3\sigma(F_o^2)$]/0/730	11 881 [$F_o^2 \geq -3\sigma(F_o^2)$]/0/754	11004 [$F_o^2 \geq -3\sigma(F_o^2)$] / 26 ^d / 628
residual density, e/Å ³	0.936 to –0.529	1.394 to –0.635	1.605 to –1.272
$R_1(F_o^2 > 2\sigma(F_o^2))^e$	0.0488	0.0393	0.0571
$wR_2[F_o^2 \geq -3\sigma(F_o^2)]^e$	0.1083	0.1076	0.1653
GOF (s) ^d	1.011 [$F_o^2 \geq -3\sigma(F_o^2)$]	1.054 [$F_o^2 \geq -3\sigma(F_o^2)$]	0.992 [$F_o^2 \geq -3\sigma(F_o^2)$]

^a Cell parameters obtained from least-squares refinement of 5538 centered reflections. ^b Cell parameters obtained from least-squares refinement of 7413 centered reflections. ^c Cell parameters obtained from least-squares refinement of 5538 centered reflections. ^d An idealized geometry was imposed upon the disordered tetrafluoroborate ion and solvent dichloromethane molecule through imposition of idealized F–B (1.36 Å), F···F (2.22 Å), Cl–C (1.80 Å) and Cl···Cl (2.95 Å) distances. ^e $R_1 = \Sigma ||F_o| - |F_c|| / \Sigma |F_o|$; $wR_2 = [\Sigma w(F_o^2 - F_c^2)^2 / \Sigma w(F_o^4)]^{1/2}$ Refinement on F_o^2 for all reflections (having $F_o^2 \geq -3\sigma(F_o^2)$). wR_2 and S based on F_o^2 ; R_1 based on F_o , with F_o set to zero for negative F_o^2 . The observed criterion of $F_o^2 > 2\sigma(F_o^2)$ is used only for calculating R_1 and is not relevant to the choice of reflections for refinement. ^d $S = [\Sigma w(F_o^2 - F_c^2)^2 / (n - p)]^{1/2}$ (n = number of data, p = number of parameters varied; $w = [\sigma^2(F_o^2) + (a_0P)^2 + a_1P]^{-1}$, where $P = [\max(F_o^2, 0) = 2F_c^2]/3$. For **20** $a_0 = 0.0467$ and $a_1 = 0.00$; for **23** $a_0 = 0.0485$ and $a_1 = 13.904$. For **25** $a_0 = 0.0904$ and $a_1 = 0.00$.

Results and Compound Characterization

Protonation of the methylene-bridged compound $[\text{RhRu}(\text{CO})_4(\mu\text{-CH}_2)(\text{dppm})_2][\text{CF}_3\text{SO}_3]$ (**3**) using triflic acid at $-80\text{ }^\circ\text{C}$ affords the dicationic methyl compound $[\text{RhRu}(\text{CO})_4(\mu\text{-CH}_3)(\text{dppm})_2][\text{CF}_3\text{SO}_3]_2$ (**21**) (Scheme 5.1). No other species was observed at this temperature. The $^{31}\text{P}\{^1\text{H}\}$ NMR spectrum of **21** contains two signals for the two ends of the diphosphine ligands at δ 24.2 and 20.8 with patterns typical of an

Scheme 5.1



AA'BB'X spin system found in Rh/M (M = Ru, Os) systems. The ^1H NMR spectrum of **21** displays two multiplets at δ 4.10 and 3.63 corresponding to the dppm methylene protons, and a broad singlet at δ 0.30. Unfortunately the close proximity of the two phosphorus signals in the $^{31}\text{P}\{^1\text{H}\}$ NMR spectrum prevented use of selective $^1\text{H}\{^{31}\text{P}\}$

experiments to aid in the determination of the binding mode of the methyl ligand. In an analogous Rh/Os complex, also having a broad unresolved methyl signal, $^1\text{H}\{^{31}\text{P}\}$ selective decoupling experiments demonstrated coupling of these methyl protons to all four phosphorus nuclei, indicative of a bridging CH_3 group. To examine the bonding involving the methyl group in the Rh/Ru analogue, isotopomers of **21** incorporating CH_2D , CD_2H and $^{13}\text{CH}_3$ were prepared. The CH_2D isotopomer (**21-CH₂D**) was prepared via the reaction between $[\text{RhRu}(\text{CO})_4(\mu\text{-CH}_2)(\text{dppm})_2][\text{CF}_3\text{SO}_3]$ (**3**) and $\text{CF}_3\text{SO}_3\text{D}$, whereas the CD_2H isotopomer (as well as detectable amounts of the other isotopomers¹⁷) was synthesized from protonation of $[\text{RhRu}(\text{CO})_4(\mu\text{-CD}_2)(\text{dppm})_2][\text{CF}_3\text{SO}_3]$ (**3-CD₂**) with triflic acid. At $-60\text{ }^\circ\text{C}$, the ^1H NMR spectrum displays the CH_3 resonance of **21** at δ 0.30, for **21-CDH₂** at δ 0.13 and finally for **21-CHD₂** at δ -0.09 (see Figure 5.1).

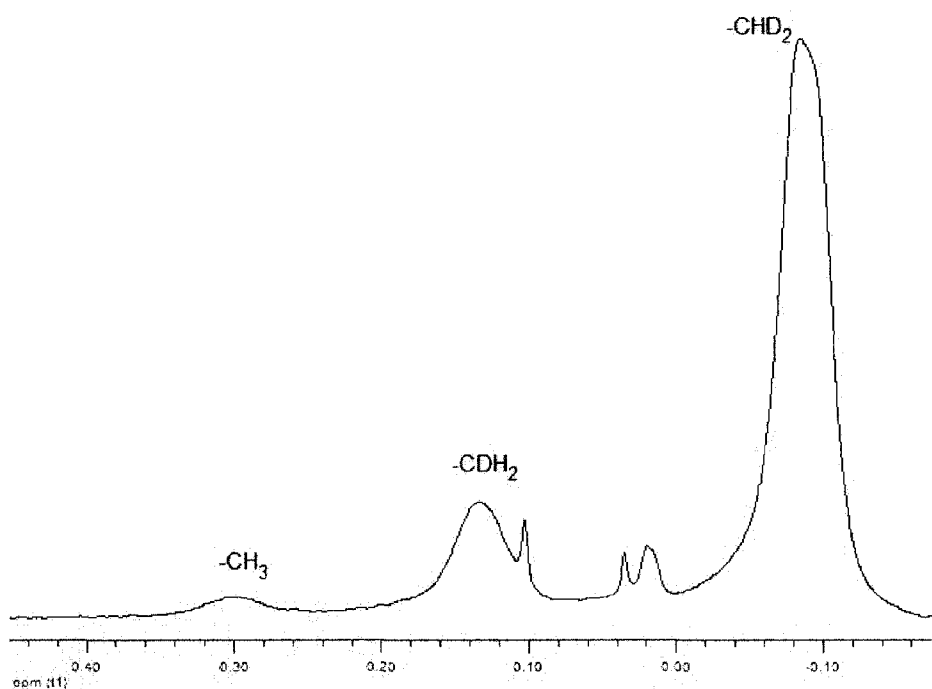


Figure 5.1: ^1H NMR spectrum of the methyl region of **21**, **21-CDH₂** and **21-CH₂D**.

The upfield shift of the protons of the bridging methyl group as the level of deuterium incorporation is increased is characteristic of an agostic interaction. The lower zero-point energy of the C–D bond relative to the C–H bond renders the C–H agostic interaction favored over agostic interactions involving the C–D bond. With the increased presence of deuterium the remaining protons of the methyl group will tend to spend more time in the C–H agostic mode rather than a C–H terminal mode, resulting in a high-field shift of the proton signals in the ^1H NMR spectrum. As noted earlier, this type of agostic bonding of the bridging methyl group has previously been reported in an analogous Rh/Os complex,⁹ and in a dppm-bridged diruthenium compound.⁷ This NMR technique of observing changes in chemical shift with isotopic labeling is referred to as Isotopic Perturbation of Resonance (IPR) was first used by Shapley¹⁸ and subsequently by others¹⁹⁻²¹ to probe the nature of bridging and/or agostic methyl groups in transition metal complexes. Further evidence supporting the agostic methyl interaction was obtained from the ^1H NMR spectrum of a $^{13}\text{CH}_3$ -enriched sample of **21**. Although the observed one-bond carbon-hydrogen coupling of 127 Hz is within the accepted range for terminal methyl groups (120 – 145 Hz for typical late-metal complexes²²), it is also close to the 121 Hz observed for the late-metal complexes $[\text{Os}_3(\text{CO})_{10}(\mu\text{-H})(\mu\text{-CH}_3)]$,¹⁸ $[\text{Cp}_2\text{Fe}_2(\text{CO})_2(\mu\text{-CH}_3)(\mu\text{-CO})]$ ²⁰ and to the value of 127 Hz for the Rh/Os analogue $[\text{RhOs}(\text{CO})_4(\mu\text{-CH}_3)(\text{dppm})_2][\text{CF}_3\text{SO}_3]_2$ ⁹ which have all been previously shown by IPR to possess bridged-agostic methyl groups. In addition, the value of 127 Hz is smaller than the $^1J_{\text{CH}}$ for complex **22** (139 Hz) in which methyl group is terminally bound (vide infra). On this basis and on the basis of the IPR experiments we conclude that the methyl

group bridges both metals, being σ -bound to one and involved in an agostic interaction with the other.

An alternate explanation of the observed chemical shift change upon deuterium incorporation, involves facile exchange of protons in a methylene-hydride species, as has been observed previously for a methylene-bridged diiridium complex $[\text{Ir}_2(\text{H})(\text{CO})_2(\mu\text{-CH}_2)(\mu\text{-SO}_2)(\text{dppm})_2][\text{CF}_3\text{SO}_3]$.²³ In an agostic methyl compound, the average spin-spin coupling constant between the methyl carbon and the hydrogens is a weighted average of one agostic C-H bond ($^1J_{\text{CH}} \approx 90$ Hz) and two terminal C-H bonds ($^1J_{\text{CH}} \approx 140$ Hz). In a methylene hydride species the observed coupling is a weighted average of the two terminal C-H bonds ($^1J_{\text{CH}} \approx 140$ Hz) and the 2-bond coupling between the methylene carbon and the metal hydride ligand, which is generally near zero, resulting in a much smaller observed coupling.^{20,21,24} In the aforementioned diiridium methylene hydride species,²⁵ the coupling was observed to be 98 Hz, an average of two ≈ 140 Hz couplings and one ≈ 0 Hz coupling. For compound **21**, significantly higher coupling constant (127 Hz) is clearly inconsistent with a methylene-hydride formalism.

The $^{13}\text{C}\{^1\text{H}\}$ NMR spectrum of **21** at -40 °C shows the methyl signal as a sharp singlet at $\delta -20.7$ with no apparent coupling to either the ^{103}Rh or ^{31}P nuclei. The absence of Rh-coupling argues strongly against a bridging methylene formulation (for example in **3** the coupling between Rh and the methylene carbon is 16 Hz) and also establishes that this group is σ -bound to Ru and not to Rh. The high-field chemical shift of this carbon is also in line with that observed for the Rh/Os methyl complex ($\delta -32.2$) and is far upfield from the methylene group in **3** ($\delta 48.3$). In the carbonyl region, two broad signals,

observed at δ 190.4 and 187.7, are assigned as terminally-bound to Ru, due to the lack of any observable Rh coupling, whereas the doublet of triplets at δ 183.4 is assigned as a terminal Rh-bound carbonyl ($^1J_{\text{RhC}} = 79$ Hz, $^2J_{\text{P(Rh)C}} = 15$ Hz). A fourth signal, at δ 219.5, is assigned as a Ru-bound semibridging carbonyl. Although no coupling to Rh could be ascertained, the low-field shift of this carbon is indicative of semi-bridging interactions.

On warming a solution of **21** to 0 °C, a new compound, [RhRu(CO)₄(CH₃)-(dppm)₂][CF₃SO₃]₂ (**22**) is formed. Compound **22** is an isomer of **21**, with the formerly Ru-bound agostic methyl group now bound terminally to Rh. The $^{31}\text{P}\{^1\text{H}\}$ NMR spectrum of **22** contains two signals at δ 28.7 and 23.0, similar in appearance to that of **21**. The ^1H NMR spectrum of **22** shows one broad multiplet at δ 3.41, assigned to the four equivalent dppm methylene protons. These protons owe their equivalence to the front-back symmetry of the complex, where the environment on one side of the RhRuP₄ plane is equivalent to that on the other side. The remaining signal at δ 1.66 appears as a triplet of doublets due to coupling to Rh ($^2J_{\text{RhH}} = 4$ Hz) and to the Rh-end of the diphosphine ligands ($^3J_{\text{PH}} = 8$ Hz). An ^1H NMR experiment using a $^{13}\text{CH}_3$ -enriched sample of **22** displays a one-bond C-H coupling of 139 Hz, consistent with a terminally-bound methyl group. The $^{13}\text{C}\{^1\text{H}\}$ NMR spectrum of **22** shows two broad signals in the carbonyl region at δ 221.6 and 186.3. The high-field signal is attributed to the pair of chemically equivalent terminally-bound carbonyls on Ru while the low-field signal is assigned to the two semibridging CO ligands. The methyl carbon appears as a doublet at δ 42.2 ($^1J_{\text{RhC}} = 25$ Hz) and represents a considerable down-field shift from that of the methyl group in the precursor **21**.

Further warming causes **22** to transform into a third compound, $[\text{RhRu}(\text{OSO}_2\text{CF}_3)(\text{CO})_3(\mu\text{-C}(\text{O})\text{CH}_3)(\text{dppm})_2][\text{CF}_3\text{SO}_3]$ (**23**), the $^{31}\text{P}\{^1\text{H}\}$ NMR spectrum which is typical of these Rh/Ru species. In the ^1H NMR spectrum two resonances appear for the dppm methylene protons, indicating that the “front-back” symmetry of the precursor (**22**) is broken and that now the environment on one side of the RhRuP_4 plane differs from that on the other side. The methyl resonance now appears as a broad singlet at δ 2.03, with no obvious coupling to either ^{103}Rh or ^{31}P . In addition, when the sample is ^{13}CO enriched the methyl proton signal broadens noticeably, although no coupling is resolved. These data suggest an acyl formulation for compound **23** which is further supported by the $^{13}\text{C}\{^1\text{H}\}$ NMR spectrum with the appearance of a low-field resonance at δ 304.8 showing strong coupling to Rh ($^1J_{\text{RhC}} = 38$ Hz). This very low-field shift for the acyl carbon has been observed previously in dmpm and/or dppm complexes of Rh/Rh,⁶ Ru/Ru,^{7,8} and Rh/Os,⁹ and suggests a bridging acyl group having significant carbene-like character, and not likely that of a terminal acyl moiety, which appear at much higher fields (δ 240 – 260).^{6-8,26} Two carbonyls appear at δ 196.6 and 184.9, and are clearly identified as Ru-bound on the basis that no Rh coupling is observed. The third carbonyl, at δ 250.3, appears as a complex multiplet and appears to correspond to a bridging carbonyl in which the coupling to Rh is unresolved from coupling to the four ^{31}P nuclei and the other carbonyls. The methyl group of the acyl appears as a broad singlet at δ 45.2, showing what is likely unresolved Rh coupling.

The IR spectrum of **23** shows two terminal carbonyl bands at 2090, 2016 cm^{-1} , and a bridging carbonyl at 1732 cm^{-1} . The presumed carbene character of the acyl carbon in **23** should reduce the C-O bond order enough to red-shift this band into the fingerprint

region of the IR spectrum. No stretch for this group was observed for this group, even for a ^{13}CO -enriched sample of **23**. The acyl group IR stretch was also absent in other binuclear dppm and dmpm complexes containing similar metals.⁶⁻⁸

The structural assignment for **23** has been confirmed by an X-ray structure determination, for which the cation is diagrammed in Figure 5.2 (with relevant bond lengths and angles given in Table 5.3). What is immediately evident from this determination is that migration of the methyl ligand of **22** to a carbonyl has occurred and that the resulting acyl group is carbon-bound to Rh and oxygen-bound to Ru. At Ru, the resulting geometry is octahedral, with the oxygen of the bridging acyl and a bridging carbonyl being directly trans to the two terminal carbonyl ligands. The geometry about Rh appears to be a distorted tetragonal pyramid, with the two ends of the diphosphine ligands, along with the acyl carbon and coordinated triflate anion occupying the basal sites, and the bridging carbonyl occupying the apical site. The Rh-C(4) bond of the bridging-acyl group (1.924(3) Å) is significantly shorter than that reported by Eisenberg (2.05(2) Å) for a related Rh₂ system,⁶ however the C(4)-O(4) acyl distance in **23** (1.243(4) Å) is comparable to that for the Rh₂ system (1.28(2) Å).⁶ The present C-O distance is somewhat longer than the typical distances in aldehydes and ketones (between 1.19 and 1.23 Å) but still much shorter than C-O single bonds in enols (*ca.* 1.33 Å) for example.²⁷ All the angles at the acyl carbon (C(4)) are close to the idealized value for sp² hybridization.

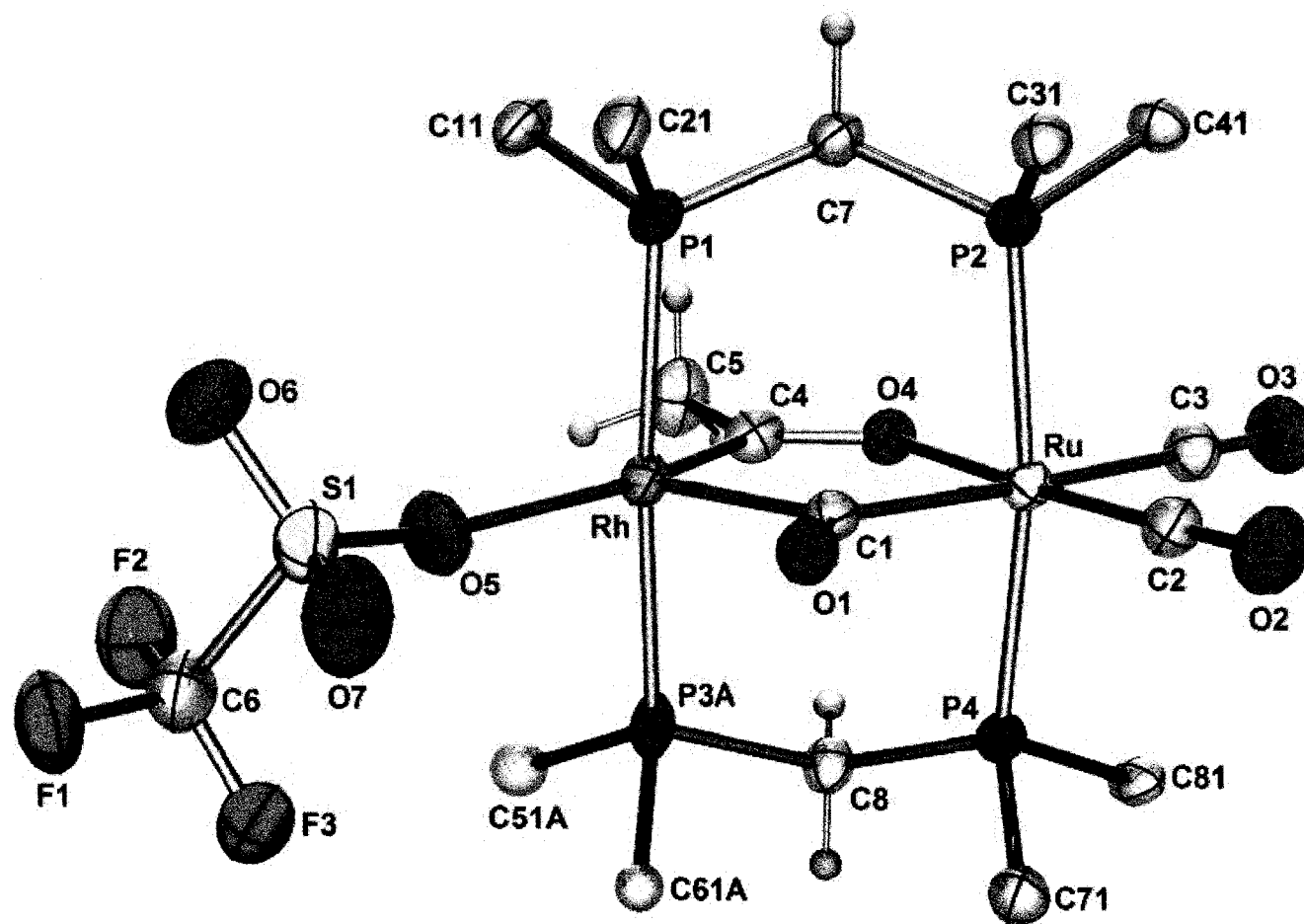


Figure 5.2: Perspective view of the complex cation of compound **23**, showing the numbering scheme. Thermal ellipsoids are drawn at the 50% level except for hydrogens, which are drawn arbitrarily small. Phenyl groups, except for ipso carbons, are omitted.

Table 5.3: Selected Distances and Angles for Compound **23**.*(i) Distances (Å)*

Atom 1	Atom 2	Distance	Atom 1	Atom 2	Distance
Rh	Ru	3.3992(4) [†]	S(1)	C(6)	1.831(5)
Rh	P(1)	2.3691(8)	P(1)	P(2)	3.132(1) [†]
Rh	P(3A)	2.34(1)	P(1)	C(7)	1.845(3)
Rh	P(3B)	2.40(1)	P(2)	C(7)	1.835(3)
Rh	O(5)	2.241(3)	P(3A)	P(4)	3.16(1) [†]
Rh	C(1)	2.011(3)	P(3A)	C(8)	1.92(2)
Rh	C(4)	1.924(3)	P(4)	C(8)	1.838(3)
Ru	P(2)	2.3895(8)	F(1)	C(6)	1.332(5)
Ru	P(4)	2.3995(8)	F(2)	C(6)	1.305(5)
Ru	O(4)	2.114(2)	F(3)	C(6)	1.337(5)
Ru	C(1)	2.068(3)	O(1)	C(1)	1.190(4)
Ru	C(2)	1.865(3)	O(2)	C(2)	1.137(4)
Ru	C(3)	1.991(3)	O(3)	C(3)	1.117(4)
S(1)	O(5)	1.444(3)	O(4)	C(4)	1.243(4)
S(1)	O(6)	1.420(3)	C(4)	C(5)	1.502(5)
S(1)	O(7)	1.446(4)			

[†] Non-bonded distance

(ii) Angles (deg)

Atom 1	Atom 2	Atom 3	Angle	Atom 1	Atom 2	Atom 3	Angle
P(1)	Rh	P(3A)	173.8(6)	O(4)	Ru	C(1)	88.8 (1)
P(1)	Rh	O(5)	97.15(8)	O(4)	Ru	C(2)	176.7(1)
P(1)	Rh	C(1)	90.26(9)	O(4)	Ru	C(3)	86.6(1)
P(1)	Rh	C(4)	85.6 (1)	C(1)	Ru	C(2)	94.3(1)
P(3A)	Rh	O(5)	88.9(6)	C(1)	Ru	C(3)	175.4(1)
P(3A)	Rh	C(1)	89.1(4)	C(2)	Ru	C(3)	90.30(1)
P(3A)	Rh	C(4)	88.3(6)	Ru	O(4)	C(4)	120.1(2)
O(5)	Rh	C(1)	106.3(1)	Rh	O(5)	S(1)	166.9(2)
O(5)	Rh	C(4)	159.7(1)	Rh	C(1)	Ru	112.9(1)
C(1)	Rh	C(4)	93.8(1)	Rh	C(1)	O(1)	113.8(2)
P(2)	Ru	P(4)	171.42(3)	Ru	C(1)	O(1)	133.3(2)
P(2)	Ru	O(4)	86.69(6)	Ru	C(2)	O(2)	176.8(3)
P(2)	Ru	C(1)	87.16(8)	Ru	C(3)	O(3)	178.9(3)
P(2)	Ru	C(2)	92.4(1)	Rh	C(4)	O(4)	124.4(2)
P(2)	Ru	C(3)	92.0(1)	Rh	C(4)	C(5)	119.1(3)
P(4)	Ru	O(4)	86.58(6)	O(4)	C(4)	C(5)	116.5(3)
P(4)	Ru	C(1)	87.39(8)	P(1)	C(7)	P(2)	116.6(1)
P(4)	Ru	C(2)	94.6(1)	P(3A)	C(8)	P(4)	114.7(6)
P(4)	Ru	C(3)	92.9(1)				

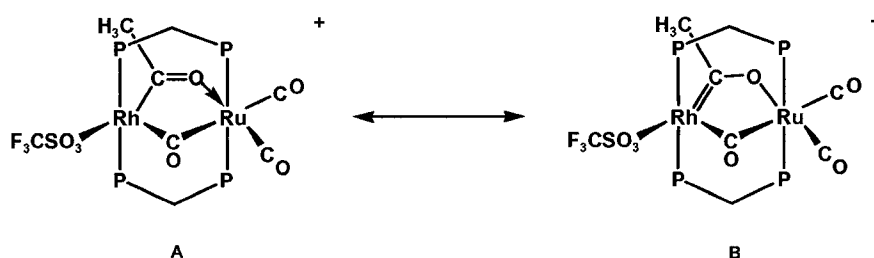
The Rh-Ru separation of 3.3992(4) Å is significantly longer than either of the intraligand P-P distances (3.132(1) and 3.16(1) Å) and indicates that no metal-metal bond is present. This large metal-metal separation leads to a slightly wider than normal Rh-C(1)-Ru angle of 112.9(1)°, suggesting sp² hybridization of this carbonyl carbon and the C(1)-O(1) distance (1.190(4) Å) as a result, is substantially longer than those of the terminal carbonyls, although not quite as long as that of the bridging acyl group. As noted earlier, this distance compares favourably with C=O bonds in aldehydes and ketones. The bond angles around C(1) suggest a large asymmetry in the bridging carbonyl (Rh-C(1)-O(1) 113.8(2)° and Ru-C(1)-O(1) 133.3(2)°), which may be caused by short non-bonding contacts (H(22)-O(1) = 2.66 Å, H(62a)-O(1) = 2.48 Å, H(32)-O(1) = 2.41 Å and H(72)-O(1) = 2.50 Å) between the ortho hydrogens of the phenyl ring and O(1). The resulting average O-H contact of 2.51 Å can be compared with that of 2.71 Å in compound **3**. Clearly, these contacts can have a strong influence on the orientation of bridging carbonyls in these complexes.

Figure 5.2 also clearly shows that one of the triflate ions is coordinating to Rh, directly opposite the acyl group (C(4)-Rh-O(5) = 159.7(1)°), with a normal Rh-O(5) distance of 2.241(3) Å. It is assumed that this structure is maintained in solution. Not only is this necessary for a 16-electron configuration at Rh, but the ¹³C{¹H} NMR unequivocally show that the carbonyl and acyl ligands are in the arrangement shown in Scheme 5.1 and Figure 5.2. Solvent coordination was ruled out by ¹H NMR spectroscopy; the spectra were identical when recorded in either acetone d₆ or CD₂Cl₂. The IR spectrum of **23** in solution shows a strong band at 1265 cm⁻¹, indicative of the presence of a coordinated triflate.²⁸ The ¹⁹F NMR spectrum is not diagnostic for

differentiating between coordinated and free triflate ions, so only one fluorine resonance is observed in **23**.

These X-Ray and spectroscopy data are consistent with a significant degree of carbene-like character^{29,30} as diagrammed in structure **B** in Chart 5.1.

Chart 5.1



If a solution of compound **23** is purged with argon, or exposed to vacuum, at temperatures above 20 °C, quantitative conversion to a new compound is observed in the ³¹P{¹H} NMR spectrum within minutes. This compound can also be obtained by direct treatment of **3** with triflic acid at room temperature. Complex **23** can be regenerated by exposure to CO. The ¹H NMR spectrum of this new complex contains a singlet at δ 1.99, indicative of the methyl group of an acyl moiety. The ¹³C{¹H} NMR spectrum of a ¹³CO-enriched sample of this compound reveals the presence of two terminal carbonyls at δ 204.2 and 180.4, and a low-field doublet resonance at δ 270.3 displaying 33 Hz coupling to Rh. These data are supportive of a dicarbonyl species with the acyl group remaining intact, and carbon-bound to Rh, so is formulated as [RhRu(OSO₂CF₃)(CO)₂(μ-C(O)CH₃)(dppm)₂][CF₃SO₃] (**20**). The IR spectrum confirms the dicarbonyl nature of **20**, showing two bands at 2045 and 1989 cm⁻¹; once again no acyl stretch is obvious.

The structure of **20** was also confirmed by an X-ray structure determination, and the cation is shown in Figure 5.3 with relevant bond lengths and angles given in Table 5.4. The obvious differences between the structures for compounds **23** and **20** are the absence of a bridging carbonyl in **20** and the substantial compression of the Rh-Ru distance compared to **23** (2.6953(4) Å vs. 3.3992(4) Å). The metal-metal separation is typical for a single bond between Rh and Ru. This drastic change in the metal-metal separation has little effect on the bond lengths and angles within the bridging acetyl group. As with **23**, these bond lengths suggest significant carbene character in the acyl group (Rh-C(3) = 1.912(4) Å and C(3)-O(3) = 1.266(5) Å). In this case, the acyl C(3)-O(3) distance is elongated compared to that in compound **23** and is now intermediate between the double bond of aldehydes (1.19 Å) and the single bond in enols (1.33 Å).²⁷ The angles at the acyl group are all near the idealized value of 120°. The major change in binding of the acyl group that results from the metal-metal bond compression is the compression of the C(3)-O(3)-Ru angle from 120.1(2)° in **23** to 100.6(2)° in **20**.

The geometry about the metals can best be described as being distorted octahedral at Ru, and again tetragonal pyramidal at Rh. The two ends of the dppm ligands as well as the acyl and triflate ligands form the base of the pyramid, with Ru occupying the coordinated apical site. Any major distortions from octahedral geometry at Ru occurs because of the bridging acyl ligand. As a result, the Rh-Ru-O(3) angle is acute (69.27(7)°) and the O(3)-Ru-C(2) angle is obtuse (107.8(1)°) compared to the ideal 90° value. The phosphines are in a distorted trans arrangement (P(3)-Rh-P(1) = 167.45(4)°) with respect to each other, whereas the acyl and triflate ligands are perfectly trans to each other (O(4)-Rh-C(3) = 178.3(1)°). The distance between

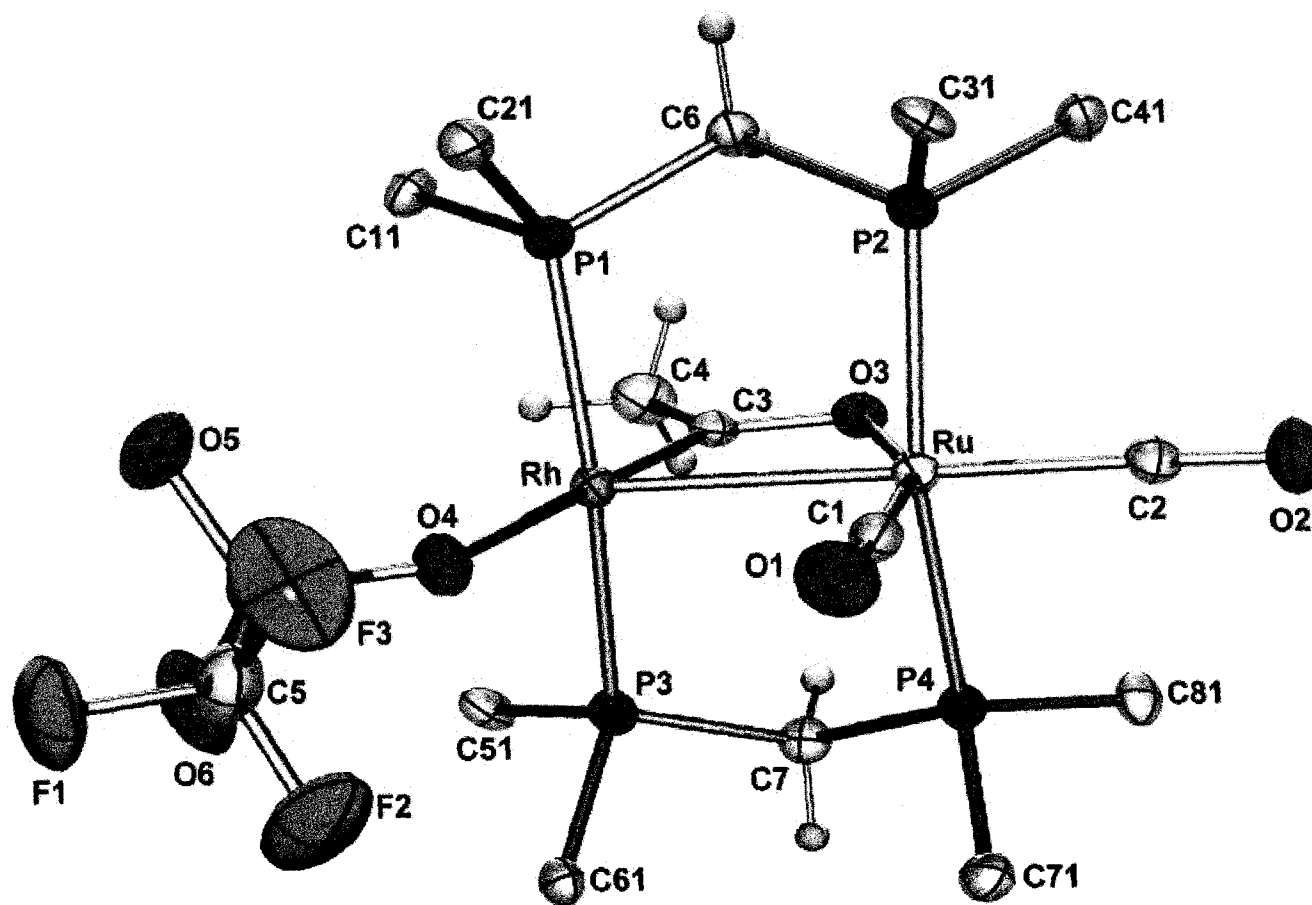


Figure 5.3: Perspective view of the complex cation of compound **20**, showing the numbering scheme. Thermal ellipsoids are drawn at the 50% level except for hydrogens, which are drawn arbitrarily small. Phenyl groups, except for ipso carbons, are omitted.

Table 5.4: Selected Distances and Angles for Compound 20.*(i) Distances (Å)*

Atom 1	Atom 2	Distance	Atom 1	Atom 2	Distance
Rh	Ru	2.6953(4)	P(1)	C(6)	1.820(4)
Rh	P(1)	2.333(1)	P(2)	C(6)	1.834(4)
Rh	P(3)	2.332 (1)	P(3)	C(7)	1.831(4)
Rh	O(4)	2.219(3)	P(4)	C(7)	1.830(4)
Rh	C(3)	1.912(4)	P(4)	P(3)	2.98(1) [†]
Ru	P(2)	2.409(1)	P(2)	P(1)	2.98(1) [†]
Ru	P(4)	2.412(1)	F(1)	C(5)	1.321(5)
Ru	O(3)	2.146(3)	F(2)	C(5)	1.298(6)
Ru	C(1)	1.877(5)	F(3)	C(5)	1.328(6)
Ru	C(2)	1.898(4)	O(1)	C(1)	1.138(5)
S(1)	O(4)	1.465(3)	O(2)	C(2)	1.127(5)
S(1)	O(5)	1.422(4)	O(3)	C(3)	1.266(5)
S(1)	O(6)	1.425(4)	C(3)	C(4)	1.510(6)
S(1)	C(5)	1.822(5)			

† Non-bonded distance

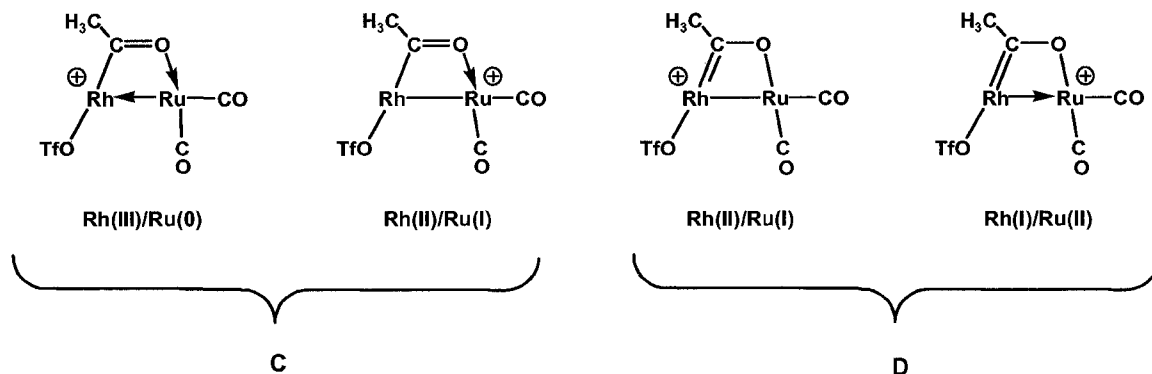
(ii) Angles (deg)

Atom 1	Atom 2	Atom 3	Angle	Atom 1	Atom 2	Atom 3	Angle
Ru	Rh	P(1)	93.44(3)	P(2)	Ru	C(2)	86.7(1)
Ru	Rh	P(3)	93.57(3)	P(4)	Ru	O(3)	84.83(8)
Ru	Rh	O(4)	109.57(8)	P(4)	Ru	C(1)	96.8(13)
Ru	Rh	C(3)	68.88(12)	P(4)	Ru	C(2)	86.0(1)
P(1)	Rh	P(3)	167.45(4)	O(3)	Ru	C(1)	157.4(1)
P(1)	Rh	O(4)	93.90(8)	O(3)	Ru	C(2)	107.8(1)
P(1)	Rh	C(3)	86.99(12)	C(1)	Ru	C(2)	94.8(1)
P(3)	Rh	O(4)	93.54(8)	Rh	P(1)	C(6)	111.5(1)
P(3)	Rh	C(3)	85.8(1)	Ru	P(2)	C(6)	109.5(1)
O(4)	Rh	C(3)	178.3(1)	Rh	P(3)	C(7)	111.6(1)
Rh	Ru	P(2)	93.39(3)	Ru	P(4)	C(7)	109.5(1)
Rh	Ru	P(4)	93.27(3)	Ru	O(3)	C(3)	100.6(2)
Rh	Ru	O(3)	69.27(7)	Rh	O(4)	S(1)	131.2(1)
Rh	Ru	C(1)	88.1(1)	Ru	C(1)	O(1)	175.6(4)
Rh	Ru	C(2)	177.1(1)	Ru	C(2)	O(2)	176.0(4)
P(2)	Ru	P(4)	165.21(4)	Rh	C(3)	O(3)	121.3(3)
P(2)	Ru	O(3)	85.21(8)	Rh	C(3)	C(4)	123.6(3)
P(2)	Ru	C(1)	96.6(1)	O(3)	C(3)	C(4)	115.1(4)

the oxygen of the triflate and rhodium (2.219(3) Å) is similar to that for **23**. Again the $^{13}\text{C}\{^1\text{H}\}$ NMR spectrum and X-ray structure support an oxy-carbene contribution to the structure of compound **20**.

Two bonding formalisms for compound **20** are shown in Chart 5.2. If one considers a normal acetyl bonding mode, shown in structure **C**, the oxidation states can be either $\text{Rh}^{+3}/\text{Ru}^0$, in which the positive charge on the complex is localized on the Rh^{+3}

Chart 5.2

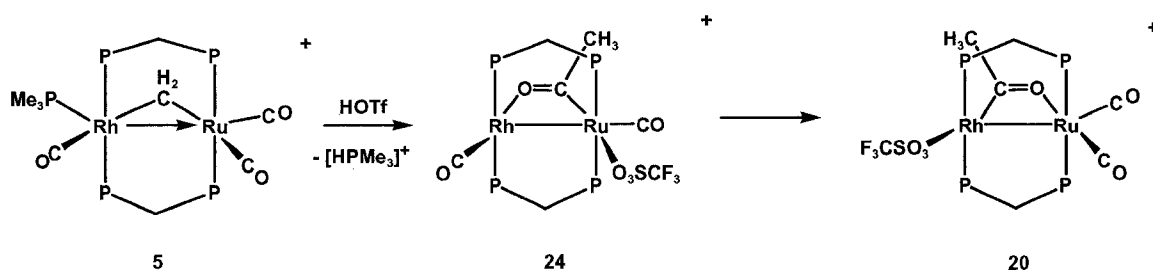


centre, achieving a 16e configuration by dative bond formation with Ru^0 . An alternate description gives the oxidation states as $\text{Rh}^{+2}/\text{Ru}^{+1}$, in which the positive charge now resides on the Ru^{+1} centre and a covalent metal-metal bond results, giving a 16e/18e configuration at the metals. The other formalism, structure **D** in Chart 5.2, invokes the oxy-carbene bonding scheme, in which the oxidation states of the two metals can be either $\text{Rh}^{+2}/\text{Ru}^{+1}$ or $\text{Rh}^{+1}/\text{Ru}^{+2}$. Solid-state structure and ^{13}C NMR experiments suggest that the latter is preferred, in which there is substantial contribution from the oxy-carbene resonance form, **D**. The $\text{Rh}^{+1}/\text{Ru}^{+2}$ formulation is also preferred on the basis of the common oxidation states observed for these metals.

It is important to note that substitution of the triflate anion for fluoroborate anion by protonation of $[\text{RhRu}(\text{CO})_4(\mu\text{-CH}_2)(\text{dppm})_2][\text{BF}_4]$ with HBF_4 at room temperature, does not give the BF_4^- -coordinated analogue to compounds **20** or **23**. Instead, decomposition into a complex mixture of products results. Apparently the BF_4^- anion is too weakly coordinating³¹ to stabilize the acyl complexes **20** and **23**.

Protonation of the phosphine adduct $[\text{RhRu}(\text{CO})_3(\text{PMe}_3)(\mu\text{-CH}_2)(\text{dppm})_2]^+$ (**5**), which is isoelectronic with the tetracarbonyl (**3**), with a slight excess of triflic acid gave quantitative conversion to $[\text{HPMe}_3]^+$ and a new complex, $[\text{RhRu}(\text{OSO}_2\text{CF}_3)(\text{CO})_2(\mu\text{-C}(\text{O})\text{CH}_3)(\text{dppm})_2][\text{CF}_3\text{SO}_3]$ (**24**), as shown in Scheme 5.2. Compound **24** is an isomer of **20**, in which the bridging acyl group is now carbon-bound to Ru. This new isomer displays a singlet in the ^1H NMR spectrum at δ 1.93, again suggesting the presence of an acyl group. The $^{13}\text{C}\{^1\text{H}\}$ NMR spectrum of a ^{13}C enriched sample of **24** showed three

Scheme 5.2



carbonyl resonances, a triplet at δ 196.3 and a doublet of triplets at δ 186.8 ($^1J_{\text{RhC}} = 75$ Hz), suggesting that there is one terminal carbonyl on each metal. The low-field resonance at δ 293.3 is a broad singlet, with no resolvable coupling to Rh, suggesting that the acyl is now carbon-bound to Ru. In order to maintain the electron count, the triflate

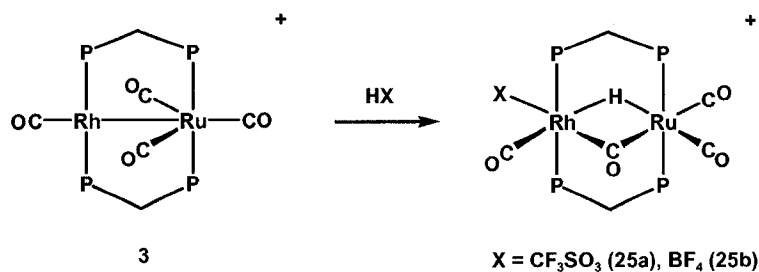
must now also be on Ru, giving this metal an 18-electron configuration. The IR spectrum displays two terminal CO bands at 2015 and 1956 cm^{-1} , with no observable stretch for the acyl group or the $\nu_{(\text{SO})}$ of the covalent triflate group. Complex **24** is unstable in solution, converting to the original isomer **20** within a few hours.

This rearrangement of the acyl group has also been observed in the RhOs system, where treatment of the RhOs analogue of **23**, $[\text{RhOs}(\text{OSO}_2\text{CF}_3)(\mu\text{-C}(\text{O})\text{CH}_3)(\text{CO})_3(\text{dppm})_2][\text{CF}_3\text{SO}_3]$ with PMe_3 at room temperature afforded the acyl dicationic complex $[\text{RhOs}(\text{CO})_3(\text{PMe}_3)(\mu\text{-C}(\text{O})\text{CH}_3)(\text{dppm})_2][\text{CF}_3\text{SO}_3]_2$, in which the acyl carbon is bound to Os.⁹ Unfortunately, the reactions of **23** and **20** with PMe_3 do not yield tractable products, instead giving a complex mixture of several products, none of which could be isolated or properly characterized due to overlap of multiple signals in both the $^{31}\text{P}\{^1\text{H}\}$ and ^1H NMR spectra.

An attempt was made to generate the acyl bridged species **20** in a reverse order, by reaction of an appropriate hydride species with diazomethane. The precursor hydride complexes $[\text{RhRu}(\text{X})(\mu\text{-H})(\text{CO})_4(\text{dppm})_2][\text{X}]$ ($\text{X} = \text{CF}_3\text{SO}_3$ (**25a**), BF_4 (**25b**)), were obtained by protonation of $[\text{RhRu}(\text{CO})_4(\text{dppm})_2][\text{X}]$ as shown in Scheme 5.3. For complex **25a**, the hydride resonance appears as a complex multiplet at $\delta - 10.41$ in the ^1H NMR spectrum, for **25b**, the hydride appears at $\delta - 11.07$. Upon broad-band ^{31}P decoupling, the hydride resonance simplifies to a doublet with coupling to Rh of 19 Hz. The coupling to each of the two sets of ^{31}P nuclei could not be determined, due to the close proximity of these two resonances in the $^{31}\text{P}\{^1\text{H}\}$ NMR spectrum, which prevented selective decoupling experiments from determining the exact nature of the hydride. The IR spectrum of **25a** shows four carbonyl bands, three terminal stretches at 2072, 2040 and

1999 cm^{-1} . The fourth band is slightly red-shifted at 1880 cm^{-1} , and this could be due to a semi-bridging interaction with Rh. There is also a stretch at 1284 cm^{-1} , suggesting triflate coordination.

Scheme 5.3

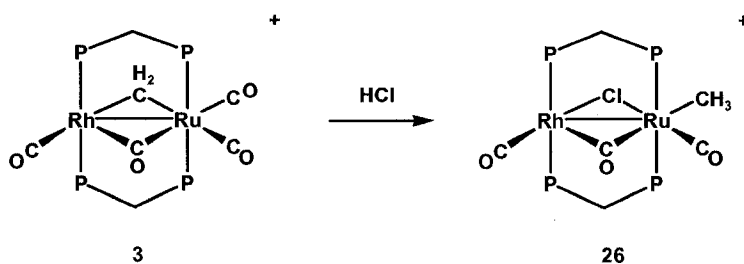


The spectroscopic parameters for both **25a** and **25b** are similar to the analogous RhOs complexes, $[\text{RhOs}(\text{X})(\mu\text{-H})(\text{CO})_4(\text{dppm})_2][\text{X}]$ ($\text{X} = \text{CF}_3\text{SO}_3$ or BF_4). In addition, the low temperature ^{19}F NMR spectrum of $[\text{RhOs}(\text{FBF}_3)(\mu\text{-H})(\text{CO})_4(\text{dppm})_2][\text{BF}_4]$ revealed the presence of two signals, one for the free BF_4 ligand, and one for coordinated BF_4 .⁹ In addition, an X-ray structure determinations for the RhOs analogues of both **25a** and **25b** showed both BF_4^- and CF_3SO_3^- groups bound to Rh in each structure respectively.⁹ It is quite likely that a similar phenomenon is occurring in **25**.

Complexes **25a** and **25b** do not react with diazomethane; even after several days under an atmosphere of CH_2N_2 , only **25** was observed in the $^{31}\text{P}\{^1\text{H}\}$ NMR spectrum.

Unlike the reactions with triflic acid and tetrafluoroboric acid, protonation of **3** with HCl does not yield an acyl complex. Instead the methyl complex $[\text{RhRu}(\text{CH}_3)(\text{CO})_2(\mu\text{-Cl})(\mu\text{-CO})(\text{dppm})_2][\text{CF}_3\text{SO}_3]$ (**26a**), is formed as shown in Scheme 5.4. The ^1H NMR spectrum shows a triplet at high field (δ -0.21) typical of a

Scheme 5.4



metal-bound methyl group. The IR spectrum of this new compound contains two terminal carbonyl bands at 2013 and 1986 cm^{-1} , as well as what appears to be a bridging CO stretch at 1711 cm^{-1} . The $^{13}\text{C}\{^1\text{H}\}$ NMR spectrum of a ^{13}CO -enriched sample of **26** shows three resonances in the carbonyl region. A low-field signal at δ 246.4 appears as a complex multiplet, and can be assigned as a bridging or semi-bridging carbonyl showing unresolved coupling to Rh and the Rh-ends of the diphosphines. The remaining two resonances appear at δ 199.4 (triplet) and 188.8 (doublet of triplets, $^1J_{\text{RhC}} = 76$ Hz) and are assigned to the terminally-bound carbonyls on Ru and Rh, respectively.

The structure of the cation of **26** was confirmed with an X-ray structure determination, as shown in Figure 5.4. Relevant bond lengths and angles are depicted in Table 5.5. Clearly the chloride anion is coordinated, acting as a bridge to both metals. The geometry at rhodium (if the metal-metal interaction is ignored) can best be described

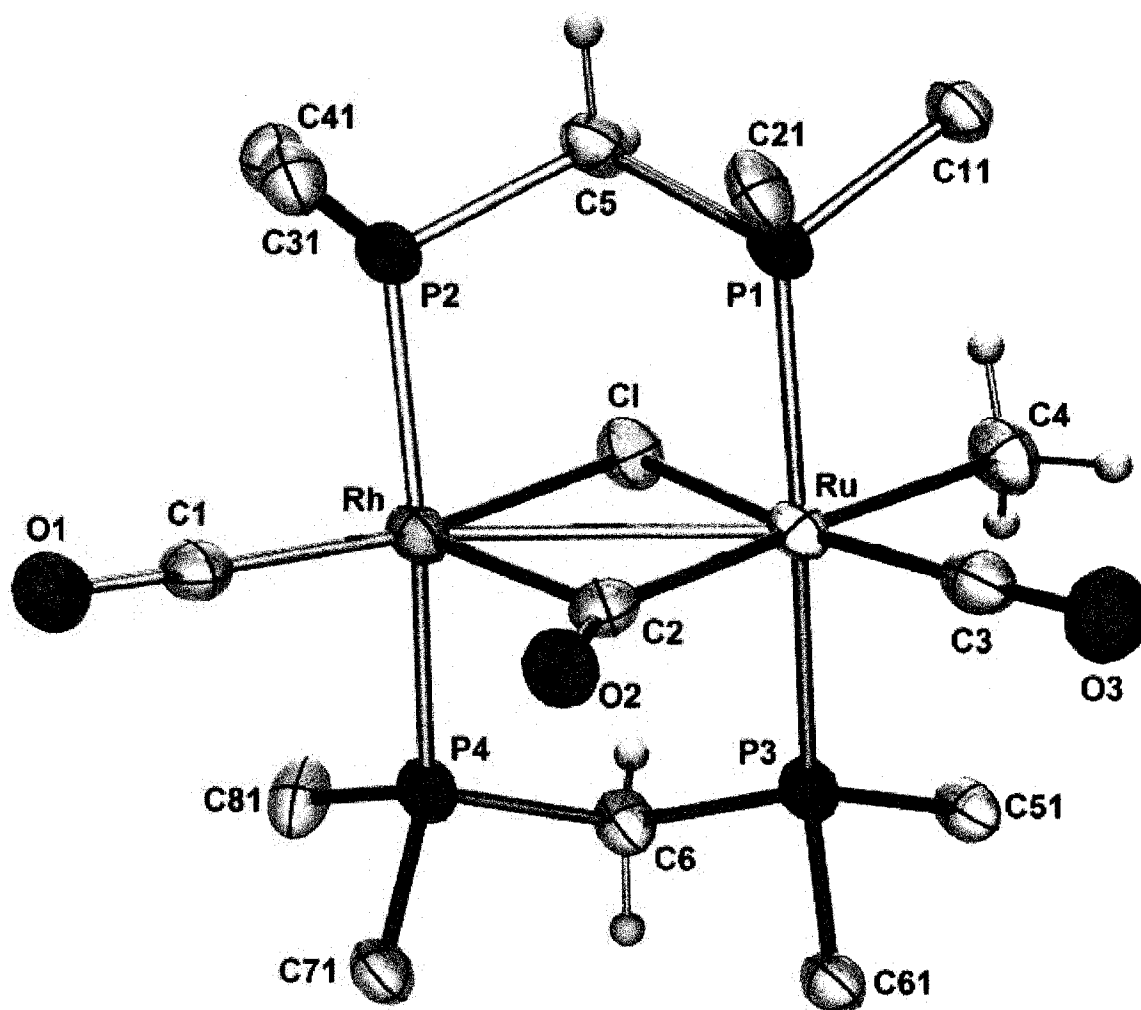


Figure 5.4: Perspective view of the complex cation of compound **26b**, showing the numbering scheme. Thermal ellipsoids are drawn at the 50% level except for hydrogens, which are drawn arbitrarily small. Phenyl groups, except for ipso carbons, are omitted.

Table 5.5: Selected Distances and Angles for Compound **26b**.*(i) Distances (Å)*

Atom 1	Atom 2	Distance	Atom 1	Atom 2	Distance
Rh	Ru	3.0115(7)	Ru	C(4)	2.180(6)
Rh	Cl	2.446(1)	P(1)	P(2)	3.082(2) [†]
Rh	P(2)	2.337(1)	P(1)	C(5)	1.827(6)
Rh	P(4)	2.330(1)	P(2)	C(5)	1.829(6)
Rh	C(1)	1.827(7)	P(3)	P(4)	3.098(2) [†]
Rh	C(2)	2.249(6)	P(3)	C(6)	1.840(6)
Ru	Cl	2.480(1)	P(4)	C(6)	1.826(6)
Ru	P(1)	2.395(1)	O(1)	C(1)	1.131(7)
Ru	P(3)	2.392(1)	O(2)	C(2)	1.141(7)
Ru	C(2)	2.056(6)	O(3)	C(3)	1.150(7)
Ru	C(3)	1.824(7)			

[†] Non-bonded distance

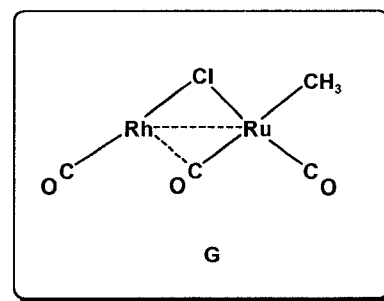
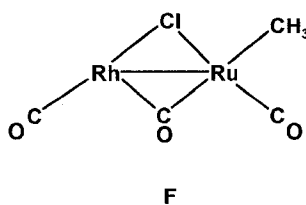
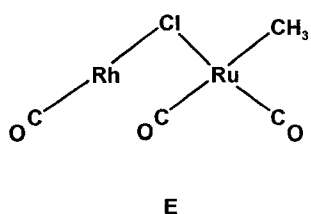
(ii) Angles (deg)

Atom 1	Atom 2	Atom 3	Angle	Atom 1	Atom 2	Atom 3	Angle
Ru	Rh	Cl	52.83(4)	Cl	Ru	P(1)	88.59(5)
Ru	Rh	P(2)	93.14(4)	Cl	Ru	P(3)	86.50(5)
Ru	Rh	P(4)	92.22(4)	Cl	Ru	C(2)	100.1(1)
Ru	Rh	C(1)	151.4(2)	Cl	Ru	C(3)	167.1(1)
Ru	Rh	C(2)	43.0(1)	Cl	Ru	C(4)	84.1(1)
Cl	Rh	P(2)	85.97(5)	P(1)	Ru	P(3)	174.9(6)
Cl	Rh	P(4)	90.21(5)	P(1)	Ru	C(2)	91.0(1)
Cl	Rh	C(1)	155.8(2)	P(1)	Ru	C(3)	92.3(1)
Cl	Rh	C(2)	95.8(1)	P(1)	Ru	C(4)	88.4(1)
P(2)	Rh	P(4)	169.62(6)	P(3)	Ru	C(2)	91.4(1)
P(2)	Rh	C(1)	90.1(1)	P(3)	Ru	C(3)	92.2(1)
P(2)	Rh	C(2)	99.0(1)	P(3)	Ru	C(4)	89.6(1)
P(4)	Rh	C(1)	89.5(1)	C(2)	Ru	C(3)	92.8(3)
P(4)	Rh	C(2)	91.0(1)	C(2)	Ru	C(4)	175.7(2)
C(1)	Rh	C(2)	108.4(3)	C(3)	Ru	C(4)	83.0(3)
Rh	Ru	Cl	51.81(4)	Rh	Cl	Ru	75.37(4)
Rh	Ru	P(1)	88.30(4)	Rh	C(1)	O(1)	178.0(7)
Rh	Ru	P(3)	89.85(4)	Rh	C(2)	Ru	88.7(2)
Rh	Ru	C(2)	48.3(1)	Rh	C(2)	O(2)	123.0(5)
Rh	Ru	C(3)	141.1(1)	Ru	C(2)	O(2)	148.3(5)
Rh	Ru	C(4)	135.9(1)	Ru	C(3)	O(3)	176.1(6)

as a tetragonal pyramid, with the equatorial sites occupied by the trans phosphines, the chloride and the terminal carbonyl, with the apical site occupied by the bridging CO.

Chart 5.3 depicts the two possible extremes in bonding for compound **26**: structure **E** contains a terminally-bound carbonyl ligand with no metal-metal interaction, whereas **F** shows an arrangement with a conventional metal-metal bond and a conventional bridging carbonyl geometry. Clearly the greater the interaction of CO with Rh the stronger the corresponding Rh-Ru interaction. The bridging carbonyl appears to be intermediate between these extremes, as depicted in structure **G**, with distances (Rh-

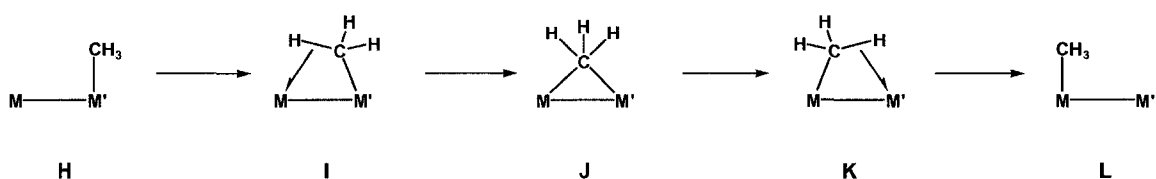
Chart 5.3



$C(2) = 2.249(6) \text{ \AA}$ and $Ru-C(2) = 2.056 \text{ \AA}$) and angles ($Rh-C(2)-O(2) = 123.0(5)^\circ$ and $Ru-C(2)-O(2) = 148.3(5)^\circ$) suggesting a semi-bridging nature for this carbonyl. In addition the metal-metal separation ($3.0115(7) \text{ \AA}$) appears to fall in the intermediate category, being significantly longer than typical Rh-Ru bonds yet still being slightly less than the intraligand P-P distances ($3.082(2) \text{ \AA}$ and $3.098(2) \text{ \AA}$). Whether this comparison of the Rh-Ru distance corresponds to any real metal-metal interaction or whether the metals are drawn together by the semi-bridging interaction is not clear.

Discussion:

Protonation of the methylene-bridged species $[\text{RhRu}(\text{CO})_4(\mu\text{-CH}_2)(\text{dppm})_2][\text{CF}_3\text{SO}_3]$ (**3**) using $\text{CF}_3\text{SO}_3\text{H}$ at $-80\text{ }^\circ\text{C}$ gives a dicationic, Ru-bound methyl complex $[\text{RhRu}(\text{CO})_4(\mu\text{-CH}_3)(\text{dppm})_2][\text{CF}_3\text{SO}_3]_2$ (**21**), in which the methyl group is asymmetrically bridging, being σ -bound to Ru and having an agostic interaction with the adjacent Rh atom. This 2e donation by the C–H bond to rhodium is assumed to be necessary to alleviate some of the electron deficiency due to the dicationic charge of the complex. Surface methyl groups have been proposed as intermediates in the Fischer-Tropsch process,^{4,32,33} and the use of cluster compounds containing $\mu\text{-CH}_3$ groups as models has been previously discussed.³⁴ Surface-bound methyl groups are known to migrate readily over the surface of a heterogeneous catalyst, and a proposed mechanism for this migration involves an agostic methyl species as intermediates in the migration of methyl groups from metal to metal, as diagrammed in Scheme 5.5. The transformation of a terminally-bound methyl group to one having an agostic interaction to an adjacent metal to a symmetrically-bridged species would readily accomplish half of a translation

Scheme 5.5

from metal to metal; the remaining part of the transformation would involve the reverse of the above, as shown in Scheme 5.5. The transformation of complex **21** into **22**

demonstrates part of this migration, in which the movement of the agostic methyl group from Ru to a terminal position on Rh is observed. The agostic interaction appears to assist in the migration of this methyl group from Ru to Rh, which occurs at temperatures above $-40\text{ }^{\circ}\text{C}$ to form a Rh-bound methyl complex **22**, which also models intermediate **L** in Scheme 5.6. The reasons for this migration are not clear. In the Rh/Os analogue,⁹ it was argued that a trade-off was made between the metal-carbon bond strengths between the 2nd and 3rd row metals. The gain in energy made by a new Os-CO bond might be greater than the loss of energy resulting from a new Rh-CH₃ bond.³⁵⁻³⁷ This disparity is not likely to exist between two adjacent 2nd row transition metals.

Warming complex **22** to ambient temperature in a closed system results in migratory insertion of the methyl and carbonyl group affording a bridging-acyl complex **23**. Recent calculations show that migratory insertion of a carbonyl and methyl group are both kinetically and thermodynamically favoured at a rhodium centre compared to the same reaction occurring at a ruthenium centre.^{38,39} Clearly migratory insertion occurs at Rh exclusively, since complex **21**, containing a Ru-CH₃ bond, does not undergo migratory insertion. Instead, the aforementioned Ru-to-Rh migration of the methyl group occurs prior to acyl formation at Rh.

Protonation of **3b** with HBF₄ at ambient temperature did not yield the acyl complex analogous to **20**, but instead gives a complex mixture of products suggesting that BF₄⁻ anion is too weakly bound to stabilize this acyl-bridged complex. Although triflate is considered to be a weakly coordinating ligand, it is nucleophilic enough to coordinate to what would otherwise be a dicationic complex without coordination; apparently the weaker coordinating BF₄⁻ anion is not sufficiently nucleophilic to stabilize

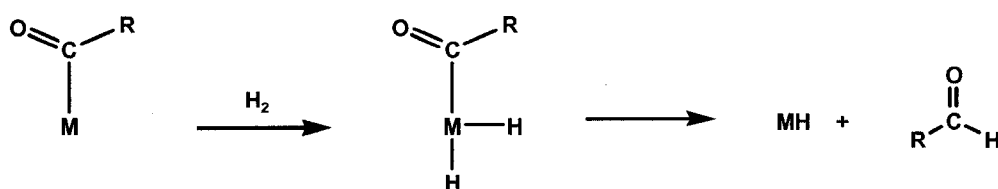
these species. In a similar study, treatment of the diruthenium species, $[\text{Ru}_2(\text{CO})_4(\mu\text{-CH}_2)(\text{dppm})_2]$, analogous to **3** with a series of acids (triflic, fluoroboric, formic and acetic) afforded the cationic methyl-bridged complex $[\text{Ru}_2(\text{CO})_4(\text{CH}_3)(\text{dppm})_2]^+$ at low temperature, although in this case only the formate and acetate complexes survived elevated temperatures to yield the acetyl-bridged species.⁷ In this system, the triflate and fluoroborate anions were not sufficiently coordinating, resulting in decomposition of the complex at higher temperatures.

The asymmetric bridging methyl group is an important species in methyl group migration, as discussed earlier, and in the facile C-H bond cleavage by an adjacent metal. In the latter of these processes, the agostic interaction is a prelude to bond cleavage through the usual sequence of donation of electron density from the C-H bonding orbital to the metal and by an accompanying back donation from the metal to the corresponding C-H anti-bonding orbital. We were interested in learning more about these bridged methyl groups in this system and looked for ways to stabilize such species to allow their subsequent reactivity to be studied. In a related study of the Rh/Os system it has been discovered that protonation of a series of phosphine adducts $[\text{RhOs}(\text{L})(\text{CO})_3(\mu\text{-CH}_2)(\text{dppm})_2]^+$ ($\text{L} = \text{PEt}_3, \text{PMe}_3, \text{PPh}_2\text{Me}, \text{P}(\text{OMe})_3$ and $\text{P}(\text{OPh})_3$)⁴⁰ yielded the targeted species containing bridged agostic methyl complexes. However, attempts to repeat this with the Rh/Ru analogue, through protonation of $[\text{RhRu}(\text{CO})_3(\text{PMe}_3)(\mu\text{-CH}_2)(\text{dppm})_2]^+$ (**5**) did not yield a methyl-bridged complex. Instead, protonation of the PMe_3 group occurs, accompanied by protonation of the resultant methylene-bridged tricarbonyl complex to give an isomer of **20** in which the acyl moiety is reversed from that in **20**, having the acyl carbon now bound to Ru and the

oxygen bound to Rh. This Ru-bound acyl is short-lived, as it quickly converts to **20** within a few hours in solution. In addition, this isomerization also involves coordination of triflate to Ru in **24**, instead of being Rh-bound in **20**. Clearly our failure to obtain the targeted asymmetrically-bridged-methyl complex demonstrates that the PMe_3 site in **5** is more basic than the methylene bridge, and the reverse is true in the Rh/Os case. Protonation of the methylene-bridged tricarbonyl complex $[\text{RhRu}(\text{CO})_3(\mu\text{-CH}_2)(\text{dppm})_2]^+$ (**4**) gave a multitude of products, so there is clearly a role that the PMe_3 plays in the formation of **24**.

One important impetus for studying the chemistry of binuclear complexes is the possibility that these complexes can display bridged-bonding modes of ligands that can lead to reactivity differences of these ligands that differ from the terminally-bound groups in mononuclear complexes. We can imagine such a reactivity difference for the acyl ligands. Reaction of a complex, containing a terminally-bound acyl group, with H_2 would generally be accepted to yield the corresponding aldehyde by reductive elimination of the acyl and hydride moieties, as outlined in Scheme 5.6. The formulation

Scheme 5.6



of these bridging-acyl complexes as oxycarbenes has implications in the production of ethanol from these groups. If initial hydrogen transfer occurred at the carbene carbon, a bridged oxyethyl group would result, and ethanol could result by H-transfer to the oxygen

of the oxyethyl group followed by subsequent hydrogenolysis. If instead initial H-transfer to the oxygen of the bridging oxycarbene occurred and a hydroxycarbene would result. Subsequent hydrogenation of the metal-carbene linkage followed by reductive elimination will give ethanol. The regiochemistry of the bridging acyl group now becomes relevant to ethanol formation. We assume that H₂ oxidative addition in our system will occur at the unsaturated Rh centre. Addition of H₂ to complex **20**, in which the bridging acyl is carbon-bound to Rh, would likely proceed by H-transfer to the acetyl carbon. This would likely result in formation of acetaldehyde, although formation of ethanol by the aforementioned steps is also possible. Alternatively, H₂ addition to the “reverse acyl” complex **24**, in which the acyl is now oxygen-bound to Rh, could lead to H-transfer directly to the oxygen atom of the bridging acyl to give a hydroxycarbene, which could eliminate ethanol by subsequent hydrogen transfers.

Neither complex **20** nor **24** afforded any detectable amounts of ethanol upon treatment with H₂. Instead, complex **20** reacted with H₂ slowly to give a complex mixture of products, with the major organometallic species being [RhRu(CO)₃(μ-H)₂(dppm)₂][CF₂SO₃] (**1**). No ethanol or acetaldehyde was detected by ¹H NMR spectroscopy. Treatment of complex **24** with H₂ resulted in rapid isomerization to **20**, followed by formation a similar mixture of products that direct hydrogenolysis of **20** afforded.

Summary:

Protonation of the methylene-bridged complex **3** affords a bridging-acyl complex, $[\text{RhRu}(\text{OSO}_2\text{CF}_3)(\text{CO})_2(\mu\text{-C}(\text{O})\text{CH}_3)(\text{dppm})_2][\text{CF}_3\text{SO}_3]$ (**20**), proceeding through three detectable intermediates: a Ru-bound agostic methyl complex, a Rh-bound methyl complex, then a tricarbonyl-containing acyl complex. The two methyl-containing complexes are good models for the proposed migration of methyl groups on the surface of bimetallic heterogeneous catalysts. $^{13}\text{C}\{^1\text{H}\}$ NMR spectroscopy and X-ray crystallography support an oxy-carbene formulation for these acyl complexes. The roles of these complexes in ethanol formation in the FT process were examined, but no detectable amounts of any oxygenates were found. Isomerization of **20** was observed indirectly, through protonation of a PMe_3 adduct of a methylene-bridged complex forming a Ru-bound acyl complex, **24**. This “reverse acyl” complex has implications with regard to ethanol formation in the FT process; however **24** quickly isomerized back to **20** over a short period of time, rendering a study of the hydrogenolysis products impossible. An attempt was made to generate an acyl-complex through diazomethane addition to the hydride species $[\text{RhRu}(\text{X})(\mu\text{-H})(\text{CO})_4(\text{dppm})_2][\text{X}]$ ($\text{X} = \text{CF}_3\text{SO}_3$ (**25a**) or BF_4 (**25b**)). Unfortunately, **25** proved to be unreactive toward diazomethane. Protonation of **3** with an acid that possesses a strongly-coordinating conjugate base (HCl) results in the formation of a Ru-bound methyl complex, $[\text{RhRu}(\text{CH}_3)(\text{CO})_2(\mu\text{-Cl})(\mu\text{-CO})(\text{dppm})_2][\text{CF}_3\text{SO}_3]$ (**26**).

References:

1. Vannice, M.A. *J. Catal.* **1975**, *37*, 449.
2. Pichler, H.; Schulz, H. *Chem. Ing. Technol.* **1970**, *12*, 1160.
3. Henrici-Olive, G.; Olive, S. *Angew. Chem.-Int. Ed. Engl.* **1976**, *15*, 136.
4. Masters, C. *Adv. Organomet. Chem.* **1979**, *19*, 63.
5. Crabtree, R.H. *The Organometallic Chemistry of the Transition Metals*; John Wiley & Sons: New York, 1988, Chapter 7.
6. Shafiq, F.; Kramarz, K.W.; Eisenberg, R. *Inorg. Chim. Acta* **1993**, *213*, 111.
7. Gao, Y.; Jennings, M.C.; Puddephatt, R.J. *Organometallics* **2001**, *20*, 1882.
8. Johnson, K.A.; Gladfelter, W.L. *Organometallics* **1990**, *9*, 2101.
9. Trepanier, S.J.; McDonald, R.; Cowie, M. *Organometallics* **2003**, *22*, 2638.
10. DMA·HCl was prepared by bubbling HCl(g) through a benzene solution of DMA. The white solid was dried in vacuo and stored under dry argon (DMA·HCl is extremely hygroscopic).
11. Further information may be obtained by contacting Dr. Robert McDonald (bob.mcdonald@ualberta.ca) and inquiring about sample numbers COW0107 (compound **20**), COW0319 (compound **23**) and COW0013 (compound **26**).
12. Programs for diffractometer operation, data reduction, and absorption correction were those supplied by Bruker.
13. Beurskens, P.T.; Beurskens, G.; de Gelder, R.; Garcia-Granda, S.; Isreal, R.; Gould, R.O.; Smits, J.M.M. *DIRDIF-96 program system*; Crystallography Laboratory, University of Nijmegen: The Netherlands, 1996.

14. Sheldrick, G.M. *SHELXL-93*: Program for crystal structure determination; University of Gottingen: Gottingen, Germany, 1993.
15. Beurskens, P.T.; Beurskens, G.; de Gelder, R.; Garcia-Granda, S.; Isreal, R.; Gould, R.O.; Smits, J.M.M. *DIRDIF-99 program system*; Crystallography Laboratory, University of Nijmegen: The Netherlands, 1999.
16. Sheldrick, G.M. *Acta Crystallogr. Sect. A* **1990**, *46*, 467.
17. The presence of all three isotopomers of **21** arose due to partial hydrolysis of CF₃SO₃D before protonation of **3**, and due to small amounts of **3** present upon treatment of **3-CD**₂ with CF₃SO₃H.
18. Calvert, R.B.; Shapley, J.R. *J. Am. Chem. Soc.* **1978**, *100*, 7726.
19. Dawkins, G.M.; Green, M.; Orpen, A.G.; Stone, F.G.A. *J. Chem. Soc., Chem. Commun.* **1982**, 41.
20. Casey, C.P.; Fagan, P.J.; Miles, W.H. *J. Am. Chem. Soc.* **1982**, *104*, 1134.
21. Green, M.L.H.; Hughes, A.K.; Popham, N.A.; Stephens, A.H.H.; Wong, L.L. *J. Chem. Soc.-Dalton Trans.* **1992**, 3077.
22. Haynes, A.; Mann, B.E.; Morris, G.E.; Maitlis, P.M. *J. Am. Chem. Soc.* **1993**, *115*, 4093.
23. Torkelson, J.R.; Antwi-Nsiah, F.H.; McDonald, R.; Cowie, M.; Pruis, J.G.; Jalkanen, K.J.; DeKock, R.L. *J. Am. Chem. Soc.* **1999**, *121*, 3666.
24. Brookhart, M.; Green, M.L.H.; Wong, L.L. *Prog. Inorganic Chem.* **1988**, *36*, 1.
25. Torkelson, J.R.; McDonald, R.; Cowie, M. *Organometallics* **1999**, *18*, 4134.
26. Jeffery, J.C.; Orpen, A.G.; Stone, F.G.A.; Went, M.J. *J. Chem. Soc.-Dalton Trans.* **1986**, 173.

27. Allen, F.H.; Kennard, O.; Watson, D.G.; Brammer, L.; Orpen, A.G.; Taylor, R. *J. Chem. Soc.-Perkin Trans. 2* **1987**, S1.
28. Lawrance, G.A. *Chem. Rev.* **1986**, *86*, 17.
29. Erker, G. *Angew. Chem.-Int. Ed. Engl.* **1989**, *28*, 397.
30. Schubert, U. *Coord. Chem. Rev.* **1984**, *55*, 261.
31. Beck, W.; Sunkel, K. *Chem. Rev.* **1988**, *88*, 1405.
32. Brady, R.C.; Pettit, R. *J. Am. Chem. Soc.* **1980**, *102*, 6181.
33. Muetterties, E.L.; Stein, J. *Chem. Rev.* **1979**, *79*, 479.
34. Muetterties, E.L.; Rhodin, T.N.; Bard, E.; Brucker, C.F.; Pretzer, W.R. *Chem. Rev.* **1979**, *79*, 91.
35. Ziegler, T.; Tschinke, V.; Ursenbach, C. *J. Am. Chem. Soc.* **1987**, *109*, 4825.
36. Armentrout, P.B. In *Bonding Energetics in Organometallic Coumpounds*; Marks, T. J., Ed.; American Chemical Society: Washington, DC, 1990, Chapter 2.
37. Ziegler, T.; Tschinke, V. In *Bonding Energetics in Organometallic Coumpounds*; Marks, T. J., Ed.; American Chemical Society: Washington, DC, 1990, Chapter 19.
38. Niu, S.; Hall, M.B. *Chem. Rev.* **2000**, *100*, 353.
39. Blomberg, M.R.A.; Karlsson, C.A.M.; Siegbahn, P.E.M. *J. Phys. Chem.* **1993**, *97*, 9341.
40. Wigginton, J.R.; Trepanier, S.J.; Cowie, M. Unpublished results.

Chapter 6

Summary, Conclusions and Future Work:

The primary goal of this thesis was to synthesize and investigate the reactivity of Rh/Ru complexes containing bridging methylene groups, as models for bimetallic Fischer-Tropsch (FT) catalysts. Monometallic catalysts of the group 8 or 9 metals have shown high FT activity, although more recent work has shown that bimetallic systems containing *combinations* of metals from groups 8 and 9 have shown higher activity than their respective monometallic counterparts in a series of chemical transformations.¹⁻⁶ The introduction of a second metal substantially increases the complexity of the system and the roles of the different metals need to be determined. We therefore undertook a study of a series of mixed-metal binuclear complexes containing group 8 and 9 metals as potential models for bimetallic FT catalysts,⁷⁻¹¹ with the goal of determining the roles of the metals in carbon-carbon bond formation related to the FT process. To date, the most successful system contains the Rh/Os combination of metals, with diazomethane addition to $[\text{RhOs}(\text{CO})_4(\text{dppm})_2][\text{CF}_3\text{SO}_3]$ showing unprecedented CH_2 coupling to form metal-bound C_1 , C_3 or C_4 fragments, depending on reaction conditions (Scheme 1.9).^{7,12} The importance of the methylene group in FT chemistry cannot be underestimated; inspection of all of the accepted proposals discussed in Chapter 1 shows the involvement of surface-bound methylene units together with other hydrocarbyl fragments in the chain-propagating steps. The success of the above Rh/Os complex in methylene-coupling reactions suggested that complexes of rhodium and ruthenium might also prove to be

successful. Certainly, substituting Os by the less expensive Ru was of obvious interest and it was assumed that substitution of the more labile Ru for Os would also give rise to interesting reactivity.

Unfortunately, the anticipated reactivity of the Rh/Ru system was not fully realized, as treatment of the complex $[\text{RhRu}(\text{CO})_4(\text{dppm})_2][\text{CF}_3\text{SO}_3]$ (**2**) with diazomethane afforded *only* the C₁-containing species $[\text{RhRu}(\text{CO})_4(\mu\text{-CH}_2)(\text{dppm})_2][\text{CF}_3\text{SO}_3]$ (**3**), with no further CH₂ incorporation beyond the initial unit. This reactivity fell far short of that noted above for the Rh/Os system which readily incorporated up to four CH₂ units.^{7,12} Although the solid-state structure of **3** proved to be nearly identical to that of the RhOs analogue, $[\text{RhOs}(\text{CO})_4(\mu\text{-CH}_2)(\text{dppm})_2][\text{CF}_3\text{SO}_3]$, the subtle differences observed can help explain the changes in reactivity upon substitution of Os for Ru. The structure of the Rh/Os analogue was *slightly* closer to structure **E** in Chart 2.2, in which one of the carbonyls was semi-bridging with Rh; in this extreme Rh is coordinatively unsaturated. Complex **3** on the other hand appeared to be closer to structure **F**, in which this carbonyl is bridging both metals accompanied by a metal-metal bond, giving both metals an 18-electron configuration. Our contention is that the less this “bridging” carbonyl interacts with Rh, the more easily it can be displaced from this metal by a nucleophile. Thus, the Rh/Os complex will undergo nucleophilic substitution more readily than the Rh/Ru counterpart. The concept of greater carbonyl lability for the Rh/Os system was supported by substitution reactions that showed nucleophilic attack of PMe_3 on $[\text{RhM}(\text{CO})_4(\mu\text{-CH}_2)(\text{dppm})_2]^+$ (M = Ru (**3**), Os), affording $[\text{RhM}(\text{CO})_3(\text{PMe}_3)(\mu\text{-CH}_2)(\text{dppm})_2]^+$ (M = Ru (**5**), Os), occurs significantly faster for the Rh/Os complex than for the Rh/Ru species.¹³ The inability of the Rh/Ru system to

incorporate a second methylene group is due to the inability of the relatively weak nucleophile CH_2N_2 to displace a carbonyl from Rh. Apparently in the Rh/Os analogue the subtle difference in binding mode of the semi-bridging carbonyl allows diazomethane to displace this group, leading to incorporation of the second and subsequent methylene groups. It was reasoned that carbonyl removal from **3** using trimethylamine-N-oxide should give a tricarbonyl species, $[\text{RhRu}(\text{CO})_3(\mu\text{-CH}_2)(\text{dppm})_2][\text{CF}_3\text{SO}_3]$ (**4**), that might prove more reactive than the tetracarbonyl counterpart. As anticipated, complex **4** did react readily with CH_2N_2 , however a multitude of unidentifiable products were obtained, in which the degree of methylene incorporation has not been established.

Clearly the chemical differences between the Rh/Ru and Rh/Os complexes are not solely related to the replacement of Os by Ru. Other factors are involved such as the nature of bridging carbonyl ligands and the strength of the metal-metal bond; a more symmetrically bridging carbonyl is accompanied by a stronger metal-metal bond leading to lower lability of the carbonyl group

Although we were unable to generate higher than C_1 complexes through the coupling of methylene units in the Rh/Ru system, we proposed that models for such species could be generated in other ways. We were particularly interested in C_3 -bridged species as models for the putative C_3H_6 -bridged intermediate in the aforementioned methylene condensation reactions of the Rh/Os system. Dry has recently alluded to the possible importance of surface-bound C_3 units in the FT process, produced by the condensation of bridging methylene groups and surface-bound olefins as the C_2 fragments.¹⁴ It was suggested that the generation of C_3 -bridged complexes should be possible through the coupling of a C_1 unit (methylene group) and a C_2 unit (alkynes or

allenes). The strategy for the synthesis of these complexes was fairly simple: reaction of a methylene-bridged complex with the C₂ source such as alkynes or allenes (in which it was anticipated that only one of the π-systems would act as a 2e donor) or reaction of a C₂-bridged complex with diazomethane as the C₁ source. Each of these strategies should give rise to different isomeric forms in the hydrocarbyl chain; in the Rh/Ru case the methylene unit(s) could either be adjacent to Rh or to Ru. Presumably, propagation to C₄- and higher chains might also be possible by incorporation of additional C₁ or C₂ units into the C₃ unit.

Success in generating C₃-bridged products was achieved by reacting the symmetric, activated alkynes dimethyl acetylenedicarboxylate (DMAD), hexafluoro-2-butyne (HFB) and diethyl acetylenedicarboxylate (DEAD) with complex **4**, giving the insertion products [RhRu(CO)₃(μ-η¹:η¹-C(R)=C(R)CH₂)(dppm)₂][CF₃SO₃] (R = CO₂Me (**6**), CF₃ (**7**), CO₂Et (**8**)). The resultant C₃ fragments have the “C(R)=C(R)CH₂” unit bound in an η¹:η¹-fashion, bridging both metals, in which the vinylic end is bound to Rh and the methylene group is bound to Ru, indicating that insertion into the Rh-CH₂ bond has occurred. Similarly, the unsymmetrical alkynes, 2-butyne-1-ol dimethylacetal (BDA) and 2-butyne-1-ol also react readily with **4**, again giving products [RhRu(CO)₃(μ-η¹:η¹-C(R)=C(R')CH₂)(dppm)₂][CF₃SO₃] (R = CH₃; R' = CH(CO₂Et)₂ (**9**), CH₂OH (**10**)), in which alkyne insertion into the Rh-CH₂ bond had occurred. In the case of the unsymmetrical alkynes the more sterically-hindered carbon was found to be adjacent to the methylene unit. We assume that this regiospecific insertion is dictated by steric factors in which the alkyne substituents interact with the phenyl groups on the dppm ligand, which serve to protect the region between the carbonyl and methylene ligands.

This regioselectivity appears to be in contrast with that observed by other research groups where it was found that alkyne insertion into a bridging methylene occurred such that the carbon with the less bulky substituent was adjacent to the incumbent methylene unit.¹⁵⁻²³

It was presumed that these C₃-bridging groups could be transformed from 2e donors (propenediyl) to 4e donors (vinyl carbene) by creating an electronic deficiency at Ru through carbonyl loss. Although addition of Me₃NO to [RhRu(CO)₃(μ-η¹:η¹-C(CO₂Me)=C(CO₂Me)CH₂)(dppm)₂][CF₃SO₃] (**6**) did afford the desired product containing a 4e donor vinyl-carbene ligand, [RhRu(CO)₂(μ-η¹:η³-CHC(CO₂CH₃)=CH(CO₂CH₃))(dppm)₂][CF₃SO₃] (**14**), the targeted ligand transformation was accompanied by an unexplained 1,3-hydrogen shift and accompanying rearrangement.

An alternative method to producing C₃-bridged complexes would be to add the C₁ unit (in the form of diazomethane) to the appropriate C₂-bridged complex. This strategy failed for the DMAD-bridged complex [RhRu(CO)₃(μ-η¹:η¹-C(CO₂Me)=C(CO₂Me))(dppm)₂][CF₃SO₃] (**11**) (C₂ source), which failed to react with diazomethane. Carbonyl removal from this species afforded the neutral dicarbonyl complex [RhRu(OSO₂CF₃)(CO)₂(μ-η¹:η¹-C(CO₂CH₃)=C(CO₂CH₃))(dppm)₂] (**12**) having a coordinating triflate ligand, and this product did prove to be reactive toward diazomethane. However, methylene incorporation did not give rise to a targeted C₃ species isomeric with **6**, but instead yielded [RhRu(OSO₂CF₃)(CO)₂(μ-η¹:η¹-C(CO₂CH₃)=C(CO₂CH₃))(μ-CH₂)(dppm)₂] (**13**), containing two separate C₂ and C₁ units.

It is unclear why methylene incorporation into the metal-metal bond is preferred over insertion into the metal-carbon bond.

As noted earlier, one goal of this work was to model steps in the sequence of carbon-carbon bond formation by sequentially increasing the length of the hydrocarbyl fragment by the selective addition of C₁ or C₂ fragments. Having generated a C₃-bridged fragment by alkyne insertion into the Rh-CH₂ bond of **4**, we next attempted extending this C₃ fragment to C₄ by incorporation of a second methylene unit. However, this extension did not prove fruitful with compounds **6** and **7**, being unreactive to diazomethane. Success was achieved in extending the C₃ fragment to C₅ when the alkyne, propargyl alcohol, was used. Reaction of **4** with propargyl alcohol yielded the double-insertion product [RhRu(CO)₂(μ-η²:η⁴-CH=C(CH₂OH)CH=C(CH₂OH)-CH₂)(dppm)₂][CF₃SO₃] (**15**) in which the two propargyl alcohol moieties have inserted in a head-to-tail arrangement to give the observed C₅ fragment. This result clearly shows that complexes with higher chain lengths are possible, although not, in this case, from CH₂ coupling as previously hoped.

Given the propensity for alkynes to undergo insertion reactions forming C₃-bridged complexes, allenes also seemed to be viable candidates for the generation of model C₃-bridged species. Allenes are ideal candidates as potential insertion substrates, due their tunable steric bulk in the form of varying substituents and to their readily available π-systems for initial coordination to the metal centre. Although allene and 1,1-dimethylallene were shown to undergo insertion into the Rh-CH₂ bond, neither of these substrates afforded the targeted C₃-bridged species outlined in Scheme 4.1. Allene inserted into the Rh-CH₂ bond with similar regiochemistry to the alkyne molecules, with

the sterically-hindered carbon being adjacent to the bridging methylene unit. However, instead of forming a C₃-bridged, “CH₂C(=CH₂)CH₂” moiety, rearrangement ensued forming an η³:η¹-trimethylenemethane species [RhRu(CO)₂(μ-η³:η¹-C(CH₂)₃)(dppm)₂][CF₃SO₃] (**16**). This type of rearrangement of an η¹-allyl group to a more stable η³ form is common.^{24,25} Although further methylene incorporation into the TMM complex was not successful, the complex proved susceptible to nucleophilic attack by both CO and PMe₃ affording the adducts [RhRu(CO)₂(L)(μ-η³:η¹-C(CH₂)₃)(dppm)₂][CF₃SO₃] (L = CO (**17**), PMe₃ (**18**)) in which the TMM moiety has remained intact. This result once again demonstrates the weak nucleophilicity of diazomethane.

The more sterically demanding 1,1-dimethylallene (DMA) reacts in a very different manner than that of its smaller counterpart. Once again the simple insertion product forming a species with either “CH₂C(=CMe₂)CH₂” or “Me₂CC(=CH₂)CH₂” bridging groups are not observed. Instead, insertion into the Rh-CH₂ bond occurs in which the *less* sterically hindered carbon of DMA forms a new bond with the bridging methylene carbon. This is followed by migratory insertion of this fragment and a Ru-bound carbonyl ligand with accompanying migration forming the complex [RhRu(CO)₃(C(O)CH₂CH₂C(=C(CH₃)₂)(dppm)₂][CF₃SO₃] (**19**).

The above reactions display both similarities and differences when compared to reactions involving the Rh/Os analogue. With allene, both the Rh/Ru and Rh/Os complexes yield analogous trimethylenemethane-bridged products. However, with 1,1-dimethylallene different products result from reactions with the two mixed-metal complexes. Instead of generating a metallacyclopentanone complex analogous to **19**,

reaction of the Rh/Os compound yields the targeted $[\text{RhOs}(\text{CO})_3(\mu\text{-}\eta^1\text{:}\eta^1\text{-}(\text{CH}_3)_2\text{C}=\text{CCH}_2\text{CH}_2)(\text{dppm})_2][\text{CF}_3\text{SO}_3]$ complex, which subsequently decomposed yielding 1,1-dimethyl-1,3-butadiene. It is proposed that both the Rh/Os and Rh/Ru systems give rise to such a C_3 -bridged complex. But, whereas the greater tendency of Os for β -hydrogen elimination gives rise to elimination of the butadiene, the greater tendency of Ru for migratory insertion to a carbonyl group gives rise to the metallacyclopentanone group in the Rh/Ru complex. This difference in reactivities involving the different metal combinations supports our contention that the use of different metals can influence the type of product(s) observed.

A secondary goal of this thesis was to use these mixed-metal complexes to model the formation of oxygenates in the FT process. Although usually produced in small quantities, Rh-based catalysts have a greater tendency than other metals to produce oxygenates such as aldehydes, ketones and alcohols.²⁶ The transformation of a bridging methylene group into a bridging acyl group was achieved by protonation of **3** yielding $[\text{RhRu}(\text{CO})_2(\mu\text{-C}(\text{O})\text{CH}_3)(\text{dppm})_2][\text{CF}_3\text{SO}_3]$ (**20**). In this transformation, a number of intermediates were observed at lower temperatures, having features that mimic important species and processes occurring on a metal surface. The appearance of the two methyl-containing intermediates, $[\text{RhRu}(\text{CO})_3(\mu\text{-CH}_3)(\text{dppm})_2]$ (**21**) and $[\text{RhRu}(\text{CH}_3)(\text{CO})_3(\text{dppm})_2]$ (**22**), observed in the transformation of **3** to **20** appear to model proposed intermediates in the migration of a methyl group from one metal to another (Scheme 5.5).

It is interesting to speculate how a bridging acyl group on a model surface might have relevance to oxygenate formation that differs from a terminally-bound group, and

how the orientation of the bridging acyl might also influence this formation. The model system described in Chapter 5 suggests some possibilities. Although hydrogenolysis of a terminal acetyl group invariably gives acetaldehyde, the bridging acyl group can, in principle, form other products. The formation of different oxygen-containing species from a bridging acyl can be dependent, not only on the orientation of the acyl, but also on the bonding within that group. In the classical acyl formulation, the expected product upon hydrogenolysis is acetaldehyde. However, if the acyl binds as an oxycarbene, as in compound **20**, we might expect a different outcome in reactions with H₂, possibly with the formation of a hydroxycarbene-hydroxyalkyl sequence yielding ethanol instead of acetaldehyde. Unfortunately, neither acetaldehyde nor ethanol were observed in the reaction of **20** with H₂.

In principle, the orientation of the bridging acyl might also influence the products obtained. In the binding mode for **20**, in which the acyl carbon is adjacent to Rh, the site of coordinative unsaturation, hydrogen transfer to the acyl will most likely occur at carbon first. It may be difficult under such circumstances to obtain a hydroxy group by hydrogen transfer to oxygen. In the reverse acyl geometry, in which the acyl-oxygen binds to Rh, hydrogen transfer directly to oxygen might occur. A reverse acyl complex, [RhRu(OSO₂CF₃)(CO)₂(μ-C(O)CH₃)(dppm)₂][CF₃SO₃] (**24**), was obtained from the protonation of complex **5**. However, this product quickly isomerizes in solution to **20**, and as such no observable oxygen-containing products are observed when **24** is treated with hydrogen.

The results contained herein, coupled with those obtained with other group 8/9 metal combinations studied within the Cowie group^{7,8,10,12,27} all share one central

foundation on which the chemistry is based: the tendency for coordinative unsaturation at rhodium in Rh/Os and Rh/Ru complexes to facilitate substrate coordination at the metal and subsequent insertion into the adjacent Rh-CH₂ bond of the bridging methylene group. Other work within this group has shown that more subtle effects such as metal-metal bonding and metal-ligand bonding in bridging ligands cannot be overlooked and can have pronounced effects on the products observed.^{7,10,12,28,29}

The study of one particular combination of metals (in this case, Rh/Ru) can certainly yield valuable information about the roles of the different metals in carbon-carbon bond formation. Naturally, an equally intensive study of complexes with similar combinations of metals (such as Rh/Fe, Rh/Os, Ir/Ru and Ir/Os) must also be performed, in order to observe not only what products are obtained in each case, but what differences in reactivity are obtained with the different metal combinations, in order to ascertain what role each metal plays in the transformation(s) of interest.

Clearly, more work needs to be done on the Rh/Ru system, in order to gain insight into the reasons why the reactivity of these complexes differs from their Rh/Os counterparts. Although significant strides toward understanding the nature of these differences has been made, further insight into the mechanism of some of the transformations caused by both metal combinations might help explain these differences.

Although the study of RhRu complexes might be a natural progression from RhOs, an obvious limiting factor in using RhM (M = Ru, Os) as models for bimetallic FT catalysts is their low utilization in industry. Rhodium, ruthenium and (especially) osmium are very expensive compared to cobalt and iron, which are more common metals used in commercial FT plants.³⁰ Ideally, bis-dppm-bridged complexes including Co/Fe,

or perhaps Co/Ru, would be ideal from the standpoint of modeling what is used in industry. However, neither Co, Fe nor Ru have tendencies to form stable complexes in which these metals possess coordinative unsaturation. Instead, complexes containing these metals prefer to achieve a saturated 18e configuration at the metals, usually requiring photolysis and/or reflux conditions to generate coordinatively unsaturated 16e species. In addition, the dpmm ligands might prove to be too “soft” to effectively bind two first row transition metals such as cobalt and iron. This has been observed previously, where the binuclear complex $[\text{RhCo}(\text{CO})_3(\text{dpmm})_2]$ fragments upon exposure to CO, and forms an equilibrium with the two mononuclear species $[\text{Rh}(\text{CO})(\text{dpmm})_2]^+$ and $[\text{Co}(\text{CO})_4]^-$.^{31,32} In any case, some work has been done in our group with the Rh/Fe combination of metals, namely the synthesis of the methylene-bridged complex $[\text{RhFe}(\text{CO})_4(\mu\text{-CH}_2)(\text{dpmm})_2][\text{CF}_3\text{SO}_3]$.³³ The Rh/Fe combination of metals is ideal from the standpoint of modeling oxygenate formation, since both of these metals tend to form oxygenates when used as FT catalysts.²⁶

The next problem that arises would be the utility of these detailed studies toward elucidation of the fundamental processes at work in *heterogeneous* catalysts containing the same combination of metals. Although the fundamental steps in the chemical transformations that occur on a surface should closely resemble those observed in soluble organometallic complexes of the type described in this thesis, the application of these complexes as accurate models is limited in scope. Clearly the presence of ancillary ligand(s) in model complexes can limit their use as models for heterogeneous surfaces. In addition, limitations in describing an extended metal surface by a *pair* of metals are obvious.

Nevertheless, the use of complexes such as those described in this thesis as models for organic transformations occurring on a metal surface can allow for significant insight into the nature of these transformations. The presence of an adjacent metal allows for the incorporation of such surface-catalysis phenomena as synergism and metal-metal cooperativity effects in modeling reactivity of surface-bound substrates that bridge adjacent metals.

References:

1. Sinfelt, J.H. *Bimetallic Catalysts: Discoveries, Concepts and Applications*; Wiley: New York, 1983
2. da Silva, A.C.; Piotrowski, H.; Mayer, P.; Polborn, K.; Severin, K. *Eur. J. Inorg. Chem.* **2001**, 685.
3. Alexeev, O.S.; Gates, B.C. *Ind. Eng. Chem. Res.* **2003**, *42*, 1571.
4. Iglesia, E.; Soled, S.L.; Fiato, R.A.; Via, G.H. *J. Catal.* **1993**, *143*, 345.
5. Huang, L.; Xu, Y. *Catalysis Letters* **2000**, *69*, 145.
6. Dombek, B.D. *Organometallics* **1985**, *4*, 1707.
7. Trepanier, S.J.; Sterenberg, B.T.; McDonald, R.; Cowie, M. *J. Am. Chem. Soc.* **1999**, *121*, 2613.
8. Trepanier, S.J.; McDonald, R.; Cowie, M. *Organometallics* **2003**, *22*, 2638.
9. Rowsell, B.D.; Trepanier, S.J.; Lam, R.; McDonald, R.; Cowie, M. *Organometallics* **2002**, *21*, 3228.
10. Dell'Anna, M.M.; Trepanier, S.J.; McDonald, R.; Cowie, M. *Organometallics* **2001**, *20*, 88.

11. Torkelson, J.R.; McDonald, R.; Cowie, M. *J. Am. Chem. Soc.* **1998**, *120*, 4047.
12. Trepanier, S.J.; Dennett, J.N.L.; Sterenberg, B.T.; McDonald, R.; Cowie, M. Manuscript to be submitted.
13. Trepanier, S.J.; Rowsell, B.D.; Cowie, M. Unpublished Results.
14. Dry, M.E. *Appl. Catal. A* **1996**, *138*, 319.
15. Dyke, A.F.; Knox, S.A.R.; Naish, P.J.; Taylor, G.E. *J. Chem. Soc.-Chem. Commun.* **1980**, 803.
16. Gracey, B.P.; Knox, S.A.R.; Macpherson, K.A.; Orpen, A.G.; Stobart, S.R. *J. Chem. Soc.-Dalton Trans.* **1985**, 1935.
17. Sumner, C.E.; Collier, J.A.; Pettit, R. *Organometallics* **1982**, *1*, 1350.
18. Akita, M.; Hua, R.; Nakanishi, S.; Tanaka, M.; Morooka, Y. *Organometallics* **1997**, *16*, 5572.
19. Adams, P.Q.; Davies, D.L.; Dyke, A.F.; Knox, S.A.R.; Mead, K.A.; Woodward, P. *J. Chem. Soc.-Chem. Commun.* **1983**, 222.
20. Colborn, R.E.; Dyke, A.F.; Knox, S.A.R.; Macpherson, K.A.; Orpen, A.G. *J. Organomet. Chem.* **1982**, *239*, C15.
21. Colborn, R.E.; Davies, D.L.; Dyke, A.F.; Knox, S.A.R.; Mead, K.A.; Orpen, A.G.; Guerchais, J.E.; Roue, J. *J. Chem. Soc.-Dalton Trans.* **1989**, 1799.
22. Dennett, J.N.L., Ph.D. Thesis, Chapter 4, University of Bristol, Bristol, UK, 2000.
23. Kaneko, Y.; Suzuki, T.; Isobe, K.; Maitlis, P.M. *J. Organomet. Chem.* **1998**, *554*, 155.
24. Crabtree, R.H. *The Organometallic Chemistry of the Transition Metals*; John Wiley & Sons: New York, 1988, Chapter 7.

25. Solin, N.; Szabo, K.J. *Organometallics* **2001**, *20*, 5464.
26. Vannice, M.A. *J. Catal.* **1975**, *37*, 449.
27. Chokshi, A., M.Sc. Thesis, University of Alberta, Edmonton, Alberta, Canada, 2004.
28. Ristic-Petrovic, D.; Anderson, D.J.; Torkelson, J.R.; McDonald, R.; Cowie, M. *Organometallics* **2003**, *22*, 4647.
29. Ristic-Petrovic, D.; Wang, M.; McDonald, R.; Cowie, M. **2002**, *21*, 5172.
30. Tullo, A.H. *Chem. Eng. News* **2003**, *July 21*, 18.
31. Elliot, D.J.; Holah, D.G.; Hughes, A.N.; Vittal, J.J.; Puddephatt, R.J. *Organometallics* **1993**, *12*, 1225.
32. Antonelli, D.M.; Cowie, M. *Organometallics* **1990**, *9*, 1818.
33. Lo, J.; Cowie, M. Unpublished results.

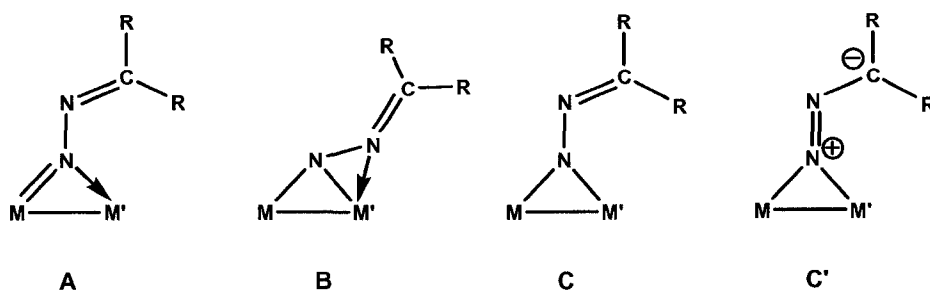
Appendix

Diazoalkane Complexes of Rh/Ru

Introduction:

Diazoalkane complexes of transition metals are important because they have been presumed as intermediates in the formation of alkylidene complexes^{1,2} that might be relevant in the FT process.³ These complexes are also of interest because they can be used as models for nitrogen fixation⁴ giving diazo-organometallic compounds. Although there are numerous bridging modes for coordination of diazoalkanes to binuclear transition metal complexes,⁵ it is quite common to find them in early transition metals acting as a 4-electron donor ligand, as shown as **A** and **B** in Chart A.1. Less common is to find the diazoalkane ligand acting as a 2-electron donor, as diagrammed for one possible valence bond formulation in Chart A.1 as structure **C**. There are very few

Chart A.1



examples in which the diazoalkane ligand bridges late transition metals, but previous work from the groups of Puddephatt⁶ and Eisenberg⁷ show that this type of coordination with late metals is possible. In both of these cases, ethyl diazoacetate was added to Ru₂ and Rh₂ complexes to afford the highly-conjugated species [Ru₂(CO)₄(μ-N₂CHCO₂Et)(dppm)₂] and [Rh₂(CO)₂(μ-N₂CHCO₂Et)(dppm)₂] respectively.

In this appendix, we report attempts to synthesize complexes containing a bridging alkylidene other than methylene in addition to the attempted synthesis of new diazoalkane complexes with the Rh/Ru combination of metals.

Experimental:

General Comments. All solvents were dried (using appropriate desiccants), distilled before use, and stored under a dinitrogen atmosphere. Reactions were performed under an argon atmosphere using standard Schlenk techniques. Diazoethane was generated from ENNG (1-ethyl-3-nitro-1-nitrosoguanidine), which was purchased from Aldrich, as was the diphenyldiazomethane, trimethylsilyldiazomethane and the 2-diazo-malonic acid diethyl ester. Ethyl diazoacetate was purchased from Fluka, Inc.

The ¹H, ¹³C{¹H}, and ³¹P{¹H} NMR spectra were recorded on a Varian iNova-400 spectrometer operating at 399.8 MHz for ¹H, 161.8 MHz for ³¹P, and 100.6 MHz for ¹³C. Infrared spectra were obtained on a Bomem MB-100 spectrometer. The elemental analyses were performed by the microanalytical service within the department.

Spectroscopic data for the compounds are available in Table A.1.

Table A.1. Spectroscopic Data For Compounds.

Compound	IR (cm ⁻¹) ^{a,b}	NMR ^{c,d}	
		³¹ P{ ¹ H} (ppm) ^e	¹ H (ppm) ^{f,g}
[RhRu(CO) ₃ (μ-N ₂ C(COH)- (CO ₂ Et))(dppm) ₂][CF ₃ SO ₃] (27)	2035 (m), 1996 (s), 1985 (m)	29.6 (m), 28.2 (dm)	10.96 (s, br, 1H), 4.36 (q, ³ J _{HH} = 8 Hz, 2H), 3.18 (m, 2H), 2.63 (m, 2H), 1.45 (t, ³ J _{HH} = 8 Hz, 3H)
[RhRu(CO) ₃ (μ-N ₂ C(CO ₂ Et) ₂ - (dppm) ₂][CF ₃ SO ₃] (28)	2045 (m), 2027 (s), 1996 (s), 1694 (m) ^h 1374 (m) ⁱ	36.9 (m), 28.2 (dm)	4.28 (q, ³ J _{HH} = 7 Hz, 2H), 3.14 (m, 2H), 3.07 (m, 2H), 1.83 (q, ³ J _{HH} = 7 Hz, 3H), 1.33 (t, ³ J _{HH} = 7 Hz, 3H), 0.57 (t, ³ J _{HH} = 7 Hz, 3H)

^a IR abbreviations: s = strong, m = medium. ^b CH₂Cl₂ solutions unless otherwise stated, in units of cm⁻¹. ^c NMR abbreviations: s = singlet, d = doublet, t = triplet, q = quartet, m = multiplet, dm = doublet of multiplets. ^d NMR data at 25 °C in CD₂Cl₂ unless otherwise stated. ^e ³¹P chemical shifts referenced to external 85% H₃PO₄. ^f Chemical shifts for the phenyl hydrogens are not given. ^g ¹H chemical shifts referenced to TMS. ^h ν(CO₂Et). ⁱ ν(N₂)

Preparation of Compounds:

(a) **[RhRu(CO)₃(μ-N₂C(COH)(CO₂Et))(dppm)₂][CF₃SO₃]·0.1CH₂Cl₂ (27).**

[RhRu(CO)₄(dppm)₂][CF₃SO₃] (2) (25 mg, 0.020 mmol) was dissolved in 15 mL of CH₂Cl₂, to which 55 μL (0.053 mmol, 2.65 equiv) of ethyl diazoacetate was added. The solution was stirred for 1 h, after which the solution was concentrated to 2 mL, followed by dropwise addition of 15 mL of Et₂O causing the precipitation of an orange powder. The supernatant was removed and the orange residue was recrystallized from CH₂Cl₂/Et₂O (1 mL/10 mL) affording bright orange microcrystals which were dried *in vacuo* (75% yield, 21 mg). Anal. Calcd for C_{62.1}H_{55.2}Cl_{0.2}F₃N₂O₁₁P₄RhRuS: C, 52.33; H, 3.73; N, 2.07; Cl, 0.52. Found: C, 52.16; H, 3.74; N, 1.98; Cl, 0.54.

(b) **[RhRu(CO)₃(μ-N₂C(CO₂Et)₂)(dppm)₂][CF₃SO₃] (28).** Compound 2 (36 mg, 0.028 mmol) was dissolved in 20 mL of CH₂Cl₂. To the solution, 0.5 mL of a 0.1 M solution of 2-diazo-malonic acid diethyl ester (0.05 mmol) was added, causing a colour change from yellow to orange over the course of 1 h. The solution was stirred for an additional 1 h, after which it was concentrated to 2 mL. Dropwise addition of 15 mL of Et₂O afforded an orange powder. The supernatant was removed and the orange residue was recrystallized from CH₂Cl₂/Et₂O (2 mL/15 mL) affording an orange powder which was dried *in vacuo* (82% yield, 32.0 mg). Anal. Calcd for C₆₁H₅₄F₃N₂O₁₀P₄RhRuS: C, 52.63; H, 3.91; N, 2.01. Found: C, 52.26; H, 3.93; N, 1.91.

(c) **Reaction of 4 with N₂CH(CO₂Et).** [RhRu(CO)₃(μ-CH₂)(dppm)₂][CF₃SO₃] (4) was prepared from a mixture of compound 3 (37 mg, 0.030 mmol) and Me₃NO (3.83 mg, 0.051 mmol, 1.7 equiv) in 0.7 mL of acetone-d₆ in an NMR tube. The solution immediately changed colour from dark red to a lighter red upon addition of 3.2 μL (0.031

mmol, 1.03 equiv.). $^{31}\text{P}\{^1\text{H}\}$ NMR spectroscopy detected the presence of numerous unidentified products, but ^1H NMR spectroscopy detected the presence of ethyl acrylate.

(d) Attempted reaction of 2 with N_2CPh_2 . Compound 2 (24 mg, 0.020 mmol) and diphenyldiazomethane (3.7 mg, 0.020 mmol) was dissolved in 0.7 mL of CD_2Cl_2 in an NMR tube. After 5 days, $^{31}\text{P}\{^1\text{H}\}$ NMR and ^1H NMR spectroscopy detected only the presence of 2.

(e) Attempted reaction of 2 with $\text{N}_2\text{CH}(\text{SiMe}_3)$. Compound 2 (99.5 mg, 0.081 mmol) was dissolved in 10 mL of CH_2Cl_2 . To this solution, 50 μL of $\text{N}_2\text{CH}(\text{SiMe}_3)$ (0.100 mmol) was added, causing no colour change. A 0.5 mL aliquot was removed after 20 h, and $^{31}\text{P}\{^1\text{H}\}$ NMR and ^1H NMR spectroscopy detected only the presence of 2.

(f) Attempted reaction of 2 with $\text{N}_2\text{CH}(\text{Me})$. Compound 2 (153 mg, 0.124 mmol) was dissolved in 10 mL of CH_2Cl_2 and the solution was cooled to $-78\text{ }^\circ\text{C}$. Diazoethane, generated from ENNG (100 mg, 0.621 mmol) was bubbled over the solution and the mixture was stirred for 2.5 h. The solution was allowed to warm to room temperature and a 0.5 mL aliquot was removed, and $^{31}\text{P}\{^1\text{H}\}$ NMR and ^1H NMR spectroscopy detected only the presence of 2 and diazoethane. Even after *ca.* 24 h, NMR spectroscopy detected only starting materials.

Results and Compound Characterization:

Compound **2** reacts with ethyl diazoacetate forming one new complex, **27**, as observed in the $^{31}\text{P}\{^1\text{H}\}$ NMR spectrum as two nearly-overlapping signals at δ 29.6 and 28.2. The ^1H NMR spectrum of **27** indicated that one CHCO_2Et group has been incorporated into this new complex, with the CH_3 and CH_2 resonances appearing at δ 1.45 and 4.36, respectively, and one low-field resonance at δ 10.96. This low-field signal shows no coupling to either Rh or P, suggesting the diazoalkane has not formed a bridging alkylidene analogous to diazomethane addition to **2**. Elemental analysis confirms that N_2 loss has not occurred, suggesting that the diazoalkane moiety has remained intact. The IR spectrum of **27** contains three terminal carbonyl bands at 2035, 1996 and 1985 cm^{-1} . Unfortunately there are a myriad of bands appearing from 1700 to 1200 cm^{-1} , giving little additional information about the binding of the ethyl diazoacetate molecule, presumably due to the large degree of unsaturation that might be present (vide infra). However, the NMR data for **27** closely match that observed for the analogous Rh/Os compound, in which the reaction between $[\text{RhOs}(\text{CO})_4(\text{dppm})_2][\text{OTf}]$ and ethyl diazoacetate gave the complex $[\text{RhOs}(\text{CO})_3(\mu\text{-N}_2\text{C}(\text{COH})(\text{CO}_2\text{Et}))(\text{dppm})_2][\text{CF}_3\text{SO}_3]$.⁸ The X-ray structure determination of this Rh/Os complex indicates that the N_2 portion of the diazoalkane has remained intact, affording a bridging diazoalkane complex similar to structure **C** in Chart A.1. In addition, however, the hydrogen of the diazoalkane carbon has migrated to the oxygen of a metal-bound carbonyl accompanied by formation of a C-C bond between the α carbon of the diazoalkane ligand and the carbonyl to which the hydrogen migrated. Although no structural data exists for the Rh/Ru complex **27**, the structure of the Rh/Os analogue was determined by X-ray crystallography^{8,9} and the

cation is shown in Figure A.1 with relevant bond lengths and angles given in Table A.3. Based on the spectral similarities between these RhOs and RhRu analogues, the structure of **27** is presumed to be similar to that determined for RhOs. Clearly the diazoalkane moiety has remained intact, and has coupled to a carbonyl forming the “diazometallacyclopentenol” moiety. Although one can envision the possibility of delocalized bonding within this group, the solid-state structure supports a more localized view of the bonding within this ligand. The C(4)-O(4) distance of 1.328(4) Å is in excellent agreement with the single C-O bonds of enols and the C(4)-C(5) distance is close to that expected for a C=C double bond (1.391(4) Å).¹⁰ The N(1)-N(2) distance of 1.270(4) Å is within the accepted range for an N=N bond (≈ 1.240 Å), and the C(5)-N(2) distance (1.402(4) Å) is as expected for a single bond between sp² hybridized carbon and nitrogen atoms. The average angles about C(4), C(5) and N(1), (120.0, 120.0 and 119.8 respectively) are also clearly consistent with sp² hybridization for these three atoms, as expected for the structure diagrammed in Scheme A.1.

With the success of ethyl diazoacetate in forming isolable diazoalkane complexes in this work and elsewhere,^{6,7} complex **2** was treated with a series of diazoalkanes in attempts to generate other diazoalkane complexes. One goal was to attempt to isolate diazoalkane complexes like **27** in which condensation of the diazoalkane and a metal bound carbonyl did *not* occur. Since hydrogen migration accompanied this condensation, it was believed that using disubstituted diazoalkanes might prevent this condensation. In addition, we were interested in generating bridging carbene fragments as models for FT-relevant fragments on metal surfaces. With diazoethane, trimethylsilyldiazomethane,

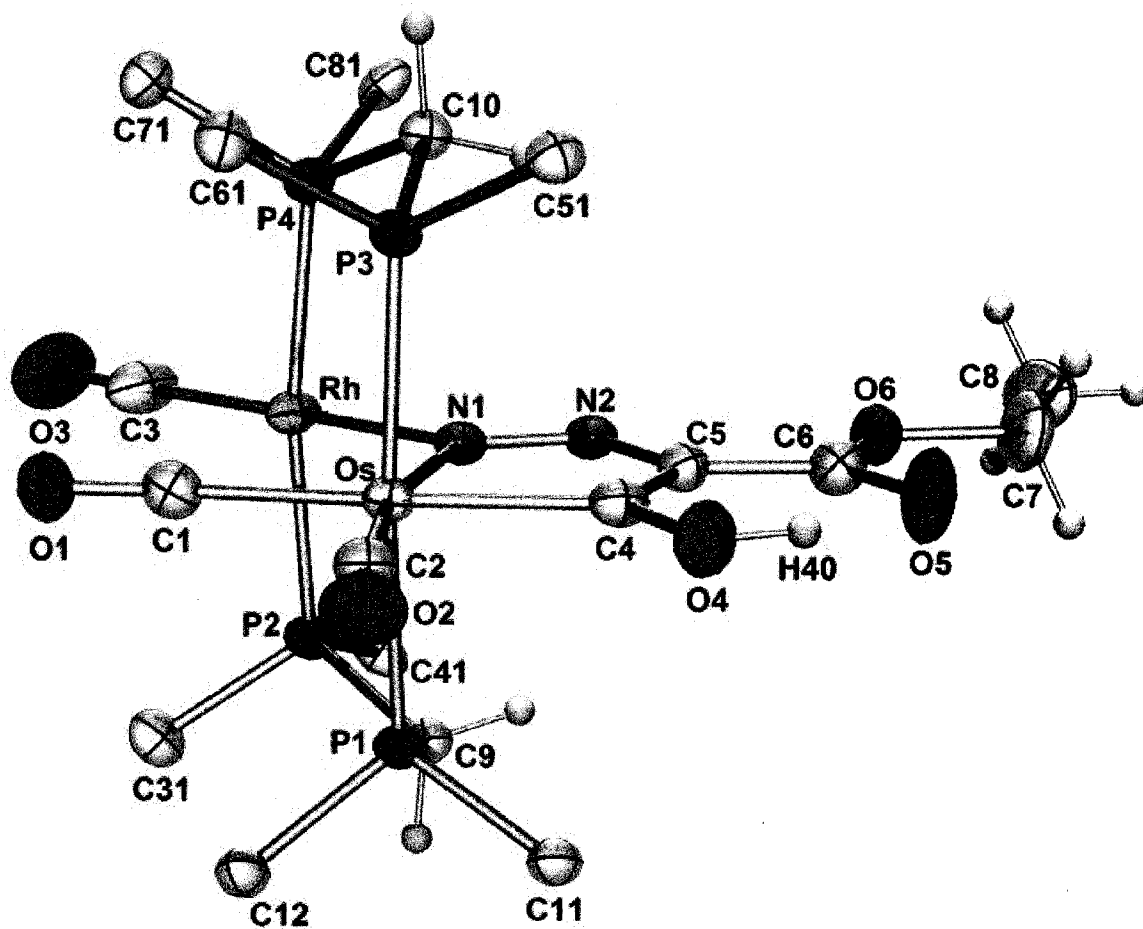


Figure A.1: Perspective view of the complex cation of compound $[\text{RhOs}(\text{CO})_3(\mu\text{-N}_2\text{C}(\text{COH})(\text{CO}_2\text{Et}))(\text{dppm})_2][\text{CF}_3\text{SO}_3]$. Thermal ellipsoids are drawn at the 50% level except for hydrogens, which are drawn arbitrarily small. Phenyl groups, except for ipso carbons, are omitted.

Table A.2: Selected Distances and Angles for [RhOs(μ -N₂C(COH)(CO₂Et))-(CO)₃(dppm)₂][CF₃SO₃].(i) Distances (\AA)

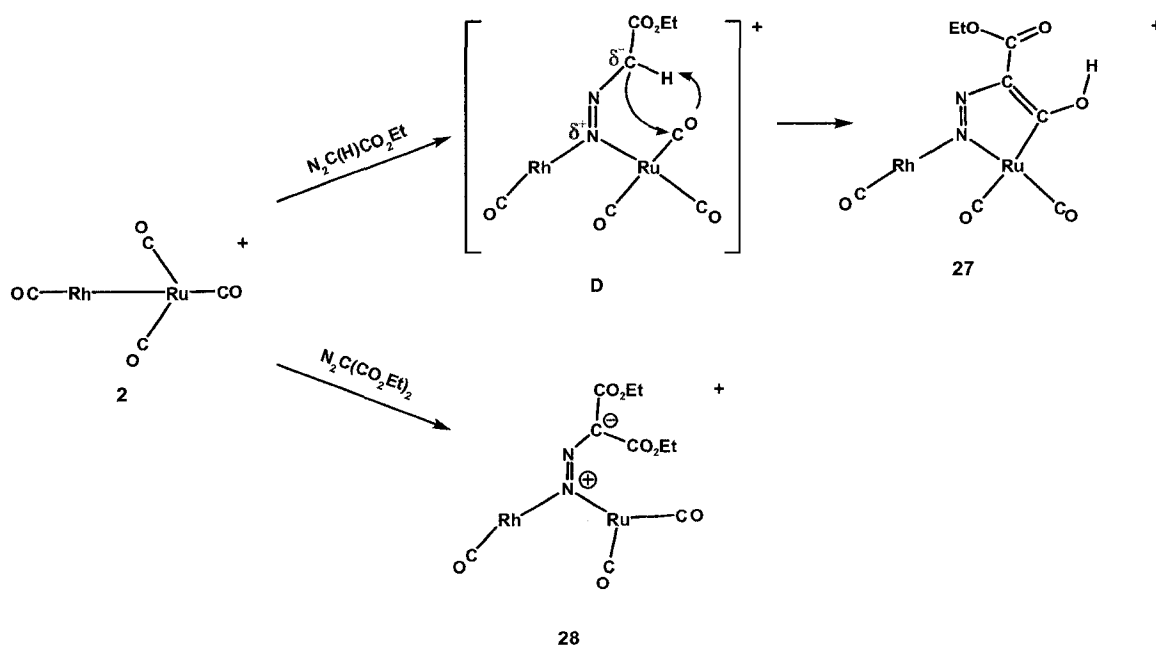
Atom 1	Atom 2	Distance	Atom 1	Atom 2	Distance
Os	P(1)	2.3978(8)	O(1)	C(1)	1.139(4)
Os	P(3)	2.4012(8)	O(2)	C(2)	1.145(4)
Os	N(1)	2.088(2)	O(3)	C(3)	1.143(5)
Os	C(1)	1.976(3)	O(4)	C(4)	1.328(4)
Os	C(2)	1.904(3)	O(4)	H(40)	0.87(6)
Os	C(4)	2.055(3)	O(5)	C(6)	1.227(5)
Rh	P(2)	2.3107(9)	O(5)	H(40)	1.85(6) [†]
Rh	P(4)	2.3052(8)	O(6)	C(6)	1.326(4)
Rh	N(1)	2.023(3)	O(6)	C(7)	1.464(5)
Rh	C(3)	1.842(4)	N(1)	N(2)	1.270(4)
P(1)	C(9)	1.839(3)	N(2)	C(5)	1.402(4)
P(2)	C(9)	1.833(3)	C(4)	C(5)	1.391(4)
P(3)	C(10)	1.836(3)	C(5)	C(6)	1.455(5)
P(4)	C(10)	1.839(3)	C(7)	C(8)	1.473(7)

[†] Non-bonded distance

(ii) Angles (deg)

Atom 1	Atom 2	Atom 3	Angle	Atom 1	Atom 2	Atom 3	Angle
P(1)	Os	P(3)	170.91(3)	Rh	P(2)	C(9)	113.4(1)
P(1)	Os	N(1)	85.39(7)	Os	P(3)	C(10)	112.3(1)
P(1)	Os	C(1)	91.5(1)	Rh	P(4)	C(10)	113.2(1)
P(1)	Os	C(2)	93.3(1)	C(4)	O(4)	H(40)	114(4)
P(1)	Os	C(4)	88.31(9)	C(6)	O(6)	C(7)	115.9(3)
P(3)	Os	N(1)	85.57(7)	Os	N(1)	Rh	107.8(1)
P(3)	Os	C(1)	90.8(1)	Os	N(1)	N(2)	119.9(2)
P(3)	Os	C(2)	95.3(1)	Rh	N(1)	N(2)	132.3(2)
P(3)	Os	C(4)	88.53(9)	N(1)	N(2)	C(5)	113.3(3)
N(1)	Os	C(1)	98.9(1)	Os	C(1)	O(1)	173.3(3)
N(1)	Os	C(2)	166.8(1)	Os	C(2)	O(2)	174.3(3)
N(1)	Os	C(4)	75.6(1)	Rh	C(3)	O(3)	178.9(4)
C(1)	Os	C(2)	94.2(1)	Os	C(4)	O(4)	125.0(2)
C(1)	Os	C(4)	174.5(1)	Os	C(4)	C(5)	114.1(2)
C(2)	Os	C(4)	91.3(1)	O(4)	C(4)	C(5)	120.9(3)
P(2)	Rh	P(4)	171.72(3)	N(2)	C(5)	C(4)	117.1(3)
P(2)	Rh	N(1)	86.84(7)	N(2)	C(5)	C(6)	121.3(3)
P(2)	Rh	C(3)	93.6(1)	C(4)	C(5)	C(6)	121.6(3)
P(4)	Rh	N(1)	87.05(7)	O(5)	C(6)	O(6)	122.3(3)
P(4)	Rh	C(3)	92.9(1)	O(5)	C(6)	C(5)	121.8(3)
N(1)	Rh	C(3)	176.5(1)	O(6)	C(6)	C(5)	115.9(3)
Os	P(1)	C(9)	112.3(1)	O(6)	C(7)	C(8)	108.0(4)

Scheme A.1



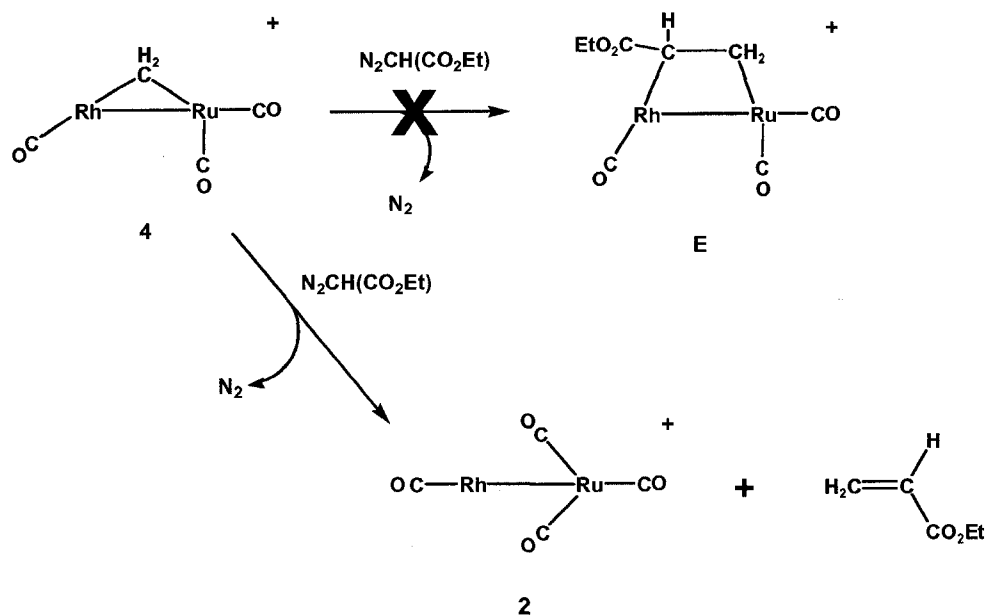
diphenyldiazomethane, neither was the case, as complex **2** failed to react with any of these diazoalkanes.

Success was achieved in the reaction of diazoalkane 2-diazo-malonic acid diethyl ester with **2**, affording a new complex with a similar $^{31}\text{P}\{^1\text{H}\}$ NMR spectrum to that of **27** (see Table A.1). This new complex, $[\text{RhRu}(\text{CO})_3(\mu\text{-N}_2\text{C}(\text{CO}_2\text{Et})_2)(\text{dppm})_2][\text{CF}_3\text{SO}_3]$ (**28**), as diagrammed in Scheme A.1, is shown to contain two ethyl groups, as observed in the ^1H NMR spectrum. Furthermore, elemental analysis suggests that, as with **27**, N_2 loss has not occurred. The IR spectrum of **28** shows three distinct terminal CO bands at 2045, 2027 and 1996 cm^{-1} , along with bands attributed to the CO_2Et ligand (1694 cm^{-1}) and the N_2 group (1374 cm^{-1}). This type of complex has been observed before by Eisenberg and coworkers,⁷ in which $\text{Rh}_2(\text{CO})_2(\mu\text{-H})_2(\text{dppm})_2$ reacts with 2-diazo-malonic acid diethyl

ester to give $[\text{Rh}_2(\text{CO})_2(\mu\text{-N}_2\text{C}(\text{CO}_2\text{Et})_2)(\text{dppm})_2]$. Spectroscopically, Eisenberg's Rh_2 species and complex **28** are very similar, with strong correlations in the IR spectra for both. However, resonance structure **C'**, as shown in Chart A.1, cannot be ruled out as a contributor to the overall structure of **28**, since some degree of conjugation was used to explain the structure of Eisenberg's complexes and is consistent with the delocalized structure observed in the solid-state structure for Puddephatt's Ru_2 complex.^{6,7}

In attempts to generate carbon-containing species analogous to those resulting from methylene coupling in the Rh/Os system, the methylene-bridged complex

Scheme A.2



$[\text{RhRu}(\text{CO})_3(\mu\text{-CH}_2)(\text{dppm})_2][\text{CF}_3\text{SO}_3]$ (**4**) was treated with ethyl diazoacetate. It was anticipated that a C_2 species **E**, as shown in Scheme A.2, or some compound that might model a precursor to such a C_2 species might be observed. This type of C-C coupling has

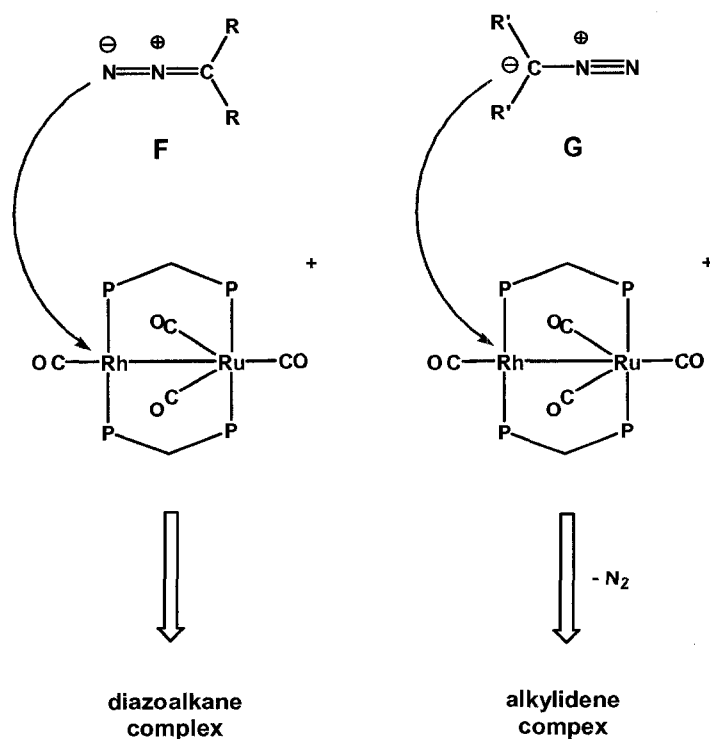
been observed by Akita et al.,¹¹ in which the complex $\text{Cp}_2\text{Ru}_2(\mu\text{-CH}_2)(\text{CO})_2(\text{NCMe})$ reacts with diazoalkanes of the general formula N_2CHR to give μ -alkenyl- μ -hydride species $\text{Cp}_2\text{Ru}_2(\mu\text{-CH=CHR})(\mu\text{-H})(\text{CO})_2$. Although C-C coupling is observed in our system, no new organometallic species is observed. Instead, the $^{31}\text{P}\{^1\text{H}\}$ and ^1H NMR spectra show the presence of a mixture of organometallic species, the major of which is compound **2** (likely arising from CO scavenging from other decomposition products) and the presence of ethyl acrylate resulting from the coupling of the methylene group from **4** and the carbene generated from ethyl diazoacetate. This type of C-C coupling was also observed in the aforementioned Ru_2 species when the disubstituted diazoalkanes (N_2CR_2 ; $\text{R} \neq \text{H}$),¹¹ were used. Similarly, in the Rh/Os system methyl acrylate is observed upon treatment of the Rh/Os analogue of **3** with ethyl diazoacetate.¹²

Discussion:

Addition of both ethyl diazoacetate and 2-diazo-malonic acid diethyl ester to the RhRu complex, $[\text{RhRu}(\text{CO})_4(\text{dppm})_2]^+$ (**2**) gives two different diazoalkane complexes that share their coordination mode: a bridging $\text{N}_2\text{CRR}'$ unit. This is in contrast to the reactions of the diazoalkanes without strong electron withdrawing groups such as N_2CH_2 , which formed a methylene bridge by N_2 loss, or the substituted analogues N_2CHCH_3 , N_2CPh_2 and $\text{N}_2\text{CHSi}(\text{CH}_3)_3$ which failed to react. These results suggest two different schemes for diazoalkane coordination to a metal centre, as diagrammed in Chart A.2. The two major resonance structures for the N_2CR_2 ligand are shown for structures **F** and **G**. If the diazoalkane carbon is the most nucleophilic site in the molecule (structure **G**)

we anticipate coordination of this atom to the metal followed by N_2 loss and generation of a metal-bound carbene. If the terminal nitrogen (structure F) is the more nucleophilic site, coordination via nitrogen occurs, leading possibly to complexes such as **27** and **28**. It is expected that electron withdrawing substituents, such as CO_2Et groups, on carbon will lower the nucleophilicity of the attached carbon, favouring coordination at nitrogen instead. The diazoalkanes N_2CHCH_3 , N_2CPh_2 and $N_2CHSi(CH_3)_3$ are electronically similar to diazomethane, so should presumably react with **2** to form bridging alkylidenes. However, we assume that the bulk of the substituents in these cases prevents coordination at carbon, resulting in no reactivity and carbene formation. Large substituents are of less significance in N-bonded diazoalkanes since these substituents are remote from the metal.

Chart A.2

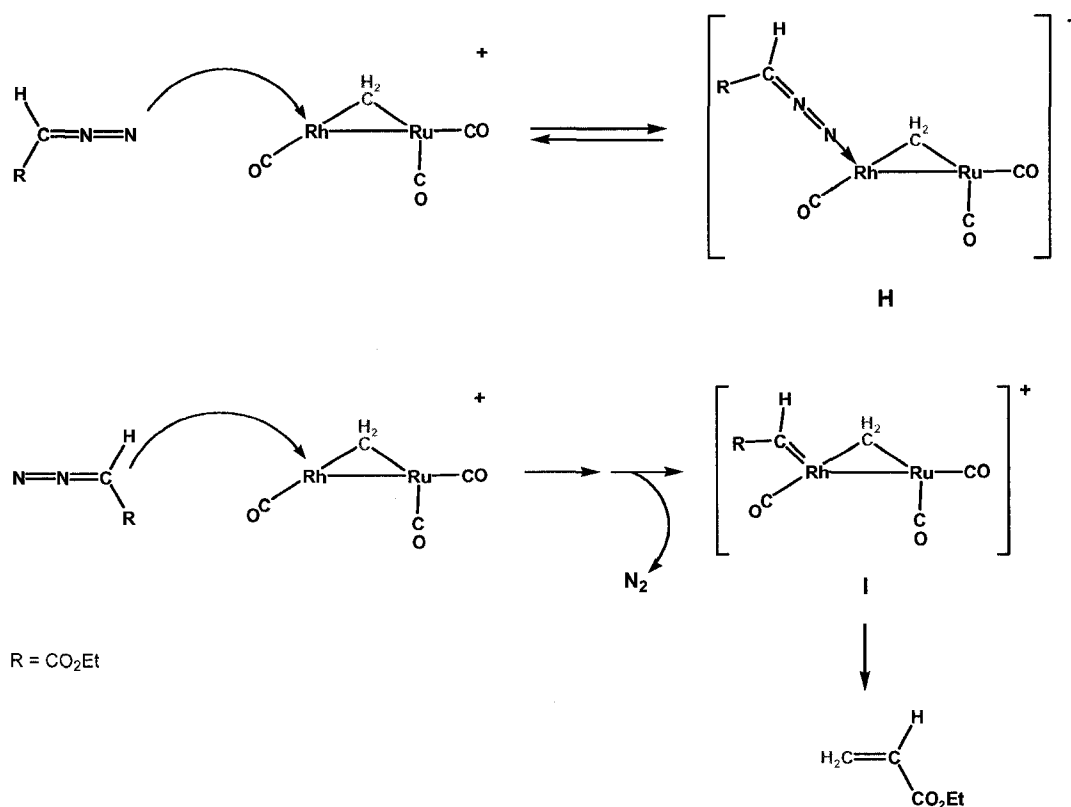


Although complex **28** appears to be a “typical” bridging diazoalkane complex, clearly the formation of **27** is significantly more complicated, and a more complex mechanism must be invoked in order to explain the condensation with a carbonyl and the hydrogen migration steps that occur. Although it is unclear why one of the carbonyls “inserts” into the C-H bond of the diazoalkane forming the “diazometallacyclopentenol”, any mechanism would likely involve diazoalkane coordination affording a similar complex to that of **28**, shown as intermediate **D** in Scheme A.1. Nucleophilic attack by the carbene carbon onto the carbon of one of the Ru-bound carbonyls along with deprotonation by the carbonyl oxygen must follow, affording the observed condensation product. Clearly the major difference in these two diazoalkane ligands is that for ethyl diazoacetate deprotonation of the original carbon-hydrogen bond by the carbonyl can occur, whereas for 2-diazo-malonic acid diethyl ester no deprotonation is possible.

Carbon-carbon coupling is also observed when ethyl diazoacetate is reacted with the unsaturated complex $[\text{RhRu}(\text{CO})_3(\mu\text{-CH}_2)(\text{dppm})_2]^+$ (**4**) yielding ethyl acrylate and primarily $[\text{RhRu}(\text{CO})_4(\text{dppm})_2]^+$ (**2**). This type of coupling has been observed previously,¹¹ and the proposed mechanism involves coordination of ethyl diazoacetate through the nucleophilic carbon atom followed by loss of N_2 giving a bridging methylene and a carbene, which subsequently couple. Although our earlier argument suggested that coordination of ethyl diazoacetate via the more nucleophilic nitrogen rather than carbon is preferred, this coordination does not lead to the presumed favoured bridging mode in this case, since the bridging site is occupied by the methylene group, leading to loss of the diazoalkane molecule (presumably ligand addition to Rh is reversible). Under these circumstances, attack via the diazoalkane carbon can compete, resulting in irreversible N_2

loss and carbene formation, as diagrammed in Scheme A.3. The proposed methylene/carbene intermediate (structure I) is analogous to that proposed by Akita et al. in their Ru₂ system,¹¹ and can proceed to produce the observed ethyl acrylate.

Scheme A.3



Conclusions:

The results reported herein clearly reveal that diazoalkane complexes of RhRu can be prepared in which the N₂ moiety remains intact. Two different types of diazoalkane complex are obtained, [RhRu(CO)₃(μ-N₂C(COH)(CO₂Et))-(dppm)₂][CF₃SO₃] (**27**) in which nucleophilic attack of the carbene carbon on a carbonyl carbon is accompanied by proton transfer to the carbonyl oxygen; and the complex [RhRu(CO)₃(μ-N₂C(CO₂Et)₂)(dppm)₂][CF₃SO₃] (**28**) in which simple coordination of the

diazoalkane results. Although diazomethane reacts with **2** to form the methylene-bridged complex $[\text{RhRu}(\text{CO})_4(\mu\text{-CH}_2)(\text{dppm})_2][\text{CF}_3\text{SO}_3]$ (**3**), the substituted diazoalkanes N_2CPh_2 , N_2CHCH_3 and $\text{N}_2\text{CHSi}(\text{CH}_3)_3$ failed to react with **2**, leaving only starting materials. These results lead to the conclusion that the steric bulk of the substituents on the carbene carbon hinder coordination of this nucleophilic centre, preventing alkylidene formation.

The bridging methylene complex $[\text{RhRu}(\text{CO})_3(\mu\text{-CH}_2)(\text{dppm})_2][\text{CF}_3\text{SO}_3]$ (**4**) readily reacts with ethyl diazoacetate to give the olefinic product ethyl acrylate via C-C coupling of the methylene bridge and the CHCO_2Et of the diazoalkane. The failure of the resulting C_2 fragment to remain bound to the Rh/Ru centres is probably a result of the unfavourable interactions between the olefin substituent and the phenyls of the dppm groups. It should be noted that we have been unsuccessful in isolating olefin complexes of any of these Rh/Ru systems in which any olefin substituents were present.

References

1. Sutton, D. *Chem. Rev.* **1993**, *93*, 995.
2. Doyle, M.P. *Chem. Rev.* **1986**, *86*, 919.
3. Muetterties, E.L.; Stein, J. *Chem. Rev.* **1979**, *79*, 479.
4. Hidai, M.; Mizobe, Y. *Chem. Rev.* **1995**, *95*, 1115.
5. Mizobe, Y.; Ishii, Y.; Hidai, M. *Coord. Chem. Rev.* **1995**, *139*, 281.

6. Gao, Y.; Jennings, M.C.; Puddephatt, R.J.; Jenkins, J.A. *Organometallics* **2001**, *20*, 3500.
7. Woodcock, C.; Eisenberg, R. *Organometallics* **1985**, *4*, 4.
8. Graham, T.W.; McDonald, R.; Cowie, M. Unpublished Results.
9. crystallographic information may be obtained by contacting Dr. Robert McDonald (bob.mcdonald@ualberta.ca) and inquiring about sample number COW0120.
10. Allen, F.H.; Kennard, O.; Watson, D.G.; Brammer, L.; Orpen, A.G.; Taylor, R. *J. Chem. Soc.-Perkin Trans. 2* **1987**, S1.
11. Akita, M.; Hua, R.; Knox, S.A.R.; Moro-oka, Y.; Nakanishi, S.; Yates, M.I. *J. Organomet. Chem.* **1998**, *569*, 71.
12. Graham, T.W.; Cowie, M. Unpublished Results.